Drug Discoveries & Therapeutics

ISSN 1881-7831 Online ISSN 1881-784X
Volume 1, Number 1, July 2007
www.ddtjournal.com

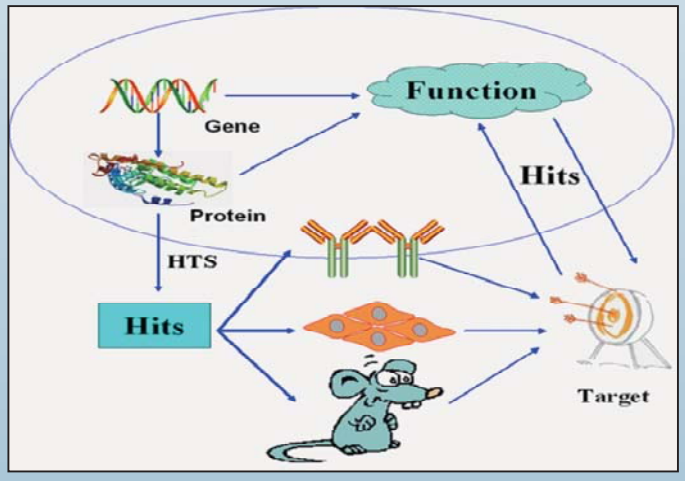

Shandong University China-Japan Cooperation Center for Drug Discovery & Screen
International Advancement Center for Medicine & Health Research

Drug Discoveries & Therapeutics

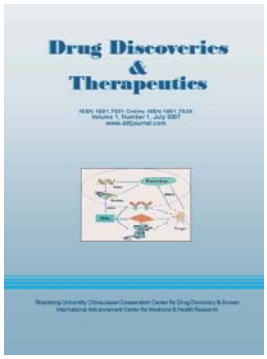

Editor-in-Chief:

Kazuhisa SEKIMIZU
(*The University of Tokyo, Tokyo, Japan*)

Associate Editor:

Norihiro KOKUDO
(*The University of Tokyo, Tokyo, Japan*)

Drug Discoveries & Therapeutics is an international journal published by *Shandong University China-Japan Cooperation Center for Drug Discovery & Screen* (SDU-DDSC) and *International Advancement Center for Medicine & Health Research Co., Ltd.* (IACMHR Co., Ltd.).

Drug Discoveries & Therapeutics mainly publishes articles related to basic and clinical pharmaceutical research such as pharmaceutical and therapeutical chemistry, pharmacology, pharmacy, pharmacokinetics, industrial pharmacy, pharmaceutical manufacturing, pharmaceutical technology, drug delivery, toxicology, and traditional herb medicine. Studies on drug-related fields such as biology, biochemistry, physiology, microbiology, and immunology are also within the scope of this journal.

Subject Coverage: Basic and clinical pharmaceutical research including Pharmaceutical and therapeutical chemistry, Pharmacology, Pharmacy, Pharmacokinetics, Industrial pharmacy, Pharmaceutical manufacturing, Pharmaceutical technology, Drug delivery, Toxicology, and Traditional herb medicine.

Langage: English
Issues/Year: 12
Published by: IACMHR and SDU-DDSC
ISSN: 1881-7831 (**Online ISSN** 1881-784X)

Editorial and Head Office

Wei TANG, MD PhD
Secretary-in-General

TSUIN-IKIZAKA 410
2-17-5 Hongo, Bunkyo-ku
Tokyo 113-0033, Japan
Tel: 03-5840-9697
Fax: 03-5840-9698
E-mail: office@ddtjournal.com
URL: http://www.ddtjournal.com

IACMHR CO., LTD.

Drug Discoveries & Therapeutics

Editorial Board

Editor-in-Chief:
Kazuhisa SEKIMIZU (*The University of Tokyo, Tokyo, Japan*)

Associate Editor:
Norihiro KOKUDO (*The University of Tokyo, Tokyo, Japan*)

Secretary-in-General:
Wei TANG (*The University of Tokyo, Tokyo, Japan*)

Office Manager:
Munehiro NAKATA *(Tokai University, Kanagawa, Japan*)

Web Editor:
Yu CHEN (*The University of Tokyo, Tokyo, Japan*)

English Editor:
Curtis BENTLEY (*Roswell, GA, USA*)

China Office:
Wenfang XU (*Shandong University, Shandong, China*)

Editors:

Yoshihiro ARAKAWA (*Tokyo, Japan*)
Fen Er CHEN (*Shanghai, China*)
Mohamed F. EL-MILIGI (*Cairo, Egypt*)
Hiroshi HAMAMOTO (*Tokyo, Japan*)
Langchong HE (*Xi'an, China*)
Hans E. JUNGINGER (*Phitsanulok, Thailand*)
Ibrahim S. KHATTAB (*Safat, Kuwait*)
Shiroh KISHIOKA (*Wakayama, Japan*)
Nobuyuki KOBAYASHI (*Nagasaki, Japan*)
Masahiro KUROYANAGI (*Hiroshima, Japan*)
Hongmin LIU (*Zhengzhou, China*)
Hongxiang LOU (*Jinan, China*)
Norio MATSUKI (*Tokyo, Japan*)
Abdulla M. MOLOKHIA (*Alexandria, Egypt*)
Yoshinobu NAKANISHI (*Ishikawa, Japan*)
Xiao-Ming OU (*Jackson, MS, USA*)
Adel SAKR (*Cincinnati, OH, USA*)
Tomofumi SANTA (*Tokyo, Japan*)
Hongbin SUN (*Nanjing, China*)
Ren-Xiang TAN (*Nanjing, China*)
Stephen G. WARD (*Bath, UK*)
Liangren ZHANG (*Beijing, China*)
Santad CHANPRAPAPH (*Bangkok, Thailand*)
Guanhua DU (*Beijing, China*)
Harald HAMACHER (*Tuebingen, Germany*)
Xiao-Jiang HAO (*Yunnan, China*)
Yongzhou HU (*Hangzhou, China*)
Toshiaki KATADA (*Tokyo, Japan*)
Hiromichi KIMURA (*Tokyo, Japan*)
Kam Ming KO (*Hong Kong, China*)
Toshiro KONISHI (*Tokyo, Japan*)
Chun Guang LI (*Victoria, Australia*)
Ji-Kai LIU (*Yunnan, China*)
Ken-ichi MAFUNE (*Tokyo, Japan*)
Tohru MIZUSHIMA (*Kumamoto, Japan*)
Masahiro MURAKAMI (*Osaka, Japan*)
Yutaka ORIHARA (*Tokyo, Japan*)
Wei-San PAN (*Liaoning, China*)
Abdel Aziz M. SALEH (*Cairo, Egypt*)
Yasufumi SAWADA (*Tokyo, Japan*)
Benny K. H. TAN (*Singapore, Singapore*)
Murat TURKOGLU (*Istanbul, Turkey*)
Takako YOKOZAWA (*Toyama, Japan*)
Jian-Ping ZUO (*Shanghai, China*)

CONTENTS

Volume 1, Number 1, 2007

Editorial

News

Brief Report

Review

CONTENTS (*Continued*)

Original Article

Guide for Authors

Copyright

Editorial

Kazuhisa Sekimizu, Ph.D.

Professor,
Laboratory of Microbiology,
Graduate School of Pharmaceutical Sciences,
The University of Tokyo, Tokyo, Japan.

In the 21st century, mankind is faced with the previously unseen reality of aging societies. Developed countries have a strong social need for the development of advanced medical technology, including the establishment of treatment for diseases affecting the elderly, such as cancer and metabolic syndrome. Meanwhile, in other parts of the world, many people are struggling with war and poverty and face the threats of starvation and infection. Given this complex situation, the role played by technological development in the field of medicine is of great significance.

In addition, the 21st century may belong to Asia, which has gained significant global recognition due to its rapid economic development. Accordingly, greater expectations have been placed on the role played by Asian researchers. However, research conducted in Asia has been criticized for its tendency to follow research conducted in Western countries. Therefore, development of original world-class research is urgently required in Asia.

Journals provide researchers with valuable opportunities to present their research findings. With the cooperation of my close friends Dr. Wei Tang and Dr. Munehiro Nakata, I decided to participate in the launch of *Drug Discovery and Therapeutics* with the objective of contributing to the advancement of pharmaceutical research in Asia. This journal will cover not only laboratory science related to drug discovery, but also the broad field of social pharmacy. Submission of highly original articles that contribute to pharmaceutical sciences will be welcomed. I sincerely hope that *Drug Discovery and Therapeutics* will contribute to the field of pharmaceutical sciences as an esteemed journal for researchers in Asia and worldwide.

July 21, 2007

Kazuhisa Sekimizu

Editor-in-Chief
Drug Discoveries & Therapeutics

China-Japan enhance joint research cooperation for drug discoveries and development:
News from CJMWDDT 2007 in Jinan, China

Xin-Yong Liu[1], Xian-Jun Qu[1], Wei Tang[1, 2]

Viral hepatitis is currently a major global cause of morbidity and mortality. In some Asian countries like China and Japan, Hepatitis B and C in particular are the most common extremely infectious diseases and are likely to develop into liver cirrhosis. Furthermore, statistics indicate that patients with liver cirrhosis resulting from hepatitis B and C have an increased risk of developing hepatocellular carcinoma (HCC). Scientists have worked tirelessly to find curative therapeutic strategies to control chronic hepatitis and liver cirrhosis, accompanied by improvements in public health and living conditions.

China's Shandong University and the University of Tokyo in Japan previously established a long-term cooperative relationship. Cooperative programs include co-training of postgraduates, exchanges of visiting scholars, academic symposia, and a bilateral international joint research program.

Some substantive progress has been made as a result of bilateral endeavors. For instance, the Shandong University China-Japan Cooperation Center for Drug Discovery & Screening (SDU-DDSC) has enhanced to serve as an important platform for further close cooperation. At the same time, the International Advancement Center for Medicine & Health Research (IACMHR) – "Drug Discoveries and Therapeutics" and International Research and Cooperation Association for Bio & Socio-Sciences Advancement (IRCA-BSSA) – "BioScience Trends" were established (Visit *http://www.ddtjournal.com* and *http://www.biosciencetrends.com*).

The first China-Japan conference on new drug discoveries and therapeutics (CJMWDDT 2007) was recently held in Jinan, China May 27-29, 2007, which provided opportunities for further communication and cooperation and increased knowledge of new drug research and clinical cures for hepatitis.

Financially supported by the National Natural Science Foundation of China (NSFC) and the Japan Society for the Promotion of Science (JSPS), the conference covered a wide range of topics in different areas of chemical biology, phytochemistry, medicinal chemistry, and pharmacology and it resulted in informed and genial discussions of hepatitis cures that yielded fruitful results. The active involvement and participation by attendees gave the conference a congenial atmosphere. In the end, an agreement was reached to work together on new drug discovery and effective hepatitis therapeutic strategies, and some agreements have resulted in the creation of handover protocols.

China-Japan conference on new drug discoveries and therapeutics (CJMWDDT), May 27-29, 2007, Jinan, China.

The CJMWDDT 2007 was a highly successful scientific event that strengthened and promoted extensive cooperation between China and Japan for the development of new pharmaceutical products and hepatitis cures. (*[1] Shandong University, Jinan, China; [2] the University of Tokyo, Tokyo, Japan.*)

CJMWDDT 2007, May 27-29, 2007, Jinan, China

Section 1: Overview of chemotherapy for viral hepatitis and hepatic cancer

Section 2: Current progress in natural product chemistry

- *New technological applications in discovery of active natural products*
- *Biotransformation of active natural products*
- *Modernization of Chinese traditional medicines*

Section 3: Current progress in drugs design and synthesis

- *Drug design based on the structural biology*
- *New methodology and technology in drug synthesis*

Section 4: New approach for drug screening and evaluation

- *Introduction of new drug evaluation in Japan*
- *Application of High throughput screening in drug discovery*
- *Models and mechanism in screening for ant-tumor drugs*
- *Therapeutic targets in anti-tumors, antiviral and cardiovascular drugs*
- *Models of neuropharmacology and cardiovascular pharmacology*

China's new drug R&D is steadily advancing

Wen-Fang Xu

China appears to consistently lag behind developed countries like the US, Japan, and the nations of Europe in the development of pharmaceuticals, putting China in an embarrassing situation. In fact, China is still dependent on foreign imports for most highly effective cures to major diseases such as cancer, diabetes, hepatitis, and neurodegenerative disease. There is no denying the fact that governmental support, and especially a significant amount of financial support and political assistance to include government restructuring, is needed for the establishment of new drug Research and Development (R&D).

Fortunately, China's authorities have recently recognized the importance of new drug development and have committed to implementing strong measures to help establish new drug R&D. This improvement in the government's status is showing immediate and substantial promise in the field of pharmaceuticals.

On January 4, 2007, a research group directed by Wang Ming-Wei, Head of the National Center for Drug Screening, Shanghai Institute of Materia Medica (SIMM), made a breakthrough in the development of novel category I anti-diabetes drugs with the support of the Ministry of Science & Technology of China, the National Natural Science Foundation (NSFC) of China, and the Shanghai municipal government. Taking almost four years, the group finally developed a non-peptide agonist of small molecule glucagon-like peptide 1 receptors with efficacy in diabetic db/db mice (*Proc Natl Acad Sci U S A 2007;104:943-948*). As an anti-diabetes drug, a peptide hormone traditionally had to be taken as an injection, which greatly limited its clinical application. In contrast, the new compound can be taken orally. This offers hope for the development of a new field of peptidomimetics for orally-available non-peptide small molecules.

Today, the ever-growing prevalence of major diseases worldwide is driving growth in new drug spending, encouraging the marketing of newly developed and efficacious therapies. This achievement appears to have significantly boosted the field of new drug research in China. While "China's pharmaceutical firms lag far behind [their Western counterparts] in terms of biological preparations" "today's achievement, with the attention it has garnered, has important scientific significance and potential social and economic value," said Chen Zhu, the minister of health PRC and also the former associate dean of the China Academy of Sciences (*http://www.simm.ac.cn/News/20071417649.htm, available as of January 4, 2007*).

Other encouraging news came from the Shanghai Life Sciences Institute. A novel anti-HIV compound named Nifeviroc was developed with the support of the municipal government and licensed for clinical trials on April 17, 2007 (*Shanghai Daily, April 17, 2007*). This is expected to become the world's first oral HIV entry-inhibitor. Thus far, applications to patent Nifeviroc have been submitted in 14 countries and regions, including the United States, Japan, and the European Union. Recently, Shanghai Targetdrug Pharmaceutical Company and Avexa, a Melbourne-based drug-research company in Australian, announced that they will jointly develop Nifeviroc for global distribution. Avexa will handle post-research expenses, develop the drug in the international marketplace, and share global profits with Targetdrug.

Thus, China may have justified rationale and confidence to believe that the day will come when China's pharmaceutical products will boast a strong presence in the global market. (Wen-Fang Xu: *Shandong University, Jinan, China.)*

Analysis on productivity of clinical studies across Asian countries — a case comparison

Ken Takahashi, Shintaro Sengoku, Hiromichi Kimura*

Pharmaco-Business Innovation Laboratory, Graduate School of Pharmaceutical Science, The University of Tokyo, Tokyo, Japan.

ABSTRACT: In an era of increasing global competition and an increased interest in global clinical studies Japan has been concerned with the risk of losing its attractiveness due to perceived longer execution times and higher cost structure. In contrast, other Asian countries particularly China and Singapore are widely recognized as potential key centers for fast conduction of global clinical studies. We conducted a case comparison based on two clinical studies performed by a multinational pharmaceutical company in order to measure the productivity of clinical studies by region and country. We focused on the site-related study cost which constituted the largest portion of the cost breakdown and also impacted both time and quality management. For investigation of the productivity we propose a breakdown model with two Key Performance Indicators (KPIs), enrollment efficiency and site-related cost efficiency, for the comparison of the number of enrolled subject per site and cost, respectively. Through the comparative analysis we found that the Asian countries (excluding Japan) on average achieved higher efficiency than Japan in both indicators. In the Asian group, China and Singapore stood out as the most efficient on both speed and site-related cost. However, when the site-related cost efficiency was adjusted for Purchasing Power Parity (PPP) the cost advantage in China disappeared, implying the price level was critical for productivity management. Although quality aspects remain to be investigated we postulate that introducing a comparative approach based on a productivity framework would be useful for an accurate productivity comparison.

Key Words: Productivity, clinical development, clinical study, regulatory science

**Correspondence to:* Pharmaco-Business Innovation Laboratory, Graduate School of Pharmaceutical Science, The University of Tokyo, 7-3-1 Hongo, Bunkyo-ku, Tokyo 113-0033, Japan;
e-mail: kimura@mol.f.u-tokyo.ac.jp

Received June 1, 2007
Accepted July 2, 2007

Introduction

It is a critical issue for large pharmaceutical companies to achieve competitive cost and speed in clinical study execution. Recently the principles of International Conference on Harmonization of Technical Requirements for Registration of Pharmaceuticals for Human use (ICH) have been embraced by most Asian countries for the facilitation of global alignment of clinical studies. Through the globalization of pharmaceutical and medical products for the past decades Japan has been one of the centers of pharmaceutical clinical studies by virtue of its large market potential. However, Japan has received a reputation that clinical study-related cost is high in comparison with that in other countries (*1-3*). The underlying reasons have not been fully understood, however, site-related inefficiency was suggested as one of reasons for the high cost level. Particularly, over-quality in execution of clinical studies, which creates laborious work processes leading to longer time to completion, has been pointed out through comparative observations (*4*). This, in turn, resulted in a decrease in the number of clinical studies conducted in Japan over the last decade (*1-3*).

In order to address the issue of low productivity in clinical studies the government and its affiliates have been implementing various actions. For example, Japanese Pharmaceuticals and Medical Devices Agency (PMDA) endorses global clinical studies involving Japan and Asian countries, as well as Asian clinical studies including Japan and other Asian countries. To design and conduct Asian-wide uniformed clinical studies in an effective way it is essential to capture precise information of cost and subject enrollment efficiencies in Asian countries. However, such basal information has not been readily available, although some limited information exists (*1-3,5*). Thus, quantitative investigations need to be initiated. For better understanding of the current situation it is necessary to provide qualified case examples which are eligible for cross-regional comparison and exploration of essential underlying mechanisms to describe identified differences.

In this report we present a case comparison of

two clinical studies with a considerable focus on the site-related study cost, which was spent by the pharmaceutical company to fund and support the studies at each study site. One of the studies was conducted globally and involved representative Asian countries including Greater China, Singapore, Taiwan, Hong Kong and Thailand. The other study was conducted in Japan with the study protocol almost identical to the global trial. We here present the results of a quantitative comparison on specific cost items and describe potential underlying explanations for the typical differences observed.

Materials and Methods

Cost related information on both the Japanese and global study was kindly provided by Novo Nordisk A/S and its Japanese affiliate, Novo Nordisk Pharma Limited. The information of cost was external payment from Novo Nordisk and available from the start of the program in 2004 to its completion in 2007. Since study-related payment is requested sometimes even long after completing a study we adopted forecasted figures for the uncovered period of study to keep to the difference an absolute minimal. Site-related study cost in Japan was calculated for the separate clinical trial executed in parallel to the global trial with the almost identical study protocol. The studies performed to document safety and efficacy for treatment of an acute disease in a new therapeutic area of drug development. Very few similar studies have been conducted globally and the study in Japan was a novel case.

In each clinical study investigators were carefully nominated from a pool of similar background and expertise. In the actual clinical studies the medicine (or placebo) was administered to each subject in a very short period of time after disease onset soon after informed consent was obtained from a patient or his/her legally accepted representative. The enrolled subjects were followed-up for three months after drug administration. Inclusion/exclusion criteria, treatment period, follow-up period, evaluation items and visit intervals were almost identical between the Japanese study and the global study. Both cases were placebo-controlled, double blind studies. The Japan study was a three-tier dose escalation trial, while the global study had a three-arm parallel design.

Twenty two countries or areas (the USA and Canada from North America, Spain, Germany, France, Netherlands, Sweden, Finland, Denmark, Italy, Austria, Belgium, Norway and Croatia from Europe, China, Singapore, Taiwan, Hong Kong and Thailand from Asia, Australia from Oceania, Israel and Brazil) participated into the said global study. Top level clinical study sites in each country were involved in both of the clinical studies. However, only two to three study sites in each Asian country were involved in the global study, while in total 29 study sites participated into the Japan Study.

The number of subjects enrolled in the global study was in total 821 consisting of 282 from North America, 380 from Europe, 113 from Asia, 21 from Oceania and 25 from other countries. In the Japan study 91 subjects were enrolled. The enrollment period of the global study from the first-patient-in to the last-patient-in was 18 months. That for the Japan study was nine months by adjusting total three months of enrollment suspension for dose tier up evaluation and decision. Both of the studies were compliant with Good Clinical Practice (GCP) of ICH (ICH-GCP). The quality in the trials was secured through monitoring activities, which fulfilled the requirements for regulatory submission to Food and Drug Agency (FDA), European Medicines Evaluation Agency (EMEA), PMDA and other regulatory authorities. Therefore, comparison of investigator site-related study costs was able to be done with negligible bias.

For the comparative analysis we defined site-related study cost as consisting of investigator grant, clinical research coordinators' (research nurses') cost, indirect cost charged by the site, Institutional Review Board (IRB)/Ethics Committee (EC) cost, study specific examination cost, study specific equipment cost, patient allowance, printing cost, translation cost, courier cost and investigator related information and education cost. For comparison amongst countries in the Asian region, Japan, China, Singapore and Taiwan were selected whereas Hong Kong and Thailand were eliminated due to few enrolled subjects (n = 2 and 1, respectively).

For the analysis of site-related cost efficiency adjusted with comparative price levels, the figures of Purchasing Power Parity (PPP) in 2005 for each country were obtained from annual report from World Bank and International Monetary Fund (for Taiwan).

Results and Discussion

The breakdown of external clinical study costs of the Japanese and the global clinical studies paid by the pharmaceutical company were as follows. The external cost of the global study consisted of site-related study cost (32.0%), outsourced monitoring cost (17.5%), external laboratory cost (14.8%), other outsourcing cost such as data management (11.9%), drug and packaging cost (3.1%) and others (20.6%). The external cost of the Japan study consisted of outsourced monitoring cost (59.0%), site-related study cost (21.2%), other outsourcing cost such as data management (9.0%), external laboratory cost (8.0%), drug and packaging cost (0.2%) and others (2.6%). Since execution of the Japan study was fully outsourced whereas the global study was performed basically by internal resource, the ratio of monitoring cost and other cost varied between them. However, it was obvious that the site-related study cost was the predominant cost portion of a clinical study when the study was managed by

internal resource. This observation showed good correspondence to a previous report (*3*).

A productivity breakdown model and the results of the enrollment efficiency, site-related cost efficiency, site-related cost efficiency adjusted with PPP, and speed of enrollment are summarized in the Figure 1 and Table 1, respectively. As for relative enrollment efficiency (indices of subjects per site), the numbers for Japan, global average (ex-Japan), Asian average (ex-Japan), North American average, European average, Oceania and others were 1.00, 1.60, 3.27, 1.38, 2.52, 1,67 and 1.99, respectively. Thus, Asian countries (ex-Japan) were on average 3.3 times more efficient than Japan which had the lowest enrollment efficiency of all the regions. Regarding site-related cost efficiency (indices of subject per cost), the figures for Japan, global average (ex-Japan), Asian average (ex-Japan), North American average, European average, Oceanian average and others were 1.00, 1.89, 3.50, 1.22, 2.28, 2.42 and 1.97, respectively. Thus, the Asian average (ex-Japan) was the most cost-efficient in the world and 3.5 times more efficient than Japan.

Considering differences in price levels across countries, we also tested to adjust site-related cost efficiency with PPP. This method utilizes the long-run equilibrium exchange rate of two currencies to equalize the currencies' purchasing power. PPP-adjusted site-related cost efficiency is considered to be useful from perspective of governments, study sites and companies to evaluate real cost efficiency of the study execution at each study site by eliminating impact of price level although only nominal site-related cost efficiency is usually discussed. Through this adjustment we obtained relative ratios of 1.00, 1.53, 1.02, 1.04, 2.19, 2.15 and 1.10 for Japan, global average (ex-Japan), Asian average (ex-Japan), North American average, European average, Oceanian average and others, respectively. This indicated that PPP-adjusted site-related cost efficiency of Japan was at an almost similar level to those of Asian average (ex-Japan), North American average and others, while those of European average and Oceanian average were about 2.2 times higher than that of Japan.

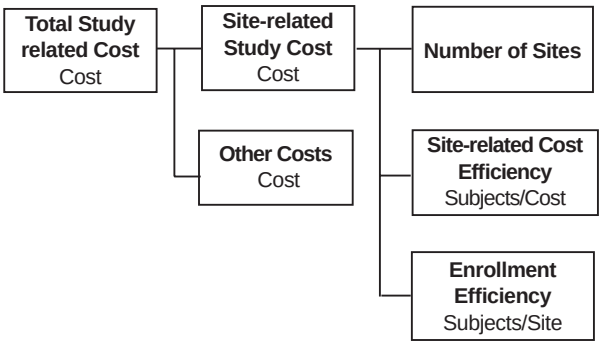

Figure 1. Productivity breakdown model of clinical studies. For comparative analysis we newly synthesized a breakdown model for the measurement of clinical study productivity. Two performance indicators, so called enrollment efficiency and site-related cost efficiency correspond to the number of subjects per site and the number of subjects per cost, respectively. Dividing enrollment efficiency by site-related cost efficiency and multiplying it by number of sites makes site-related study cost.

When we compared speed of enrollment (subjects per site per month) across regions, these were 1.00, 0.80, 1.64, 0.69, 1.26, 0.84 and 0.99 for Japan, global average (ex-Japan), Asian average (ex-Japan), North American average, European average, Oceania and others respectively, demonstrating clear advantage of Asian countries compared to other regions. Speed of enrollment in Japan was higher than in North American average and Oceanian average, as well as in the global trial as a whole.

To obtain more precise understanding of site performance in Japan we selected top 10% performing study sites for comparison. When these three sites were analyzed, the indices of average enrollment efficiency and speed of enrollment were 3.01, and the site-related cost efficiency index was 1.39. These results indicated that the higher performing Japanese sites were fairly competitive in speed of enrollment. This indicates that with careful site selection Japan can be a notable contributor to global and Asian-wide clinical studies.

We then conducted a country-level comparison in the same manner in the Asian region for the indices of enrollment efficiency, site-related cost efficiency, PPP-adjusted site-related cost efficiency and speed of

Table 1. Comparison of selected performance indicators for clinical study efficiency (Unit: Index (Japan = 1.00))

Items	Definition	Japan Study		Global Study (ex-Japan)								
		Japan		Global	Asia				North America	Europe	Oceania	Others
		Total	Top 10%	Total	Total	China	Singapore	Taiwan	Total	Total	Total	Total
Number of Subjects	Subjects	91	28	821	113	81	20	9	282	380	21	25
Site-related Cost Efficiency	Subjects/Cost	1.00	1.39	1.89	3.50	4.55	2.70	1.68	1.22	2.28	2.42	1.97
Site-related Cost Efficiency adjusted with PPP		1.00	1.39	1.53	1.02	0.77	2.00	0.76	1.04	2.19	2.15	1.10
Enrollment Efficiency	Subjects/Site	1.00	3.01	1.60	3.27	8.60	3.19	0.96	1.38	2.52	1.67	1.99
Speed of Enrollment	Subjects/Site/Month	1.00	3.01	0.80	1.64	4.30	1.59	0.48	0.69	1.26	0.84	0.99
Comparative Price Levels (PPP)		1.00	1.00	0.81	0.29	0.17	0.74	0.45	0.85	0.96	0.89	0.56

Based on the shown in Figure 1 enrollment efficiency, site-related cost efficiency (nominal and PPP-adjusted) and speed of enrollment were selected as representative efficiency indicators for the clinical studies. All indicators were transformed indices (here Japan was set to 1.00) due to a confidentiality requirement from the information provider. Along with this manger the global and Asian average (ex-Japan) were calculated. North American average, European average, Oceanian average and other countries' average were also deduced herewith for reference. To compare speed of enrollment the indexed figures were calculated by dividing enrollment efficiency of each country by the number of enrollment period of each study and setting that of Japan to 1.00.

enrollment. All comparative data were transformed into indices, setting the Japanese case to 1.00.

In the Chinese case 81 subjects were enrolled to the global study. Here we observed 4.55 and 0.77 for nominal and PPP-adjusted site-related cost efficiencies, respectively, and the speed of enrollment was 4.30. These results indicated that China retained a strong potential to contribute to global studies in terms of speed and site-related cost even in a new therapeutic area of drug development with challenges in preparing and implementing studies. However, the PPP-adjusted site-related cost efficiency suggested that the current Chinese sites' cost efficiency was sustained by virtue of low price levels compared to other regions and countries.

As per other countries, the Singaporean sites (n=20 for subject enrollment) showed well balanced performance with regard to nominal and PPP-adjusted site-related cost efficiencies and speed of enrollment (2.70, 2.00 and 1.59, respectively), implying that Singapore was another excellent contributor to global studies. Taiwan's nominal and PPP-adjusted site-related cost efficiencies and speed of enrollment indices were 1.68, 0.76 and 0.48, respectively. We do not have clear rationale for the low level of speed of enrollment, but anticipating that these performance indicators could be influenced with conditional factors such as nomination of clinical investigators and selection of sites due to relatively smaller number of subject (n = 9).

Among Asian countries the Chinese and Singaporean sites demonstrated excellent nominal site-related cost efficiency and speed of enrollment profiles. Furthermore, Asian average site-related cost efficiency and speed of enrollment were greater than North American and European average, which strongly suggested further contribution of Asian regions as a driver of global studies for new drugs and the potential for running competitive Asian-wide drug development programs. From the series of comparison we concluded that Japanese sites were not as efficient on execution and site-related cost as Asian sites. This supported our initial hypothesis that Japan was facing challenges and needed to improve its capabilities from both speed and cost aspects.

Chinese and Singaporean sites showed higher performance in speed and site-related cost compared to any other regions. The high enrolment efficiency in China could be due to a centralization of clinical research and development functions to a few medical institutions. Furthermore, the two studies of analyzed required a high level of specialization within the relevant therapeutic area, which might further facilitate a concentration to specific study sites. This explanation also fit to the observed lower PPP-adjusted site-related cost efficiency. Hypothesizing that a high level of specialization is required, there would be an associated increase in the need for medical tasks and expenses. In Singapore, institutional development of clinical research has prospered under the government's initiative for the last few years. This national approach generates a strong infrastructure for clinical studies, for instance, cross-border invitation of clinical researchers and key investigators, intensive investment in information technology systems and, subsequently, enhanced on-line networking of medical institutions. Although we need further investigation in order to fully understand the observed differences, there are clearly better practices in the Asian region that could be used for the improvement of Japanese study sites' competitiveness.

Around year 2000 Japanese study sites had obtained the following reputation: clinical study cost in Japan was by far more expensive than in other countries; Japanese standard was still not fully aligned with ICH-GCP; Japanese clinical studies often required a longer period of time to completion. However, in our analysis these high performing Japanese study sites exhibited almost competitive performance to sites in other Asian countries and in the rest of the world. This result strongly endorses the importance of the uptake and diffusion of domestic best practices in parallel with benchmarking approaches to other countries. Indeed, it was recently communicated that the quality issues of clinical studies and floundering speed of enrollment were being resolved while the high cost structure still remained as an issue (*4*). The result of our comparative analysis supports these statements and was in accordance with reported improvement in speed of enrollment over global studies.

Comparison of the PPP-adjusted site-related cost efficiency provided a different perspective on the study cost management. The PPP-adjusted cost efficiency of the Japanese sites was comparable to the Asian, North American and other regions' study sites, taking differences in the price level of each country into account. This observation also revealed a potential risk for future clinical studies. An increase in a price level in China may lead significant increase in level of site-related cost in a longer term. When looking at Japan it is clear that the price level keeps impacting site-related study costs despite internal efforts for improvement. A nation-wide, systemic approach to reduce structural costs, for instance, compensating sunk cost for investment, subsidies, would be required to restore Japan's competitive position in the Asian region and globally.

From the sponsor company's perspective the quality of Asian sites including Chinese sites' performance was comparable to North American and European sites. However, there are still quality-related issues especially in some Asian countries that remain as a concern.

For instance, there are still local practices that differ from international practices and there are still barriers to overcome for example in China. Several precedent observations (*6*) including what Liang Kong highlighted (*7*) also have suggested the following quality-related issues in Chinese clinical trials: 1) the overall clinical

study levels lag behind the requirements of ICH-GCP, 2) compared to developed countries GCP history in China is quite short and there are few people with GCP knowledge and experience, 3) the regulatory approval process is lengthy and the local language and hardware can present challenges for multi-national companies, and 4) sponsors conducting studies in China must be prepared to devote substantial resources to understanding the nuances of the distinct system in which they are operating. Therefore, quality aspects of Asian sites should be considered in detail when plans are made to a clinical study in these countries. We may also need to explore ways of evaluating quality-adjusted study productivity.

In this report the site-related study cost was investigated using several performance indicators. This cost item constituted 21.2% of the total external study cost in the Japanese study as described above. On the other hand, approximately over half of the total study cost was spent for monitoring tasks, which was a much larger portion than in the global study. This can be explained by the fact that monitoring work in Japan was fully outsourced to a Contract Research Organization (CRO). If the monitoring activities in both of the clinical studies had been fully outsourced to CROs we could have discussed difference in cost and price of monitoring outsourcing between Japan and other countries. The difference in project team structure made it difficult to compare the monitoring cost across regions. However, in general, there is an issue with high costs for monitoring activities in Japan. This concern has also been raised by Japanese pharmaceutical industry and by the government.

To address this issue a questionnaire survey-based research was conducted in 2006 in order to investigate current condition of Japanese study sites (*8*). The survey unraveled following findings: 1) there were not enough number of Clinical Research Coordinators (CRCs), research nurses or medical doctors who were educated and experienced well about clinical studies and GCP, 2) Japanese investigators were often too busy to supervise clinical study activities, 3) motivation of Japanese investigators was relatively low due to lack of incentives and mind-set on punctuality for company-sponsored clinical studies, and 4) study application formats differed amongst sites. Another observation, a questionnaire-based surveillance over 24 clinical research associates (CRAs) of a Japanese subsidiary of a foreign affiliated pharmaceutical company, pointed out pursuit of excessive goal of company-sponsored clinical studies in Japan (*4*). This was potentially due to a requirement of the Japanese GCP guideline and a strict attitude of Japanese regulatory authority. Therefore, it seems that pharmaceutical companies are forced to support and motivate investigators and clinical research coordinators in Japan which may require considerable incremental labor cost. This point needs to be clarified in further cross-regional research on the dynamics of study sites, investigators, CRCs and CRAs.

In conclusion, we obtained the following findings throughout this comparative case example by analyzing enrollment and site-related cost efficiencies following a proposed productivity framework. Asian sites, particularly the Chinese and Singaporean sites, were shown to be achieving much higher efficiency in both speed and site-related cost than other regions. A comparison of PPP-adjusted site-related cost efficiency provided a different interpretation projecting a significant reduction in site-related cost efficiency when price in these Asian countries may increase. Finally, Japanese study sites should consider adoption of internal and other countries' best practices to be competitive going forward. These initiatives may require a concerted action between investigators, medical societies, regulators, and pharmaceutical industry organizations. Although quality aspects remain to be investigated further, we believe that this approach should be effective to accurately forecast effectiveness of execution and cost across regions and countries.

Acknowledgements

Cost data of the referred two clinical studies was very kindly provided by Novo Nordisk A/S and Novo Nordisk Pharma Limited. We also thank Dr. Per Falk of Novo Nordisk Pharma Limited, Dr. Sakuo Hoshi of the University of Tokyo Hospital and Dr. Tomohiro Anzai of Fast Track Initiative, Inc. for critical reading of manuscript.

References

1. Takeuchi M. The issues on research and development strategies of new drugs. J Health Care and Society 2005;15:17-23.
2. Uden S. Drug development in Asia - An industry perspective -, Simultaneous, worldwide development strategies - Implementation of global clinical studies and introduction of new sciences and technologies edited by Masahiro Takeuchi & Stephan W. Lagakos. 257-265 Digital Press (2003).
3. Urushidani A. Recommendation for appropriate clinical study cost in Japan. The Pharmaceuticals Monthly (Gekkan Yakuji) 2005;47:2239-2250.
4. Umehara S, Iwasaki M. Consideration for the current status of the clinical studies in Japan-The proposals of the more sufficient monitoring from the sponsor. Journal of Clinical Therapeutics & Medicines 2006;22:795-803.
5. Group 2 Task Force 5 Clinical Evaluation Panel Drug Evaluation Committee Japanese Pharmaceutical Manufacturers Association, Recent Clinical Study Environment in Asian countries, Center for Pharmaceutical Publication, 2005.
6. Tassignon JP. The globalization of clinical studies, Applied Clinical Studies, Jan, 2006.
7. Kong L. Challenges clinical studies in China. DIA TODAY 2007;7:18-20.
8. Results and raw data available at www.jmacct.med.or.jp/topics/topic_group.html

Lack of polymorphisms in the coding region of the highly conserved gene encoding transcription elongation factor S-II (*TCEA1*)

Takahiro Ito[1], Kent Doi[2, 3], Naoko Matsumoto[4], Fumiko Kakihara[4], Eisei Noiri[2], Setsuo Hasegawa[4], Katsushi Tokunaga[3], Kazuhisa Sekimizu[1, *]

[1] *Division of Developmental Biochemistry, Graduate School of Pharmaceutical Sciences, University of Tokyo, Tokyo, Japan;*
[2] *Department of Nephrology and Endocrinology, Graduate School of Medicine, University of Tokyo, Tokyo, Japan;*
[3] *Department of Human Genetics, Graduate School of Medicine, University of Tokyo, Tokyo, Japan;*
[4] *Sekino Clinical Pharmacology Clinic, Tokyo, Japan.*

ABSTRACT: Transcription elongation factor S-II stimulates mRNA chain elongation catalyzed by RNA polymerase II. S-II is highly conserved among eukaryotes and is essential for definitive hematopoiesis in mice. In the present study, we report the identification of five novel nucleotide variations in the human S-II gene in the Japanese population. All five variations were located in introns, and no polymorphisms were found in the protein-coding region, suggesting strong negative selection during gene evolution. Together with the SNPs (single nucleotide polymorphisms) reported in the National Center for Biotechnology Information SNP database, our results provide tools for evaluating the role of S-II in complex genetic diseases, such as congenital hematopoietic disorders.

Key Words: Transcription elongation factor, S-II, Japanese population, nucleotide variation

Introduction

Transcription factor S-II, also known as TFIIS, was originally identified as a specific stimulatory protein of RNA polymerase II *in vitro* (*1*). Further biochemical, structural, and genetic studies demonstrated that S-II stimulates transcript elongation by promoting the read-through of transcription arrest sites by RNA polymerase II (*2-5*). The genes encoding S-II have been identified in many eukaryotes including budding yeast, fruit fly, mouse, and human (*6-9*). The human S-II gene, designated *TCEA1*, was initially reported to be a 2.5-kb intronless gene mapped on 3p22- > p21.3 (*10*). We previously reported that the murine S-II gene consists of 10 exons and maps on the proximal region of mouse chromosome 1, which is syntenic to human chromosome 8q (*11*). Consistent with the synteny between the mouse and human chromosomes, recent progress in the human genome project identified another gene composed of 10 exons on 8q11 (UCSC Genome Browser, http://genome.ucsc.edu/). These results suggest that the S-II gene on 8q encodes a functional S-II protein, whereas the other gene on 3q is a pseudogene as proposed by HGNC (HUGO Gene Nomenclature Committee, http://www.gene.ucl.ac.uk/nomenclature/). In the present study, we screened 125 Japanese volunteers for single nucleotide polymorphisms in *TCEA1*, and found 5 nucleotide variations that were not previously reported in the NCBI (National Center for Biotechnology Information) SNP database.

Materials and Methods

Study subjects

Blood samples were collected after obtaining written informed consent from 125 Japanese adult volunteers for this study, which was approved by the ethics committees of the Graduate School of Pharmaceutical Sciences, University of Tokyo, and Sekino Clinical Pharmacology Clinic. Genomic DNAs were purified from whole blood samples using MagExtractor-genome (TOYOBO, Shiga, Japan) and an automated system (SX-6G; Precision System Science, Chiba, Japan).

Amplification of human S-II genomic DNA fragments

**Correspondence to:* Graduate School of Pharmaceutical Sciences, University of Tokyo, Hongo 7-3-1, Bunkyo-ku, Tokyo 113-0033, Japan;
e-mail: sekimizu@mol.f.u-tokyo.ac.jp

Received May 1, 2007
Accepted May 15, 2007

Table 1. Primer sequences for amplification and sequencing used in this study

Amplicon ID	Feature	PCR Primer sequence (5' to 3')	Amplified Region[1]	Sequencing Primer Sequence (5' to 3')	Sequenced region[1]
E1	Covers exon 1	FW - AGCGATCTGCAGTCAGTTGGTAGC RV - CAGGGACTGGAAATACAAGAGCGA	-256 - 284	FW - TTCGTAAGGAAGGGGGCCTA RV - same as PCR	-143 - 284
E2	Covers exon 2	FW - AGGTGGTGCTGTTGCTCCTTATC RV - GAGATTTCACTGCTACTGCCAAC	11500 - 11940	FW, RV - same as PCR	11500 - 11940
E3	Covers exon 3	FW - GCAGCTGGTGCTCTATGAAGTAATCCATG RV - TCGCCTTTATTACGAGGCACTGCTTTCAG	21663 - 22326	FW, RV - same as PCR	21663 - 22326
E4	Covers exon 4	FW - GGGAGTGTTGACTGAACTTGCATTG RV - AGACAGGGGAATTGATGCAGGAAGT	28189 - 28529	FW, RV - same as PCR	28189 - 28529
E56	Covers exons 5& 6	FW - AGCTGTCATTCTCTGGTCCCATC RV - ACCGTGCCTGGCATTTGCATATG	33501 - 35236	FW - same as PCR RV - CCCGTATCAGCAACAACTTC	33501 - 34162 and
				FW - GCAGTGAAGTGATCAGATTC RV - same as PCR	34944 - 35236
E7	Covers exon 7	FW - GGTGACAGAGTGAGACTCCTTCTACCCA RV - CCTAATCAGTCAGCAGCCGTCAACATCC	37057 - 39065	FW - CCAGGTCAAGTGGTTGTCCTGCCT RV - AGATCGTGCCATTGCACTCCAGCCT	37318 - 38076
E8	Covers exon 8	FW - GACAGCCAGCCTGTGACACTAGAAG RV - TCCGTGGTTTCAGGCATCCACTCAG	42629 - 43256	FW, RV - same as PCR	42629 - 43256
E9	Covers exon 9	FW - GGAAGTGCGTGCTCTGTTGACAT RV - GTCAGGGAGTACAAGAGTACTGT	51489 - 51870	FW, RV - same as PCR	51489 - 51870
E10	Covers exon 10	FW - GGAAAGTCAGGCACTTAAGATAGG RV - GGAAAACTAGTTGCTTGGCCTAGTT	53847 - 54107	FW, RV - same as PCR	53847 - 54107

[1] Nucleotide numbering is according to the mutation nomenclature *(den Dunnen and Antonarakis 2000).*

for sequencing

To amplify the coding regions and exon-intron boundaries from genomic DNA, we developed primer sets using the human chromosome 8 sequence assembled by the International Human Genome Sequencing Consortium (Nucleotide number 55041469-55097366, May 2004 freeze, hg17, http://genome.ucsc.edu/). Using the primers listed in Table I, we amplified nine genomic DNA fragments covering all the coding exons of human S-II by polymerase chain reactions (PCR) using individual genomic DNAs extracted from blood samples as templates. The reactions were performed with LA Taq DNA polymerase and its reaction buffer (Takara Bio Inc. Shiga, Japan) supplemented with 2.5 mM magnesium chloride. Primer concentrations in the reaction were 0.4 μM each, except for the E56 and E8 amplicons in which 0.2 μM was used. For E1 amplification, we added dimethyl sulfoxide at a final concentration of 4% to the reaction. Amplification conditions were as follows; for the E1 amplification, 2 min at 94°C followed by 35 cycles of 30 sec at 94°C, 30 sec at 54°C, 1 min at 72°C, followed by a final extension of 1 min at 72°C; E2 amplification, 2 min at 94°C followed by 35 cycles of 30 sec at 94°C, 30 sec at 54°C, 30 sec at 72°C, followed by a final extension of 1 min at 72°C; E3, E4, E7, E9, and E10 amplifications, 2 min at 94°C followed by 35 cycles of 30 sec at 94°C, 30 sec at 56°C, 1 min at 72°C, followed by a final extension of 1 min at 72°C; E56 and E8 amplifications, 2 min at 94°C followed by 35 cycles of 30 sec at 94°C, 30 sec at 58°C, 30 sec at 72°C, followed by a final extension of 1 min at 72°C. Specific amplifications of the PCR products were evaluated by agarose gel electrophoresis before performing the sequencing reactions.

Nucleotide sequence determination and screening for polymorphisms

Nucleotide sequences of the PCR products were determined using BigDye terminator cycle sequence reaction mix Ver 3.1 (Applied Biosystems) and the sequencing primers listed on Table 1. Sequencing reactions with E1 and E7 amplicons contained dimethyl sulfoxide at final concentrations of 10% and 5%, respectively. After purification, the samples were sequenced on an ABI PRISM 3100 Genetic Analyzer (Applied Biosystems). Nucleotide variations were first identified by SeqScape software (Applied Biosystems), and verified visually. We used the human chromosome 8 genomic sequence from the International Human Genome Sequencing Consortium (Nucleotide number 55041469-55097366, May 2004 freeze, hg17) as a reference sequence.

Results and Discussion

By designing sets of PCR primers within the introns (Table 1), we could specifically amplify genomic DNA fragments encoding human S-II gene located on 8q11. Sequencing of these PCR products and comparison of these sequences with a reference sequence revealed a total of five single nucleotide variations in introns 2, 4, and 7 (Table 2; nucleotides are numbered according to the mutation nomenclature (*12*)). Comparison of our data with the SNPs deposited in the NCBI SNP database (dbSNP build 127) indicated that these five nucleotide variations were novel. Chi-square analysis revealed that the observed frequencies of the genotypes did not

Table 2. Nucleotide variations from *TCEA1* locus

ID[1]	Position[1]	Genotype	Number of genotype	Allele frequencies of		*P* value for Hardy-Weinberg equilibrium test
				Major allele	Minor allele	
		TT	101	T	C	
IVS2 (-274) T > C	21802	TC	23	0.9	0.1	0.80
		CC	1			
		AA	124	A	T	
IVS4 (-220) A > T	33647	AT	1	0.996	0.004	0.96
		TT	0			
		CC	124	C	T	
IVS4 (-169) C > T	33698	CT	1	0.996	0.004	0.96
		TT	0			
		GG	120	G	A	
IVS7 + 46 G > A	37809	GA	5	0.98	0.02	0.82
		AA	0			
		TT	124	T	C	
IVS7 (-155) T > C	42800	TC	1	0.996	0.004	0.96
		CC	0			

[1] Nucleotide numbering is according to the mutation nomenclature *(den Dunnen and Antonarakis 2000).*

deviate from the expectations according to the Hardy-Weinberg equilibrium (Table 2). No variations were detected in the protein-coding regions, suggesting the operation of negative selection due to a strong functional constraint of the transcription elongation factor S-II protein. Consistent with this notion, the genes encoding S-II are highly conserved among eukaryotes (*2*), and gene disruption in mice leads to embryonic lethality due to defects in definitive hematopoiesis (*13*). It remains to be determined whether nucleotide polymorphisms in the S-II gene are associated with congenital disorders of hematopoiesis.

Acknowledgements

This work was supported by grants from the Japan Society for the Promotion of Science, and the Ministry of Education, Science, Sports and Culture. We thank Taku Fujinawa for his excellent technical assistance.

References

1. Sekimizu K, Nakanishi Y, Mizuno D, Natori S. Purification and preparation of antibody to RNA polymerase II stimulatory factors from Ehrlich ascites tumor cells. Biochemistry 1979;18:1582-1588.
2. Wind M, Reines D. Transcription elongation factor SII. Bioessays 2000;22:327-336.
3. SivaRaman L, Reines D, Kane CM. Purified elongation factor SII is sufficient to promote read-through by purified RNA polymerase II at specific termination sites in the human histone H3.3 gene. J Biol Chem 1990;265:14554-14560.
4. Kettenberger H, Armache KJ, Cramer P. Architecture of the RNA polymerase II-TFIIS complex and implications for mRNA cleavage. Cell 2003;114:347-357.
5. Shimoaraiso M, Nakanishi T, Kubo T, Natori S. Transcription elongation factor S-II confers yeast resistance to 6-azauracil by enhancing expression of the SSM1 gene. J Biol Chem 2000;275:29623-29627.
6. Chen HC, England L, Kane CM. Characterization of a HeLa cDNA clone encoding the human SII protein, an elongation factor for RNA polymerase II. Gene 1992;116:253-258.
7. Hirashima S, Hirai H, Nakanishi Y, Natori S. Molecular cloning and characterization of cDNA for eukaryotic transcription factor S-II. J Biol Chem 1988;263:3858-3863.
8. Nakanishi T, Nakano A, Nomura K, Sekimizu K, Natori S. Purification, gene cloning, and gene disruption of the transcription elongation factor S-II in Saccharomyces cerevisiae. J Biol Chem 1992;267:13200-13204.
9. Marshall TK, Guo H, Price DH. Drosophila RNA polymerase II elongation factor DmS-II has homology to mouse S-II and sequence similarity to yeast PPR2. Nucleic Acids Res 1990;18:6293-6298.
10. DiMarco SP, Glover TW, Miller DE, Reines D, Warren ST. Transcription elongation factor SII (TCEA) maps to human chromosome 3p22 - > p21.3. Genomics 1996;36:185-188.
11. Ito T, Seldin MF, Taketo MM, Kubo T, Natori S. Gene structure and chromosome mapping of mouse transcription elongation factor S-II (Tcea1). Gene 2000;244:55-63.
12. den Dunnen JT, Antonarakis SE. Mutation nomenclature extensions and suggestions to describe complex mutations: a discussion. Hum mutat 2000;15:7-12.
13. Ito T, Arimitsu N, Takeuchi M, Kawamura N, Nagata M, Saso K, Akimitsu N, Hamamoto H, Natori S, Miyajima A, Sekimizu K. Transcription elongation factor S-II is required for definitive hematopoiesis. Mol Cell Biol 2006;26:3194-3203.

GMP implementation in China: A double-edged sword for the pharmaceutical industry

Ruoyan Gai[1, 2], Xian-Jun Qu[2], Hong-Xiang Lou[2], Jin-Xiang Han[3], Shu-Xiang Cui[3], Munehiro Nakata[2, 4], Norihiro Kokudo[5], Yasuhiko Sugawara[3, 5], Chushi Kuroiwa[1, 2], Wei Tang[2, 3, 5, *]

The "Japan-China Joint Team for Medical Research and Cooperation":
[1] *Department of Health Policy and Planning, the University of Tokyo, Tokyo, Japan;*
[2] *China-Japan Cooperation Center for Drug Discovery & Screen, Shandong University, Jinan, China;*
[3] *Shandong Academy of Medical Sciences, Jinan, China;*
[4] *Department of Applied Biochemistry, Tokai University, Kanagawa, Japan;*
[5] *Hepato-Biliary-Pancreatic Surgery Division, Department of Surgery, Graduate School of Medicine, the University of Tokyo, Tokyo, Japan.*

ABSTRACT: China's Good Manufacturing Practice (GMP) standards that mainly parallel WHO standards were made compulsory in 2004. However, GMP implementation had both positive as well as negative impacts on the pharmaceutical industry, with negatives including pharmaceutical companies suffering economic hardships, poor execution of GMP standards, and sequent health scares. This report briefly describes the problems with GMP implementation in China.

Key Words: GMP, pharmaceutical sector reform, policymaking, China

Zheng Xiaoyu, the former director of China's State Food and Drug Administration (SFDA), had promoted Good Manufacturing Practice (GMP) certification in China but was convicted of taking bribes and dereliction of duty and sentenced to death this year (2007). Many high-ranking officials were involved in the scandal. Problems with many aspects of GMP implementation were one of the key points in the accusations against Zheng. The scandal, together with many recent health scares, spotlights the paradoxical nature of GMP implementation and serious flaws with drug administration in China.

As directed by the World Health Organization (WHO), GMP is a system to ensure that products are consistently produced and controlled according to quality standards (*1*). Starting in the 1960s, GMP standards were established and revised in most developed countries. Today, GMP are internationally recognized as an effective system for safety and quality assurance. China's GMP standards, basically paralleling WHO standards in developing countries, were introduced in the early 1980s and established in the form of present legislative and compulsory standards in 2004 (*2*). However, GMP implementation has created a great deal of confusion and problems for China's pharmaceutical industry.

The background of GMP implementation involves reforms in drug legislation and regulation as well as reforms in administrative systems for drug administration as accompany economic restructuring. With its opening up to the outside world, China has, as a global strategy for its domestic pharmaceutical industry, inaugurated many reforms paralleling international practices in an attempt to devise drug regulation and administration suited to a market economy. Stimulated by high profits and government deregulation, the number of pharmaceutical companies increased substantially to approximately 6,000 before GMP implementation (*3*). However, most were small-scale companies with minimal efficiency and outdated manufacturing technology that competed viciously in the market. Amidst this chaos, the pharmaceutical market suffers from inadequate drug safety and quality and is even plagued by fake drugs. Thus, the SFDA's original intent was to improve the safety and quality of drugs, to upgrade drug manufacturing, and to optimize the composition of the pharmaceutical industry by eliminating a number of small and medium companies in poor condition.

GMP implementation was expected to strengthen

**Correspondence to:* Hepato-Biliary-Pancreatic Surgery Division, Department of Surgery, Graduate School of Medicine, the University of Tokyo, 7-3-1 Hongo, Bunkyo-ku, Tokyo 113-8655, Japan;
e-mail: TANG-SUR@h.u-tokyo.ac.jp

Received June 22, 2007
Accepted July 10, 2007

China's pharmaceutical industry. However, results have differed from what the SFDA intended. Obvious problems for which SFDA has been criticized were that more than 3,700 small and medium companies still account for the majority of firms in China's pharmaceutical industry and that many face economic hardships with a heavy debt burden and an even more severe lack of funds. The huge cost of GMP implementation has led to a worsening of their financial situation. Meanwhile, poorly planned projects to adapt the GMP guidelines led to unnecessarily excessive production capacity. A number of qualified plants with expensive GMP product lines lay idle and do little to recoup the funds invested in GMP implementation (*4*).

In addition, there were differences between GMP standards and what was actually implemented and certified at several pharmaceutical companies. One factor causing this poor state of GMP implementation is believed to be a lack of transparency in the drug administration system that has allowed financial relationships between local governments and pharmaceutical companies and regional protectionism by these forces (*5*). A typical case was the bribery scandal mentioned at the beginning. Thus, many health scares have arisen from shoddy products manufactured by companies with perfunctory GMP certification (*6*), severely hurting the credibility of GMP.

Given the issues discussed above, GMP implementation has been a double-edged sword wielded by governments supervising drug administration. All of the processes involved should serve as a good lesson for other developing countries promoting pharmaceutical sector reform. As a part of China's global strategy for its domestic pharmaceutical industry, its endeavors to enhance these regulatory and legislative standards put drug regulation on the right path early on. In this regard, the SFDA took the right tack. However, the issue of rationalization of the government structure of drug administration should be resolved incrementally in the near future; this resolution may be facilitated by interdisciplinary studies incorporating diverse views from policymakers, corporate executives, and researchers.

Acknowledgements

This study was supported by Grants-in-Aid from the Ministry of Education, Science, Sports and Culture of Japan, Yuasa International Education and Academic Exchange Fund, and Japan-China Medicine Association.

References

1. WHO. "GMP questions and answers", Available at: http://www.who.int/medicines/areas/quality_safety/quality_assurance/gmp/en/.
2. China to close medicine companies failing to pass GMP. People's Daily online. May 7, 2004. Available at: http://english.people.com.cn/200405/07/eng20040507_142573.html
3. Executive summary of "Chinese Pharmaceutical Industry" (report from Bioportfolio). This document is available at: http://www.bioportfolio.com/cgi-bin/acatalog/Chinese_Pharmaceutical_Industry.html#a369.
4. Xu FX. The Existing Problems in GMP Certified Enterprises and the Consideration of Administration. Chinese Pharmaceutical Affairs [zhong guo yao shi] 2005;8:472-473.
5. http://article.chinalawinfo.com/article/user/article_display.asp?ArticleID=34760
6. Cyranoski D. China's deadly drug problem. Nature 2007;446:598-599.

Viral infectious disease and natural products with antiviral activity

Kaio Kitazato[1], Yifei Wang[2], Nobuyuki Kobayashi[1, 3, *]

[1] *Division of Molecular Pharmacology of Infectious Agents, Department of Molecular Microbiology and Immunology, Graduate School of Biomedical Sciences, Nagasaki University, Nagasaki, Japan;*
[2] *Guangzhoujinan Biomedicine Research & Development Center, Jinan University, Guangzhou, China;*
[3] *Central Research Center, AVSS. Co., 1-22 Wakaba-machi, Nagasaki, Japan.*

ABSTRACT: Viral diseases, such as acquired immunodeficiency syndrome (AIDS), respiratory diseases, and hepatitis, are the leading causes of death in humans worldwide, despite the tremendous progress in human medicine. The lack of effective therapies and/or vaccines for several viral infections, and the rapid emergence of new drug-resistant viruses have urged a growing need for developing new and effective chemotherapeutic agents to treat viral diseases. Recent advances in the understanding of both the cellular and molecular mechanisms of virus replication have provided the basis for novel therapeutic strategies. Several hundred natural products have been isolated for screening and identifying antiviral activity, and some have been shown to have great medicinal value in preventing and/or ameliorating viral diseases in preclinical and clinical trials. There are innumerable potentially useful medicinal plants and herbs waiting to be evaluated and exploited for therapeutic applications against genetically and functionally diverse virus families. This review focuses on several selected pathogenic viruses, including the human immunodeficiency virus (HIV), influenza virus, hepatitis B and C viruses and herpes viruses, and antiviral natural compounds from medicinal plants (herbs), while paying particular attention to promising compounds in preclinical and clinical trials. We also focused our attention on the need to develop effective screening systems for antiviral activity.

Key Words: HIV-1, influenza virus, HBV/HCV, HSV-1, HSV-2, antiviral, natural product, herbs, medicinal plant

**Correspondence to:* Division of Molecular Pharmacology of Infectious Agents, Department of Molecular Microbiology and Immunology, Graduate School of Biomedical Sciences, Nagasaki University, 1-14, Bunkyo-machi, Nagasaki 852-8521, Japan;
e-mail: nobnob@net.nagasaki-u.ac.jp

Received June 25, 2007
Accepted July 1, 2007

Introduction

Viral diseases, caused by pathogenic virus infections which have high morbidity and mortality rates, are still the leading cause of death in humans worldwide. Although effective vaccines have led or might lead to the eradication of important viral pathogens, such as smallpox, polio, and mumps, other viral diseases, such as human immunodeficiency virus (HIV) and hepatitis C virus (HCV), have proven difficult to combat using the conventional vaccine approach. Moreover, the emergence of viral resistance to drugs, as well as the serious adverse effects induced by antiviral drugs, has caused serious medical problems, particularly when administered in combination over prolonged treatment periods. Although many new antiviral drugs have been approved in recent years, most of them are used for the treatment of HIV, and these drugs are quite costly, thus limiting their use in developing countries, where infection is most prevalent.

A virus is a unique pathogen which is incapable of replicating without a host cell. It utilizes the host cell environment and cellular factors for its propagation. This unique feature of viruses makes it difficult to design a treatment to attack the virus or its replication directly without any adverse effects on the infected cells. However, viruses share a common stage in their replication cycle, which includes attachment and entry to the host cell, transcription of viral mRNA, replication of viral genome, assembly and budding as progeny virus particles, regardless of different genetic materials (DNA or RNA), or whether has a different invasion strategy of which enveloped with a lipid-containing membrane (enveloped virus) or not. Whereas, viruses with an RNA genome, such as HIV, HCV, and influenza, are genetically highly variable, due to the fact that viral reverse transcriptase or RNA-dependent RNA polymerase lack a proofreading mechanism. Accumulated mutations in viral RNA genome have been proven to be associated with the emergence of drug-resistant viruses (*1-3*). The emergence of drug-

resistant viruses presents a challenge for the design of new drugs. These problems emphasize the need to develop new antiviral drugs targeting different steps in the viral replication cycle.

An understanding of the molecular mechanisms of viral invasion and replication enables us to design antiviral drugs targeting the different stages of the viral replication cycle. Although in theory, any viral molecule that is essential for viral replication is a potential drug target, most of the clinically useful antiviral drugs are the molecules that can specifically target a single viral enzyme, which is crucial in viral replication (*4*). Targeting virus molecules is likely more specific, and less toxic. However, there is a narrow spectrum of viruses and a higher risk of creating resistant viruses. Whereas drugs which target cellular molecules may possess a broader antiviral activity spectrum and less risk of developing virus resistance, but may be more toxic to the host cell. Ideally, effective therapeutic agents that target multiple stages in the viral replication cycle with combined approaches but with little or no toxicity are desirable.

Traditional medicines, such as Chinese medicine (CM), have long been used as multiple combinations of compounds in the form of processed natural products. Medicinal herbs relieve the symptoms of many different human diseases, including infectious diseases, and have been used for thousands of years. CM is typically orally administered as hot-water extracts, which can be used for the prophylactic and therapeutic treatment of viral infections. A wide variety of natural compounds derived from medicinal plants (herbs) have been extensively studied in terms of their antiviral activity. Several hundred natural active compounds have been identified worldwide (*5-9*). Many of them have complementary and overlapping mechanisms of action, either inhibiting viral replication, or synthesis of the viral genome. These natural active compounds, which contain more characteristics of high chemical diversity and biochemical specificity than standard combinatorial chemistry, offer major opportunities for finding novel lead structures that are active against a wide range of assay targets. In addition, natural products that are biologically active in assays are generally small molecules with drug-like properties. Namely, they are capable of being absorbed and metabolized by the body. Hence, the development costs of producing orally active medicines are likely to be much lower than that of biotechnological products or most compounds produced to date from combinatorial chemistry. Therefore, natural products, including traditional medicinal plants (herbs), offer great promise as potentially effective new antiviral drugs.

Selected viral diseases and antiviral agents

HIV/AIDS and antiviral agents

Human immunodeficiency virus (HIV) is the causative pathogen of acquired immunodeficiency syndrome (AIDS). HIV has cumulatively infected over 60 million individuals and caused the deaths of over 28 million people since it was first recognized in 1981, and is the most destructive epidemic of recent times. This global epidemic remains out of control, and transmission is rapidly spreading worldwide. According to the WHO 2006 global summary of the AIDS epidemic, the number of people living with HIV continues to grow; a total of 39.5 million people were living with HIV, a total of 4.3 million people were newly infected with HIV, and a total of 2.9 million people died due to AIDS in 2006. The majority of people living with HIV are in developing countries, such as sub-Saharan Africa and East and South Asia (*10*). Induction of the highly active antiretroviral therapy (HAART), a combination therapy with reverse transcriptase and protease inhibitors, has significantly improved the clinical outcome of HIV infection and AIDS, greatly reduced morbidity and mortality in HIV-1-infected individuals, and dramatically improved the life expectancy of AIDS patients. However, the treatment cannot eradicate the virus from infected individuals and is quite often limited by the emergence of drug-resistant HIV-1 strains and long-term toxicity. In addition, the high cost of anti-HIV drugs limits the ability of HIV-infected people and AIDS patients in developing countries to access HARRT (*11*). The discovery of low cost, effective medicinal agents is therefore urgently needed.

HIV-1 is unique in terms of its transmission and replication. HIV-1 is transmitted both by sexual contact and heamatogenously through contaminated needles or blood products, so the virus can initiate infection by crossing a mucosal barrier or by direct entry into a T cell or monocyte/macrophage lineage cell in the peripheral blood. HIV-1 can spread after a long latent period of infection. Recent advances in the understanding of the cellular and molecular mechanisms of HIV-1 entry and replication have provided the basis for novel therapeutic strategies to prevent viral penetration of the target cell-membrane and inhibit virus multiplication (Figure 1). HIV-1 entry into host cells represents a complex sequence of events involving several viral and cellular proteins that are potential targets for drug development. Targeting the host cell factors involved in the regulation of HIV-1 replication might be one way to overcome the resistance of HIV-1 to antiviral drugs. Both CXCR4 and CCR5 chemokine receptors are co-receptors for HIV entry to the host cell, and their antagonists are being investigated as HIV entry inhibitors in controlled clinical trials (*12*). The inhibitors will be needed in combination in order to inhibit viral replication, and even in combinations of antiviral drugs that also target other aspects of the HIV replication cycle, such as reverse transcriptase and protease, to obtain optimum therapeutic effects. Currently, the number of anti-

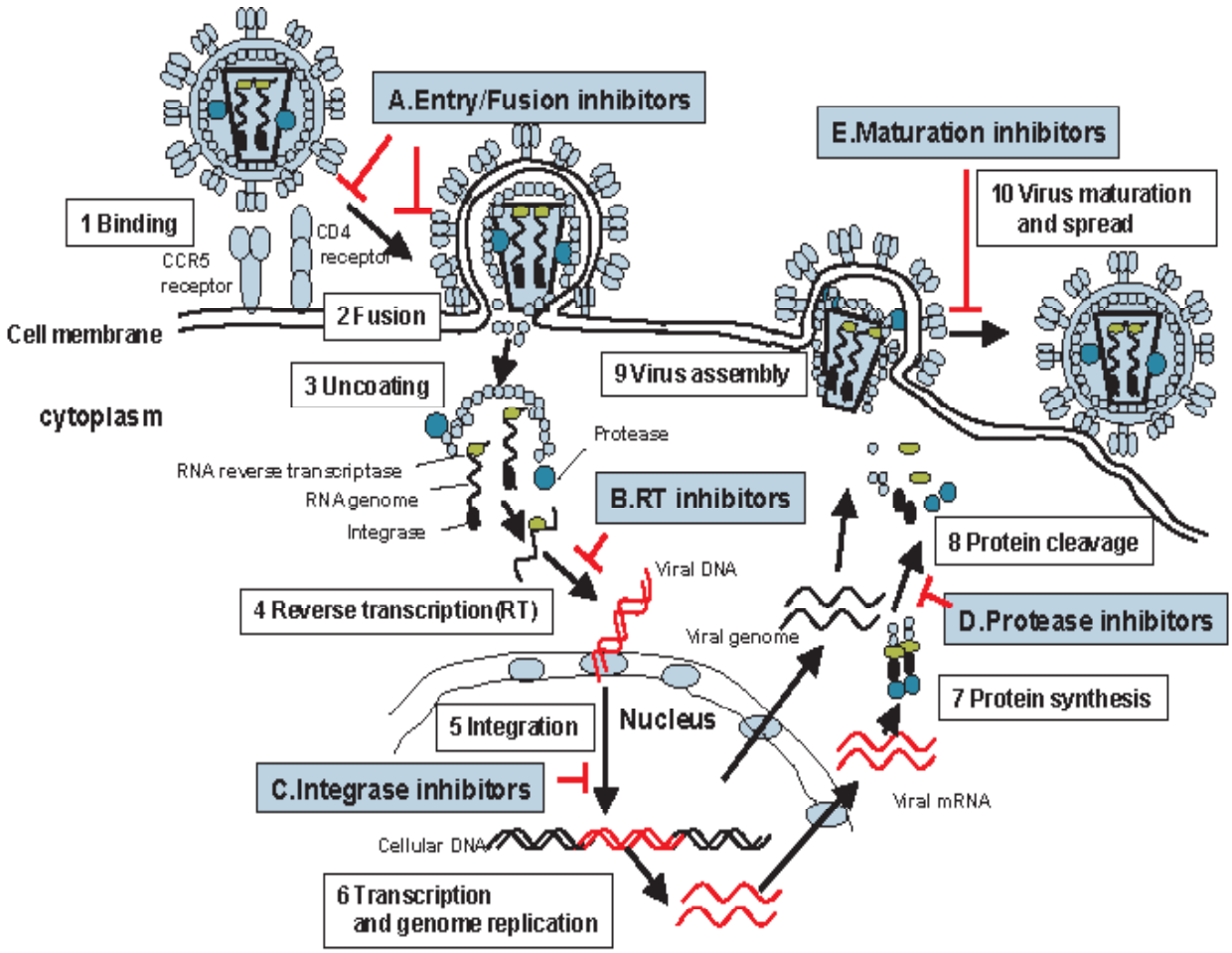

Figure 1. The HIV-1 replication life cycle. The replication life cycle of human immunodeficiency virus (HIV) have several specific steps (1-10), many of which are targets for antiviral drugs (A-E).

HIV/AIDS therapeutic drugs approved by the FDA has increased to 26 drugs from the first approved drug, AZT, in 1987 (*13*). These anti-HIV/AIDS drugs can be categorized into fusion inhibitors (FIs), nucleoside/nucleotide reverse transcriptase inhibitors (NRTIs), nonnucleoside reverse transcriptase inhibitors (NNRTIs), and protease inhibitors (PIs) (*14-17*). However, HIV-1 has developed an extraordinary degree of genetic diversity. To date, a high number of mutations in protease, reverse transcriptase, and gp41 have been associated with reduced susceptibility to the antiretroviral drugs currently available. In addition, new integrase inhibitors and maturation inhibitors that target Gag have shown promising effects in preclinical and clinical trials (*17-20*).

Substantial progress has been made on the use of natural products as anti-HIV agents, and several natural products, mostly of plant origin, have been shown to possess promising activities that could assist in the prevention and/or amelioration of the disease. Table 1 summarizes some major natural compounds with anti-HIV activity derived from plants or herbs (*19-35*). The following natural products from plant origin have been cited as promising anti-HIV agents: Betulinic acid (a pentacyclic triterpene) isolated from the bark of the white birch tree, has been demonstrated to inhibit maturation of the HIV-1 Gag precursor assembled *in vitro* (*23-26*), Chinese herbal medicine, *Scutellaria baicalensis* Georgi and its identified components, Baicalin (a flavonoid), calanolides (coumarins), have been shown to inhibit infectivity and replication of HIV (*17,28-35*). Flavonoids inhibit HIV-1 activation via a novel mechanism, and these agents are potential candidates for therapeutic strategies aimed at maintaining a cellular state of HIV-1 latency. Acute HIV-1 infection has been shown to be suppressed by certain flavonoids *in vitro*, and evidence for inhibition of HIV-1 protease, integrase, and reverse transcriptase by flavonoids also exists (*28-32*). Calanolide A, a coumarins, is a potent non-nucleoside reverse transcriptase inhibitor (NNRTI) of human immunodeficiency virus type 1 (HIV-1) (*33-35*), recently discovered in extracts from the tropical rainforest tree, *Calophyllum lanigerum*. Recent studies have also shown that several polysaccharides are effective inhibitors of HIV replication. Some of the presented compounds demonstrated *in vitro* synergism; thus there is the rationale of their combined use in HIV-infected individuals (*9,26,34*). Although extensive research has been performed to assess both

Table 1. Natural products with anti-HIV activity

Compounds	Origin of plant	Activity/Target	References
Terpenoids			
Agastanol and Agastaquinone	*Agastache rugosa*	Protease	*19*
Uvaol and Ursolic acid	*Crataegus pinnatifida*	Protease	*20*
Garciosaterpene A,C	*Garcinia speciosa*	Reverse transcriptase Inhibition in syncytium	*21*
Vaticinone	*Vatica cinerea*	Inhibited replication	*22*
Betulinic acid	Widely distributed	Inhibited maturation	*23-26*
Glycyrrhizin	*Glycyeehiza spp.*	Inhibited Infectivity, cytopathic activity, replication	*27*
Flavonoids			
Baicalin	*Scutellaria baicalensis*	Reverse transcriptase infection/entry, replication	*28* *29*
Taxifolin (dihydroquercetin)	*Juglans mandshurica*	Inhibited cytopathic activity	*30*
(-)-Epigallocatechin-3-gallate (EGCG)	Green tea	Reverse transcriptase	*31*
Flavonoid glucuronide	*Charysanthemum morifolium*	Integrase	*32*
Coumarins			
Calanolide A	*Calophyllum lanigerum*	Reverse transcriptase	*33-35*

the beneficial effects and the risks of herbal medicines in patients with HIV infection and AIDS, the potential beneficial effects need to be confirmed in large, rigorous trials. There is insufficient evidence to support the use of herbal medicines in HIV-infected individuals and AIDS patients.

Influenza virus and antiviral agents

Influenza A virus is one of the most common infectious pathogens in humans. It is a seasonal, acute, highly transmissible respiratory disease. Influenza in humans is caused by two subtypes of influenza virus A and B. Influenza virus A mutates easily, thereby often causing new antigenic variants of each subtype to emerge. The threat of a human influenza pandemic has greatly increased over the past several years with the emergence and continuing global spread of the highly pathogenic avian influenza viruses, notably H5N1 virus. The current widespread circulation of H5N1 viruses among avian populations in several Asian, African and European countries and the transmission from avian species to humans with a high mortality rate of more than 50%, warn us to prepare for the next pandemic threat.

The control and treatment of influenza depends mainly on chemical and biochemical agents. There are two classes of anti-influenza drugs currently available for influenza therapy, which target either the influenza A M2 ion channel or neuraminidase (NA) (*36*). However, the emergence of resistance to these drugs has been detected, which raises concerns regarding their widespread use (*37*). The viral particles have two surface antigens, haemagglutinin and sialidase (neuraminidase), that decorate the surface of the virus and have been implicated in viral attachment and fusion, and the release of virion progeny, respectively. The receptor for haemagglutinin is the terminal sialic acid residue of the host cell surface sialyloligosaccharides, while sialidase catalyses the hydrolysis of terminal sialic acid residues from sialyloligosaccharides. The enzyme neuraminidase (NA) is an attractive target for antiviral strategy because of its essential role in the pathogenicity of many respiratory viruses. NA removes sialic acid from the surface of infected cells and virus particles, thereby preventing viral self-aggregation and promoting efficient viral spread; NA also plays a role in the initial penetration of the mucosal lining of the respiratory tract. Since the influenza virus genome does not have the processing protease for the viral membrane fusion glycoprotein precursors, entry of this virus into cells is determined primarily by host cellular, trypsin-like proteases that proteolytically activate the fusion glycoprotein precursors of Influenza A virus. The protease determine the infectious organ tropism of Influenza A virus infection as well as the efficiency of viral multiplication in the airway. Administration of protease inhibitors in the early-stage of infection significantly suppresses viral entry and viral multiplication (*38*).

To date, some of the anti-influenza agents that have been isolated from plants include a variety of polyphenols, flavonoids, and alkaloids (*39*), summarized in Table 2. Polyphenol-rich extract from the medicinal plant *Geranium sanguineum* L. has been reported to show a strong anti-influenza virus activity, as well as antioxidant and radical scavenging capacities (*40*). A biflavonoids, ginkgetin isolated from *Ginkgo biloba* L. and *Cephalotaxus harringtonia* K. Koch show a potent inhibitory activity against influenza virus sialidase (*41*,*42*). A combination of NA inhibitors and protease inhibitors could be potentially used as a potent anti-influenza therapy in order to minimize the emergence of drug-resistant mutant viruses. Although most clinical trials have reported some benefits from the use of antiviral herbal medicines, there remains a need for larger, stringently designed, randomized clinical trials to provide conclusive evidence of their efficacy. An indole alkaloid from *Uncaria rhynchophylla* and the pavine alkaloid (-)-thalimonie (Th1) from *Thalictrum*

Table 2. Natural products with anti-influenza activity

Compounds	Origin of plant	Activity/Target	References
Polyphenols			
Polyphenolic complex	*Geranium sanguineum* L.	Influenza virus	*40*
Flavonoids			
biflavonoids (Ginkgetin)	*Ginkgo biloba* L.	influenza virus sialidase	*41*
tetrahydroxyflavone	*Scutellaria baicalensis*	influenza virus sialidase	*42*
Alkaloids			
Thalimonine	*Thalictrum simplex* L.	influenza virus replication	*43*
Indole alkaloid	*Uncaria rhynchophylla*	influenza virus replication	*44*
Lignans			
rhinacanthin E,F	*Rhinacanthus nasutus*	Influenza virus	*45*

simplex also exhibit potent inhibitory effects against influenza A viruses (*43*). Many medicinal plants (herbs) including the *Bergenia ligulata*, *Nerium indicum* and *Holoptelia integrifolia* plants, exhibit considerable antiviral activities against the influenza virus (*44*). Furthermore, two new lignans with activity against the influenza virus from the medicinal plant *Rhinacanthus nasutus* have also been reported (*45*).

Hepatitis B and C viruses and antiviral agents

Hepatitis B virus (HBV) infection is a serious global health problem. According to WHO estimation, of the 2 billion people who have been infected with the hepatitis B virus (HBV), more than 350 million suffer from chronic HBV infection. These chronically infected persons are at a high risk of death from cirrhosis of the liver and liver cancer, diseases that kill about one million persons each year (*46,47*). On the other hand, hepatitis C virus (HCV) is a major cause of acute hepatitis and chronic liver disease, including cirrhosis and liver cancer. Globally, an estimated 170 million persons are chronically infected with HCV and 3 to 4 million persons are newly infected each year. HCV spreads primarily by direct contact with human blood. The major causes of HCV infection worldwide are use of unscreened blood transfusions, and re-use of needles and syringes that have not been adequately sterilized. No vaccine is currently available to prevent hepatitis C (*48,49*). Liver disease due to chronic HBV and HCV infection is becoming a leading cause of death among persons with HIV infection worldwide (*50*).

Currently available Anti-HBV and HCV drugs include interferon, lamivudine and ribavirin. The therapeutic effects of interferon for HBV are around 30%. The effect of interferon for HCV is 20%~30%. A combination therapy of interferon and ribavirin for HCV can increase the therapeutic efficacy up to 50%, but has serious side effects and can be prohibitively expensive for low-income countries with a high prevalence of HCV. Lamivudine inhibits HBV multiplication and significantly decreases the viral load, but can easily induce resistance (*51*). Many patients who use natural products, including those who are not eligible for IFN/ribavirin, cannot afford treatment, or fail to respond to IFN.

Oxymatrine and matrine are the two major alkaloid components found in sophora roots. They are obtained primarily from the above ground portion of *Sophora alopecuroides* L., *Sophora flavescens* and *Sophora subprostrata* (shandougen). An intensive investigation into the pharmacology and clinical applications of these alkaloids has been performed in China during the past decade. The sophora alkaloids appear to inhibit viral replication, reduce destruction of liver cells, inhibit liver fibrosis and promote the flow of bile. Most of the clinical trials have been performed on HBV using oxymatrine extracted from *S. flavescens* and *S. subprostata*. Oxymatrine has been shown to be effective in normalizing ALT levels and clearing the HBV virus. The clinical effectiveness of oxymatrine for patients with hepatitis C has also been reported to show a reduction of viral load and inhibition of liver fibrosis, which appears to be a separate additional function of sophora alkaloids beyond inhibiting viral activity (*52-56*). Matrine was shown to reduce the formation of liver fibrosis that was caused by chemical damage to the liver (*57-58*). However, further research is needed to elucidate the effectiveness of these natural products for the treatment of chronic HCV, including their preparation and standardization.

The HCV genome possesses a unique open reading frame (ORF), encoding for a single long polyprotein that is processed by both host cellular peptidases and virus-encoded proteases (PR). HCV-PR is a primary and rational target in the development of anti-HCV agents. The medicinal herbs *Acacia nilotica, Boswellia carterii, Embelia schimperi, Piper cubeba, Quercus infectoria, Trachyspermum ammi* and *Syzygium aromaticum* extracts were investigated *in vitro* and showed significant inhibitory activity against HCV protease (*59*). In addition, the use of the botanical components glycyrrhizin, catechin, silymarin and phytosterols, and the antioxidants *N*-acetylcysteine were investigated for their efficacy in treating chronic hepatitis and affecting liver damage (*60*).

Herpes viruses and antiviral agents

Herpes viruses are common human pathogenic viruses, which include at least eight unique pathogenic strains, the neurotropic herpes simplex virus 1 (HSV-1) and

herpes simplex virus 2 (HSV-2), varicella zoster virus (VZV) (HSV-3), and lymphotropic human cytomegarovirus (HCMV) (HSV-4), EBV (HSV-5), HHV-6, HHV-7, and HHV-8. HSV-1 usually causes orolabial disease, and HSV-2 is associated more frequently with genital and newborn infections. HSV causes mild and self-limited disease of the mouth and lips or genitals. However, this disease can sometimes be life-threatening. Such is the case with neonatal HSV infection and HSV infections of the central nervous system. Furthermore, in the immunocompromised host, severe infection has been encountered and is a source of morbidity. Both viruses establish latent infections in sensory neurons and recurrent lesions at or near the point of entry into the body. Among HSV-related pathologies, genital herpes is an important sexually transmitted disease (STD) commonly caused by HSV-2. HSV-1 infections are very common and mostly affect adult people (*57*). In addition, HSV-2 infection may be a risk factor for the transmission of HIV (*61-62*).

Effective anti-herpes drugs, such as acyclovir, ganciclovir, valaciclovir, penciclovir, famciclovir, and vidarabine, are available for treatment. Acyclovir is the most commonly used drug for the treatment of HSV infection. However, a serious problem with the use of acyclovir is the emergence of drug resistance in treated patients. Drug-resistant strains of HSV frequently develop following therapeutic treatment. Resistance to acyclovir and related nucleoside analogues can occur following mutation in either HSV thymidine kinase (TK) or DNA polymerase. Virus strains associated with clinical resistance are almost always defective in TK production (*63*). Therefore, new antiviral agents exhibiting different mechanisms of action are urgently needed.

A large number of natural compounds from medicinal plant extracts, such as phenolics, polyphenols, terpenes (*e.g.*, mono-, di-, tri-), flavonoids, sugar-containing compounds, have been found to be promising anti-herpetic agents (*64*). Different kinds of anthraquinones from extracts of *Rheum officinale*, *Aloe barbadensis* (Aloe vera), *Rhamnus frangula, Rhamnus purshianus*, and *Cassia angustifolia* have been found to be quite active against HSV-1. Furthermore, inactivation of HSV-1 and HSV-2 and prevention of cell-to-cell virus spread by *Santolina insularis* essential oil has been found (*65*). Recently, 18 plants with ethnomedical backgrounds from different families were screened for antiviral activity against HSV-1, and three extracts, from *Hypericum mysorense, Hypericum hookerianum* and *Usnea complanta*, exhibited significant anti-HSV-1 activity at concentrations without toxic effects on cells *in vitro* (*66*). Furthermore, the study evaluated extracts of 23 medicinal species widely used in the traditional medicine of Nepal for the treatment of infectious and other diseases on their *in vitro* antiviral activity against influenza virus and herpes simplex-virus (HSV). Two species, *Bergenia ligulata* and *Nerium indicum*, showed the highest anti-influenza activity. *Holoptelia integrifolia* and *Nerium indicum* exhibited considerable antiviral activity against the herpes simplex virus. None of these extracts have shown any cytotoxic effects (*67*).

Development of screening systems for antiviral agents

Although the development of new anti-viral drugs for the treatment of many viral infected diseases is urgent, some viruses are not even established to propagate *in vitro*. The development of an effective screening system is crucial for the discovery of new antiviral drugs. However, safety concerns regarding using dangerous viruses have limited many laboratories to screen the antiviral activity of compounds, despite having the resources of active compounds either chemically synthesized or extracted from natural resources. We herein describe one example of the development of a new screening system for HIV-1 protease inhibitors, which was recently established in our laboratory. This system uses a cell line in which HIV-1 PR is expressed in a chimeric protein with the green fluorescent protein (GFP) by the tet-off system (*68*). This system can measure HIV-1 PR activity as a function of either the fluorescence of GFP or the cytotoxic activity of HIV-1 PR, which suppresses cell attachment when re-plated to a culture dish after the induction of HIV-1 PR expression (Figure 2). The system is virus-free, but the sensitivity is compatible with that of a system which uses a live virus for infection.

Perspective

Based on the specific assay system or screening approach, a large number of structurally unique antiviral compounds from medicinal plants (herbs) have been identified. The advantages of natural compounds are fewer side effects in comparison to orthodox medical drugs, and the production of synergistic effects for a more positive treatment outcome. However, the potential beneficial effects of these natural compounds need to be confirmed in large, rigorous trials. The continued discovery and development of new formulations of herbal medicines, containing a combination of multiple ingredients that synergistically act to potently and selectively inhibit virus replication at different stages and strengthen the impaired immune system, should be a potential therapeutic option in the future.

These natural lead structures can be chemically modified and improved through knowledge of the structure-activity relationship, mechanism of action, drug metabolism, molecular modeling and combinatorial chemistry studies. For the antiviral activity of these compounds, it is important to identify

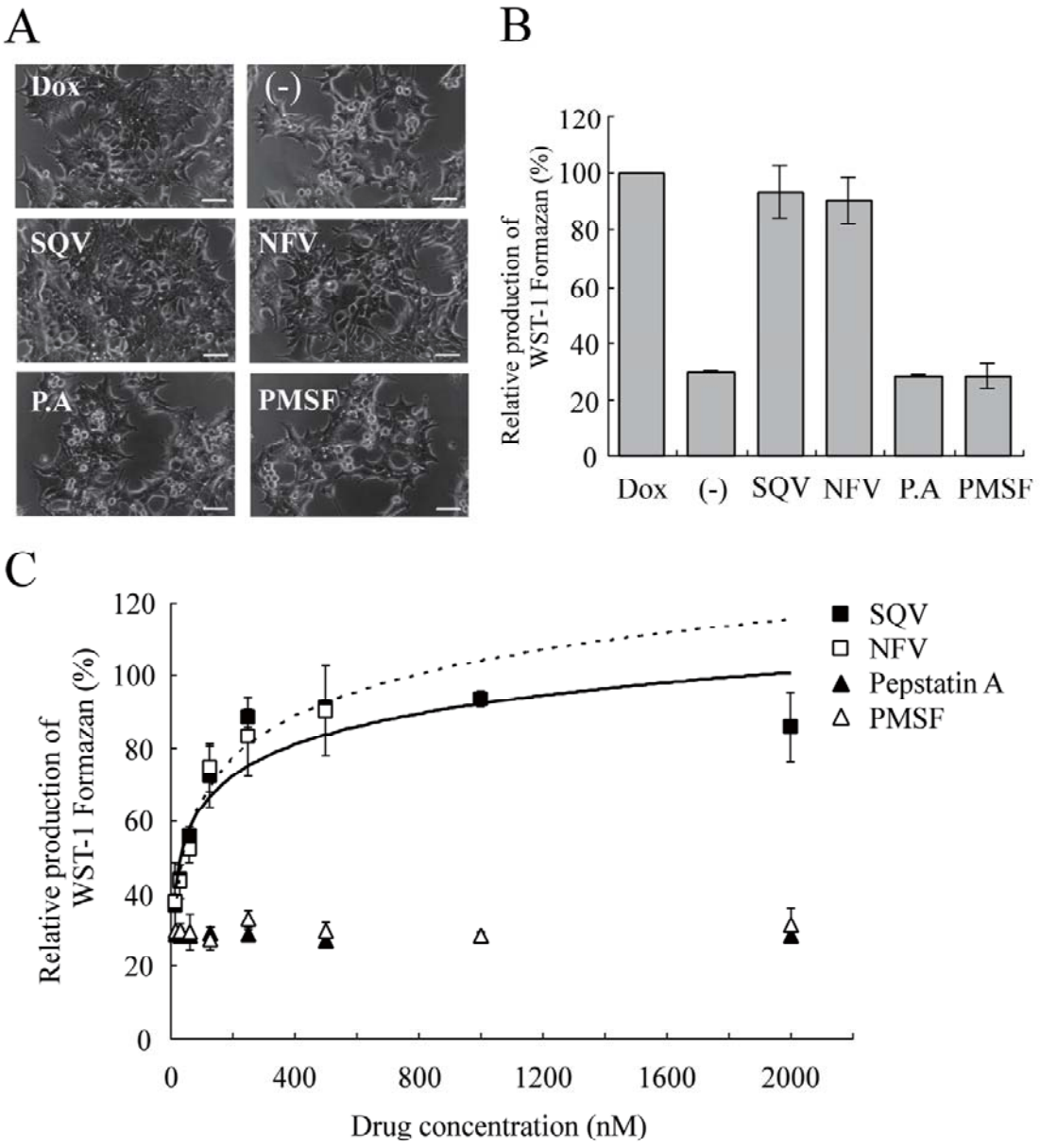

Figure 2. Development of a highly sensitive screening method for HIV-1 PR inhibitors. (A), Morphological change in the E-PR293. The E-PR293 cells were treated with 100 ng/mL of Dox or 1 mM of PR inhibitors, SQV, NFV, pepstain A (P.A) or PMSF. The scale bar indicates 50 mm; (B), The growth Figure 1. The HIV-1 replication life cycle. The replication life cycle of human immunodeficiency virus (HIV) have several specific steps (1-10), many of which are targets for antiviral drugs (A-E). of cells monitored by a WST-1 assay. The relative amount of WST-1 formazan to Dox-treated cells was calculated; (C), The dose-dependent activity of specific HIV-1 PR inhibitors on the cytotoxicty-based system. The cells were re-plated and then treated with SQV (closed square), NFV (opened square), pepstatin A (closed triangle), and PMSF (opened triangle) at various concentrations as indicated in the figure. The data represent the mean ± SD percentage.

virus specific targets and, when possible, to determine if this substance selectively interacts with the target. The assessment of the cytotoxicity of an antiviral compound is clearly an important part of the evaluation of a potential chemotherapeutic agent, since it should show neither acute nor long-term toxicity against the host. Determining the efficacy and toxicity of these agents as well as performing clinical trials together is expected to contribute to the generation of new drugs from such natural products.

Moreover, drug discovery must be improved greatly by new technologies emerging in the post-genomic era. Gene expression profile studies employing microarray technology could help to identify molecular targets of the biological activity of antiviral agents from natural products. On the other hand, the pathways for new drug discovery are broadened by the continuous improvement of technological platforms, including computer-aided drug design, high throughput screening, biochip, transgenic and RNAi technology. The continued investigation of active formulations, bioactive fractions, and isolated compounds is thus critical for continuing drug development in the 21st century.

References

1. Richman DD. Antiviral drug resistance. Antiviral Res

2006;71:117-121.
2. Yin PD, Das D, Mitsuya H. Overcoming HIV drug resistance through rational drug design based on molecular, biochemical, and structural profiles of HIV resistance. Cell Mol Life Sci 2006;63:1706-1724.
3. Shafer RW, Rhee SY, Pillay D, Miller V, Sandstrom P, Schapiro JM, Kuritzkes DR, Bennett D. HIV-1 protease and reverse transcriptase mutations for drug resistance surveillance. AIDS 2007;21:215-223.
4. De Clercq E. Strategies in the design of antiviral drugs. Nat Rev Drug Discov 2002;1:13-25.
5. Cragg GM, Newman DJ, Snader KM. Natural products in drug discovery and development. J Nat Prod 1997;60:52-60.
6. Harvey A. Strategies for discovering drugs from previously unexplored natural products. Drug Discov Today 2000;5:294-300.
7. Koehn FE, Carter GT. The evolving role of natural products in drug discovery. Nat Rev Drug Discov 2005;4:206-220.
8. Newman DJ, Cragg GM. Natural products as sources of new drugs over the last 25 years. J Nat Prod 2007;70:461-477
9. Jassim SAA, Naji MA. Novel antiviral agents: a medicinal plant perspective. J Applied Microbiol 2003;95:412-427.
10. UNAIDS/WHO "AIDS Epidemic Update: December 2006", http://data.unaids.org/pub/EpiReport/2006/2006_EpiUpdate_en.pdf
11. Simon V, Ho DD, Abdool Karim Q. HIV/AIDS epidemiology, pathogenesis, prevention, and treatment. Lancet 2006;368:489-504.
12. Opar A. New HIV drug classes on the horizon. Nat Rev Drug Discov 2007;6:258-259.
13. De Clercq E. Current lead natural products for the chemotherapy of human immunodeficiency virus (HIV) infection. Med Res Rev 2000;20:323-349.
14. El Safadi Y, Vivet-Boudou V, Marquet R. HIV-1 reverse transcriptase inhibitors. Appl Microbiol Biotechnol 2007;75:723-737.
15. Camarasa MJ, Velázquez S, San-Félix A, Pérez-Pérez MJ, Gago F. Dimerization inhibitors of HIV-1 reverse transcriptase, protease and integrase: a single mode of inhibition for the three HIV enzymes? Antiviral Res 2006;71:260-267.
16. Nair V, Chi G. HIV integrase inhibitors as therapeutic agents in AIDS. Rev Med Viol (in press).
17. Pommier Y, Johnson AA, Marchand C. Integrase inhibitors to treat HIV/AIDS. Nat Rev Drug Discov 2005;4:236-248.
18. Grinsztejn B, Nguyen BY, Katlama C, Gatell JM, Lazzarin A, Vittecoq D, Gonzalez CJ, Chen J, Harvey CM, Isaacs RD. Safety and efficacy of the HIV-1 integrase inhibitor raltegravir (MK-0518) in treatment-experienced patients with multidrug-resistant virus: a phase II randomized controlled trial. Lancet 2007;369:1261-1269.
19. Min BS, Hattori M, Lee HK, Kim YH. Inhibitory constituents against HIV-1 protease from Agastache rugosa. Arch Pharm Res 1999;22:75-77.
20. Min BS, Jung HJ, Lee JS, Kim YH, Bok SH, Ma CM, Nakamura N, Hattori M, Bae K. Inhibitory effect of triterpenes from Crataegus pinatifida on HIV-I protease. Planta Med 1999;65:374-375.
21. Rukachaisirikul V, Pailee P, Hiranrat A, Tuchinda P, Yoosook C, Kasisit J, Taylor WC, Reutrakul V. Anti-HIV-1 protostane triterpenes and digeranylbenzophenone from trunk bark and stems of Garcinia speciosa. Planta Med 2003;69:1141-1146.
22. Zhang HJ, Tan GT, Hoang VD, Hung NV, Cuong NM, Soejarto DD, Pezzuto JM, Fong HH. Natural anti-HIV agents. Part IV. Anti-HIV constituents from Vatica cinerea. J Nat Prod 2003;66:263-268.
23. Kashiwada Y, Hashimoto F, Cosentino LM, Chen CH, Garrett PE, Lee KH. Betulinic acid and dihydrobetulinic acid derivatives as potent anti-HIV agents. J Med Chem 1996;39:1016-1017.
24. Li F, Goila-Gaur R, Salzwedel K, Kilgore NR, Reddick M, Matallana C, Castillo A, Zoumplis D, Martin DE, Orenstein JM, Allaway GP, Freed EO, Wild CT. PA-457: a potent HIV inhibitor that disrupts core condensation by targeting a late step in Gag processing. Proc Natl Acad Sci U S A 2003;100:13555-13560.
25. Yu D, Wild CT, Martin DE, Morris-Natschke SL, Chen CH, Allaway GP, Lee KH. The discovery of a class of novel HIV-1 maturation inhibitors and their potential in the therapy of HIV. Expert Opin Investig Drugs 2005;14:681-693.
26. Yu D, Morris-Natschke SL, Lee KH. New developments in natural products-based anti-AIDS research. Med Res Rev 2007;27:108-132.
27. Ito M, Sato A, Hirabayashi K, Tanabe F, Shigeta S, Baba M, De Clercq E, Nakashima H, Yamamoto N. Mechanism of inhibitory effect of glycyrrhizin on replication of human immunodeficiency virus (HIV). Antiviral Res 1988;10:289-298.
28. Kitamura K, Honda M, Yoshizaki H, Yamamoto S, Nakane H, Fukushima M, Ono K, Tokunaga T. Baicalin, an inhibitor of HIV-1 production *in vitro*. Antiviral Res 1998;37:131-140.
29. Li BQ, Fu T, Dongyan Y, Mikovits JA, Ruscetti FW, Wang JM. Flavonoid baicalin inhibits HIV-1 infection at the level of viral entry. Biochem Biophys Res Commun 2000;276:534-538.
30. Min BS, Lee HK, Lee SM, Kim YH, Bae KH, Otake T, Nakamura N, Hattori M. Anti-human immunodeficiency virus-type 1 activity of constituents from Juglans mandshurica. Arch Pharm Res 2002;25:441-445.
31. Fassina G, Buffa A, Benelli R, Varnier OE, Noonan DM, Albini A. Polyphenolic antioxidant (-)-epigallocatechin-3-gallate from green tea as a candidate anti-HIV agent. AIDS 2002;16:939-941.
32. Lee JS, Kim HJ, Lee YS. A new anti-HIV flavonoid glucuronide from Chrysanthemum morifolium. Planta Med 2003;69:859-861.
33. Creagh T, Ruckle JL, Tolbert DT, Giltner J, Eiznhamer DA, Dutta B, Flavin MT, Xu ZQ. Safety and pharmacokinetics of single doses of (+)-calanolide a, a novel, naturally occurring nonnucleoside reverse transcriptase inhibitor, in healthy, human immunodeficiency virus-negative human subjects. Antimicrob Agents Chemother 2001;45:1379-1386.
34. Asres K, Seyoum A, Veeresham C, Bucar F, Gibbons S. Naturally derived anti-HIV agents. Phytother Res 2005;19:557-581.
35. Kostova I. Coumarins as inhibitors of HIV reverse transcriptase. Curr HIV Res 2006;4:347-363.
36. De Clercq E. Antiviral agents active against influenza A viruses. Nat Rev Drug Discov 2006;5:1015-1025.
37. Guan Y, Chen H. Resistance to anti-influenza agents. Lancet 2005;366:1139-1140.
38. Serkedjieva J, Toshkova R, Antonova-Nikolova S, Stefanova T, Teodosieva A, Ivanova I. Effect of a plant polyphenol-rich extract on the lung protease activities of influenza-virus-infected mice. Antivir Chem Chemother 2007;18:75-82.
39. Wang X, Jia W, Zhao A, Wang X. Anti-influenza agents from plants and traditional Chinese medicine. Phytother Res 2006;20:335-341.
40. Sokmen M, Angelova M, Krumova E, Pashova S, Ivancheva S, Sokmen A, Serkedjieva J. *In vitro* antioxidant activity of polyphenol extracts with antiviral

properties from *Geranium sanguineum* L. Life Sci 2005;76:2981-2993.
41. Miki K, Nagai T, Suzuki K, Tsujimura R, Koyama K, Kinoshita K, Furuhata K, Yamada H, Takahashi K. Anti-influenza virus activity of biflavonoids. Bioorg Med Chem Lett 2007;17:772-775.
42. Nagai T, Miyaichi Y, Tomimori T, Suzuki Y, Yamada H. *In vivo* anti-influenza virus activity of plant flavonoids possessing inhibitory activity for influenza virus sialidase. Antiviral Res 1992;19:207-217.
43. Serkedjieva J, Velcheva M. *In vitro* anti-influenza virus activity of the pavine alkaloid (-)-thalimonine isolated from Thalictrum simplex L. Antivir Chem Chemother 2003;14:75-80.
44. Rajbhandari M, Wegner U, Jülich M, Schöpke T, Mentel R. Screening of Nepalese medicinal plants for antiviral activity. J Ethnopharmacol 2001;74:251-255.
45. Kernan MR, Sendl A, Chen JL, Jolad SD, Blanc P, Murphy JT, Stoddart CA, Nanakorn W, Balick MJ, Rozhon EJ. Two new lignans with activity against influenza virus from the medicinal plant Rhinacanthus nasutus. J Nat Prod 1997;60:635-637.
46. Lai CL, Ratziu V, Yuen MF, Poynard T. Viral hepatitis B. Lancet 2003;362:2089-2094.
47. Lavanchy D. Hepatitis B virus epidemiology, disease burden, treatment, and current and emerging prevention and control measures. J Viral Hepat 2004;11:97-107.
48. Patrick L. Hepatitis C: epidemiology and review of complementary/alternative medicine treatments. Altern Med Rev 1999;4:220-238.
49. Lauer G, Walker BD. Hepatitis C virus infection. N Engl J Med 2001;345:41-52.
50. Koziel MJ, Peters MG. Viral Hepatitis in HIV infection. N Engl J Med 2007;356:1445-1454.
51. Van Rossum TG, Vulto AG, De Man RA, Brouwer JT, Schalm SW. Review article: glycyrrhizin as a potential treatment for chronic hepatitis C. Aliment Pharmacol Ther 1998;12:199-205.
52. Liu J, Zhu M, Shi R, Yang M. Radix Sophorae flavescentis for chronic hepatitis B: a systematic review of randomized trials. Am J Chin Med 2003;31:337-354.
53. Lu LG, Zeng MD, Mao YM, *et al*. Oxymatrine therapy for chronic hepatitis B: a randomized double-blind and placebocontrolled multi-center trial. World J Gastroenterol 2003;9:2480-2483.
54. Lu LG, Zeng MD, Mao YM, Fang JY, Song YL, Shen ZH, Cao AP. Inhibitory effect of oxymatrine on serum hepatitis B virus DNA in HBV transgenic mice. World J Gastroenterol 2004;10:1176-1179.
55. Yu YY, Wang QH, Zhu LM, Zhang QB, Xu DZ, Guo YB, Wang CQ, Guo SH, Zhou XQ, Zhang LX. A clinical research on oxymatrine for the treatment of chronic hepatitis B. Zhonghua Gan Zang Bing Za Zhi 2002;10:280-281.
56. Mao YM, Zeng MD, Lu LG, *et al*. Capsule oxymatrine in treatment of hepatic fibrosis due to chronic viral hepatitis: a randomized, double blind, placebo-controlled, multicenter clinical study. World J Gastroenterol 2004;10:3269-3273.
57. Liu J, Manheimer E, Tsutani K, Gluud C. Medicinal herbs for hepatitis C virus infection: a Cochrane hepatobiliary systematic review of randomized trials. Am J Gastroenterol 2003;98:538-544.
58. Azzam HS, Goertz C, Fritts M, Jonas WB. Natural products and chronic hepatitis C virus. Liver Int 2007;27:17-25.
59. Hussein G, Miyashiro H, Nakamura N, Hattori M, Kakiuchi N, Shimotohno K. Inhibitory effects of Sudanese medicinal plant extracts on hepatitis C virus (HCV) protease. Phytother Res 2000;14:510-516.
60. Patrick L. Hepatitis C: epidemiology and review of complementary/alternative medicine treatments. Altern Med Rev 1999;4:220-238.
61. Whitley RJ, Roizman B. Herpes simplex virus infections. Lancet 2001;357:1513-1518.
62. Lingappa JR, Celum C. Clinical and therapeutic issues for herpes simplex virus-2 and HIV co-infection. Drugs 2007;67:155-174.
63. Coen DM, Schaffer PA. Antiherpesvirus drugs: a promising spectrum of new drugs and drug targets. Nat Rev Drug Discov 2003;2:278-288.
64. Khan MT, Ather A, Thompson KD, Gambari R. Extracts and molecules from medicinal plants against herpes simplex viruses. Antiviral Res 2005;67:107-119.
65. De Logu A, Loy G, Pellerano ML, Bonsignore L, Schivo ML. Inactivation of HSV-1 and HSV-2 and prevention of cell-to-cell virus spread by Santolina insularis essential oil. Antiviral Res 2000;48:177-185.
66. Vijayan P, Raghu C, Ashok G, Dhanaraj SA, Suresh B. Antiviral activity of medicinal plants of Nilgiris. Indian J Med Res 2004;120:24-29.
67. Rajbhandari M, Wegner U, Julich M, Schopke T, Mentel R. Screening of Nepalese medicinal plants for antiviral activity. J Ethnopharmacol 2001;74:251-255.
68. Fuse T, Watanabe K, Kitazato K, Kobayashi N. Establishment of a new cell line inducibly expressing HIV-1 protease for performing safe and highly sensitive screening of HIV protease inhibitors. Microbes Infect 2006;8:1783-1789.

Target validation: A door to drug discovery

Xiu-Ping Chen, Guan-Hua Du*

Institute of Materia Medica, Chinese Academy of Medical Sciences and Peking Union Medical College, Beijing, China.

ABSTRACT: From ancient times to today, drug discovery transitioned from serendipity to rationality over its long history. Proper drug target selection and validation are crucial to the discovery of new drugs. This review discusses the definition of drug targets and proposes several characteristics for drug targets. The limitations of the term 'target' itself are summarized. The drug target validation process is also discussed in detail and pitfalls during this process are outlined. Small active chemical compounds obtained from the target validation process are useful tools in target validation and target function research. The validation of lectin-like oxidized low-density lipoprotein receptor-1 (LOX-1) as a new potential anti-atherosclerotic drug target is cited as an example in order to elucidate the target validation process.

Key Words: Drug discovery, drug target, drug target validation, high-throughput screening, lectin-like oxidized low-density lipoprotein receptor-1

Introduction

In medicine, biotechnology, and pharmacology, drug discovery is generally thought of as the discovery, creation, or design of a compound or a complex that possesses the potential to become a useful therapeutic. It is really an expensive, time-consuming, and difficult process that involves the identification of candidates and synthesis, characterization, screening, and assays of their therapeutic efficacy. The word 'target' has been widely used in both medical and pharmaceutical research. However, the definition of "target" itself is vague and is debated within the pharmaceutical industry. The number of drug targets is also controversial, due in large degree to disputes over the definition of what a target is. The exact connotation of the term "drug target" needs to be elucidated. Target validation is the first step in completely new drug discovery. Validation of new drug targets is the process of physiologically, pathologically, and pharmacologically evaluating a biomolecule and might be performed at the molecular, cellular, or whole animal level.

Lectin-like oxidized low-density lipoprotein receptor-1 (LOX-1) was identified as a special receptor for oxidized low-density lipoprotein (ox-LDL) in endothelial cells (*1*). Accumulated studies revealed that LOX-1 might play an important role in the pathogenesis of atherosclerosis (*2-7*). Review of ten years of studies on LOX-1 suggested that LOX-1 might be a specific new drug target, and validation results here revealed that LOX-1 is a new promising anti-atherosclerotic drug target.

Drug discovery: From serendipity to rationality

Drug discovery is one of the most crucial components of the pharmaceutical industry's Research and Development (R&D) process and is the essential step in the generation of any robust, innovative drug pipeline. However, new drug discovery is an expensive, time-consuming, and difficult process. Moreover, the end result is never guaranteed. A single new drug can cost 1.2 billion euros and take 10 years to develop (*8*).

The early history of drug discovery is all about natural products and herbal remedies, the use of which dates back thousands of years. In ancient times, drug discovery was mainly based on the accumulation of experience from generation to generation. It is a rather long process that involves huge costs in both money and even lives. Just like the discovery of penicillin, serendipity has been the key to the pharmaceutical industry's success over many decades. Now with the development of modern chemistry, hundreds and sometimes thousands of chemical compounds have to be made and tested in an effort to find one that can achieve a desirable result. Thus, traditional drug discovery strategy based on experience and serendipity is no longer able to meet the needs of pharmaceutical companies. A shift from serendipity to rationality in drug discovery is underway (Figure 1). Rational drug discovery based on knowledge of the biological system being investigated allows highly specific selective

**Correspondence to:* Guan-Hua Du, Institute of Materia Medica, Chinese Academy of Medical Sciences and Peking Union Medical College, Beijing 100050, China; e-mail: dugh@imm.ac.cn

Received June 29, 2007
Accepted July 6, 2007

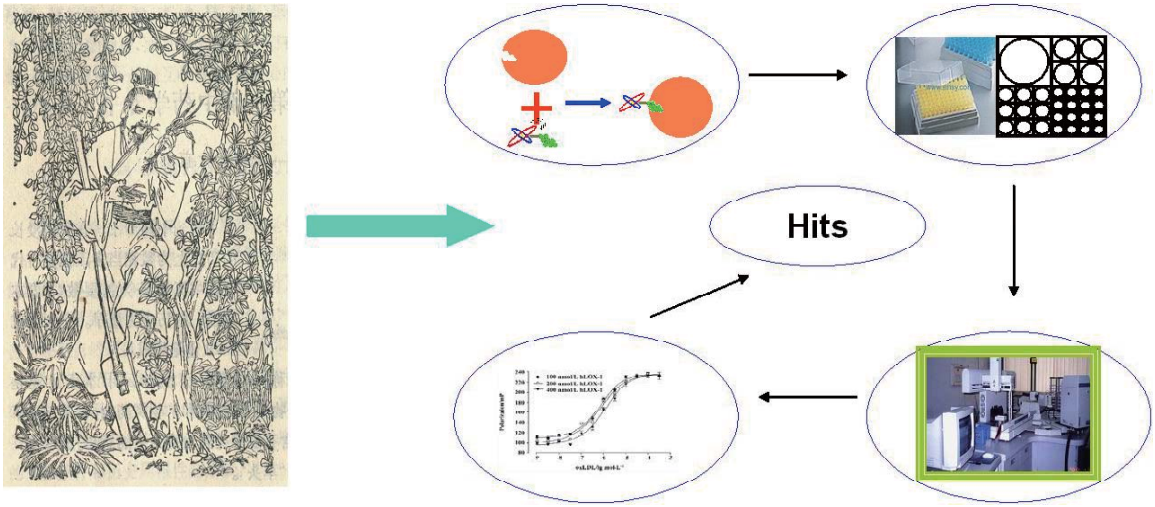

Figure 1. Drug discovery: From 'Tasting to Testing.' The emergence of an "accidental" approach to drug discovery has its origins in early history with traditional natural herbal remedies that were passed from generation to generation in local communities or tribes. The ancient Chinese legend that "Shen Nong tastes a hundred herbs in a single day and meets seventy toxins" demonstrates the great sufferings of our ancestors encountered during the discovery of new drugs. This experience-based drug discovery mode lasted for several thousands years. It was not until the late 18th and early 19th centuries that the active components of medicinal plants and herbal remedies were analyzed, resulting in the discovery of alkaloids. HTS and ultra-HTS developed during the later 1980s represent a new mode of drug discovery. These methods represent a multifunctional, multiskilled environment that connects a range of discovery functions in a high-capacity, integrated process producing a product that consists of a cohort of tractable chemical leads with respect to targets of interest.

antagonists and agonists to be developed. These molecules can then be developed as lead compounds, drug candidates, and even drugs.

What are drug targets?

Target identification and validation are the first key stages in the drug discovery pipeline (*9*). But what is a drug target? Generally speaking, a drug target is the specific binding site of a drug *in vivo* through which the drug exerts its action. A specific drug target might have the following characteristics: 1) The drug target is a biomolecule(s), normally a protein that could exist in isolated or complex modality. 2) The biomolecules have special sites that match other molecules (commonly small molecules with special structures). These molecules could be endogenous or extraneous substances such as chemical molecules (drugs). 3) The biomolecular structure might change when the biomolecule binds to small molecules and the changes in structure normally are reversible. 4) Following the change in the biomolecule's structure various physiological responses occur and induce regulation of the cell, organ, tissue, or body status. 5) The physiological responses triggered by the changes in biomolecule structure play a major role in complex regulation and have a therapeutic effect on pathological conditions. 6) The expression, activity, and structure of the biomolecule might change over the duration of the pathological process. 7) Small molecules binding to the biomolecules are drugs (*10*).

As is apparent from the above discussion, a drug target is a key molecule involved in a particular metabolic or signal transduction pathway that is specific to a disease condition or a specific disease. However, the term 'drug target' itself has several limitations and is debated within the pharmaceutical industry. In this respect, several points should be kept in mind.

First, a drug target is a relative concept. For starters, a drug target is, just like other biomolecules, also a biomolecule involved in a transduction pathway. The difference between the two is only in their location and role in the transduction pathway. Another aspect is that a drug target is disease-dependent, that is, every target is involved in a special spectrum of diseases.

Second, most human diseases are rather complicated and involve many risk factors, so there are clearly many different drug targets with respect to a specific disease. Targeting a specific target could not conceivably cure a kind of disease. However, the involvement of many targets in a disease does not mean that each target shares equally in the pathogenesis of the disease and thus drugs targeting these targets would not be equally effective in the therapy of the disease.

Third, drug targets can change, which means that with the development of insights into biomolecules and their role in the pathogenesis of a certain disease, drug targets might be not as important as or may be much more important than currently believed. In fact, the establishment of drug targets is based on understanding of the pathogenesis of the disease.

Fourth, there are many drugs targeting the same target and one drug may have more than one target. The relationship between a drug and its target is not one-to-

one but one-to-many or many-to-one.

Fifth, when a new drug target is discovered and validated, researchers usually hope to obtain more specific drugs targeting the target. However, a key understanding to keep in mind is that the body is a subtle organism and a more specific drug might disrupt the homeostasis of the body. Compared to aspirin, rofecoxib is a specific COX-2 inhibitor. However, studies had shown that rofecoxib increases cardiovascular risks, resulting in rofecoxib's withdrawal from the drug market.

Sixth, a drug target usually refers to a single biomolecule. This connotation should be revised. Recent research has noted that a complex, like HDL, for example, or even a kind of cell, like an endothelial cell, could be a potential drug target. However, drug target validation based on this concept is very difficult since reliable, accurate, and robust indexes to evaluate the effect of drugs targeting these targets are rare.

According to whether there are drugs available, a drug target can be classified into two classes: established drug targets and potential drug targets. The former are those for which there is a good scientific understanding, supported by a lengthy publication history regarding both how the target functions in normal physiology and how it is involved in human pathology. Furthermore, there are many drugs targeting this target. The latter are those biomolecules whose functions are not fully understood and which lack drugs targeting them. Potential targets suggest directions for completely new drug research.

How many drug targets are there?

With the development of modern science and technology, humans became more informed about themselves than at any time in history. Thousands of drugs had been discovered and created. However, the mechanisms of their action and the targets of their action were poorly understood. Furthermore, the number of drug targets in the body is less consistent than the definition of a drug target. How many drug targets are there in the body? Drews and Reiser were the first to systematically pose and answer this question, identifying 483 drug targets. Later, Hopkins and Groom revised this figure downward to only 120 underlying molecular targets. Subsequently, Golden proposed that all then-approved drugs acted through 273 proteins. By contrast, Wishart *et al*. reported 14,000 targets for all approved and experimental drugs, although they revised this number to 6,000 targets on the Drug Bank database website (*11*). Imming *et al*. catalogued 218 molecular targets for approved drug substances (*12*), whereas Zheng *et al*. cited 268 'successful' targets in the current version of the Therapeutic Targets Database. John *et al*. proposed a consensus number of 324 drug targets for all classes of approved therapeutic drugs (*11*). With the publication of draft maps of the human genome and an interim agreement that the human genome consists of approximately 21,000 genes, there has been considerable anticipation that many novel disease-specific molecular targets will be rapidly identified and that these will form the basis of many new drug discovery programs (*13*). According to the current definition, one could rationally predict that there are 5,000 to 10,000 established and potential drug targets in humans (*10*).

Target validation

New target validation is the basis of completely new drug exploration and the initial step of drug discovery. New drug target validation might be of great help not only to new drug research and development but also provide more insight into the pathogenesis of target-related diseases. Basically, the target validation process might include six steps:

1. Discovering a biomolecule of interest.
2. Evaluating its potential as a target.
3. Designing a bioassay to measure biological activity.
4. Constructing a high-throughput screen.
5. Performing screening to find hits.
6. Evaluating the hits.

The drug discovery process starts with the identification, or growing evidence of, biological targets that are believed to be connected to a particular condition or pathology. Information supporting the role of these targets in disease modulation can come from a variety of sources. Traditionally, the targets have been researched and largely discovered in academic laboratories, and to a lesser extent in the laboratories of pharmaceutical and biotechnology companies. Basic research into understanding the fundamental, essential processes for signaling within and between cells and their perturbation in conditions has been the basic approach for establishing potential targets suitable for drug intervention (*14*).

After the identification of a biological target of interest, the next challenge begins with the conversion of the target into a bioassay that can give a readout of biological activity. The range of potential targets is large, from enzymes and receptors to cellular systems that represent an entire biochemical pathway or a disease process. Consequently, the range of assay design techniques and types of assay available have to be correspondingly comprehensive. Once an assay that measures the biological activity of the target, by some direct or indirect means, has been developed, then compounds can be tested in the bioassay to see if they inhibit, enhance, or do nothing to this activity (*14*).

After a bioassay to measure biological activity is designed, the next key step is the establishment of a high-throughput screening (HTS) method. The basic requirements for HTS assay are that it be sensitive,

stable, highly reproducible, and robust and suitable for screening thousands or even millions of samples. With sufficient luck, several 'hit' compounds will be discovered by primary screening.

The 'hit' compounds must be rescreened to exclude false positive results. Then, the next step is 'hit' identification, which may include its chemical characteristics, *i.e.* mainly its stability, its toxicity *in vivo* and *in vitro*, and its pharmacological evaluation, and particularly its effects in cells and animal models.

In summary, target validation should be performed at three levels: the molecular level, the cellular level, and the whole animal model level (Figure 2). Small chemicals obtained from HTS provide useful tools for the validation of new drug targets. Most HTS models are at the molecular level, that is, cell-free systems. For example, screening of a specific enzyme inhibitor usually involves mixing the enzyme and samples together to detect a decrease in the substrate or to determine an increase in the product in this enzyme catalytic process. The results obtained from this level are not absolutely reliable since there are many predictable and unpredictable factors. However, true results from this level convey the point that hits truly act with the target. There is a significant difference between a cell and cell-free system. Validation at the cell level provides confirmation of cell-free results. At this level, the pathological significance of the target might be rendered more apparent using small chemicals. The effect of the small chemicals on a cell system will provide a tentative outline of these chemicals. Animal models are used to validate the target at the whole level. At this level, the primary concern is the effect of the 'hit'. If the hit obtained from HTS displays a therapeutic effect in animal models, then it may be promising. However, more often than not a 'hit' displays no effect in an animal model and the result should be interpreted with caution. Common shortfalls and/or pitfalls that need to be considered include (*15*):

1. Using the wrong animal model.
2. Using the wrong route or dosing regimen.
3. Using the wrong vehicle or formulation of test material.
4. Using the wrong dose level. In studies where several dose levels are studied, the worst outcome is to have an effect at the lowest dose level tested (*i.e.*, the safe dosage in animals remains unknown). The next worst outcome is to have no effect at the highest dose tested (generally meaning that the signs of toxicity remain unknown, invalidating the study in the eyes of many regulatory agencies).
5. Making leaps of faith. An example is to set dosage levels based on others' data and to then dose all test animals. Ultimately, all animals at all dose levels die, the study ends, and the problem remains.
6. Using the wrong concentration of test materials in screening. Many effects are very concentration-dependent.

Validation of LOX-1 as a new potential anti-atherosclerotic drug target

LOX-1 is a new kind of ox-LDL receptor discovered from bovine aortic endothelial cells (BAEC) by Sawamura *et al.* in 1997 (*1*). Studies have shown that LOX-1 is the major receptor for ox-LDL in endothelial cells of large arteries although other ox-LDL receptors have also been reported (*1*). Accumulated studies revealed several ligands for LOX-1 that are expressed in different types of cells and that could be regulated at the level of transcription. Changed expression of LOX-1 at the mRNA and protein level has been reported in several cardiovascular processes such as atherosclerosis, hypertension, myocardial ischemia, ischemia-reperfusion injury, and diabetes (*2-6*). Identification, regulation, and understanding of LOX-1 signal transduction pathways might improve current insights on the pathogenesis of some cardiovascular diseases and provide a selective treatment tool for physicians. LOX-1 might be a potential and promising target for cardiovascular drug research.

The relationship between LOX-1 and atherosclerosis could be summarized as six e's: endocytosis of ox-LDL, expression co-location with atherosclerosis, enhanced by atherosclerosis-related risk factors, elevated LOX-1 protein in cardiovascular diseases, effects involved in pathogenesis of atherosclerosis, and eliminated by anti-atherosclerotic drugs. Furthermore, LOX-1 is related to the stability of atherosclerotic plaque (*6*).

A review of ten years of studies on LOX-1 reveals that in principle LOX-1 is consistent with these characteristics for a specific drug target. LOX-1 is a 50 kDa type II membrane protein that structurally belongs to the C-type lectin family with a short intracellular N-terminal hydrophilic and a long extracelluar C-terminal hydrophilic domain separated by a hydrophobic domain of 26 amino acids (*1*). The lectin domain is the ligand recognition site and the binding activity of LOX-1 to its ligands depends on the interaction of positively charged residues with negatively charged ligands (*16,17*). Based on the arrangement of critical binding residues on the LOX-1 structure and comparing the size of the dimmer surface of LOX-1 with the diameter of ox-LDL, the binding mode for the recognition of ox-LDL was proposed, indicating that three LOX-1 molecules are needed to bind to one ox-LDL molecule (*18,19*). Furthermore, two different fragments of the ligand-binding domain of human LOX-1 have been crystallized and analyzed by X-ray (*20*). The binding of LOX-1 to ox-LDL induces intracellular reactive oxygen species (ROS) production, p38 mitogen-activated protein kinase (p38 MAPK) and nuclear factor kappa B (NF-κB) activation, and expression of intercellular adhesion molecule-1

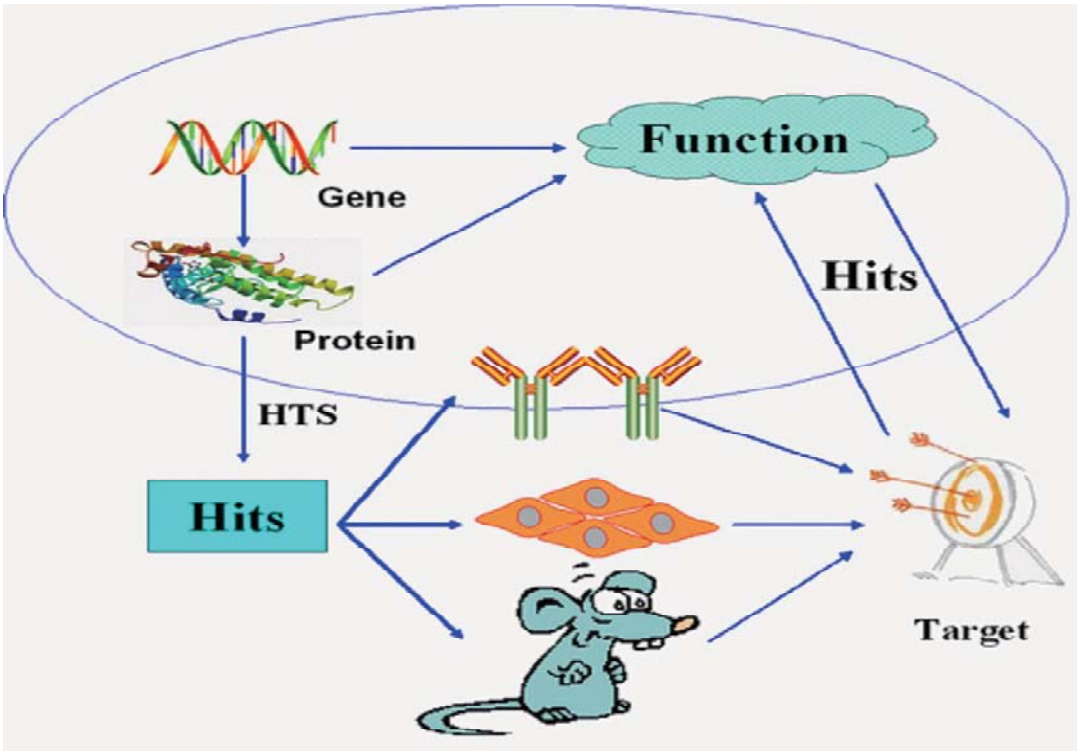

Figure 2. Drug target validation: hit discovery and target function research. New drug target validation is a difficult process. However, hit compounds obtained from HTS could be a useful tool for target validation and target function research. A HTS model is established to obtain hits. The screened hits will be evaluated at the molecular, cellular, and whole animal level and their effects will be of great use in validating the target. At the same time, a drug target validation process based on this strategy also serves as the process of target function research.

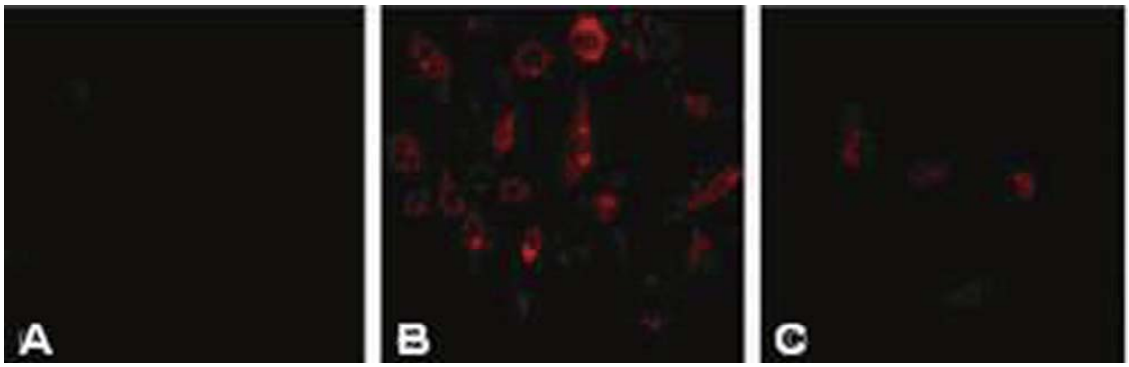

Figure 3. LOX-1 ligand 6306 obtained from HTS inhibits LOX-1 mediated DiI-ox-LDL uptake. hLOX-1-CHO-K1 cells were incubated with DiI-ox-LDL (10 μg/mL) with and without 6306. The uptake of DiI-ox-LDL was measured with a fluorescence microscope. A, blank; B, without 6306; C, 20 μM 6306.

(ICAM-1), vascular cell adhesion molecule-1 (VCAM-1), and monocyte chemoattractant protein-1 (MCP-1). Changed expression of LOX-1 had been reported in several cardiovascular diseases such as atherosclerosis, hypertension, myocardial ischemia, ischemia-reperfusion injury, and cardiovascular complications of diabetes (*2-7*). However, further study is needed to provide more evidence that LOX-1 is a promising drug target.

To validate whether LOX-1 could serve as a new potential target, a competitive fluorescence polarization-based (FP) HTS method was first established to screen LOX-1 ligands in a 384-well microplate using recombinant human LOX-1 protein. The human LOX-1 gene was obtained by RT-PCR from THP-1 cells stimulated with histamine. The purified hLOX-1 gene was cloned into a pMD 18-T vector, which was amplified in Escherichia coli strain DH5α. hLOX-1 cDNA was subcloned into pPIC9K to provide the recombinant plasmid pPIC9K-His-hLOX-1. The plasmid pPIC9K-His-hLOX-1 was transformed into Pichia pastoris GS115. The hLOX-1 protein was

purified with HiTrap Chelating HP and labeled with fluorescein isothiocyanate (FITC).

Assay was based on receptor-ligand interaction: human LOX-1 was labeled with FITC and bound to its special ligand, ox-LDL and different chemicals from the sample bank were used to compete with ox-LDL. A total of 12,700 compounds were screened with an excitation filter of 485 nm and emission filter of 530 nm. This yielded a Z' factor of 0.75, and three chemicals of LOX-1 mimic ligands with an EC_{50} below 40 μM were identified (*21*,*22*).

To further evaluate the binding activity of these chemicals, one of the three compounds, 6306, was studied further using cell models. Ox-LDL was labeled by DiI and the uptake of DiI-oxLDL was studied with hLOX-1-CHO-K1 cells (CHO-K1 cells transfected with the human LOX-1 gene). Fluorescence microscopy of hLOX-1-CHO-K1 cells incubated with DiI-ox-LDL showed that hLOX-1-CCHO-K1 cells internalized significant amounts of DiI-ox-LDL (Figure 3B) although the control did not (Figure 3A); this internalization was also blocked by excess amounts of unlabeled ox-LDL (200 μg/mL). Pre-cultured 6306 (20 μM) significantly decreased LOX-1 mediated DiI-ox-LDL endocytosis (Figure 3C). This suggests that 6306 has a high affinity to hLOX-1 protein under physiological conditions.

Previous studies revealed that the binding of ox-LDL to LOX-1 induced intracellular reactive oxygen species (ROS) production (*23-25*). Ox-LDL may decrease intracellular nitric oxide (NO) concentration due to the increase in intracellular O_2^-. Using hLOX-1-CHO-K1 cells, the effects of the screened LOX-1 ligand 6306 on ROS and O_2^- production were determined.

Results showed that 6306 had similar effects to ox-LDL on the ROS and O_2^- production in LOX-1-CHO-K1 cells. 6306 significantly reduced the NO_2^- level in the supernatant of cultured cells (data not shown). These results suggest that 6306 might activate LOX-1 and result in effects similar to those of ox-LDL. Due to the important role ox-LDL plays in atherosclerosis, 6306 was not used in animal studies.

Another ligand, 6302, may inhibit ox-LDL induced hLOX-1-CHO-K1 cell intracellular ROS and O_2^- formation and NO_2^- decrease. A rat model of atherosclerosis induced by a high-fat diet was established to explore the role of LOX-1 in the pathogenesis of atherosclerosis and to test if LOX-1 ligand had potential to serve as a leading anti-atherosclerotic compound, and the effects of LOX-1 ligand 6302 were studied in this model.

The results revealed that LOX-1 ligand 6302 attenuated aortic intima injury induced by a high-fat diet in rats and inhibited atherosclerotic plaque formation. The serum levels of total cholesterol (TC), triglyceride (TG), and low-density lipoprotein-cholesterol (LDL-C) decreased while the high-density lipoprotein-cholesterol (HDL-C) level increased in a model of atherosclerosis where 6302 was administered. The serum malondialdehyde (MDA) level also decreased (data not shown). These results suggest that LOX-1 inhibition might have a beneficial effect on atherosclerosis.

Conclusion

Drugs are a physician's most powerful weapon to combat disease. The discovery of new drug targets is the basis of new drug development and examination of new drug mechanisms. Though the advent of a pharmacogenomics era opens the door for new drug target research, there are still numerous obstacles to the identification and validation of new drug targets and a great deal of work must be done.

Acknowledgements

This work is supported by the Natural Science Fundation of China (No: 30630073), National Scientific and Technological Basic Conditions Platform Construction Program (No: 2005DKA32400).

References

1. Sawamura T, Kume N, Aoyama T, Moriwaki H, Hoshikawa H, Aiba Y, Tanaka T, Miwa S, Katsura Y, Kita T, Masaki T. An endothelial receptor for oxidized low-density lipoprotein. Nature 1997;386:73-77.
2. Vohra RS, Murphy JE, Walker JH, Ponnambalam S, Homer-Vanniasinkam S. Atherosclerosis and the lectin-like oxidized low-density lipoprotein scavenger receptor. Trends Cardiovasc Med 2006;16:60-64.
3. Mehta JL, Chen J, Hermonat PL, Romeo F, Novelli G. Lectin-like, oxidized low- density lipoprotein receptor-1 (LOX-1): a critical player in the development of atherosclerosis and related disorders. Cardiovasc Res 2006;69:36-45.
4. Chen M, Masaki T, Sawamura T. LOX-1, the receptor for oxidized low-density lipoprotein identified from endothelial cells: implications in endothelial dysfunction and atherosclerosis. Pharmacol Ther 2002;95:89-100.
5. Mehta JL, Li D. Identification, regulation and function of a novel lectin-like oxidized low-density lipoprotein receptor. J Am Coll Cardiol 2002;39:1429-1435.
6. Chen XP, Zhang TT, Du GH. Lectin-like oxidized low-density lipoprotein receptor-1, a new promising target for the therapy of atherosclerosis? Cardiovascular Drug Review 2007;25:1-16.
7. Chen XP, Du GH. Lectin-like oxidized low-density lipoprotein receptor-1: protein, ligands, expression and pathophysiological significance. Chin Med J 2007;120:421-426.
8. http://www.eurograduate.com/showarticle.php?article_id_show=29
9. Wang S, Sim TB, Kim YS, Chang YT. Tools for target identification and validation. Curr Opin Chem Biol 2004;8:371-377.
10. Du GH. Evaluation and validation of drug targets. Acta Pharmacol Sin 2004;25:1566.
11. Overington JP, Al-Lazikani B, Hopkins AL. How many drug targets are there? Nat Rev Drug Discov 2006;5:993-996.

12. Imming P, Sinning C, Meyer A. Drugs, their targets and the nature and number of drug targets. Nature Rev Drug Discov 2006;5:821-834.
13. Williams M. Target validation. Curr Opin Pharmacol 2003;3:571-577.
14. John GH, Martyn NB, Bristol-Myers S. High throughput screening for lead discovery. Burger's Medicinal Chemistry and Drug Discovery, sixth edition, Vol 2: Drug Discovery and Drug Development 2002, Wiley Press, pp37-70.
15. Shayne CG. Introduction: drug Discovery in the 21st Century. Drug Discovery Handbook. 2005, Wiley Press, pp1-10.
16. Chen M, Narumiya S, Masaki T, Sawamura T. Conserved C-terminal residues within the lectin-like domain of LOX-1 are essential for oxidized low-density-lipoprotein binding. Biochem J 2001;355:289-296.
17. Shi X, Niimi S, Ohtani T, Machida S. Characterization of residues and sequences of the carbohydrate recognition domain required for cell surface localization and ligand binding of human lectin-like oxidized LDL receptor. J Cell Sci 2001;114:1273-1282.
18. Park H, Adsit FG, Boyington JC. The crystal structure of the human oxidized low density lipoprotein receptor Lox-1. J Biol Chem 2005;280:13593-13599.
19. Ohki I, Ishigaki T, Oyama T, Matsunaga S, Xie Q, Ohnishi-Kameyama M, Murata T, Tsuchiya D, Machida S, Morikawa K, Tate S. Crystal structure of human lectin-like, oxidized low-density lipoprotein receptor 1 ligand binding domain and its ligand recognition mode to OxLDL. Structure 2005;13:905-917.
20. Ishigaki T, Ohki I, Oyama T, Machida S, Morikawa K, Tate S. Purification, crystallization and preliminary X-ray analysis of the ligand-binding domain of human lectin-like oxidized low-density lipoprotein receptor 1 (LOX-1). Acta Crystallograph Sect F Struct Biol Cryst Commun 2005;61:524-527.
21. Zhang T, Huang Z, Dai Y, Chen X, Zhu P, Du G. The expression of recombinant human LOX-1 and identifying its mimic ligands by fluorescence polarization-based high throughput screening. J Biotechnol 2006;125:492-502.
22. Zhang TT, Huang ZT, Dai Y, Chen XP, Zhu P, Du GH. High-throughput fluorescence polarization method for identifying ligands of LOX-1. Acta Pharmacol Sin 2006;27:447-452.
23. Nishimura S, Akagi M, Yoshida K, Hayakawa S, Sawamura T, Munakata H, Hamanishi C. Oxidized low-density lipoprotein (ox-LDL) binding to lectin-like ox-LDL receptor-1 (LOX-1) in cultured bovine articular chondrocytes increases production of intracellular reactive oxygen species (ROS) resulting in the activation of NF-kappaB. Osteoarthritis Cartilage 2004;12:568-576.
24. Cominacini L, Pasini AF, Garbin U, Davoli A, Tosetti ML, Campagnola M, Rigoni A, Pastorino AM, Lo Cascio V, Sawamura T. Oxidized low density lipoprotein (ox-LDL) binding to ox-LDL receptor-1 in endothelial cells induces the activation of NF-kappaB through an increased production of intracellular reactive oxygen species. J Biol Chem 2000;275:12633-12638.
25. Chen XP, Xun KL, Wu Q, Zhang TT, Shi JS, Du GH. Oxidized low density lipoprotein receptor-1 mediates oxidized low density lipoprotein-induced apoptosis in human umbilical vein endothelial cells: Role of reactive oxygen species. Vascul Pharmacol 2007;47:1-9.

Therapeutic potential of heat-processed *Panax ginseng* with respect to oxidative tissue damage

Takako Yokozawa[1,*], Ki Sung Kang[1], Noriko Yamabe[1], Hyun Young Kim[2]

[1] *Institute of Natural Medicine, University of Toyama, 2630 Sugitani, Toyama, Japan;*
[2] *College of Pharmacy, Seoul National University, San 56-1, Shillim-Dong, Kwanak-gu, Seoul, Korea.*

ABSTRACT: *Panax ginseng* has been reported to exhibit a wide range of pharmacological and physiological actions. A method of heat-processing to enhance the efficacy of ginseng is well established in South Korea based on a long history of ethnopharmacological evidence. We investigated the increase in free radical-scavenging activity of *Panax ginseng* as a result of heat-processing and its active compounds related to fortified antioxidant activity. In addition, the therapeutic potential of heat-processed ginseng (HPG) with respect to oxidative tissue damage was examined using rat models. Based upon chemical and biological activity tests, the free radical-scavenging active components such as less-polar ginsenosides and maltol in *Panax ginseng* significantly increased depending on the temperature of heat-processing. According to animal experiments related to oxidative tissue damage, HPG displayed hepatoprotective action by reducing the elevated thiobarbituric acid reactive substance (TBA-RS) level, as well as nuclear factor-kappa B (NF-κB) and inducible nitric oxide synthase (iNOS) protein expressions, while increasing heme oxygenase-1 in the lipopolysaccharide-treated rat liver, and HPG also displayed renal protective action by ameliorating physiological abnormalities and reducing elevated TBA-RS, advanced glycation endproduct (AGE) levels, NF-κB, cyclooxygenase-2, iNOS, 3-nitrotyrosine, N^{ε}-(carboxymethyl)lysine, and receptors for AGE protein expression in the diabetic rat kidney. Therefore, HPG clearly has a therapeutic potential with respect to oxidative tissue damage by inhibiting protein expression related to oxidative stress and AGEs, and further investigations of active compounds are underway. This investigation of specified bioactive constituents is important for the development of scientific ginseng-derived drugs as part of ethnomedicine.

Key Words: *Panax ginseng*, heat-processing, less-polar ginsenosides, maltol, oxidative tissue damage, advanced glycation endproducts

1. Introduction

Herbs have been used for centuries to treat illness and improve health and still account for about 80% of medical treatments in the developing world, with approximately one-third of drugs being derived from plant sources (*1-3*). Since free radical-induced damage and subsequent lipid, protein, and DNA peroxidations are implicated in many kinds of human pathologies, great efforts have been made to examine various herbs or nutraceuticals in the search for therapeutic agents that safely and effectively act against oxidative stress-induced disease (*4,5*).

Panax ginseng C.A. Meyer (Araliaceae) is a medicinal herb that is mainly cultivated in Korea and Northeast China. Considered a valued medicine, it has been used in the Orient for more than 2000 years. The genus name *Panax* means 'cure-all' in Greek and as the plant is considered to be the lord or king of herbs (*6-8*). Ginseng and its components have been reported to exhibit a wide range of pharmacological and physiological actions, such as antiaging, antidiabetic, anticarcinogenic, analgesic, antipyretic, antistress, antifatigue, and tranquilizing properties, as well as the stimulation of DNA, RNA, and protein synthesis (*9-18*). These medicinal properties of ginseng have been suggested to be linked, although not totally, to ginseng's action to protect against free radical attack (*19-23*).

Although traditional Chinese medicine and many current research studies often use products that combine ginseng with other medicinal herbs or vitamins, a method of heat-processing to enhance the efficacy of ginseng is well established in Korea based

**Correspondence to:* Institute of Natural Medicine, University of Toyama, 2630 Sugitani, Toyama 930-0194, Japan;
e-mail: yokozawa@inm.u-toyama.ac.jp

Received June 2, 2007
Accepted June 16, 2007

on its long history of ethnopharmacological evidence (*24-28*). In his book, Xu-Jing, an attendant to a special envoy of the Chinese Emperor to Korea, described two kinds of ginseng products in Korea, sun-dried and steamed ginseng, in 1123. *Panax ginseng* cultivated in Korea is harvested after 4 to 6 years of cultivation and is classified into three types depending on how it is processed. Fresh ginseng can be consumed in an unprocessed state. White ginseng (WG, harvested when 4-6 years old) is dried ginseng root after peeling. Red ginseng (RG, harvested when 6 years old) is ginseng root steamed at 98-100°C without peeling (Figure 1) (*6-8,29*).

Generally, RG is more common as a medicinal herb than WG in Asia because steaming induces changes in the chemical constituents and enhances the biological activity of ginseng (*8,29-31*). On the other hand, a novel heat-processing method in which ginseng is autoclaved at a higher temperature than RG was recently developed to achieve an even stronger activity than that of RG, and this ginseng product was termed heat-processed ginseng (HPG, Figure 1) (*25,32,33*). HPG has been reported to exhibit more potent pharmacological activities, such as vasorelaxation, anxiolytic-like activity, antioxidant activity, and antitumor activity, than conventional WG or RG (*32,34-37*).

Based upon this evidence, this study investigated the increase in free radical-scavenging activity of *Panax ginseng* as a result of heat-processing and its active compounds related to enhanced antioxidant activity. In addition, the therapeutic potential of HPG with respect to oxidative tissue damage was examined using rat models. The aim of this paper was to review scientific evidence underlying the therapeutic potential of HPG with respect to oxidative tissue damage, which should prove helpful in understanding the complex efficacy changes of ginseng brought about by heat-processing.

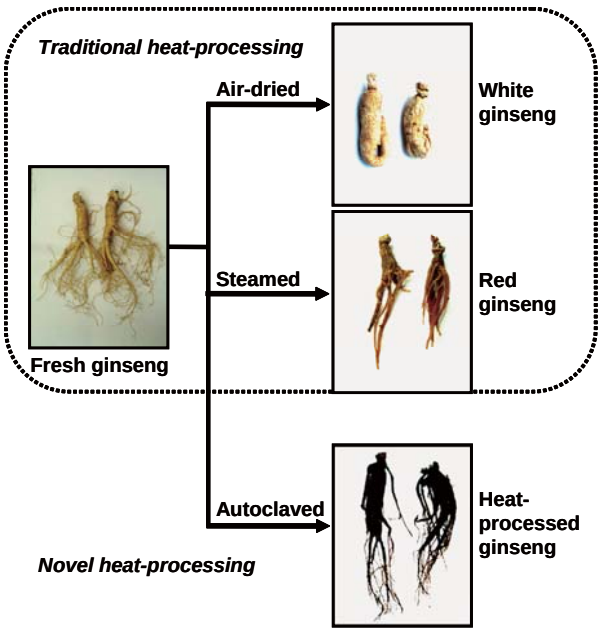

Figure 1. Classification of *Panax ginseng* by heat-processing methods.

2. Increase in the free radical-scavenging activity of ginseng as a result of heat-processing

Reactive oxygen metabolites, including free radicals such as nitric oxide ($^{\bullet}NO$), superoxide anion ($O_2^{\bullet-}$), hydroxyl radical (•OH), and peroxynitrite ($ONOO^-$), are toxic and play an important role in tissue injury (*38-41*). $O_2^{\bullet-}$ reacts rapidly with $^{\bullet}NO$ to produce the more toxic $ONOO^-$. $ONOO^-$ is protonated and forms peroxynitrous acid (ONOOH) under physiological conditions, and ONOOH easily decays to yield strong oxidants such as nitrogen dioxide, nitryl cations, and •OH. $ONOO^-$ and its decomposition products contribute to antioxidant depletion, alterations of protein structure, and oxidative damage observed in human disease (*42-45*). As antioxidants may attenuate oxidative damage by free radical-scavenging or metal chelation, many studies have been performed to identify medicinal herbs' potential action to protect against free radical attack.

Ginseng extract is known to exhibit free radical-scavenging activity with respect to radicals such as 1,1-diphenyl-2-picrylhydrazyl (DPPH), carbon-centered radical, $O_2^{\bullet-}$, $ONOO^-$, and •OH. Although there have been many reports on ginseng's action to protect against free radical attack, ginseng has been found to possess no $^{\bullet}NO$-scavenging activity (*20,32,46*). According to the authors' own *in vitro* studies of free radical-scavenging activity with WG, RG, and HPG (*37,47*), WG had no or little effect on $^{\bullet}NO$-scavenging activity but RG and HPG displayed stronger inhibitory effects than WG, as shown in Figure 2A. In addition, HPG exhibited greater $O_2^{\bullet-}$-scavenging activity than WG and RG; however, there was no difference in the $O_2^{\bullet-}$-scavenging activity of WG and RG (Figure 2B). In particular, HPG effectively scavenged $ONOO^-$ and •OH in a concentration-dependent manner, as shown in Figure 2C and D. Therefore, the free radical-scavenging activity of ginseng increased as a result of heat-processing (*37,47*), and HPG is suggested to have stronger action to protect against reactive oxygen species (ROS) related to tissue damage than conventional ginseng products.

3. Identification of free radical-scavenging active components of HPG

Although the beneficial effects of ginseng with respect to free radical attack and their enhancement by heat-processing have been well documented, the quality of ginseng is important to ensure its safety and efficacy (*48*). The contents of ginseng change with the cultivation period, location, harvesting time, or the parts utilized, and there are wide variations in pharmacological activity and components such as ginsenoside in the ginseng (*49-51*). The employment

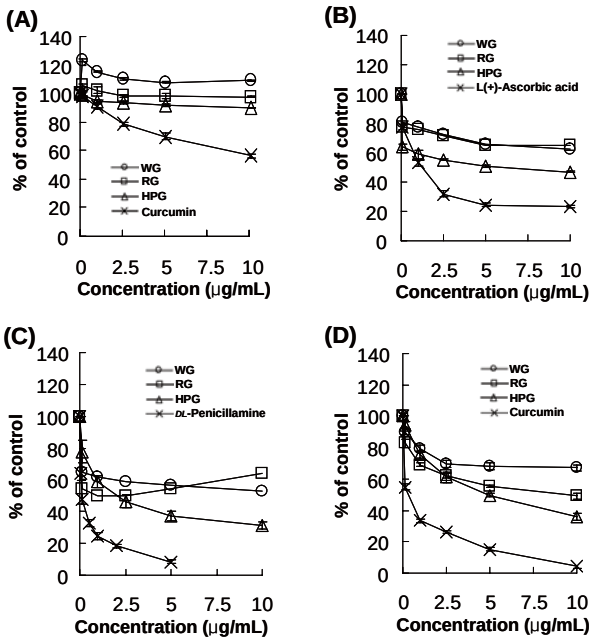

Figure 2. Effects of ginsengs on (A) $^{\bullet}NO$, (B) $O_2^{\bullet-}$, (C) $ONOO^-$, and (D) •OH production.

of standardized extracts of ginseng with specified bioactive constituents has been suggested to be the first step in assessing its efficacy and safety and ensuring optimal quality control of ginseng products (*23*). Therefore, the active components of ginseng produced by heat-processing were investigated by elucidating changes in chemical and free radical-scavenging activity.

3.1. Changes in the chemical and free radical-scavenging activity of ginsenosides

Ginsenosides, unique constituents of ginseng, are glycosides of thirty carbon derivatives of the triterpenoid dammarane, as shown in Figure 3. They have a hydrophobic four-ring steroid-like structure with hydrophilic sugar moieties. About 30 different types of ginsenosides have been isolated and identified from the root of *Panax ginseng*. Each also has at least two (carbon-3 and -20) or three (carbon-3, -6 and -20) hydroxyl groups, which are free or bound to monomeric, dimeric, or trimeric sugars (*6*,*52*).

The HPLC profile of each prepared ginseng extract is illustrated in Figure 4. WG shows typical ginsenosides consisting of Re, Rg_1, Rb_1, Rc, and Rb_2. In the case of RG, the contents of polar ginsenosides (peaks 1 and 2) decreased slightly and less-polar ginsenosides (peaks 5-8) increased. Moreover, major polar ginsenosides (peaks 1-4) in WG decreased greatly and less-polar ginsenosides (peaks 5-10) became major constituents in HPG. This elevation in the content of less-polar ginsenosides was also shown in a heat-processing model experiment using glycine-Rb_2 (Figure 5 and 6), that is, Rb_2 was gradually changed into 20(*S*)-Rg_3, 20(*R*)-Rg_3, Rk_1, and Rg_5 by heat-processing at 100 and 120°C (Figure 5) (*53*). 20(*R*)-ginsenosides and 20(*S*)-

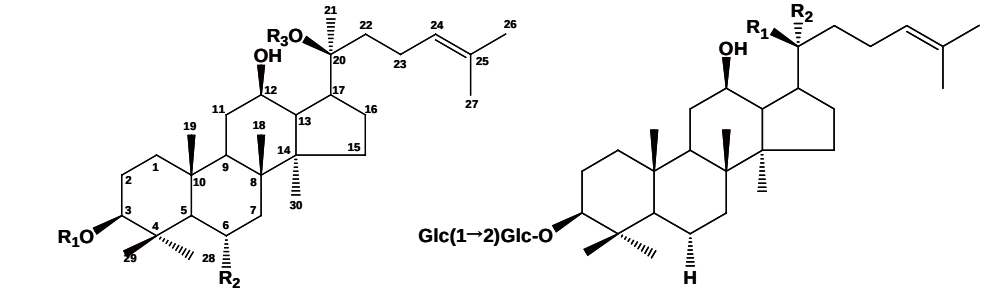

Rb_1 : R_1 = Glc(2←1)Glc, R_2 = H, R_3 = Glc(6←1)Glc
Rb_2 : R_1 = Glc(2←1)Glc, R_2 = H, R_3 = Glc(6←1)Ara(p)
Rc : R_1 = Glc(2←1)Glc, R_2 = H, R_3 = Glc(6←1)Ara(f)
Rd : R_1 = Glc(2←1)Glc, R_2 = H, R_3 = Glc
Re : R_1 = H, R_2 = O-Glc(2←1)Rha, R_3 = Glc
Rg_1 : R_1 = H, R_2 = O-Glc, R_3 = Glc

20(*R*)-Rg_3 : R_1 = CH_3, R_2 = OH
20(*S*)-Rg_3 : R_1 = OH, R_2 = CH_3

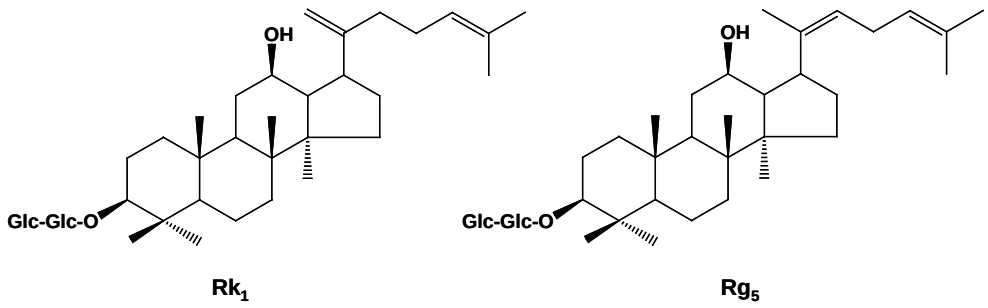

Figure 3. Structures of ginsenosides. –Glc: *D*-glucopyranosyl, -Rha: *L*-rhamnopyranosyl, -Ara(p): *L*-arabinopyranosyl, -Ara(f): *L*-arabinofuranosyl.

ginsenosides are epimers of each other depending on the position of the hydroxyl group on carbon-20. This epimerization is known to occur by the selective attack of the hydroxyl group after the elimination of a glycosyl residue at carbon-20 during the steaming process (*6*,*52*). In addition, more less-polar ginsenosides such as Rk_1 and Rg_5 are known to be easily produced by the elimination of H_2O at carbon-20 of Rg_3 under high pressure and temperature conditions, like in autoclaving

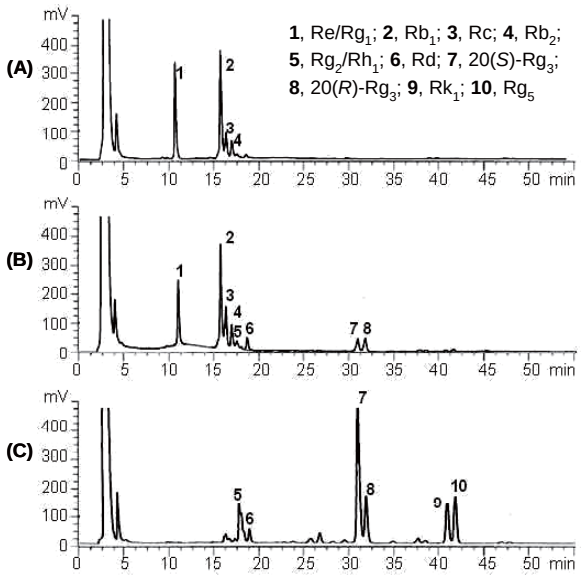

Figure 4. HPLC-ELSD chromatogram of the total ginsenoside fractions of (A) WG, (B) RG, and (C) HPG.

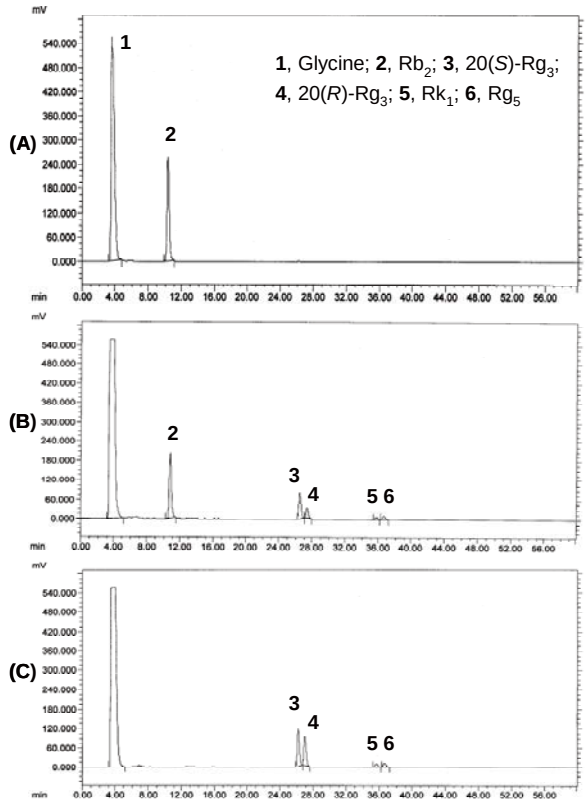

Figure 5. HPLC chromatograms of (A) glycine-Rb_2 mixture, (B) glycine-Rb_2 mixture steamed at 100°C for 3 h, and (C) glycine-Rb_2 mixture steamed at 120°C for 3 h.

(Figure 6) (*25*).

Despite the long history of ginseng research, there have been virtually no *in vitro* reports describing the direct free radical-scavenging mechanisms of ginsenosides. Table 1 shows the •NO-scavenging activity of ginsenoside-Re, Rg_1, Rb_1, 20(*S*)-Rg_3, 20(*R*)-Rg_3, Rk_1, and Rg_5, but no ginsenosides displayed •NO-scavenging activity or increased •NO generation in high concentrations (*47*). However, the *n*-BuOH fraction, mainly consisting of ginsenosides, displayed the strongest activity based on •OH-scavenging activity-guided fractionation of HPG when determined with an electron spin resonance spectrometer (ESR) (Figure 7). The *n*-BuOH fraction was analyzed by HPLC (Figure 8A), and relatively high contents of four ginsenosides, 20(*S*)-Rg_3 32.8%, 20(*R*)-Rg_3 7.3%, Rk_1 15.7%, and Rg_5 18.6%, were detected and isolated, all known to be major ginsenoside constituents of HPG (*32*,*33*). Among them, 20(*S*)-Rg_3 displayed the strongest activity, and the next were, in decreasing order, Rg_5, 20(*R*)-Rg_3, and Rk_1 at a concentration of 0.5% (Figure 8B). Therefore, 20(*S*)-Rg_3 and Rg_5 were suggested to be the main •OH-scavenging active components of HPG (*53*,*54*).

According to the correlation between the structure

Table 1. Effects of ginsenosides on •NO production

Material	Concentration (μg/mL)	•NO (μM)	Production %
Re	12.5	13.6 ± 0.1	101.9
	25	13.5 ± 0.3	101.3
	50	13.6 ± 0.3	102.4
	125	14.6 ± 0.2[c]	109.9
	250	15.1 ± 0.1[c]	113.5
Rg_1	12.5	13.7 ± 0.2[b]	103.1
	25	13.9 ± 0.2[c]	104.6
	50	14.9 ± 0.1[c]	111.9
	125	15.5 ± 0.1[c]	116.8
	250	16.7 ± 0.1[c]	125.8
Rb_1	12.5	13.1 ± 0.1	98.5
	25	13.6 ± 0.1	102.2
	50	14.0 ± 0.1[c]	105.1
	125	15.3 ± 0.2[c]	115.2
	250	16.6 ± 0.1[c]	124.7
20(*S*)-Rg_3	12.5	12.5 ± 0.2[c]	94.0
	25	13.1 ± 0.1	98.8
	50	13.7 ± 0.3[c]	102.9
	125	14.4 ± 0.1[c]	108.4
	250	15.5 ± 0.1[c]	112.5
20(*R*)-Rg_3	12.5	12.9 ± 0.2	96.7
	25	13.0 ± 0.1	97.5
	50	14.1 ± 0.1[c]	106.4
	125	14.7 ± 0.1[c]	110.4
	250	15.5 ± 0.2[c]	116.9
Rk_1	12.5	14.4 ± 0.2[c]	108.2
	25	14.1 ± 0.2[c]	105.8
	50	14.3 ± 0.4[c]	107.7
	125	14.2 ± 0.3[c]	106.4
	250	13.9 ± 0.4[a]	104.2
Rg_5	12.5	13.7 ± 0.1[a]	102.8
	25	13.0 ± 0.3	97.9
	50	13.0 ± 0.1	97.8
	125	13.5 ± 0.1	101.5
	250	14.4 ± 0.1[c]	108.1
Control	-	13.3 ± 0.3	100.0

Significance: [a]$p < 0.05$, [b]$p < 0.01$, [c]$p < 0.001$ compared with control values.

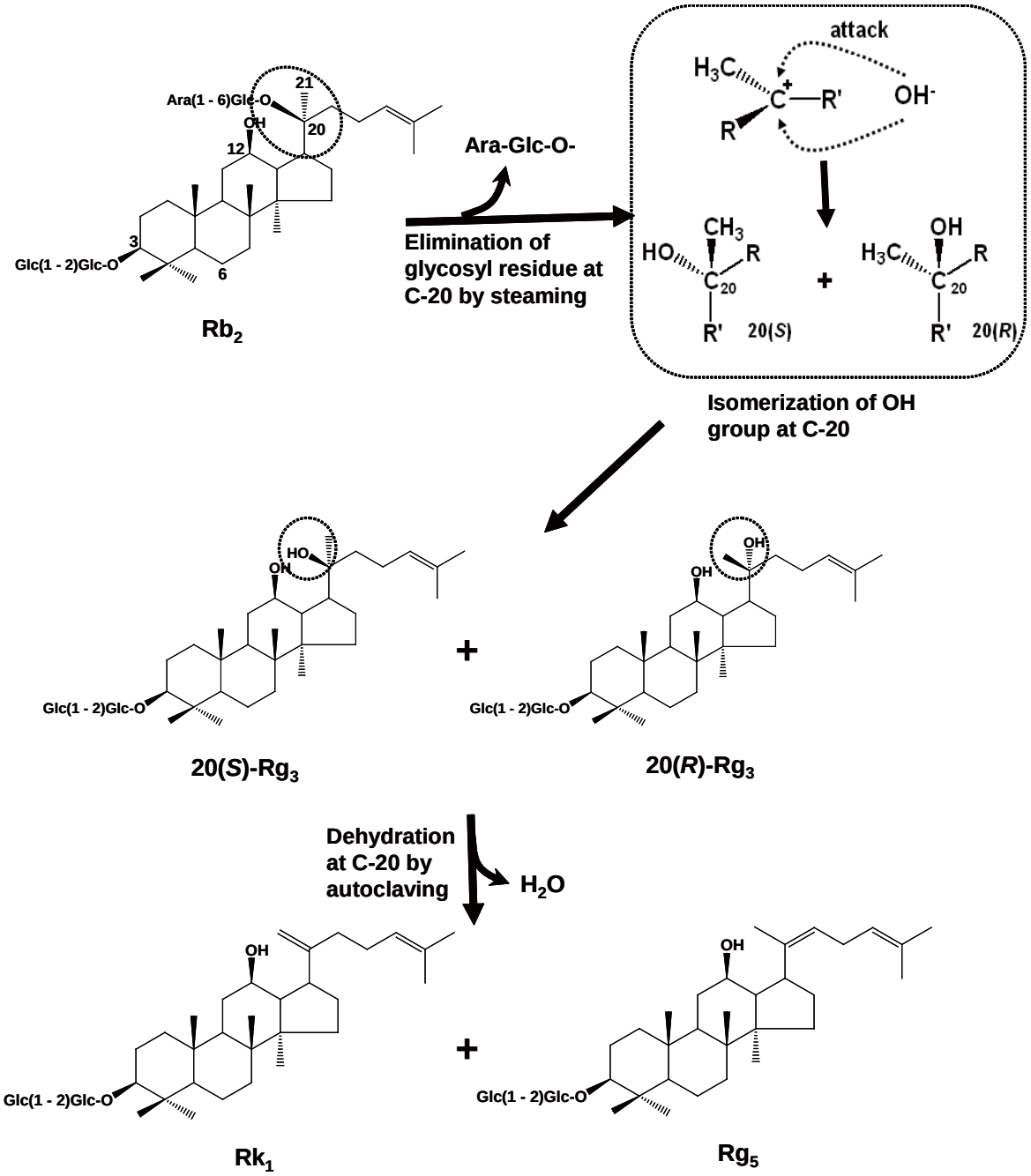

Figure 6. Structural changes of ginsenoside Rb_2 brought about by heat-processing. –Glc, *D*-glucopyranosyl; -Ara, *L*-arabinopyranosyl.

and •OH-scavenging activity of ginsenosides (Rb_1, Rb_2, Rc, Rd, Re, Rg_1, 20(*S*)-Rg_3, 20(*R*)-Rg_3) isolated from *Panax ginseng*, 20(*S*)-Rg_3 displayed the strongest activity, and the next were, in decreasing order, Rb_1, Rg_1, and Rc (Figure 9A). These ginsenosides (2 mM) displayed inhibitory activity with respect to •OH generation 50% greater than that of the control. The other ginsenosides such as Rb_2 and Rd displayed comparably lower activity, and Re and 20(*R*)-Rg_3 exhibited no significant inhibition (Figure 9A). The difference in the structures of ginsenosides is solely due to the position and type of sugar moieties connected to the ring of the triterpenoid dammarane, and this mutual interaction was suggested to play an important role in the antioxidant effects of ginsenosides (*55*).

•OH-scavenging can be accomplished by direct scavenging or *via* the prevention of •OH formation through the chelation of free metal ions or conversion of H_2O_2 to other harmless compounds (*56*). Several ginsenosides used in this study displayed no or weak H_2O_2- and DPPH radical-scavenging activity at a concentration of 2 mM based on preliminary studies (unpublished). Based on the ferrous metal ion-chelating activity tests of several ginsenosides, the •OH-scavenging mechanism of ginsenosides was related more to their transition metal-chelating activity than *via* the direct scavenging of free radicals (Figure 9) (*57*). As weakly •OH-scavenging Rb_2 was gradually changed into strongly •OH-scavenging 20(*S*)-Rg_3 and Rg_5 by heat-processing (Figure 6), the

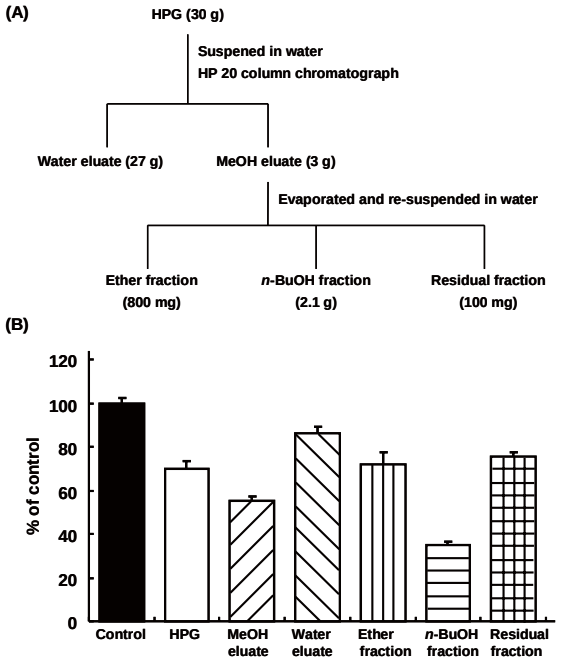

Figure 7. (A) Fractionation of HPG extract. (B) The graph compares the effects of HPG and its fractions (1 mg/mL) on •OH production.

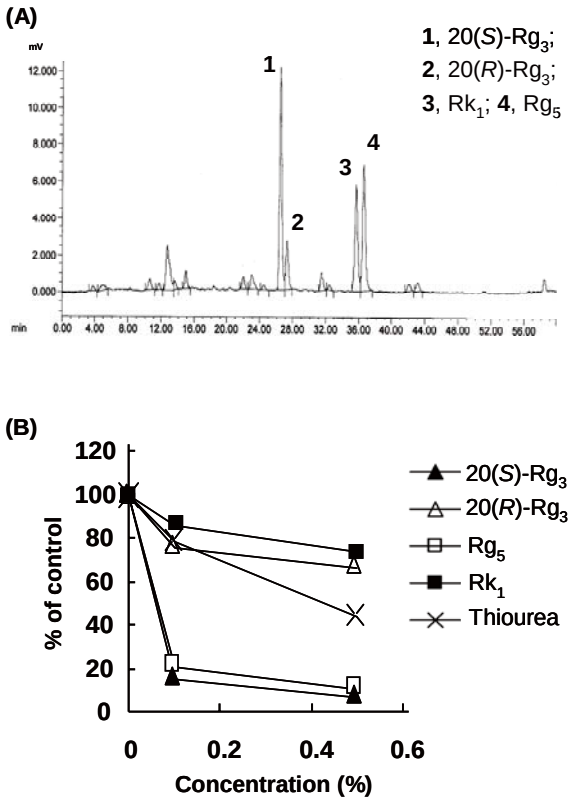

Figure 8. (A) HPLC chromatogram of *n*-BuOH fraction of HPG. (B) The graph compares the effects of less-polar ginsenosides on •OH production.

chemical changes of ginsenosides are thought to be pivotal to enhancing the antioxidant activity of ginseng by ferrous metal ion-chelating activity, and dietary nutrients containing metal chelators have received much attention because of their preventive antioxidant activity (*38*,*41*,*58*).

3.2. Changes in the chemical and free radical-scavenging activity of phenolic acids and maltol

In general, the main pharmacologically active constituents of ginseng are believed to be ginsenosides, but researchers also have investigated phenolic compounds as bioactive constituents of ginseng (*59*,*60*). Phenolic compounds are commonly found in plants, and they have been reported to exhibit multiple biological effects, including antioxidant activity. Many studies have revealed that the phenolic content of plants can be correlated with their antioxidant activity (*61*,*62*). In addition, the free radical-scavenging activity of ginsenosides was, according to previous research, limited to •OH by ferrous metal ion-chelating activity (*53*,*54*,*57*), which fails to explain the increased $^{\bullet}$NO-, $O_2^{\bullet-}$-, and $ONOO^-$-scavenging activity of ginseng as a result of heat-processing with only ginsenosides. However, the highly reactive $ONOO^-$-scavenging ability of HPG was closely related to its ether fraction containing phenolic compounds based on $ONOO^-$-scavenging activity-guided fractionation of HPG (Figure 7A) (unpublished). Therefore, focus was turned to the phenolic compounds of ginseng, *i.e.* non-saponin components such as salicylic acid, vanillic acid, *p*-coumaric acid, and maltol (Figure 10). They are also known to be the principal antioxidant components of WG and RG (*59*,*60*).

Based on GC-MS analyses of ginseng extracts, four compounds were detected in the order of increasing retention time: maltol, salicylic acid, vanillic acid, and *p*-coumaric acid (Figure 11). Maltol was found to be the compound increased most by heat-processing in comparison to the other 3 phenolic acids. In the case of phenolic acids, their contents increased in RG in comparison to those in WG (Table 2). The *p*-coumaric and vanillic acid content is known to be greater in RG than in WG (*63*); however, the contents of these compounds did not continuously increase in HPG. The decreases in some phenolic content in HPG were thought to be caused by thermal decomposition or structural changes in phenolic compounds under high pressure and temperature conditions. In particular, salicylic acid easily decomposes thermally and has a propensity to undergo hydroxylation (*64*,*65*), and the level of total phenolic compounds has been reported to decrease with heat treatment in malt (*66*). Although there were changes in the content of salicylic, vanillic,

Table 2. Quantity of maltol and phenolic acids in WG, RG, and HPG (mg/100 g)

	WG	RG	HPG
Maltol	2.6	10.7	94.0
Salicylic acid	0.1	1.6	0.4
Vanillic acid	0.4	1.0	0.6
p-Coumaric acid	0.5	0.6	0.4

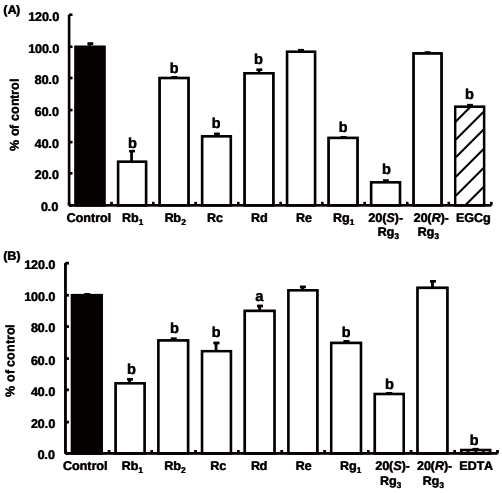

Figure 9. Comparisons of (A) •OH-scavenging and (B) ferrous metal ion-chelating activity of ginsenosides at 2 mM. $^{a}p < 0.01$, $^{b}p < 0.001$ in comparison to control values.

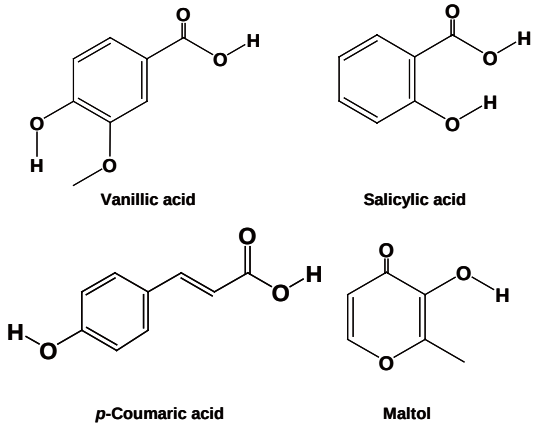

Figure 10. Structures of phenolic compounds and maltol.

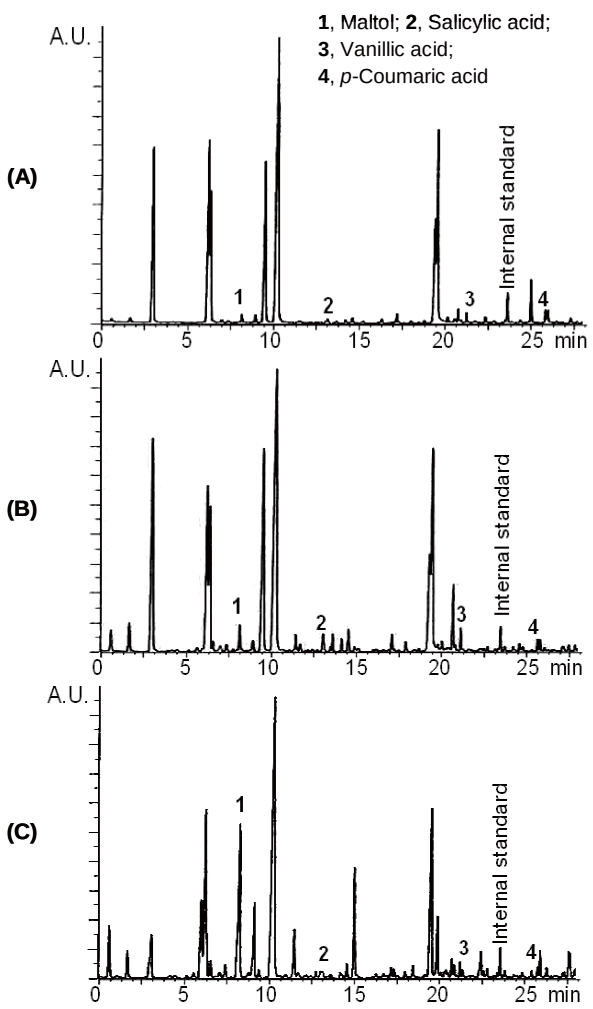

Figure 11. GC-MS chromatograms of phenolic fractions of (A) WG, (B) RG, and (C) HPG.

and *p*-coumaric acids in WG, RG, and HPG, these were considerably fewer than those of maltol (Table 2).

When each phenolic compound and maltol (10 μg/mL) were added, vanillic acid displayed the strongest $^{\bullet}$NO-scavenging activity, and the next was *p*-coumaric acid, but salicylic acid and maltol exhibited no activity (Figure 12A). Similarly, vanillic acid displayed the strongest $O_2^{\bullet -}$-scavenging activity, and the next were, in decreasing order, salicylic acid, maltol, and *p*-coumaric acid (Figure 12B). Vanillic acid, maltol, and *p*-coumaric acid displayed strong $ONOO^-$-scavenging activity, but the effect of salicylic acid decreased with the increase in concentration (Figure 12C). In particular, highly toxic •OH production was reduced to 13.1, 13.2, 39.0, and 74.2% of the control value by maltol, *p*-coumaric acid, vanillic acid, and salicylic acid, respectively (Figure 12D). The free radical-scavenging activity of phenolic compounds in ginseng was in accordance with the reported structure and activity relationships of simple phenolic acids. The number and position of hydroxyl groups or hydrogen-donating groups in the phenolic molecular structures affect their antioxidant activity (*37*,*47*,*65*). On the other hand, the strong $ONOO^-$- and •OH-scavenging activity of maltol was thought to result from ferrous metal ion-chelating action owing to its hydroxyketone structure (*67*).

Based on the quantitative analysis of phenolic contents and radical-scavenging activity tests, maltol was the main free radical-scavenging component of HPG among the 4 principal antioxidant phenolic compounds in ginseng. However, this fails to explain the free radical-scavenging activity of HPG with only phenolic acids and maltol. The most convincing proposal involves Maillard reaction products (MRPs), thought to be the major components in various crude drugs or foods that correlated with enhanced free radical-scavenging activity as a result of heat treatment. MRPs in ginseng were reported to increase as a result of heat-processing; these compounds are arg-fru-glc, arg-fru, maltol, maltol-3-*O*-β-*D*-glucoside, and so on (*68*,*69*). A detailed study of MRPs in HPG has not been conducted yet, but maltol is a typical marker of the Maillard reaction (*70*). Therefore, further studies of free radical-scavenging active components such as MRPs or new products generated during heat-processing are

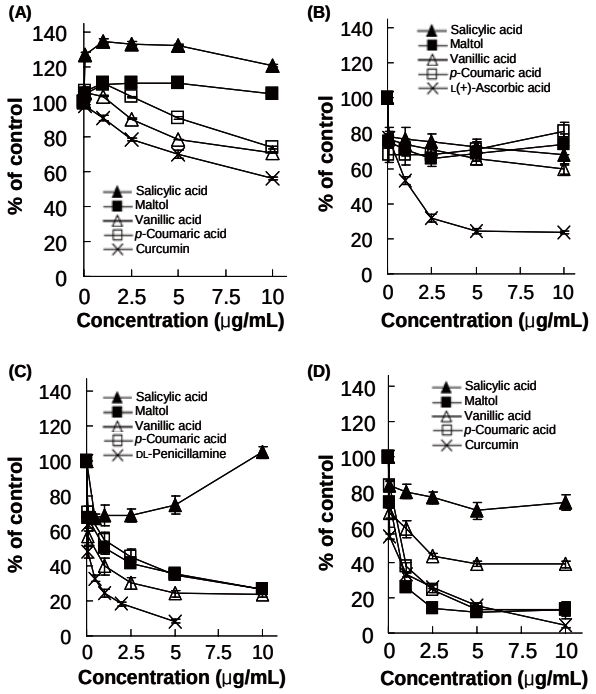

Figure 12. Effects of phenolic compounds on (A) $^{\bullet}NO$, (B) $O_2^{\bullet-}$, (C) $ONOO^-$, and (D) $\bullet OH$ productions.

underway.

4. HPG's protective action against lipopolysaccharide (LPS)-induced hepatic damage

LPS has been shown to increase the constitutive release of $^{\bullet}NO$ by the endothelium and the activity of inducible nitric oxide synthase (iNOS) (*71,72*). In addition, $^{\bullet}NO$ stimulates H_2O_2 and $O_2^{\bullet-}$ production by mitochondria (*73*), and, in turn, these ROS participate in the up-regulation of iNOS expression *via* nuclear factor-kappa B (NF-κB) activation (*74,75*). NF-κB is normally present in the cytoplasm of eukaryotic cells as an inactive complex with the inhibitory protein, IκB. When cells are exposed to various external stimuli, such as ROS or LPS, IκB undergoes rapid phosphorylation with subsequent ubiquitination, leading to the proteosome-mediated degradation of this inhibitor. The functionally active NF-κB exists mainly as a heterodimer consisting of subunits of the Rel family (*e.g.*, Rel A or p65, p50, p52, c-Rel, v-Rel, and Rel B) and translocates to the nucleus, where it binds to specific consensus sequences in the promoter or enhancer regions of target genes, thereby altering their expression (*74,76-78*). ROS also cause the peroxidation of membrane phospholipids, which can alter membrane fluidity and lead to the loss of cellular integrity. Thus, the impaired activity of mitochondrial enzymes leads to decreased energy levels and failure of organs such as of the heart, kidney, lung, and liver (*42,79*). On the other hand, heme oxygenase-1 (HO-1) is believed to play an important role in attenuating tissue injury caused by inflammatory stimuli, and the up-regulation of HO-1 has been shown to protect against LPS-induced cardiovascular collapse or liver damage (*80,81*).

Among the major organs affected by LPS toxicity, the liver plays an important physiological role in LPS detoxification (*82,83*). In addition, there has been growing interest regarding the effects of RG-specific ginsenosides on hepatotoxicity and the antioxidative enzyme activity of the liver because the metabolites of ginsenosides are known to be esterified with fatty acid in the liver without structural variation, and the esterified metabolites accumulate in the liver (*84-87*). Therefore, the effect of HPG, which has increased RG-specific ginsenoside content, on LPS-induced liver injury in rats was examined to identify its hepatoprotective action.

To examine the hepatoprotective action of HPG, male Wistar rats were divided into four groups while avoiding any inter-group differences in body weight. The control groups were given water, while the other groups were orally administered HPG extracts at a dose of 50 or 100 mg/kg body weight daily using a stomach tube. After 15 consecutive days of administration, the rats were given intravenous LPS (from *Escherichia coli* serotype 055: B5, Sigma Chemical Co., USA), at 5 mg/kg body weight. At 6 h after the LPS challenge, the rats were sacrificed, and blood and liver samples were collected.

As shown in Table 3, there was a significantly elevated serum nitrite/nitrate (NO_2^-/NO_3^-) level in LPS-treated control rats. However, HPG administration either failed to ameliorate or only slightly (not significantly) increased this increased level. The fact that the administration of ginseng increases the serum

Table 3. NO_2^-/NO_3^- level of serum

Group	Dose (mg/kg body weight/day)	NO_2^-/NO_3^- (μM)
Normal	-	0.3 ± 0.2
LPS treatment		
Control	-	216.5 ± 1.0[a]
HPG	50	217.4 ± 0.7[a]
HPG	100	223.5 ± 0.1[a]

Values are the mean ± SE, [a]$p < 0.001$ compared with normal rats.

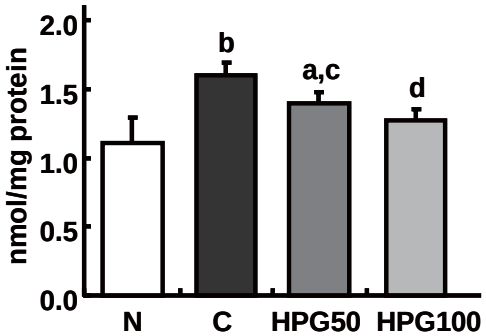

Figure 13. TBA-RS levels in hepatic mitochondria. N, normal rats; C, LPS-treated control rats; HPG50, HPG (50 mg/kg body weight/day)-administered and LPS-treated; HPG100, HPG (100 mg/kg body weight/day)-administered and LPS-treated. [a]$p < 0.01$, [b]$p < 0.001$ *vs.* normal rats; [c]$p < 0.05$, [d]$p < 0.001$ *vs.* LPS-treated control rats.

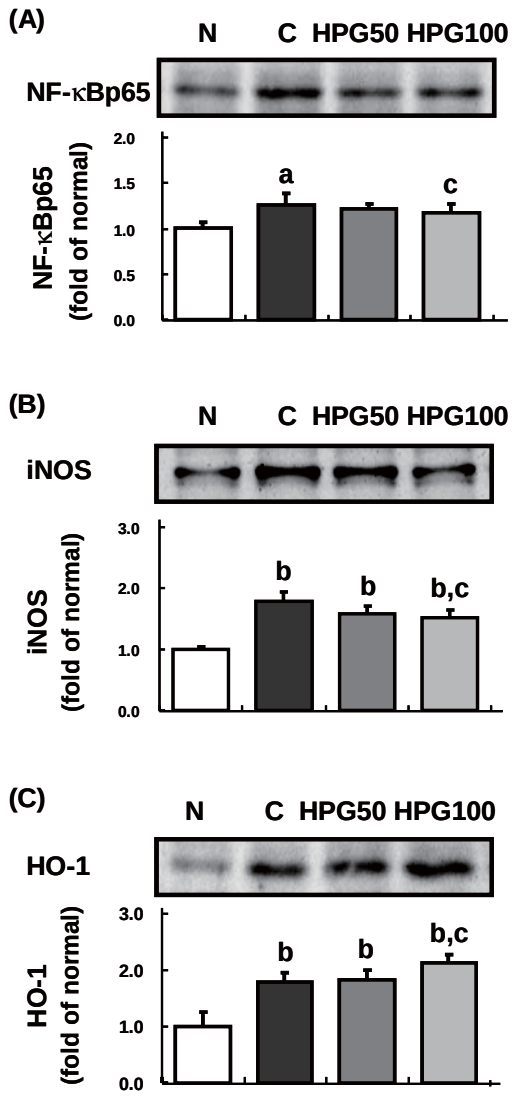

Figure 14. Effects of HPG on (A) NF-κBp65, (B) iNOS, and (C) HO-1 expressions. N, normal rats; C, LPS-treated control rats; HPG50, HPG (50 mg/kg body weight/day)-administered and LPS-treated; HPG100, HPG (100 mg/kg body weight/day)-administered and LPS-treated. $^{a}p < 0.05$, $^{b}p < 0.001$ in comparison to normal rats; $^{c}p < 0.05$ in comparison to LPS-treated control rats.

NO_2^-/NO_3^- level related to vascular relaxation has been well documented (*88,89*), and the slightly increased serum NO_2^-/NO_3^- level of HPG-administered groups in this study was also thought to have been due to the same reason.

Figure 13 shows the thiobarbituric acid reactive substance (TBA-RS) level of hepatic mitochondria, implying an index of endogenous lipid peroxidation caused by oxidative stresses. The TBA-RS level in control rats was significantly higher than that in normal rats, but it was reduced by HPG administrations in a dose-dependent manner. This amelioration of the TBA-RS level suggests the protective effect of HPG on hepatic mitochondria and its function. In addition, Figure 14 shows Western blot analyses in liver tissues related to oxidative stress. The oxidative stress-related proteins NF-κB, iNOS, and HO-1 are up-regulated in the liver during LPS challenge but have opposite roles. That is, down-regulation of NF-κB and iNOS suggests a hepatoprotective effect, but HO-1 is known to exhibit a protective role *via* up-regulation (*72,79,81*). The NF-κBp65 and iNOS levels in the LPS-treated control rats were significantly higher than those of normal rats, but these elevated levels were reduced by HPG administrations in a dose-dependent manner. Although iNOS is well known to be regulated by NF-κB (*75,76*), the deactivation of NF-κBp65 by HPG administration was thought to be too weak to have much of a significant effect on the inhibition of iNOS. Otherwise, the effect of HPG might be involved in transcriptional factors other than NF-κBp65 and post-transcriptional cytokines related to the induction of iNOS (*79*). Therefore, inhibition of the elevated iNOS level was thought to be partially related to the deactivation of NF-κBp65 as a result of HPG administration. On the other hand, the HO-1 level in LPS-treated control rats was significantly higher than that in normal rats, and it was more significantly up-regulated by the 100 mg/kg body weight/day of HPG administration. This differential modulation of iNOS and HO-1 by HPG administration appears to have a protective effect against oxidative stress in accordance with the hepatoprotective effect of ketamine on LPS-induced hepatic injury in rats (*81*). On the other hand, the anti-inflammatory effect of 20(*S*)-protopanaxadiol (20(*S*)-PPD), a metabolite of ginsenoside, was suggested to be mediated by the inactivation of NF-κB, suppression of iNOS, and induction of HO-1 (*90*) based on the study of the effect of 20(*S*)-PPD on LPS-induced RAW 264.7 cells. In addition, maltol was suggested to be a functional agent that prevents oxidative damage in the brain of mice by reducing increased TBA-RS levels (*91*). Although the synergetic antioxidant effects of multiple constituents of HPG cannot be ignored, HPG clearly has an antioxidant effect on liver injury related to acute oxidative stress, and this activity may be related to the increase in antioxidant components as a result of heat-processing (*92*).

5. HPG's action to protect against streptozotocin (STZ)-induced diabetic renal damage

Diabetes mellitus is characterized by hyperglycemia. An abnormally elevated blood glucose level causes oxidative stress and the formation of advanced glycation endproducts (AGEs), which have been closely linked to diabetic complications such as neuropathy, retinopathy, and nephropathy (*78,93*). In particular, diabetics are at increased risk for several types of kidney disease, and the predominant cause of end-stage renal disease in this disorder is diabetic nephropathy (*94,95*). Many attempts have been made to improve the treatment of diabetes. Various kinds of hypoglycemic drugs or insulin are now available for the control of hyperglycemia, but modern medicine offers

no satisfactory therapy without undesirable side effects or contraindications (*96*). Prevention of the occurrence and progression of diabetic nephropathy is crucial. Therefore, great effort has been focused on finding a novel therapeutic agent for diabetic nephropathy in traditional and herbal medicines that produce no toxic effects (*97-100*).

Antioxidants are known to protect against glycation-derived free radicals and may have a therapeutic potential (*78,93*). HPG displayed stronger $^{\bullet}NO$-, $O_2^{\bullet -}$-, $ONOO^-$-, and •OH-scavenging activity than WG and RG, as mentioned above. However, there are virtually no reports concerning the effect of HPG on diabetic oxidative stress, and the enhanced radical-scavenging activity of HPG is thought to be beneficial with respect to diabetic oxidative damage caused by hyperglycemia. Therefore, HPG's protective action against renal damage caused by oxidative stress or the formation of AGEs in diabetes and its molecular biological mechanism were investigated.

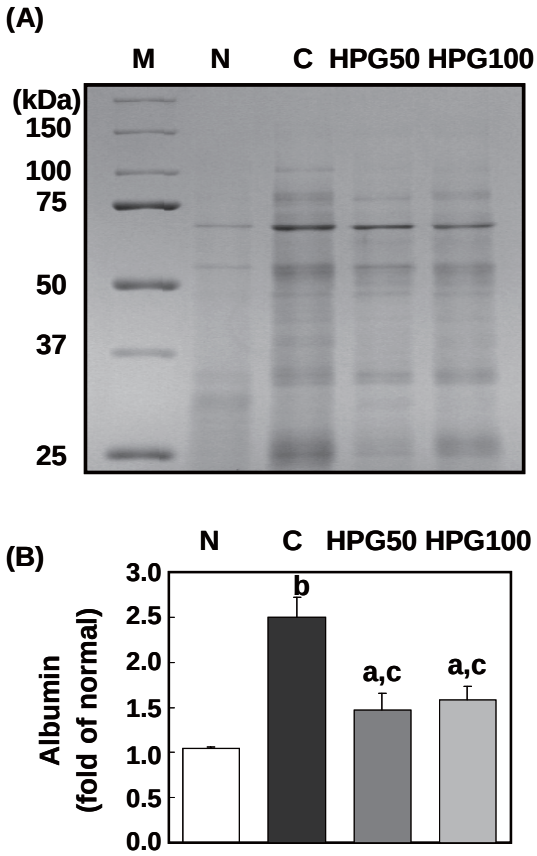

Figure 15. SDS-PAGE pattern of urinary protein. M, protein marker; N, normal rats; C, diabetic control rats; HPG50, diabetic rats treated with HPG (50 mg/kg BW/day); HPG100, diabetic rats treated with HPG (100 mg/kg BW/day). $^{a}p < 0.05$, $^{b}p < 0.001$ in comparison to normal rats; $^{c}p < 0.01$ in comparison to diabetic control rats.

To obtain Type 1 (insulin dependent) diabetic rats, STZ (50 mg/kg body weight) was injected intraperitoneally into male Wistar rats. Ten days after the injection, the glucose level of blood from the tail vein was determined and the rats were divided into three groups, avoiding any inter-group differences in blood glucose levels and body weights. The control group was given water, while the other groups were given an HPG extract orally at a dose of 50 or 100 mg/kg body weight daily using a stomach tube. After administration for 15 consecutive days, urine, blood, and kidneys were collected.

The destruction of β-cells and disorder of insulin secretion in the diabetic state causes physico-metabolic abnormalities such as a decrease in body weight gain and increases in food and water intake and urine volume. The STZ-induced diabetic rats in this study also displayed these changes. However, HPG administration significantly reduced water intake and urine excretion levels, suggesting that HPG would improve the physiological abnormalities associated with diabetes (Table 4).

Hyperglycemia, a primary characteristic of diabetes, is mainly attributed to diabetic oxidative stress caused by several factors. Hyperglycemia leads to the overproduction of free radicals by the nonenzymatic glycation of proteins through the Maillard reaction, and these free radicals exert deleterious effects on the function of β-cells vulnerable to oxidative stress (*101,102*). In addition, hyperglycemia can degrade antioxidant enzyme defences, thereby allowing ROS to cause cellular and tissue damage. As shown in Table 5, the blood glucose levels in diabetic rats significantly decreased in rats fed HPG at a dose of 100 mg. In addition, among the renal function parameters, HPG administration reduced the abnormally increased urinary albumin level in diabetic rats (Figure 15). The urinary protein level slightly increased in diabetic rats but was significantly reduced by HPG administrations. On the other hand, there were no remarkable ameliorations in serum urea nitrogen and creatinine clearance (Ccr) levels (Table 5). The sign of early diabetic nephropathy is an increased urinary albumin level, and advanced diabetic nephropathy is characterized by proteinuria and decreasing Ccr levels (*103*). Therefore, early

Table 4. Physico-metabolic symptoms

Group	Dose (mg/kg BW/day)	Body weight (initial, g)	Body weight (final, g)	Body weight (gain, g)	Food intake (g/day)	Water intake (mL/day)	Urine volume (mL/day)
Normal	-	239.2 ± 3.6	313.3 ± 11.0	72.8 ± 6.6	18.8 ± 0.8	35.9 ± 3.1	15.2 ± 1.3
Diabetic							
Control	-	196.9 ± 4.6	227.0 ± 5.8[a]	27.2 ± 5.0	29.1 ± 0.9[a]	147.1 ± 6.0[a]	120.2 ± 5.2[a]
HPG	50	196.7 ± 7.6	222.8 ± 11.5[a]	26.1 ± 5.1	28.1 ± 0.8[a]	134.8 ± 4.2[a,b]	107.9 ± 3.1[a,c]
HPG	100	196.5 ± 5.6	219.0 ± 9.1[a]	19.9 ± 5.2	26.3 ± 0.9[a,c]	124.9 ± 3.0[a,c]	98.8 ± 2.8[a,c]

$^{a}p < 0.001$ compared with normal rats; $^{b}p < 0.01$, $^{c}p < 0.001$ compared with diabetic control rats.

Table 5. Biochemical features of serum and urine

Item	Normal	Diabetic rats		
		control	HPG (50 mg/kg BW/day)	HPG (100 mg/kg BW/day)
Serum glucose, mg/dL	112 ± 4	558 ± 22[c]	526 ± 26[c]	501 ± 14[c,e]
Serum glycosylated protein,nmol/mg protein	15.5 ± 0.5	20.9 ± 0.9[c]	21.6 ± 0.4[c]	15.6 ± 0.7[f]
Serum urea nitrogen, mg/dL	15.0 ± 0.7	26.0 ± 0.6[c]	24.5 ± 1.0[c,d]	25.3 ± 0.9[c]
Serum creatinine, mg/dL	0.31 ± 0.01	0.32 ± 0.01	0.28 ± 0.01[b,f]	0.28 ± 0.01[b,f]
Urinary protein, mg/day	11.2 ± 2.3	13.0 ± 0.6	9.9 ± 1.0[a,f]	8.9 ± 0.7[b,f]
Ccr, mL/kg BW/min	7.73 ± 0.06	7.29 ± 0.38	7.89 ± 0.36	7.86 ± 0.43

[a]$p < 0.05$, [b]$p < 0.01$, [c]$p < 0.001$ compared with normal rats; [d]$p < 0.05$, [e]$p < 0.01$, [f]$p < 0.001$ compared with diabetic control rats.

diabetic renal changes were thought to have occurred in this study but not advanced nephropathy. Furthermore, hyperglycemia results in irreversible tissue damage caused by the protein glycation reaction, which leads to the formation of glycosylated protein and AGEs (*104,105*). The glycosylated serum protein level increased in the present diabetic animal model, which implies that it stimulates the oxidation of sugars, enhancing damage to both sugars and proteins in circulation and the vascular wall, continuing and reinforcing the cycle of oxidative stress and damage. In addition, accumulation of AGEs in the kidney was also observed. Excessive formation and accumulation of AGEs in tissues can alter the structure and function of tissue proteins. In people with diabetes and/or chronic renal failure, AGEs that accumulate in the kidney are responsible for pathological changes including increased kidney weight, glomerular hypertrophy, glomerular basement membrane thickening, and progressive albuminuria (*106*). Moreover, AGEs stimulate free radical mechanisms and induce membrane peroxidation, which in turn increases membrane permeability. Therefore, AGE accumulation in the kidney is regarded as an index of progressive renal damage in diabetic nephropathy. HPG decreased the levels of glycosylated serum protein and renal AGEs significantly (Table 5 and 6), suggesting that it would inhibit oxidative damage and irreversible renal damage caused by protein glycation reaction in diabetes.

A significant increase in TBA-RS, an index of endogenous lipid peroxidation, has been shown in diabetes (*107,108*). Therefore, the measurement of TBA-RS is frequently used to determine the level of oxidative stress in diabetic patients. In addition, the increased lipid peroxidation in the kidney implies the level of susceptibility to diabetic oxidative stress, which then leads to diabetic complications. From this view point, the prevention of lipid peroxidation resulting from oxidative stress is considered to play a crucial role in protection from disorders associated with diabetes. The administration of HPG reduced the renal TBA-RS level significantly and dose-dependently (Table 6). These results suggest that HPG may alleviate oxidative stress associated with diabetic pathology through the inhibition of lipid peroxidation.

To then consider hyperglycemia-induced renal function parameters and tissue damage, Western blot analyses in the kidney related to oxidative stress and AGE formation were performed. NF-κB, cyclooxygenase-2 (COX-2), and iNOS are known to be involved in the pathogenesis of many chronic diseases associated with oxidative stress. COX-2 and

Table 6. Renal AGE and TBA-RS levels

Group	Dose (mg/kg BW/day)	AGEs (AU)	TBA-RS (nmol/mg protein)
Normal	-	0.77 ± 0.02	0.83 ± 0.01
Diabetic			
Control	-	0.96 ± 0.03[a]	1.45 ± 0.11[a]
HPG	50	0.81 ± 0.03[b]	0.90 ± 0.04[b]
HPG	100	0.80 ± 0.01[b]	0.76 ± 0.05[b]

[a]$p<0.001$ compared with normal rats; [b]$p < 0.001$ compared with diabetic control rats.

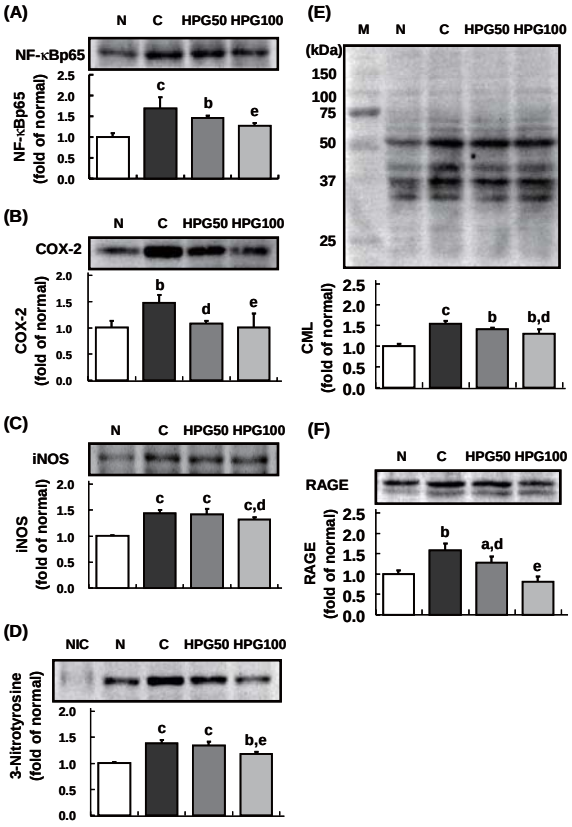

Figure 16. Effects of HPG on (A) NF-κBp65, (B) COX-2, (C) iNOS, (D) 3-nitrotyrosine, (E) CML, and (F) RAGE expressions. NIC, nitrotyrosine immunoblotting control; M, protein marker; N, normal rats; C, diabetic control rats; HPG50, diabetic rats treated with HPG (50 mg/kg BW/day); HPG100, diabetic rats treated with HPG (100 mg/kg BW/day). [a]$p < 0.05$, [b]$p < 0.01$, [c]$p < 0.001$ in comparison to normal rats; [d]$p < 0.05$, [e]$p < 0.01$ in comparison to diabetic control rats.

iNOS expression is known to be significantly enhanced in the kidneys of STZ-induced diabetic rats or mice (*96*). NF-κB is involved in the regulation of COX-2 and iNOS expression. As the current results show, NF-κBp65, COX-2, and iNOS were overexpressed in the diabetic rat kidney, and these overexpressions were concentration-dependently inhibited by HPG administrations (Figure 16A, B, and C). These findings imply that HPG inhibits COX-2 and iNOS expression as a result of the deactivation of NF-κB. Surh *et al*. (*77*) also reported that the anti-tumor promoting activity of HPG and its ingredient 20(*S*)-Rg_3 are mediated through the suppression of intracellular signaling cascades responsible for the activation of NF-κB and subsequent induction of COX-2.

3-Nitrotyrosine, a by-product of the reaction between $ONOO^-$ and proteins, is a potential biomarker for reactive-nitrogen species and increases in diabetic renal tissue. In addition, $ONOO^-$ induces the formation of N^{ε}-(carboxymethyl)lysine (CML) as a result of the oxidative cleavage of Amadori products (*109-111*). CML is a major AGE in human tissues, is known to be a marker of cumulative oxidative stress, and is involved in the development of diabetic nephropathy (*110,112*). Moreover, CML's activation of receptors for AGE (RAGE) results in the activation of NF-κB and the production of proinflammatory cytokines (*78,113*). As shown in Figure 16D, the significantly elevated 3-nitrotyrosine level in diabetic rats was reduced by HPG administrations, suggesting that HPG alleviates oxidative stress by inhibiting the generation of reactive-nitrogen species such as $ONOO^-$. In addition, the elevated renal accumulation of CML and RAGE expression in diabetic rats were significantly reduced in HPG-administered groups (Figure 16E and F). These findings imply that HPG can prevent diabetic nephropathy by inhibiting $ONOO^-$ generation, AGE formation, and RAGE activation.

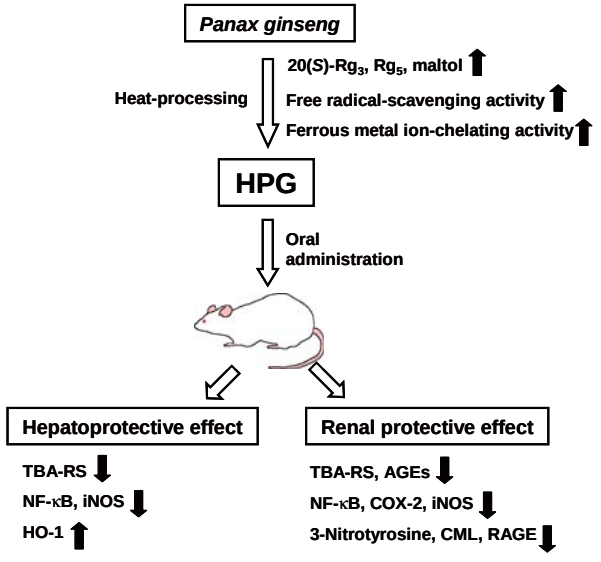

Figure 17. Schematic representation of the therapeutic potential of HPG with respect to oxidative tissue damage.

The current findings strongly suggest that the inhibition of oxidative stress and AGE formation may improve and prevent diabetes-induced tissue damage and diabetic complications. Although the anti-hyperglycemic effect of HPG was not a strong one, HPG displayed considerable action to protect against hyperglycemia-induced renal damage by inhibiting AGE formation and oxidative stress. In particular, HPG suppresses RAGE activation related to NF-κB activation by inhibiting AGE formation. HPG also protects the kidney against diabetic oxidative stress induced by expression of COX-2 and iNOS *via* the deactivation of NF-κB. Furthermore, HPG alleviates oxidative stress in diabetes through the inhibition of lipid peroxidation and the generation of reactive-nitrogen species such as $ONOO^-$. All of this evidence is thought to relate to the enhanced free radical-scavenging activity of ginseng brought about by heat-processing (*114*).

6. Conclusion and perspectives

Chemical and biological activity tests have elucidated the scientific evidence underlying the therapeutic potential of HPG with respect to oxidative tissue damage. Free radical-scavenging active components such as less-polar ginsenosides and maltol in *Panax ginseng* significantly increased depending on the temperature of heat-processing. Based on animal experiments related to oxidative tissue damage, HPG displayed hepatoprotective action by reducing the elevated TBA-RS level, and NF-κB and iNOS protein expression, while increasing HO-1 in LPS-treated rat livers, and HPG also displayed renal protective action by ameliorating physiological abnormalities and reducing elevated TBA-RS, AGEs, NF-κB, COX-2, iNOS, 3-nitrotyrosine, CML, and RAGE protein expression in the diabetic rat kidney (Figure 17). Therefore, HPG clearly has a therapeutic potential with respect to oxidative tissue damage by inhibiting protein expression related to oxidative stress and AGEs. Thus, further investigations with active compounds are underway. This investigation of specified bioactive constituents is important for the development of scientific ginseng-derived drugs as part of ethnomedicine.

References

1. Gesler WM. Therapeutic landscapes: medical issues in light of the new cultural geography. Soc Sci Med 1992;34:735-746.
2. Winslow LC, Kroll DJ. Herbs as medicines. Arch Intern Med 1998;158:2192-2199.
3. Bent S, Ko R. Commonly used herbal medicines in the United States: a review. Am J Med 2004;116:478-485.
4. Evans P, Halliwell B. Free radicals and hearing. Cause, consequence, and criteria. Ann N Y Acad Sci 1999;884:19-40.

5. Ferrari CKB. Functional foods, herbs and nutraceuticals: towards biochemical mechanisms of healthy aging. Biogerontology 2004;5:275-289.
6. Park JD. Recent studies on the chemical constituents of Korean ginseng (*Panax ginseng* C.A. Meyer). Korean J Ginseng Sci 1996;20:389-415.
7. Nocerino E, Amato M, Izzo AA. The aphrodisiac and adaptogenic properties of ginseng. Fitoterapia 2000;71: S1-5.
8. Yun TK. Brief introduction of *Panax ginseng* C.A. Meyer. J Korean Med Sci 2001;16:S3-S5.
9. Abe H, Arichi S, Hayashi T, Odashima S. Ultrastructural studies of Morris hepatoma cells reversely transformed by ginsenosides. Experientia 1979;35:1647-1649.
10. Han BH, Park MH, Han YN, Shin SC. Studies on the antioxidant components of Korean ginseng (IV). Antifatigue activity components. Yakhak Hoeji 1984;28:231-235.
11. Yokozawa T, Oura H, Kawashima Y. Effect of serial administration of ginsenoside-Rb_2 in diabetic rats: in terms of carbohydrate and lipid metabolites. Chem Pharm Bull 1987;35:4872-4877.
12. Sugaya A, Yuzurihara M, Tsuda T, Yasuda K, Kajiwara K, Sugaya E. Proliferative effect of ginseng saponin on neurite extension of primary cultured neurons of the rat cerebral cortex. J Ethnopharmacol 1988;22:173-181.
13. Yokozawa T, Oura H. Effects of ginseng powder in aging rats. J Med Pharm Soc WAKAN-YAKU 1988;5:50-55.
14. Yokozawa T, Oura H, Kawashima Y. The effect of ginsenoside-Rb_2 on nitrogen balance. J Nat Prod 1989;52:1350-1352.
15. Deng HW, Guan YY, Kwan CY. The effects of ginsenosides on lipid peroxidation in liver and cardiac muscle homogenates. Biochem Arch 1990;6:359-365.
16. Yokozawa T, Oura H. Facilitation of protein biosynthesis by ginsenoside-Rb_2 administration in diabetic rats. J Nat Prod 1990;53:1514-1518.
17. Bhattacharya SK, Mitra SK. Anxiolytic activity of *Panax ginseng* root: an experimental study. J Ethnopharmacol 1991;34:87-92.
18. Yokozawa T, Fujitsuka N, Yasui T, Oura H. Effects of ginsenoside-Rb_2 on adenine nucleotide content of rat hepatic tissue. J Pharm Pharmacol 1991;43:290-291.
19. Chen X. Cardiovascular protection by ginsenosides and their nitric oxide releasing action. Clin Exp Pharmacol Physiol 1996;23:728-732.
20. Zhang D, Yasuda T, Yu Y, Zheng P, Kawabata T, Ma Y, Okada S. Ginseng extract scavenges hydroxyl radical and protects unsaturated fatty acids from decomposition caused by iron-mediated lipid peroxidation. Free Radic Biol Med 1996;20:145-150.
21. Lee HJ, Kim DY, Chang CC. Antioxidant effects of Korean red ginseng components on the antioxidant enzymes activity and lipid peroxidation in the liver of mouse treated with paraquat. J Ginseng Res 1999;23:182-189.
22. Maffei Facino R, Carini M, Aldini G, Berti F, Rossoni G. *Panax ginseng* administration in the rat prevents myocardial ischemia-reperfusion damage induced by hyperbaric oxygen: evidence for an antioxidant intervention. Planta Med 1999;65:614-619.
23. Kitts DD, Hu C. Efficacy and safety of ginseng. Public Health Nutr 2000;3:473-485.
24. Pieralisi G, Ripari P, Vecchiet L. Effects of a standardized ginseng extract combined with dimethylaminoethanol bitartrate, vitamins, minerals, and trace elements on physical performance during exercise. Clin Ther 1991;13:373-382.
25. Park JH, Kim JM, Han SB, Kim NY, Surh YJ, Lee SK, Kim ND, Park MK. A new processed ginseng with fortified activity. Advances in Ginseng Research. Korean Society of Ginseng, Seoul, Korea, 1998, p.146-159.
26. Wesnes KA, Ward T, McGinty A, Petrini O. The memory enhancing effects of a *Ginkgo biloba/Panax ginseng* combination in healthy middle-aged volunteers. Psychopharmacology (Berl) 2000;152:353-361.
27. Kennedy DO, Scholey AB, Wesnes KA. Modulation of cognition and mood following administration of single doses of *Ginkgo biloba*, ginseng, and a ginkgo/ginseng combination to healthy young adults. Physiol Behav 2002;75:739-751.
28. Kiefer D, Pantuso T. *Panax ginseng*. Am Fam Physician 2003;68:1539-1542.
29. Kasai R, Besso H, Tanaka O, Saruwatari Y, Fuwa T. Saponins of red ginseng. Chem Pharm Bull 1983;31:2120-2125.
30. Matsuura H, Hirao Y, Yoshida S, Kunihiro K, Fuwa T, Kasai R, Tanaka O. Study of red ginseng: new glucosides and a note on the occurrence of maltol. Chem Pharm Bull 1984;32:4674-4677.
31. Oh CH, Kang PS, Kim JW, Kwon J, Oh SH. Water extracts of cultured mountain ginseng stimulate immune cells and inhibit cancer cell proliferation. Food Sci Biotechnol 2006;15:369-373.
32. Kim WY, Kim JM, Han SB, Lee SK, Kim ND, Park MK, Kim CK, Park JH. Steaming of ginseng at high temperature enhances biological activity. J Nat Prod 2000;63:1702-1704.
33. Kwon SW, Han SB, Park IH, Kim JM, Park MK, Park JH. Liquid chromatographic determination of less polar ginsenosides in processed ginseng. J Chromatogr A 2001;921:335-339.
34. Kim ND, Kang SY, Park JH, Schini-Kerth VB. Ginsenoside Rg_3 mediates endothelium-dependent relaxation in response to ginsenosides in rat aorta: role of K^+ channels. Eur J Pharmacol 1999;367:41-49.
35. Keum YS, Park KK, Lee JM, Chun KS, Park JH, Lee SK, Kwon HJ, Surh YJ. Antioxidant and anti-tumor promoting activities of the methanol extract of heat-processed ginseng. Cancer Lett 2000;150:41-48.
36. Park JH, Cha HY, Seo JJ, Hong JT, Han K, Oh KW. Anxiolytic-like effects of ginseng in the elevated plus-maze model: Comparison of red ginseng and sun ginseng. Prog Neuropsychopharmacol Biol Psychiatry 2005;29:895-900.
37. Kang KS, Kim HY, Pyo JS, Yokozawa T. Increase in the free radical scavenging activity of ginseng by heat-processing. Biol Pharm Bull 2006;29:750-754.
38. Halliwell B, Gutteridge JMC. Oxygen toxicity, oxygen radicals, transition metals and disease. Biochem J 1984;219:1-14.
39. Baud L, Ardaillou R. Reactive oxygen species: production and role in the kidney. Am J Physiol 1986;251:F765-776.
40. Radi R, Beckman JS, Bush KM, Freeman BA. Peroxynitrite-induced membrane lipid peroxidation: the cytotoxic potential of superoxide and nitric oxide. Arch Biochem Biophys 1991;288:481-487.
41. Valko M, Rhodes CJ, Moncol J, Izakovic M, Mazur M. Free radicals, metals and antioxidants in oxidative stress-induced cancer. Chem Biol Interact 2006;160:1-40.
42. Beckman JS, Koppenol WH. Nitric oxide, superoxide, and peroxynitrite: the good, the bad, and the ugly. Am J Physiol 1996;271:1424-1437.
43. Ischiropoulos H. Biological tyrosine nitration: a pathophysiological function of nitric oxide and reactive oxygen species. Arch Biochem Biophys 1998;356:1-11.
44. Nakazawa H, Fukuyama N, Takizawa S, Tsuji C, Yoshitake M, Ishida H. Nitrotyrosine formation and its

role in various pathological conditions. Free Radic Res 2000;33:771-784.
45. Ceriello A, Mercuri F, Quagliaro L, Assaloni R, Motz E, Tonutti L, Taboga C. Detection of nitrotyrosine in the diabetic plasma: evidence of oxidative stress. Diabetologia 2001;44:834-838.
46. Kim YK, Guo Q, Packer L. Free radical scavenging activity of red ginseng aqueous extracts. Toxicology 2002;172:149-156.
47. Kang KS, Yokozawa T, Kim HY, Park JH. Study on the nitric oxide scavenging effects of ginseng and its compounds. J Agric Food Chem 2006;54:2558-2562.
48. Yap KY, Chan SY, Weng Chan Y, Sing Lim C. Overview on the analytical tools for quality control of natural product-based supplements: a case study of ginseng. Assay Drug Dev Technol 2005;3:683-699.
49. Ko SR, Choi KJ, Han KW. Comparison of proximate composition, mineral nutrients, amino acid and free sugar contents of several *Panax* species. Korean J Ginseng Sci 1996;20:36-41.
50. Attele AS, Wu JA, Yuan CS. Ginseng pharmacology. Multiple constituents and multiple actions. Biochem Pharmacol 1999;58:1685-1693.
51. Sievenpiper JL, Arnason JT, Leiter LA, Vuksan V. Decreasing, null and increasing effects of eight popular types of ginseng on acute postprandial glycemic indices in healthy humans: the role of ginsenosides. J Am Coll Nutr 2004;23:248-258.
52. Shoji J. The saponins of ginseng. Recent Advances in Ginseng Studies. In: Shibata S, Ohtsuka Y, Sato S. editors, Hirokawa Publishing, Tokyo, Japan, 1990, p.11-31.
53. Kang KS, Kim HY, Baek SH, Yoo HH, Park JH, Yokozawa T. Study on the hydroxyl radical scavenging activity changes of ginseng and ginsenoside-Rb_2 by heat processing. Biol Pharm Bull 2007;30:724-728.
54. Kang KS, Kim HY, Yamabe N, Yokozawa T. Stereospecificity in hydroxyl radical scavenging activities of four ginsenosides produced by heat processing. Bioorg Med Chem Lett 2006;16:5028-5031.
55. Liu ZQ, Luo XY, Sun YX, Chen YP, Wang ZC. Can ginsenosides protect human erythrocytes against free-radical-induced hemolysis? Biochim Biophys Acta 2002;1572:58-66.
56. Huang D, Ou B, Prior R. The chemistry behind antioxidant capacity assays. J Agric Food Chem 2005;53:1841-1856.
57. Kang KS, Yokozawa T, Yamabe N, Kim HY, Park JH. ESR study on the structure and hydroxyl radical-scavenging activity relationships of ginsenosides isolated from *Panax ginseng* C.A. Meyer. Biol Pharm Bull 2007;30:917-921.
58. Halliwell B, Gutteridge JMC, Cross CE. Free radicals, antioxidants, and human disease: Where are we now? J Lab Clin Med 1992;119:598-620.
59. Han BH, Park MH, Han YN. Studies on the antioxidant components of Korean ginseng (III). Identification of phenolic acids. Arch Pharmacol Res 1981;4:53-58.
60. Han BH, Park MH, Han YN. Studies on the antioxidant components of Korean ginseng (V): the mechanism of antioxidant activity of maltol and phenolic acids. Korean Biochem J 1985;18:337-340.
61. Sato M, Ramarathnam N, Suzuki Y, Ohkubo T, Takeuchi M, Ochi H. Varietal differences in the phenolic content and superoxide radical scavenging potential of wines from different sources. J Agric Food Chem 1996;44:37-41.
62. Cai Y, Luo Q, Sun M, Corke H. Antioxidant activity and phenolic compounds of 112 traditional Chinese medicinal plants associated with anticancer. Life Sci 2004;74:2157-2184.
63. Jung MY, Jeon BS, Bock JY. Free, esterified, and insoluble-bound phenolic acids in white and red Korean ginsengs (*Panax ginseng* C.A. Meyer). Food Chem 2002;79:105-111.
64. Reepmeyer JC. Thermal decomposition of aspirin: formation of linear oligomeric salicylate esters. J Pharm Sci 1983;72:322-323.
65. Rice-Evans CA, Miller NJ, Bolwell PG, Bramley PM, Pridham JB. The relative antioxidant activities of plant-derived polyphenolic flavonoids. Free Radic Res 1995;22:375-383.
66. Samaras TS, Camburn PA, Chandra SX, Gordon MH, Ames JM. Antioxidant properties of kilned and roasted malts. J Agric Food Chem 2005;53:8068-8074.
67. Yasumoto E, Nakano K, Nakayachi T, Morshed SR, Hashimoto K, Kikuchi H, Nishikawa H, Kawase M, Sakagami H. Cytotoxic activity of deferiprone, maltol and related hydroxyketones against human tumor cell lines. Anticancer Res 2004;24:755-762.
68. Li X, Zheng Y, Liu M, Zhang L. A study on Maillard reaction and its products during processing of red ginseng. Zhongguo Zhong Yao Za Zhi 1999;24:274-278.
69. Suzuki Y, Choi KJ, Uchida K, Ko SR, Sohn HJ, Park JD. Arginyl-fructosyl-glucose and arginyl-fructose, compounds related to browning reaction in the model system of steaming and heat-drying processes for the preparation of red ginseng. J Ginseng Res 2004;28:143-148.
70. Davidek T, Clety N, Devaud S, Robert F, Blank I. Simultaneous quantitative analysis of Maillard reaction precursors and products by high-performance anion exchange chromatography. J Agric Food Chem 2003;51:7259-7265.
71. Salvemini D, Korbut R, Anggard E, Vane J. Immediate release of a nitric oxide-like factor from bovine aortic endothelial cells by *Escherichia coli* lipopolysaccharide. Proc Natl Acad Sci U S A 1990;87:2593-2597.
72. Liu S, Adcock IM, Old RW, Barnes PJ, Evans TW. Lipopolysaccharide treatment *in vivo* induces widespread tissue expression of inducible nitric oxide synthase mRNA. Biochem Biophys Res Commun 1993;196:1208-1213.
73. Poderoso JJ, Carreras MC, Lisdero C, Riobo N, Schopfer F, Boveris A. Nitric oxide inhibits electron transfer and increases superoxide radical production in rat heart mitochondria and submitochondrial particles. Arch Biochem Biophy 1996;328:85-92.
74. Gius D, Botero A, Shah S, Curry A. Intracellular oxidation/reduction status in the regulation of transcription factors NF-kappaB and AP-1. Toxicol Lett 1999;106:93-106.
75. Han YJ, Kwon YG, Chung HT, Lee SK, Simmons RL, Billiar TR, Kim YM. Antioxidant enzymes suppress nitric oxide production through the inhibition of NF-kappaB activation: role of H_2O_2 and nitric oxide in inducible nitric oxide synthase expression in macrophages. Nitric Oxide 2001;5:504-513.
76. Surh YJ, Chun KS, Cha HH, Han SS, Keum YS, Park KK, Lee SS. Molecular mechanisms underlying chemopreventive activities of anti-inflammatory phytochemicals: down-regulation of COX-2 and iNOS through suppression of NF-kappaB activation. Mutat Res 2001;480-481:243-268.
77. Surh YJ, Na HK, Lee JY, Keum YS. Molecular mechanisms underlying anti-tumor promoting activities of heat-processed *Panax ginseng* C.A. Meyer. J Korean Med Sci 2001;16:S38-41.
78. Ahmed N. Advanced glycation endproducts-role in pathology of diabetic complications. Diabetes Res Clin Prac 2005;67:3-21.
79. Cadenas S, Cadenas AM. Fighting the stranger-

antioxidant protection against endotoxin toxicity. Toxicology 2002;180:45-63.
80. Takahashi T, Morita K, Akagi R, Sassa S. Heme oxygenase-1: a novel therapeutic target in oxidative tissue injuries. Curr Med Chem 2004;11:1545-1561.
81. Suliburk JW, Gonzalez EA, Kennison SD, Helmer KS, Mercer DW. Differential effects of anesthetics on endotoxin-induced liver injury. J Trauma 2005;58:711-717.
82. Jirillo E, Caccavo D, Magrone T, Piccigallo E, Amati L, Lembo A, Kalis C, Gumenscheimer M. The role of the liver in the response to LPS: experimental and clinical findings. J Endotoxin Res 2002;8:319-327.
83. Chen T, Zamora R, Zuckerbraun B, Billiar TR. Role of nitric oxide in liver injury. Curr Mol Med 2003;3:519-526.
84. Kim JS, Kim KW, Choi KJ, Kwak YK, Im KS, Lee KH, Chung HY. Screening of antioxidative components from red ginseng saponin. Korean J Ginseng Sci 1996;20:173-178.
85. Kim HJ, Chun YJ, Park JD, Kim SI, Roh JK, Jeong TC. Protection of rat liver microsomes against carbon tetrachloride-induced lipid peroxidation by red ginseng saponin through cytochrome P450 inhibition. Planta Med 1997;63:415-418.
86. Hasegawa H. Proof of the mysterious efficacy of ginseng: basic and clinical trials: metabolic activation of ginsenoside: deglycosylation by intestinal bacteria and esterification with fatty acid. J Pharmacol Sci 2004;95:153-157.
87. Lee HU, Bae EA, Han MJ, Kim DH. Hepatoprotective effect of 20(*S*)-ginsenoside Rg_3 and its metabolite 20(*S*)-ginsenoside Rh_2 on *tert*-butyl hydroperoxide-induced liver injury. Biol Pharm Bull 2005;28:1992-1994.
88. Han SW, Kim H. Ginsenosides stimulate endogenous production of nitric oxide in rat kidney. Int J Biochem Cell Biol 1996;28:573-580.
89. Kim JY, Lee HJ, Kim JS, Ryu JH. Induction of nitric oxide synthase by saponins of heat-processed ginseng. Biosci Biotechnol Biochem 2005;69:891-895.
90. Lee SH, Seo GS, Ko G, Kim JB, Sohn DH. Anti-inflammatory activity of 20(*S*)-protopanaxadiol: enhanced heme oxygenase 1 expression in RAW 264.7 cells. Planta Med 2005;71:1165-1170.
91. Kim YB, Oh SH, Sok DE, Kim MR. Neuroprotective effect of maltol against oxidative stress in brain of mice challenged with kainic acid. Nutr Neurosci 2004;7:33-39.
92. Kang KS, Yamabe N, Kim HY, Yokozawa T. Effect of sun ginseng methanol extract on lipopolysaccharide-induced liver injury in rats. Phytomedicine 2007(*in press*).
93. Baynes JW. Role of oxidative stress in development of complications in diabetes. Diabetes 1991;40:405-412.
94. Selby JV, FitzSimmons SC, Newman JM, Katz PP, Sepe S, Showstack J. The natural history and epidemiology of diabetic nephropathy. Implications for prevention and control. JAMA 1990;263:1954-1960.
95. Held PJ, Port FK, Webb RL, Wolfe RA, Garcia JR, Blagg CR, Agodoa LY. The United States Renal Data System's 1991 annual data report: an introduction. Am J Kidney Dis 1991;18:1-16.
96. The Diabetes Control and Complications Trial Research Group. The effect of intensive treatment of diabetes on the development and progression of long-term complications in insulin-dependent diabetes mellitus. N Engl J Med 1993;329:977-986.
97. Yokozawa T, Yamabe N, Cho EJ, Nakagawa T, Oowada S. A study on the effects to diabetic nephropathy of Hachimi-jio-gan in rats. Nephron Exp Nephrol 2004;97:38-48.
98. Yamabe N, Yokozawa T, Oya T, Kim M. Therapeutic potential of (-)-epigallocatechin 3-*O*-gallate on renal damage in diabetic nephropathy model rats. J Pharmacol Exp Ther 2006;319:228-236.
99. Yokozawa T, Satoh A, Nakagawa T, Yamabe N. Attenuating effects of Wen-Pi-Tang treatment in rats with diabetic nephropathy. Am J Chin Med 2006;34:307-321.
100. Xu H, Shen J, Liu H, Shi Y, Li L, Wei M. Morroniside and loganin extracted from *Cornus officinalis* have protective effects on rat mesangial cell proliferation exposed to advanced glycation end products by preventing oxidative stress. Can J Physiol Pharmacol 2006;84:1267-1273.
101. Brownlee M, Vlassara H, Cerami A. Nonenzymatic glycosylation and the pathogenesis of diabetic complications. Ann Intern Med 1984;101:527-537.
102. Njoroge FG, Monnier VM. The chemistry of the Maillard reaction under physiological conditions: a review. Prog Clin Biol Res 1989;304:85-107.
103. Schrijvers BF, De Vriese AS, Flyvbjerg A. From hyperglycemia to diabetic kidney disease: the role of metabolic, hemodynamic, intracellular factors and growth factors/cytokines. Endocr Rev 2004;25:971-1010.
104. Cooper ME, Gilbert RE, Epstein M. Pathophysiology of diabetic nephropathy. Metabolism 1998;47:3-6.
105. Yabe-Nishimura C. Aldose reductase in glucose toxicity: a potential target for the prevention of diabetic complications. Pharmacol Rev 1998;50:21-33.
106. Vlassara H, Striker LJ, Teichberg S, Fuh H, Li YM, Steffes M. Advanced glycation end products induce glomerular sclerosis and albuminuria in normal rats. Proc Natl Acad Sci U S A 1994;91:11704-11708.
107. Gallou G, Ruelland A, Legras B, Maugendre D, Allannic H, Cloarec L. Plasma malondialdehyde in type 1 and type 2 diabetic patients. Clin Chim Acta 1993;214:227-234.
108. Turk HM, Sevinc A, Camci C, Cigli A, Buyukberber S, Savli H, Bayraktar N. Plasma lipid peroxidation products and antioxidant enzyme activities in patients with type 2 diabetes mellitus. Acta Diabetol 2002;39:117-122.
109. Komers R, Lindsley JN, Oyama TT, Schutzer WE, Reed JF, Mader SL, Anderson S. Immunohistochemical and functional correlations of renal cyclooxygenase-2 in experimental diabetes. J Clin Invest 2001;107:889-898.
110. Nagai R, Unno Y, Hayashi MC, Masuda S, Hayase F, Kinae N, Horiuchi S. Peroxynitrite induces formation of N^{ε}-(carboxylmethyl)lysine by the cleavage of Amadori product and generation of glucosone and glyoxal from glucose: novel pathways for protein modification by peroxynitrite. Diabetes 2002;51:2833-2839.
111. Virag L, Szabo E, Gergely P, Szabo C. Peroxynitrite-induced cytotoxicity: mechanism and opportunities for intervention. Toxicol Lett 2003;140-141:113-124.
112. Horie K, Miyata T, Maeda K, Miyata S, Sugiyama S, Sakai H, van Ypersole de Strihou C, Monnier VM, Witztum JL, Kurokawa K. Immunohistochemical colocalization of glycoxidation products and lipid peroxidation products in diabetic renal glomerular lesions. Implication for glycoxidative stress in the pathogenesis of diabetic nephropathy. J Clin Invest 1997;100:2995-3004.
113. Yan SD, Schmidt AM, Anderson GM, Zhang J, Brett J, Zou YS, Pinsky D, Stern D. Enhanced cellular oxidant stress by the interaction of advanced glycation end products with their receptors/binding proteins. J Biol Chem 1994;269:9889-9897.
114. Kang KS, Kim HY, Yamabe N, Nagai R, Yokozawa T. Protective effect of sun ginseng against diabetic renal damage. Biol Pharm Bull 2006;29:1678-1684.

Anti-depressant and anti-nociceptive effects of 1,4-benzodiazepine-2-ones based cholecystokinin (CCK_2) antagonists

Eric Lattmann[1,*], Jintana Sattayasai[2], Pornthip Lattmann[1], David C. Billington[1], Carl H. Schwalbe[1], Jordchai Boonprakob[2], Wanchai Airarat[2], Harjit Singh[1], Michael Offel[1], Alexander Staaf[1]

[1] *The School of Pharmacy, Aston University, Aston Triangle, Birmingham, England;*
[2] *Department of Pharmacology, Faculty of Medicine, Khon Kaen University, Khon Kaen, Thailand.*

ABSTRACT: Various 1,4-benzodiazepines were synthesized around a Diazepam, Oxazepam and the n-propyl-1,4-benzodiazepine template. SAR studies of CCK_2 binding affinity were performed and selected examples of each series were tested *in vivo* in mice. In addition to an anxiolytic effect, antidepressant effects were discovered using 8 standard CNS assays in mice. Finally, the cocomittant administration of the 1,4-benzodiazepine based CCK antagonists enhanced the response to pain with a low dose of morphine, significantly.

Key Words: 1,4-Benzodiazepine template, anxiolytics, antidepressant, anti-nociceptive agent, CCK-B antagonist, CCK_2

Introduction

Cholecystokinin, which act as a neuromodulator/gut hormone and CCK-ligands, agonists as well as antagonists (*1*) have been extensively investigated as potential drug candidates (*2*). CCK-antagonists (*3*) were studied as growth inhibitors in certain forms of cancer (*4*), as anxiolytics (*5*), in the treatment of schizophrenia (*6*), satiety (*7*) and as anti-panic agents (*8*). An agonist, the shortened CCK tetrapeptide, was found to induce panic in patients and these effects were blocked by CCK antagonists (*9*).

A phase II trial of Devazepide, a potent and CCK_1 selective antagonist (*10*) has been recently completed (*11*) showing a significant enhancement of the effect of morphine in the treatment of chronic and severe pain (*12*).

Asperlicin, a microbial metabolite, was the first non-peptidal CCK antagonist and analogues thereof, containing an indolylmethyl substituent in the 3-position were studies as CCK ligands (*13*). The 1,4-benzodiazepine template was varied by a combinatorial solid phase synthesis (*14*) and was optimised in terms of CCK binding affinity (*15*). In the search for new CCK ligands, in which the 1,4-benzodiazepine structure was replaced by an achiral template, the tryptophan-indole moiety was selected as starting point (*16*).

Here, the systematic variation of the 1,4-benzodiazepine template (*17*) and the testing of reaction intermediates resulted in CCK_2 ligands (Figure 1), which were subsequently studied in mice.

Having realized the relevance of the CCK receptor in the treatment of pain (*18*) and depression (*19*), novel

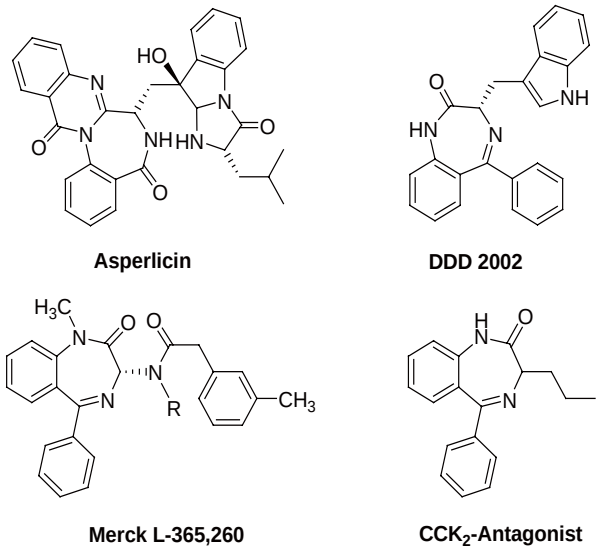

Figure 1. Chemical structures of Asperlicin, DDD 2002, Merck L-365,260, and CCK_2-antagonist.

**Correspondence to:* The School of Pharmacy, Aston University, Aston Triangle, Birmingham B4 7ET, England;
e-mail: e.lattmann@aston.ac.uk

Received May 11, 2007
Accepted June 6, 2007

1,4-benzodiazepine based compounds were prepared and fully tested for these applications.

Materials and Methods

Chemistry

Atmospheric pressure chemical ionisation mass spectrometry (APCI-MS) was carried out on a Hewlett-Packard 5989B quadrupole instrument connected to a 59987A unit with an APCI accessory. IR spectra were recorded as KBr discs on a Mattson 3000 FTIR spectrophotometer. Proton NMR spectra were obtained on a Bruker AC 250 instrument operating at 250MHz, with TMS as internal standard.

Experimental

Synthesis of Diazepam **1** [Methyl-7-chloro-5-phenyl-1,3-dihydro-2H-1,4-benzodiazepin-2-one]: 1.75 mL of Chloroacetyl chloride (22 mmol) was added under stirring to a solution of 2-amino-5-chloro-benzophenone (4.65 g, 20 mmol) in 25 mL of anhydrous ether at 0°C. The suspension containing the newly formed 2-chloroacetamido-5-chlorobenzophenone was stirred for half an hour at 0°C and for 2 h at room temperature. 64 mmoles of urotropine, 14.2 mL 2N aqueous HCl, 60 mL methanol and 5.8 mL water were added to this suspension and the mixture was heated under reflux for 16 h. It was cooled in an ice bath and the precipitate was filtered. The crystalls were washed with a 10 mL cold mixture of methanol/water. The product was dried at 60°C under reduced pressure. Yield 72% of Nor-desmethyldiazepam. APCI + m/s: m/z = 271; IR (KBr disc) υ_{max} = 3449, 3207, 2960, 1679, 1604, 1476, 1093, 794 cm^{-1}; ^{1}H-NMR ($CDCl_3$) d 4.31 (s, 2 H, C3:-$\underline{H}_2$), 7.1-7.65 (m, 8 H, arom. H), 10.0 p.p.m. (s,1 H, N1:-$\underline{H}$).

Conversion of Nor-desmethyldiazepam into Diazepam **1**: A mixture of 0.05 mole of Nor-desmethyldiazepam, 100 mL of *N,N*-dimethylformamide and 50% suspension of NaH in mineral oil (0.06 mol) was added in portions to a solution of the parent compound (0.05 mol) in DMF (100 mL). After stirring for 15 min at 0-5°C, methyliodide (0.06 mol) was added dropwise to the mixture with ice cooling and the solution was stirred for additional 30 min at RT. For work up, water was added and the suspension was extracted with EtOAc. The extract was washed with brine, dried (Na_2SO_4) and then concentrated under reduced pressure giving Diazepam in quantitative yield. The entitled compound is identical with the reference substance form Sigma-Aldrich. APCI + m/s: m/z = 285; TLC (Ether): R_f = 0.4; ^{1}H-NMR ($CDCl_3$) d 3.2 (s, 3H, N1:-C$\underline{H}_3$), 4.4 (s, 2H, C3:-$\underline{H}_2$), 7.1-7.6 p.p.m.(m, 8 arom. H).

Alkylation of Diazepam

A solution containing 20 mL of anhydrous THF and 1.6 g (16 mmol) of diisopropylamine was cooled to -60°C and 11.2 mL (16 mmol) of 1.6 M *n*-butyllithium solution in hexane was added via syringe. The solution was stirred for 10-15 min and then warmed to room temperature. After the mixture was cooled back to -60°C, a 5 mL anhydrous DCM solution of Diazepam (2.3 g, 8 mmol) was added through a syringe and the reaction mixture was brought to room temperature over 30 min. The resulting dark red solution of the Diazepam anion was cooled to -20°C. 16 mmol alkylbromide was added in 5 mL of THF. The mixture was stirred and allowed to come to room temperature. The reaction was followed by TLC and for work up dilute HCl was added until pH 6-7. The reaction mixtures were extracted with ether (3 × 100 mL). The oil, obtained after evaporation of the dried etheral extract, was chromatographed. Elution with hexane-ethyl acetate (6:1) gave the desired compounds as oils.

7-Chloro-1-methyl-5-phenyl-3-propyl-1,3-dihydro-2H-1,4-benzodiazepin-2-one ***2a***

APCI + m/s: m/z = 327; TLC (Ether): R_f = 0.75; IR (KBr) υ_{max} = 2971, 2861, 1715, 1669, 1461, 1253, 1114, 1073, 738, 705 cm^{-1}; ^{1}H-NMR ($CDCl_3$) d 0.99 (t; 3H, *J* = 7Hz, C3:-$(CH_2)_2C\underline{H}_3$), 1.35-1.52 (m, 2H, C3:-$(CH_2)_2C\underline{H}_3$), 1.99 (m, 2H, C3:-$C\underline{H}_2CH_2CH_3$), 3.48 (s, 3H, N1:-C$\underline{H}_3$); 4.17 (t, 1H, *J* = 5Hz, C3:-$\underline{H}$), 7.2-7.87 (m, 8 arom. H), ^{13}C-NMR ($CDCl_3$) d 14.1 (C3:-$(CH_2)_2\underline{C}H_3$), 19.1 (C3:-$CH_2\underline{C}H_2CH_3$), 28.9 (N1:-$\underline{C}H_3$), 35.0 (C3:-$\underline{C}H_2CH_2CH_3$), 68.0 (C-3), 122.6, 128.5, 129.5, 130.8, 131.3, 138.1, 141.2, 167.7, 171.7 p.p.m.

3-Allyl-7-chloro-1-methyl-5-phenyl-1,3-dihydro-2H-1,4-benzodiazepin-2-one ***2b***

APCI + m/s: m/z = 325 (80%), 311 (10%), 299 (5%), 285 (5%); TLC (Ether): R_f = 0.75; IR (KBr) υ_{max} = 3436, 2923, 2856, 1668, 1607, 1484, 1386, 1320, 1263, 1094, 1031, 804, 695 cm^{-1}; ^{1}H-NMR ($CDCl_3$) d 2.45 (m, 2 $\underline{H}$), 2.95 (s, 3 H, N1:-C$\underline{H}_3$), 3.85 (m, 1H, C3:-$\underline{H}$), 4.8-5.6 (br m, 3 H, C3:-$CH_2C\underline{H}$=C$\underline{H}_2$), 7.1-7.85 (m, 8 arom. H); ^{13}C-NMR ($CDCl_3$) d 32.8 (N1:-$\underline{C}H_3$), 36.8, 62.1 (C-3), 122.2, 124.4, 127.1, 127.9, 129.4, 130.1, 131.7, 133.5, 136.4, 143.2, 167.4, 168.2 p.p.m.

7-Chloro-1-methyl-5-phenyl-3-prop-2-ynyl-1,3-dihydro-2H-1,4-benzodiazepin-2-one ***2c***

APCI + m/s: m/z = 323 (80%), 285 (15%), 241(5%); TLC (Ether): R_f = 0.8; IR (KBr) υ_{max} = 3058, 2954, 2968, 1668, 1612, 1480, 1318, 1253, 1123, 819, 742, 701 cm^{-1}; ^{1}H-NMR ($CDCl_3$) d 2.0-2.4 (m, 3 H), 3.45 (s, 3 H, N1:-C$\underline{H}_3$), 5.7 (m, 1 H, C3:-$\underline{H}$), 7.2-7.75 (m, 8 arom. H); ^{13}C-NMR ($CDCl_3$) d 21.9 (C3:-$\underline{C}H_2C{\equiv}CH$), 35.4 (N1:-

$\underline{C}H_3$), 122.3, 127.1, 128.0, 129.5, 130.8, 131.7, 136.5, 141.4, 166.5, 170.8 p.p.m.

7-Nitro-5-phenyl-3-propyl-1,3-dihydro-2H-1,4-benzodiazepin-2-one 3a via Sandmeyer reaction

p-Nitrobenzophenone was reacted 1.15 eq of bromo-butyrylchloride at ambient temperature and the precipitate of *N*-(2-benzoyl-4-nitrophenyl)-2-bromopentanamide was filtered off. 0.02 mole of *N*-(2-benzoyl-4-nitrophenyl)-2-bromopentanamide containing potassium iodide as catalyst were dissolved in 100 mL of liquid ammonia. The mixture was stirred for 5 h in liquid ammonia and subsequently the ammonia was allowed to evaporate off at room temperature overnight. The residue was recrystallised in ether/petrolether. Yield 60%. APCI - m/s: m/z = 323 (75%), 241 (25%); TLC (Ether): R_f = 0.6; IR (KBr disc) υ_{max} = 3449, 3338, 1640, 1611, 1476, 1313, 1297 (-NO_2), 1093, 958, 765, 699 cm^{-1}; ^{1}H-NMR ($CDCl_3$) d 0.98 (t; 3H, *J* = 7Hz, C3:-$(CH_2)_2C\underline{H}_3$), 1.25-1.9 (m, 4H, C3:-$(C\underline{H}_2)_2CH_3$), 3.48 (tr, 1H, *J* = 4Hz, C3:-$\underline{H}$), 7.2-7.75 (m, 6 arom. H), 7.9 (d, 1 arom. H), 8.1 (d, 1 arom. H), 8.5 (s, 1H, N1:-H); ^{13}C-NMR ($CDCl_3$/MeOD) d 14.3 (C3:-$(CH_2)_2\underline{C}H_3$), 21.4, 35.4, 62.8 (C-3), 122.6, 128.5, 129.2, 129.5, 130.6, 131.4, 132.4, 137.3, 164.8, 168.9 172.8 p.p.m.

*7-Amino-5-phenyl-3-propyl-1,3,4,5-tetrahydro-2H-1,4-benzodiazepin-2-one **3b***

A solution of 3.2 mmole of 7-amino-3-propyl-benzodiazepine in 10mL of ethanol was added to an excess (15 mL) of a hot solution of 15% Sn-(II)-chloride in conc. hydrochloric acid. 25 mL of ethanol was added and the solution was filtered and concentrated in vacuum to give yellow needles, which were filtered and recrystallised from ethanol. APCI - m/s: m/z = 295 (80%), 241 (20%); TLC (Ether): R_f = 0.45; IR (KBr) υ_{max} = 3432, 3262, 2960, 2859, 1646, 1532, 1498, 1318, 1241, 825, 695 cm^{-1}; ^{1}H-NMR ($CDCl_3$) d 0.95 (s, 3H, C3:-$(CH_2)_2C\underline{H}_3$), 1.3-1.8 (two m, 4H, C3:-$(C\underline{H}_2)_2CH_3$), 2.4 (m, 2H), 3.65 (br s, 2H, C7:-$N\underline{H}_2$), 6.78 (s, 1H), 6.85 (d, 1H), 7.25-7.8 (m, 6 arom. H), 8.35 (d, 1H), 10.2 (s, 1H); ^{13}C-NMR ($CDCl_3$) d 13.7 C3:-$(CH_2)_2\underline{C}H_3$), 22.3 (C3:-$CH_2\underline{C}H_2CH_3$), 27.6 (C3:-$\underline{C}H_2CH_2CH_3$), 37.8, 118.6, 120.6, 123.4, 125.1, 128.2, 129.2, 131.6, 138.4, 141.2, 171.9 p.p.m.

*7-Chloro-5-phenyl-3-propyl-1,3-dihydro-2H-1,4-benzodiazepin-2-one **3c***

A solution of 25 mmol of the amino-benzodiazepine **3b** in 30 mL of 6N hydrochloric acid was reacted with an aqueous solution of 30 mmol sodium nitrite (2.1 g) at 0-5°C. The resulting solution was added to 12 g copper chloride in 120 mL of 3N hydrochloric acid. The mixture was allowed to come to RT until the liberation of nitrogen was completed. After cooling the green solid, which has separated, was collected and dissolved in DCM. Copper salts were removed by washing the organic phase with aq. ammonia. It was dried with sodium sulfate, evaporated off and the desired compound was recrystallised from ethanol.

APCI + m/s: m/z = 313 (80%), 268 (15%), 264 (5%); mp: 197-198°C; TLC (Ether): R_f = 0.72; IR (KBr disc) υ_{max} = 3218, 3123, 2923, 2851, 1687, 1604, 1476, 1320, 1220, 826, 699 cm^{-1}; ^{1}H-NMR ($CDCl_3$) d 0.99 (t; 3H, *J* = 7Hz, C3:-$(CH_2)_2C\underline{H}_3$), 1.3-1.5 (m, 2H, C3:-$CH_2C\underline{H}_2CH_3$), 2.23 (m, 2H, C3:-$C\underline{H}_2CH_2CH_3$), 3.53 (t, 1H, *J* = 5Hz, C3:-$\underline{H}$), 7.15-7.7 (m, 8 arom. H), 10.3 (s, 1H, N1:-H); ^{13}C-NMR ($CDCl_3$) d 14.5 (C3:-$(CH_2)_2\underline{C}H_3$), 19.3 (C3:-$CH_2\underline{C}H_2CH_3$), 33.1 (C3:-$\underline{C}H_2CH_2CH_3$), 63.2 ($\underline{C}$3:-$(CH_2)_2CH_3$), 122.8, 124.9, 129.1, 130.2, 130.8, 131.6, 135.7, 137.4, 168.0, 172.5 p.p.m.

General experimental for the N-Alkylation of 3-propyl-benzodiazepines

The N1-alkyl/aryl derivatives (Table 1) were obtained by deprotonating the parent amide **3c** with 1.1 eq. sodium hydride in DMF followed by the reaction of the in situ formed anion with 1.2 eq. of the electrophile. The alkylation towards the methyl, ethyl, propyl and butyl derivatives **4a-4d** was carried out at 20°C. The alkylation with the electrophiles (Table 1) giving the phthalimide-, piperidine-derivatives **4g-4l** was carried out at 50°C.

The N1-hydroxylmethyl-benzodiazepine **4e** was obtained from formaldehyde, generated by thermal decomposition of paraformaldehyde. After 30 min the reactions were quenched with 10% aq. hydrochloric acid. The mixture was extracted with methylenchloride (3 times), concentrated in vacuum to give the N1 alkylated benzodiazepines. The crude product was purified further by solid extraction with ether.

*7-Chloro-1-ethyl-5-phenyl-3-propyl-1,3-dihydro-2H-1,4-benzodiazepin-2-one **4a***

APCI + m/s: m/z = 343 (90%), 268 (10%); TLC (Ether): R_f = 0.85; IR (KBr) υ_{max} = 2990, 2863, 1723, 1673, 1602, 1482, 1255, 1124, 1080, 693 cm^{-1}; ^{1}H-NMR ($CDCl_3$) d 1.01 (t; 3H, *J* = 7Hz, C3: -$(CH_2)_2C\underline{H}_3$), 1.35-1.50 (m, 5H, C3:-$(CH_2C\underline{H}_2CH_3$ + N1:-$CH_2C\underline{H}_3$), 2.23 (m, 2H, C3:-$C\underline{H}_2CH_2CH_3$), 3.65 (q, 2H, N1:-$C\underline{H}_2CH_3$); 4.33 (t, 1H, *J* = 5Hz, C3:-$\underline{H}$), 7.2-7.87 (m, 8 arom. H), ^{13}C-NMR ($CDCl_3$) d 13.3, 14.1, 22.9 (C3:-$CH_2\underline{C}H_2CH_3$), 28.2 (N1:-$\underline{C}H_2CH_3$), 35.0 (C3:-$\underline{C}H_2CH_2CH_3$), 68.0 (C-3), 122.6, 128.5, 129.5, 130.8, 131.3, 138.1, 141.2, 167.7, 171.7 p.p.m.

*7-Chloro-5-phenyl-1,3-dipropyl-1,3-dihydro-2H-1,4-benzodiazepin-2-one **4b***

APCI + m/s: m/z = 356 (95%), 268 (5%); TLC (Ether): R_f = 0.88; IR (KBr) υ_{max} = 2973, 2908, 1714, 1681, 1457, 1251, 1112, 1070, 738, 695 cm^{-1}; ^{1}H-NMR ($CDCl_3$) d 0.73 (t, 3H, N1:-$CH_2CH_2C\underline{H}_3$), 1.0 (t; 3H, *J* = 7Hz, C3:-$(CH_2)_2C\underline{H}_3$), 1.43-1.7 (m, 6H, C3:-($C\underline{H}_2C\underline{H}_2CH_3$ + N1:-$CH_2C\underline{H}_2CH_3$), 3.48 (m, 2H, N1:-$C\underline{H}_2CH_2CH_3$), 4.25 (m, 1H, C3:-<u>H</u>), 7.26-7.87 (m, 8 arom. H); ^{13}C-NMR ($CDCl_3$) d 10.8, 14.1, 19.3, 22.9, 48.4 (N1:-$\underline{C}H_2CH_2CH_3$), 63.5 (<u>C</u>3:-H), 123.7, 128.4, 128.7, 130.3, 130.8, 132.4, 140.9, 166.9, 167.7 p.p.m.

1-Butyl-7-chloro-5-phenyl-3-propyl-1,3-dihydro-2H-1,4-benzodiazepin-2-one ***4c***

APCI + m/s: m/z = 369 (90%), 279 (5%), (5%); TLC (Ether): R_f = 0.9; IR (KBr) υ_{max} = 2924, 2867, 1717, 1683, 1461, 1283, 1121, 740, 695 cm^{-1}; ^{1}H-NMR ($CDCl_3$) d 0.95-1.9 (m, 14H, C3:-($C\underline{H}_2C\underline{H}_2C\underline{H}_3$ + N1:-$CH_2C\underline{H}_2C\underline{H}_2C\underline{H}_3$), 4.1-4.3 (m, 3H, C3:-<u>H</u> + N1:-$C\underline{H}_2CH_2CH_2CH_3$), 7.25-7.7 (m, 8 arom. H); ^{13}C-NMR ($CDCl_3$) d 13.5, 13.9, 19.3, 19.6, 28.8, 38.6, 68.1 (<u>C</u>3:-H), 123.7, 128.3, 128.7, 129.3, 130.8, 132.4, 139.1, 140.5, 167.7, 169.7 p.p.m.

1-Benzyl-7-chloro-5-phenyl-3-propyl-1,3-dihydro-2H-1,4-benzodiazepin-2-one ***4d***

APCI + m/s: m/z = 403 (95%), 313 (5%); TLC (Ether): R_f = 0.89; IR (KBr) υ_{max} = 2925, 2865, 1717, 1673, 1600, 1447, 1272, 1121, 738, 693 cm^{-1}; ^{1}H-NMR ($CDCl_3$) d 0.9-1.9 (m, 7H, C3:-($C\underline{H}_2C\underline{H}_2C\underline{H}_3$); 4.25 (m, 2H, N1:-$C\underline{H}_2$-Ph), 4.66 (m, 1H, C3:-<u>H</u>), 7.0-7.75 (m, 8 arom, H); ^{13}C-NMR ($CDCl_3$) d 14.2 (C3:-$(CH_2)_2\underline{C}H_3$), 22.9 (C3:-$(CH_2\underline{C}H_2CH_3)$, 33.7 (C3:-$\underline{C}H_2CH_2CH_3$), 49.9 (N1:-$\underline{C}H_2$-Ph), 63.4 (<u>C</u>3:-H), 123.9, 127.3, 127.6, 127.8, 128.4, 130.4, 130.9, 131.2, 132.4, 136.5, 138.1, 140.3, 167.4, 169.7 p.p.m.

7-Chloro-1-(hydroxymethyl)-5-phenyl-3-propyl-1,3-dihydro-2H-1,4-benzodiazepin-2-one ***4e***

APCI + m/s: m/z = 343 (95%), 313 (5%); TLC (Ether): R_f = 0.55; IR (KBr) υ_{max} = 3420, 2962, 2869, 1667, 1598, 1382, 1320, 1062, 825, 695 cm^{-1}; ^{1}H-NMR ($CDCl_3$) d 0.99 (t, 3H, *J* = 7Hz, C3:-$CH_2CH_2C\underline{H}_3$); 1.2-1.7 (m, 4H, C3:-($C\underline{H}_2C\underline{H}_2CH_3$), 3.3-3.6 (br s, 1H, N1:-CH_2-O<u>H</u>), 4.2 (q, 1H, C3:-<u>H</u>), 7.0-7.5 (m, 8 arom, H); ^{13}C-NMR ($CDCl_3$) d 14.3 (C3:-$CH_2CH_2\underline{C}H_3$), 17.9 (C3:-$CH_2\underline{C}H_2CH_3$), 29.1 (C3:-$\underline{C}H_2CH_2CH_3$), 69.2 (C-3), 96.0 N1:-$\underline{C}H_2$-OH), 121.5, 128.3, 128.5, 128.9, 130.4, 130.6, 132.2, 139.0, 141.8, 166.8, 169.3 p.p.m.

7-Chloro-1-(3-hydroxypropyl)-5-phenyl-3-propyl-1,3-dihydro-2H-1,4-benzodiazepin-2-one ***4f***

APCI + m/s: m/z = 371 (90%), 313 (10%); TLC (Ether): R_f = 0.62; IR (KBr) υ_{max} = 3428, 2954, 2925, 1675, 1579, 1405, 1326, 1076, 823, 715, 676 cm^{-1}; ^{1}H-NMR ($CDCl_3$) d 1.0 (t, 3H, *J* = 7Hz, C3:-$CH_2CH_2C\underline{H}_3$), 1.2-2.4 (m, 6H), 3.1-3.8 (m, 4H), 4.5 (m, 1H, C3:-<u>H</u>), 7.25-7.55 (m, 8 arom. H); ^{13}C-NMR ($CDCl_3$) d 14.1 (C3:-$CH_2CH_2\underline{C}H_3$), 19.3 (C3:-$CH_2\underline{C}H_2CH_3$), 30.8, 33.5 (C3:-$\underline{C}H_2CH_2CH_3$), 58.2, 63.5 (C-3), 97.2, 123.8, 128.4, 129.3, 130.2, 131.2, 136.2, 141.8, 167.4, 170.0 p.p.m.

7-Chloro-5-phenyl-1-(2-piperidin-1-ylethyl)-3-propyl-1,3-dihydro-2H-1,4-benzodiazepin-2-one ***4g***

APCI + m/s: m/z = 424; TLC (Ether): R_f = 0.85; IR (KBr) υ_{max} = 3443, 2928, 2866, 1675, 1608, 1476, 1315, 1112, 699 cm^{-1}; ^{1}H-NMR ($CDCl_3$) d 0.95 (t, 3H, *J* = 7Hz, C3:-$CH_2CH_2C\underline{H}_3$), 1.1-1.9 (m, 10H, N1:-CH_2-CH_2-<u>Pi--H</u> + C3:-$C\underline{H}_2C\underline{H}_2CH_3$), 2.1-2.4 (m, 2H), 2.65-2.8 (m, 4H, N1:-CH_2-CH_2-<u>Pi--H</u>), 3.46 (m, 1H), 4.2 (m, 1H), 4.51 (m, 1H, C3:-<u>H</u>), 7.25-7.60 (m, 8 arom. H); ^{13}C-NMR ($CDCl_3$) d 14.1 (C3:-$CH_2CH_2\underline{C}H_3$), 19.2 (C3:-$CH_2\underline{C}H_2CH_3$), 22.3, 25.4, 30.8, 33.9 (C3:-$\underline{C}H_2CH_2CH_3$), 47.3, 53.9, 58.2, 63.5 (<u>C</u>3:-H), 127.3, 128.1, 130.4, 130.7, 131.4, 136.5, 141.5, 167.4, 169.6 p.p.m.

2-[3-(7-Chloro-2-oxo-5-phenyl-3-propyl-2,3-dihydro-1H-1,4-benzodiazepin-1-yl)propyl]-1H-isoindole-1,3(2H)-dione ***4h***

APCI + m/s: m/z = 500 (75%), 313 (20%), 268 (5%); TLC (Ether): R_f = 0.88; IR (KBr) υ_{max} = 3467, 2960, 2869, 1771, 1710, 1677, 1602, 1462, 1400, 1372, 1037, 825, 726, 695 cm^{-1}; ^{1}H-NMR ($CDCl_3$) d 0.98 (t, 3H, *J* = 7Hz, C3:-$CH_2CH_2C\underline{H}_3$), 1.1-2.4 (m, 6H, C3:-$C\underline{H}_2C\underline{H}_2CH_3$) + N1:-$CH_2$-$C\underline{H}_2$-$CH_2$-Phth), 3.4-3.95 (m, 4H, N1:-$C\underline{H}_2$-CH_2-$C\underline{H}_2$-Phth), 4.45 (m, 1H, C3:-<u>H</u>), 7.1-7.9 (m, 12 arom. H); ^{13}C-NMR ($CDCl_3$) d 14.1 (C3:-$CH_2CH_2\underline{C}H_3$), 19.3 (C3:-$CH_2\underline{C}H_2CH_3$), 33.5, 35.2 (C3:-$\underline{C}H_2CH_2CH_3$), 44.8, 51.9, 63.4 (<u>C</u>3:-H), 123.3, 128.7, 129.6, 129.9, 130.2, 131.4, 131.9, 133.6, 136.2, 142.1, 166.5, 169.2 p.p.m.

Ethyl 2-(7-chloro-2-oxo-5-phenyl-3-propyl-2,3-dihydro-1H-1,4-benzodiazepin-1-yl)acetate ***4i***

APCI + m/s: m/z = 399 (90%), 313 (5%), 268 (5%); TLC (Ether): R_f = 0.65; IR (KBr) υ_{max} = 2958, 2865, 1717, 1677, 1580, 1461, 1268, 1201, 1069, 823, 740, 703 cm^{-1}; ^{1}H-NMR ($CDCl_3$) d 0.9-1.1 (m, 6H, C3:-$CH_2CH_2C\underline{H}_3$ + N1:-CH_2-$CO_2CH_2C\underline{H}_3$), 1.2-1.85 (m, 4H, C3:-$C\underline{H}_2C\underline{H}_2CH_3$), 4.1-4.3 (m, 4H, N1:-$C\underline{H}_2$-$CO_2C\underline{H}_2CH_3$), 4.5 (q, 1H, *J* = 5Hz, C3:-<u>H</u>), 7.25-7.8 (m, 8 arom. H); ^{13}C-NMR ($CDCl_3$) d 13.2 (N1:-CH_2-$CO_2CH_2\underline{C}H_3$), 14.0 (C3:-$CH_2CH_2\underline{C}H_3$), 19.6 (C3:-$CH_2\underline{C}H_2CH_3$), 33.6 (C3:-$\underline{C}H_2CH_2CH_3$), 49.2 (N1:-$\underline{C}H_2$-$CO_2CH_2CH_3$), 61.5, 63.8 (<u>C</u>3:-H), 122.8, 128.6, 128.9, 129.4, 130.6, 131.3, 136.4, 140.2, 166.9, 169.8 p.p.m.

2-(7-Chloro-2-oxo-5-phenyl-3-propyl-2,3-dihydro-1H-1,4-benzodiazepin-1-l)acetonitrile ***4j***

APCI + m/s: m/z = 352 (90%), 268 (10%); TLC (Ether): R_f = 0.81; IR (KBr) υ_{max} = 2930, 2861, 2280 (N1:-CH_2-C≡N), 1723, 1687, 1598, 1324, 1265, 825, 744, 695 cm^{-1}; ^{1}H-NMR ($CDCl_3$) d 1.01 (t, 3H, *J* = 7Hz, C3:-$CH_2CH_2CH_3$), 1.1-1.9 (m, 4H, C3:-$CH_2CH_2CH_3$), 3.45 + 3.6 (two m, 2H, N1:-CH_2-C≡N), 4.5 (q, 1H, *J* = 5Hz, C3:-H), 7.1-7.8; 7.1-7.9 (m, 8 arom, H); ^{13}C-NMR ($CDCl_3$) d 14.1 (C3:-$CH_2CH_2CH_3$), 19.3 (C3:-$CH_2CH_2CH_3$), 33.4 (C3:-$CH_2CH_2CH_3$), 38.9 (N1:-CH_2-C≡N), 62.9 (C3:-H), 115.4 (N1:-CH_2-C≡N), 122.8, 128.4, 128.9, 129.4, 130.4, 130.9, 131.5, 137.4, 139.2, 167.4, 169.3 p.p.m.

7-Chloro-1-(2-oxo-2-phenylpropyl)-5-phenyl-3-propyl-1,3-dihydro-2H-1,4-benzodiazepin-2-one ***4k***

APCI + m/s: m/z = 431 (80%), 313 (10%), 279 (10%); TLC (Ether): R_f = 0.82; IR (KBr) υ_{max} = 2969, 2871, 1717, 1688, 1598, 1465, 1255, 1116, 1076, 740, 693 cm^{-1}; ^{1}H-NMR ($CDCl_3$) d 1.0 (t, 3H, *J* = 7Hz, C3:-($CH_2CH_2CH_3$); 1.25-1.9 (m, 4H, C3:-($CH_2CH_2CH_3$), 4.27 (m, 3H, C3:-H + N1:-CH_2-CO-Ph), 7.0 - 8.0 (m, 13 arom. H); ^{13}C-NMR ($CDCl_3$) d 14.1 (C3:-$CH_2CH_2CH_3$), 22.3 (C3:-$CH_2CH_2CH_3$), 32.5 (C3:-$CH_2CH_2CH_3$), 53.3 (N1:-CH_2-CO-Ph), 63.8 (C-3), 123.2, 128.1, 128.7, 129.1, 130.9, 131.2, 131.5, 135.2, 136.9, 137.3, 139.9, 167.9, 169.0, 191.5 (N1:-CH_2-CO-Ph) p.p.m.

7-chloro-1-(3,3-dimethyl-2-oxobutyl)-3-hydroxy-5-phenyl-1,3-dihydro-2H-1,4-benzodiazepin-2-one ***5a***

Alkylation method: A 50% suspension of NaH in mineral oil (0.06 mol) was added in drops to a solution of Oxazepam (0.05 mol) in dry DMF (100 mL). After stirring for 15 min at RT, the alkylating agent (0.06 mol) was added in drops to the mixture, with ice cooling. The solution was stirred for additional 30-45 min at RT. For work up water was added (75 mL) and the suspension was added to ethylacetate (75 mL). The extract was washed with brine (2 × 100 mL), dried over sodium sulphate and the solvent was evaporated. Column chromatography was performed with ether/petrolether 1:2 as eluent.

Yield: 81%. R_f (ether/petrolether 1:2) = 0.51 Mol. Weight: 384.9 Mol. Formula: $C_{21}H_{21}ClN_2O_3$. MS (APCI(-)): 383, 385 (M-1), 285, 287 (M+) m/z. IR (KBr-disc) υ_{max}: 3450, 2933, 2358, 1710, 1677, 1596, 1482, 1322, 1131 & 693 cm^{-1}. ^{1}H-NMR ($CDCl_3$) 300K: 1.23 (s, $(CH_3)_3$), 4.81 (s, C3-H), 5.04-5.12 (m, -CH_2-), 7.05-7.67 (m, Ar-9H) p.p.m. ^{13}C-NMR (DMSO-d_6) 300K: 26.3 ((CH_3)$_3$), 43.5 ((CCH_3)$_3$), 53.2 (CH_2), 82.0 (C3), 122.9, 128.3 (2 × C), 128.4, 129.6, 129.8 (2 × C), 130.4, 130.8, 131.9, 137.4, 140.1 (Ar-C), 155.3 (C=O), 166.9 (C=N), 169.4 (C=O) p.p.m.

7-chloro-3-hydroxy-5-phenyl-1-prop-2-ynyl-1,3-dihydro-2H-1,4-benzodiazepin-2-one ***5b***

Yield: 67%. R_f (ether/petrolether 1:2) = 0.38 Mol. Weight: 324.8. Mol. Formula: $C_{18}H_{13}ClN_2O_2$. MS (APCI(-)): 323, 325 (M-1), 284, 286 (M+) m/z. IR (KBr-disc) υ_{max}: 3418, 3291, 3225, 2923, 1700, 1634, 1478, 1415, 1324, 1131, 1002 & 695 cm^{-1}. ^{1}H-NMR ($CDCl_3$) 300K: 2.10-2.34 (t, CH, *J* = 24.7, 25.0Hz), 4.51-4.66 (m, -CH_2-), 5.04 (C3), 7.21-7.63 (Ar-H) p.p.m. ^{13}C-NMR ($CDCl_3$) 300K: 37.0 (-CH_2-), 73.5, 75.19 (CH), 86.6 (C3), 123.4, 128.3 (2 × C), 128.3, 129.4 (2 × C), 130.3, 130.7, 131.1, 132.1, 137.1, 139.5 (Ar-H), 164.6 (C=O), 166.1 (C=N) p.p.m.

Preparation of 7-Chloro-5-phenyl-3-propyl-1,3-dihydro-2H-1,4-benzodiazepin-2-thione ***6***

1.8 g (6 mmol) of template **3c** and Lawesson's reagent (2.67 g, 6.6 mmol) were refluxed in 50 mL of pyridine. The reaction was completed after 8-10 h. The reaction mixture was cooled, concentrated in vacuum and the suspension of the residue in ice water was extracted with 50 mL of dichloromethane. The organic phase was filtered, dried and evaporated in vacuum. The crude product was further purified by column chromatography with ether.

Yield: 75%; MW 329; APCI + m/s: m/z = 329 (80%), 295 (10%), 268 (10%); mp: 238-242°C; TLC (ether): R_f = 0.85; IR (KBr disc) υ_{max} = 3440, 2952, 1614, 1569, 1475, 1318, 1160, 1027, 828, 698 cm^{-1}. ^{1}H-NMR ($CDCl_3$) d (ppm) 0.9-1.7 (br m, 5H), 2.1-2.5 (m, 2H), 4.09 (m, 1 H, C3:-H), 7.2-7.6 (m, 8 arom. H), 11.6 (s, 1H, N1:-H). ^{13}C-NMR ($CDCl_3$) d (ppm) 14.5 (C3:-$(CH_2)_2CH_3$), 19.5, (C3:-$CH_2CH_2CH_3$), 36.3 (C3:-$CH_2CH_2CH_3$), 67.1 (C-3), 124.9, 128.3, 128.9, 129.8, 130.2, 130.6, 131.8, 135.2, 137.8, 169.2, 202.3 (C=S).

8-Chloro-1-methyl-6-phenyl-4-propyl-4H-[1,2,4]triazolo[4,3-a][1,4]benzodiazepine ***7***

0.86 g (2.6 mmol) of template **2b** and acetylhydrazide (0.58 g, 7.8 mmol) was refluxed in 25 mL of *n*-butanol for 12 h to give the title product (0.68 g, 75%). The reaction mixture was cooled, concentrated in vacuum and the suspension of the residue in ice water was extracted with EtOAc (50 mL). The organic phase was dried with K_2CO_3, filtered, and evaporated in vacuum. The product was purified further by column chromatography with ether/10% methanol.

Yield: 34%; MW 351; APCI + m/s: m/z = 351; mp: 217-219°C; TLC (ether/10% methanol): R_f = 0.45; IR (KBr disc) υ_{max} = 3420, 2925, 2865, 1604, 1531, 1482, 1424, 1301, 1096, 695 cm^{-1}. ^{1}H-NMR ($CDCl_3$) d (ppm) 1.0 (s, 3H, (C3:-$(CH_2)_2CH_3$), 1.4-1.9 (br m, 4H, C3:-$(CH_2)_2CH_3$), 2.61 (s, 3H, C1:-CH_3), 4.52 (s, 1H, C4:-H), 7.2-7.7 (m, 8 H, arom. H). ^{13}C-NMR ($CDCl_3$) d (ppm) 12.1 (C4:-$(CH_2)_2CH_3$), 22.5, 31.7, 56.5 (C-4), 124.6, 128.3,

129.2, 130.7, 130.9, 131.2, 131.4, 132.1, 138.4, 165.9.

Pharmacology

^{131}I-CCK-8 receptor binding assay: The CCK_1 and CCK_2 receptor binding assays were performed by using guinea pig pancreas or guinea pig cerebral cortex, respectively. For the CCK_2 assay membranes from male guinea pig brain tissues were prepared according to the modification described by Saita *et al.* 1991. For the CCK_1 binding assay pancreatic membranes were obtained as described by Charpentier *et al.* 1988. All the binding assays were carried out in duplicate with L-365260 and Devazepide as internal standards.

In order to prepare the tissue the cerebral cortex was weighed after dissection and then homogenized in 25 mL ice cold 0.32 M sucrose for 15 strokes at 500 rpm. It was then centrifuged at 1,000 g (3,000 rpm) for 10 min. The supernatant was centrifuged at 20,000 g (13,000 rpm) for 20 min. This pellet was redispensed in the required volume of assay buffer as defined below with 5 strokes of homogenizer at 500 rpm. The final tissue concentration was 1 g original weight to 120 mL buffer. The tissue was stored in aliquots at -70°C.

For the receptor binding assay the radio ligand (^{125}I-Bolton Hunter labelled CCK, NEN) and the drugs to be tested were incubated at 25 pM with membranes (0.1 mg/mL) in assay buffer containing 20 mM Hepes, 1 mM EGTA, 5 mM $MgCl_2$, 150 mM NaCl at pH 6.5 for 2 h at room temperature. The incubations were terminated by centrifugation. The membrane pellets were wasted twice with water and bound radioactivity was measured in a γ-counter.

The GABA-A binding assay (*20*) was performed with ^{3}H-diazepam.

Animal studies

Experiments were conducted in male IRC mice obtained from the Animal House, Faculty of Medicine, Khon Kaen University. Each experimental group consisted of 6-8 animals and the treatment procedures were approved by the ethical committee, Faculty of Medicine, Khon Kaen University (HO 2434-76) accord with current UK legislation.

Mice were intraperitoneal injected with either test compound dissolved in 5% DMSO at the volume not more than 0.2 mL/animal. At 30 min after treatment, animals were tested as described in the following sections.

Anxiolytic activity tests

The light/dark box: Mice were placed in the light part of the light/dark box. The box was a Plexiglass cage, 25 × 50 × 20 cm, having one-third as a dark and two-third as a light compartment. A 40-W light bulb was used and positioned 10 cm above the center of the light component. The animals could walk freely between dark and light parts through the opening. The time animals spent in light part during the 5 min interval was recorded. The mouse was considered to be in the light part when its 4 legs were in the light part.

The elevated plus-maze: The wooden elevated plus-maze consisted of two open arms (30 × 10 cm) without any walls, two enclosed arms of the same size with 5-cm high side walls and end wall, and the central arena (10 × 10 cm) interconnecting all the arms. The maze was elevated approximately 30 cm height from the floor. At the beginning of the experiment the mouse was placed in the central arena facing one of the enclosed arm. During a 5 min interval, the time animals spent in the open arms of plus-maze was recorded. The mouse was considered to be in the open part when it had clearly crossed the line between the central arena and the open arm with its 4 legs.

Nociception tests

The thermal tail-flick test: The thermal response latency was measured by the tail flick test. The animals were placed into individual restraining cages leaving the tail hanging freely. The tail was immersed into water preset at 50°C. The response time, at which the animal reacted by withdrawing its tail from water, was recorded and the cut-off time was 10 sec in order to avoid damaging the animal's tissue.

The hot plate test: Mice were placed on a hot plate that was thermostatically maintained at 50°C. A Plexiglass box was used to confine the animal to the hot plate. The reaction time of each animal (either paw licking or jumping) was considered a pain response. The latency to reaction was recorded. For prevention of heat injury, the cut-off time of the test was 30 sec.

Antidepression tests

The tail suspension test: Mice were hung by their tail on the tail hanger using sticky tape for tail fixation, at approximately 1 cm from the end. The hanger was fixed in the black plastic box (20 × 20 × 45 cm) with the opening at the top front. The distance between the hanger to floor was approximately 40 cm. The mouse was suspended in the air by its tail and the immobile time was recorded during the period of 5 min. The duration of immobility was defined as the absence of all movement except for those required for respiration

The forced swim test: The forced swim test was carried out in a glass cylinder (20 cm diameter, 30 cm height) filled with water to the height of 20 cm. The water temperature was approximately 25-28°C. Mice were gently placed into the water and the immobility time was recorded by an observer during the period of 5 min. Immobility was defined as absence of all

movement and remained floating passively in the water with its head just above the water surface.

Motor activity tests

The rota-rod test: Mouse was placed on the rotating drum with the acceleration speed (Acceler. Rota-rod, Jones & Roberts, for mice 7650, Ugo Basile, Italy). The time animal spent on the rod is recorded.

The wire mesh grasping test: Mouse was placed on a wire mesh (20 × 30 cm). After a few seconds, the mesh was turned 180° and the time animal hold on the mesh was recorded.

Potentiation of morphine induced-analgesia

Each mouse received 2 injections. For the first injection, either 5% DMSO or synthetic CCK antagonists was injected intraperitoneally. Twenty min after the first injection, either normal saline or various doses of morphine were injected subcutaneously as the second injection.

The thermal response latency was measured by the tail flick test. The base line withdrawal thresholds (BT) were recorded prior to the first injection. Test thresholds (TT) were measured 60 min after the second injection. The cut off time was set to 45 sec. This was to avoid any tissue damage to the paw during the course of analgesia testing. The test thresholds were expressed as a percentage of Maximal Possible Effect (%MPE) using the equation: $\%MPE = \{(TT-BT)/(45-BT)\} \times 100$

Statistical methods

The data were expressed as mean ± SD and one-way analysis of variance (ANOVA) and supplementary Tukey test for pairwise comparison were tested to determine for any significant difference at $p < 0.05$.

Results and Discussion

Chemistry

Nor-methyldiazepam was synthesised according to the standard literature procedure (*21*) starting with aminoketones and chloroacetylchloride (*22*). Subsequent imine formation of the 7 membered ring system with urotropine, via the known α-amino intermediate, gave the target compound in 87% yield. Alkylation of the 1,4-benzodiazepin-2-one with dimethylsulfate gave Diazepam **1**, which was used as template for alkylation reactions and condensations with propionaldehyde in the 3-position (*23*).

The Diazepam **1** was deprotonated with LDA at -78°C and the alkylation with propylbromide, allylbromide and propargylbromide as electrophile with a catalytic amount of KI gave the alkylated benzodiazepines **2b-2c** in THF at ambient temperature over night (*24*) (Scheme 1).

In Scheme 2 a novel synthesis suitable for large scale preparation of the 3-propyl-1,4-benzodiazepine **3c** and the further alkylation products **4a-4k** are outlined. The route was adapted from the synthesis of Diazepam, in which bromo-butyric acid chloride was reacted to form the desired amide **I.** Bromobutyric acid chloride was obtained from the readily available bromobutyric acid with thionyl chloride. Starting material nitro-benzophenone was reacted with bromo-butyric acid chloride to give the desired amide **I** which was isolated. The treatment of this benzamide **I** with ammonia gave the 3-propyl-1,4-benzodiazepine **3a** in good yield. Unlike for the synthesis of Diazepam, Urotropine could not be used to the formation of the 7-membered ring system.

The nitro-benzodiazepine **3a** was reduced with a solution of Sn-(II)-chloride to the amino-benzodiazepine **3b**, which was converted into chloride **3c** in a Sandmeyer reaction. The amine **3b** was diazotated in situ with cupper chloride under acetic conditions.

The *N*-alkylated benzodiazepines **4a-4k** were synthesised from the benzodiazepine template **3c** with sodium hydride in DMF (*25*). No dialkylation products were obtained and no comumn chromatography was required for further purification.

Further *N*-alkylated benzodiazepines were synthesized using the Oxazepam template under same reaction conditions. With allylbromide and 3,3-dimethyloxobutyl chloride the Oxazepam derivatives **5a** and **5b** were obtained.

The preparation of the 4H-[1,2,4]triazolo[4,3-a]-1,4-benzodiazepine **7** via the thioamide intermediate **6** is outlined in the synthetic Scheme 4.

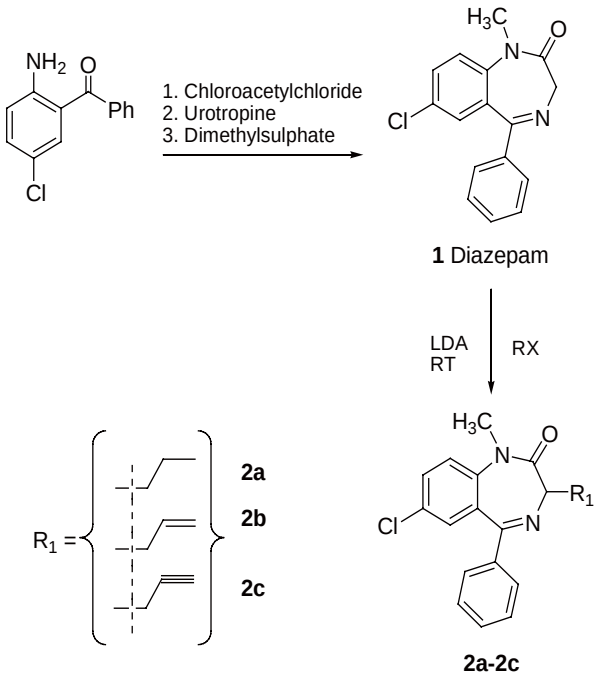

Scheme 1. *N*-Alkylation of Diazepam.

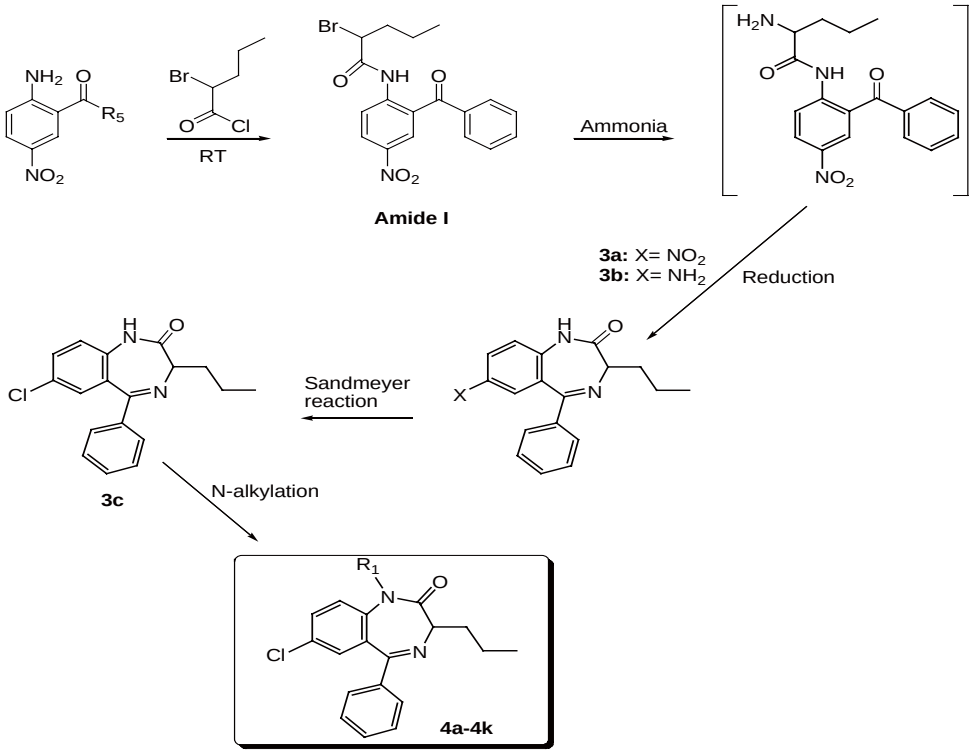

Scheme 2. *N*-alkylation of 3-propyl-1,4-benzodiazepines.

The template **3c** was converted into thioamide **6** with tetraphosphorus decasulfide (P4S10) under reflux conditions. In an improved method, tetraphosphorus decasulfide was replaced by with 2,4-bis(4-methoxyphenyl)-2-4-dithioxo-1,2,3,4-dithiadiphosphetane (Lawesson's reagent) (*26*) which gave the thioamide **6** in 75% yield.

The activated thioamide **6** was reacted with an excess of acetylhydrazide into the desired 1,2,4-triazolo-1,4-benzodiazepines **7**. *N*-butanol was essential to achieve a high reflux temperature for this conversion.

The Nva template **8** was prepared by refluxing 5-chloro-2-aminobenzophenone with 2 equivalent of *L*-Nor-valine ethylester HCl for 48 h in presence of a catalytic amount of DMAP.

X-ray analysis

As gold standard of characterization, the X-ray structure of the *N*-alkylated propyl-benzodiazepine **4i** is outlined in Figure 2.

It was found as expected, that the benzodiazepine **4i** ring was not part of a flat extended system. Torsion angles within this ring about bonds that have full or partial double bond character (N4-C5, C10-C11, N1-C2) did not exceed 4.2(4)° in magnitude. Torsion angles within the ring about the intervening bonds N1-C10 and C5-C11 attained the intermediate values of -42.3(4) and 44.2(4)°, respectively. Those about C2-C3 and C3-N4 at the opposite end of the ring had the largest magnitudes, being 78.2(3) and -73.2(3)°. The amide resonance affecting atoms N1, C2 and O17 were confirmed by the elongation of the C2-O17 distance to 1.217(3) Å compared with 1.197(4) Å for the ester C13-O18. The partial negative charge on O17 helped to attract a C23-H23…O17 hydrogen bond with H…O distance 2.48 Å and C-H…O angle 165°. Structural details were listed in Table 1.

SAR-studies - binding affinity

For the entire set of 1,4-benzodiazepines the chemical yields and the binding affinities were outlined for the CCK_2 receptor in Table 2.

Alkylated derivatives of diazepam (**2a-2c**) were

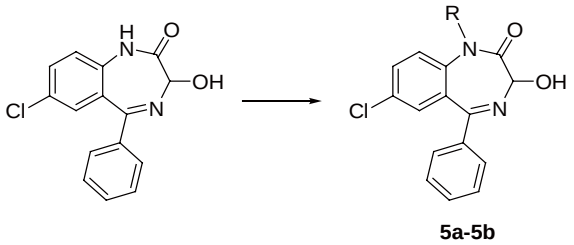

Scheme 3. *N*-Alkylation of Oxazepam.

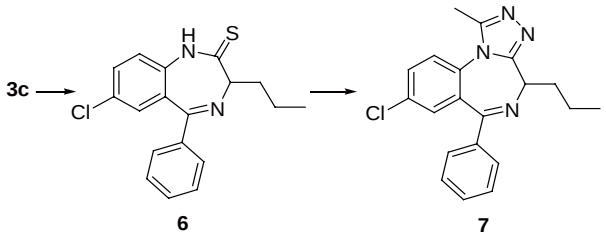

Scheme 4. Preparation of triazolo-propylbenzodiazepine **7**.

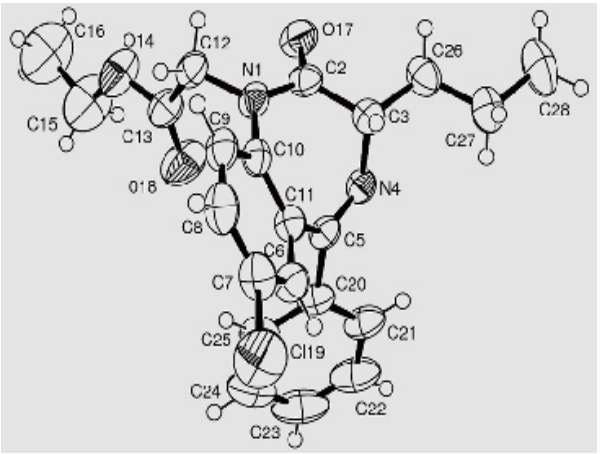

Figure 2. X-ray structure of benzodiazepine **4i**.

found to occur a very low binding affinity towards the CCK_2 receptor.

Reaction intermediate **3c** showed a good potency with an IC_{50} about 300 nM, while the precursors, the nitro-intermediate **3a**, and the amino-intermeate **3b** were relatively biologically inactive.

The ligand **3c** containing a C3 unit in the 3-position of the 1,4-benzodiazepine was previously found to bind best to a postulated lipophilic pocket at the CCK_2 receptor (*13*). In order to optimize the affinity of the 3-propyl-1,4-benzodiazepines, additional substituents were introduced in the N1-position giving the series of *N*-alkylated propylbenzodiazepines **4a-4k,** of which the nitrile **4j** occurred an enhanced binding affinity compared with parent derivative **3c**.

The more complex derivatives such as the piperidino-, and phthalimido-benzodiazepines **4g**, **4f** and **4h** did not show an enhanced binding affinity at the CCK receptor.

As previously reported for the 3-ureido-benzodiazepines, N1-alkylation (*27*) should have shown enhanced binding on the CCK_2 receptor, but with the majority of the electrophiles used here, the affinity was significantly lower than for the N1-unalkylated 1,4-benzodiazepine **3c**.

Functionalised hydrophilic substituents at the N1 position as seen for the hydroxy-alkyl derivatives **4e**, **4f** resulted in the loss of binding affinity.

In order to gain a high chemical diversity an amide **6u**, an ester **4i** and a ketone **4k** was formed of the 1,4-benzodiazepine template.

A decreased affinity was observed for the N1 alkylated propyl-1,4-benzodiazepine **4k** unlike Merck's 3-ureido-1,4-benzo-diazepines, which have previously shown an increased binding with this N1-substituent (*28*).

Table 1. Crystal structure determination for benzodiazepine **4i**

Empirical formula	$C_{22}H_{23}ClN_2O_3$
a/Å	9.2332(8)
b/Å	17.702(4)
c/Å	13.052(5)
β/°	97.466(15)
Z	4
Calculated density/g·cm^{-3}	1.253
Crystal system	Monoclinic
Space group	$P2_1/c$
Diffractometer	Enraf-Nonius CAD4
Radiation used	Mo-Kα
Monochromator	Graphite
Crystal size/mm	0.45 × 0.20 × 0.05
Temperature/K	294(2)
Data collection mode	ω-2θ scans
Theta range/°	2.22-24.98
Reciprocal lattice segments	$-10 \le h \le 10$ $-11 \le k \le 21$ $0 \le l \le 15$
Reflections measured	6512
Symmetry-independent reflections	3685
Cut-off criterion	$I > 2\sigma(I)$
Linear absorption coefficient/mm^{-1}	0.205
Method of absorption correction	psi-scan
Method of solution	direct
Method of refinement	full-matrix LS
Final *R*(obs)	0.0449
Final *wR2* (all data)	0.1478
Residual density/e Å^{-3}	-0.216, 0.275

Table 2. Chemical yields and IC_{50} receptor binding data on the Cholecystokinin (CCK_2) receptor of the 1,4-benzodiazepines. (Standard: Merck L-365260 10 nM)

Entry	Substituent	Yield (%)	CCK_2 (μM)
1	Diazepam		
2a	R_1= propyl	28	5
2b	R_1= allyl	35	2.5
2c	R_1= propargyl	22	2.2
3a	X=NO_2	60	8
3b	X=NH_2	65	>50
3c	X=Cl	52	0.3 ± 0.01
4a	R_1= ethyl	78	1.2 ± 0.6
4b	R_1= propyl	74	5 ± 2
4c	R_1= butyl	65	3 ± 1
4d	R_1= benzyl	65	35 ± 3
4e	R_1= hydroxymethyl	21	37 ± 11
4f	R_1= hydroxypropyl	31	71 ± 21
4g	R_1= 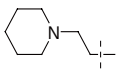	82	88 ± 12
4h	R_1= 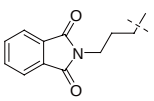	87	34 ± 6
4i	R_1= 	63	3.5 ± 0.4
4j	R_1= cyanomethy	53	0.19 ± 0.02
4k	R_1= 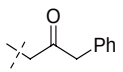	21	4 ± 1.5
5a	R= 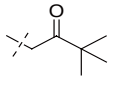	81	0.19 ± 0.02
5b	R= allyl	67	0.98
6	thioamide-	56	0.20 ± 0.02
7	triazolo-	34	32
8	L-isomer	69	0.17 ± 0.02

A cyanomethyl substituent on the N1 position is desirable, firstly to enhance the affinity and secondly to differentiate the binding profile between the cholecystokinin and the benzodiazepine receptor. It is known that most of the substiuents in the N1 position block the affinity on the GABA-A receptor (*20*).

The alkylated derivatives based on the Oxazepam structure, such as **5a** and **5b** showed potent and moderate binding affinity. Compared to Oxazepam the binding affinity was increseased 100 fold for ketone **5a**.

The biosteric modification from amide **3c** into thioamide **6** gained some binding affinity, which was lost with the indroduction of the triazolo ring system, cp **7**.

The optically pure *L*-stereoisomere **8** of the *n*-propyl derivative displayed a further improved activity and is considered a promising example of an optically and chemically pure compound derived from nor-valine in only one chemical step (Figure 3).

In Figure 3, important structures were highlighted additionally for clarity. The crystalline **4i** was suitable for X-ray analysis, but lacked of binding affinity.

Nitrile **4j** displayed the best binding affinity of the *N*-alkylated propyl series **4**. The *t*-butyl–keton side chain decreased affinity of the *n*-propyl derivatives in the **4**-series, but enhanced the affinity for the Oxazepam template as seen as for Merck' ureas.

Thioamide **6** was found of improved CCK binding affinity. The triazolo-compound **7** was supposed a GABAA ligand, possibly with a modified subtype specificity, due to the 3-propyl substituent, but was not further investigated. The *L*-propyl-1,4-benzodiazepine derivative **8** combined control of stereochemistry at the C3 centre, easy access and good CCK_2 binding affinity.

In vivo studies

The neuropharmacological effects of intermediate **3c**, the active and inactive dpropylbenzodiazepines **4i** and **4j**, the *N*-alkylated Oxazepam analogue **5a**, thioamide **6** and the *L*-propyl benzodiazepine **8** were evaluated in mice in 8 different *in vivo* assays, compared to Diazepam **1** and desimipramine as standards.

The benzodiazepine **4j**, **5a**, **6** and **8** displayed equivalent potency for the CCK_2 receptor. All test compounds have been found inactive in the evaluation of pain in the hot plate and the tail flick assays (*29*), when administered as a single agent (Table 3).

The first step of the *in vivo* evaluation (*30*), was the determination of the MED, minimum effective dose, to select *in vivo* active compounds and to compare the results with the receptor binding data. Compounds without binding affinity were not found different from the control (propylen glycol) at doses of 0.1, 0.5, 1.0, 2.0, 5.0 and 10 mg. For example, **4i** displayed no binding affinity and was found inactive in mice.

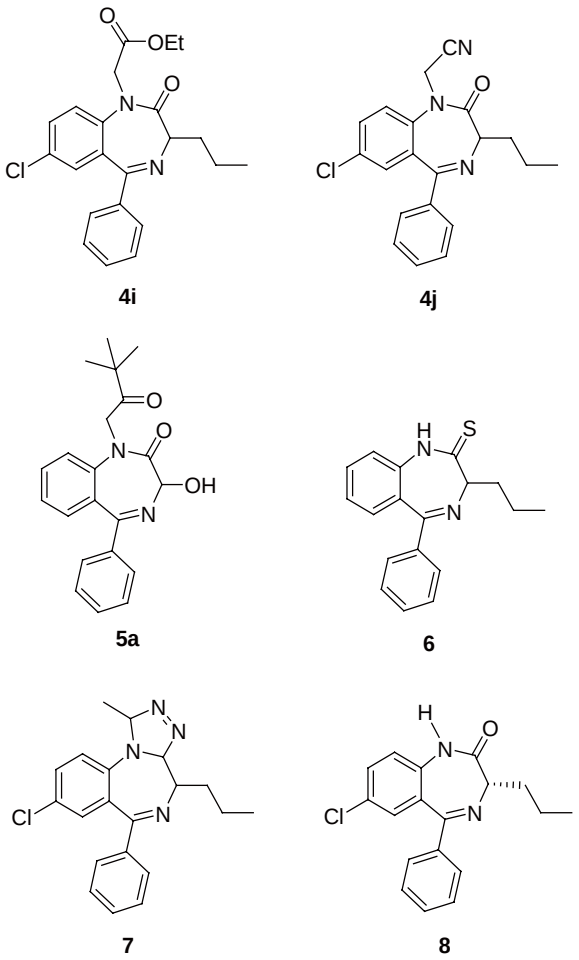

Figure 3. Important structures highlighted additional for the SAR-studies - binding affinity.

Benzodiazepine **4j**, **5a**, **6** and **8**, ligands of the same binding profile, had an MED of 1 mg/kg in both antidepressant assays and 2.5 mg/kg in the selected anxiolytic assays. The anxiolytic effect was evaluated by using the black and white box test (*31*) and the elevated x-maze (*32*) as two standard anxiolytic assays (Table 4).

Subsequently, full data of the equipotent CCK_2 selective derivatives **4j**, **5a** and **8** were collected and the ED_{50} were calculated

Anxiolytic assays: Animals have shown at high doses in the black and white test (*33*) a significantly increased preference for the light area, and also the number of crossings between the two chambers were enhanced for **4j**, **5a** and **8**. An enhanced locomotor activity was determinated with an ED_{50} of 9/11/7 mg/kg for the set of benzodiazepine derivatives. This correlated with the results of *the elevated plus maze test (X-maze)* (*34*), in which a greatly enhanced exploration of the open arms with an increased number of total crossings was observed. The anxiolytic effect is linked with CCK_2 binding affinity. The ureas (*19*) displayed as mixed CCK ligands, anxiolytic- and antidepressant effects at a similar low dose. The binding affinity correlated in this comparison well with *in vivo* results.

Table 3. *In vivo* evaluation of selected 1,4-benzodiazepines

Compound	Receptor binding IC_{50} (nM)		Elevated plus-maze	Light/dark box	Tail suspension test	Forced swim test	Thermal tail flick test	Hot plate test	Rota-rod test	Wire mesh grasping
	CCK_1	CCK_2								
1	>100000	>100000	1	1	-	-	-	-	1	1
3c	>10000	300 ± 10	5	5	2.5	2.5	-	-	-	-
4i	>10000	3500 ± 400	NS	NS	NS	NS	NS	NS	NS	NS
4j	>10000	190 ± 20	2.5	2.5	1	1	-	-	-	-
5a	>10000	190 ± 10	2.5	2.5	1	1	-	-	-	-
6	>10000	200 ± 10	2.5	2.5	1	1	-	-	-	-
8	>10000	170 ± 10	2.5	2.5	1	1	-	-	-	-

NS: no significance could be observed at 0.1, 0.5, 1.0, 2.5, 5.0 and 10 mg/kg compared to the control.
MED: minimum effective dose (mg/kg) given in above table.

Table 4. *In vivo* studies of selected CCK antagonists in mice

	ED_{50} (mg/kg ± 1 mg/kg)		
	4j	**5a**	**8**
Elevated plus maze	9	11	9
Light/dark box	9	11	7
Tail suspension test	2	4	2
Forced swim test	2	3	2
Thermal tail flick test	>100	>100	>100
Hot plate	>100	>100	>100
Rota rod test	>100	>100	>100
Wire mesh grasping	>100	>100	>100

Antidepressant assays: Antidepressant drugs have the effect of reducing the duration of immobility in *the despair swim test (immobility time test)* (*35*). The set of ligands **4j**, **5a** and **8** decreased the immobility time at a very low dose and the ED_{50} was calculated at 2/3/2 mg/kg. In the tail suspension test, which is based on a similar underlying mechanism, an ED_{50} of 2/4/2 mg/kg was determined for **4j**, **5a** and **8**. Desipramine, a tricyclic antidepressant served as positive control, which occured a similar potency and magnitude of the antidepressant effect.

Nociception and motor activity tests: In all treated groups, no effect on nociception (*36*) was observed in the tail immersion test (*37*) and the hot plate method. An impairment of motor activity could not be observed in all tested models up to a dose of 100 mg/kg in the wire mash grasping and the rota rod test.

*Potentiation effect of **4j** and **8** on morphine-induced analgesia in mice*

CCK antagonists are supposed to enhance the effect of morphine and therefore the cocomittant administration of **4j** and **8** at a dose of 5 mg/kg body weight was investigated. Assays were carried out as described in experimental section. The thermal response latency of the animals were determined by the tail flick test and the results were expressed as %MPE = {(TT-BT)/(45-BT)} × 100.

Although no intrinsic analgesic effect of **4j** and **8** was observed as single agent, both CCK antagonists

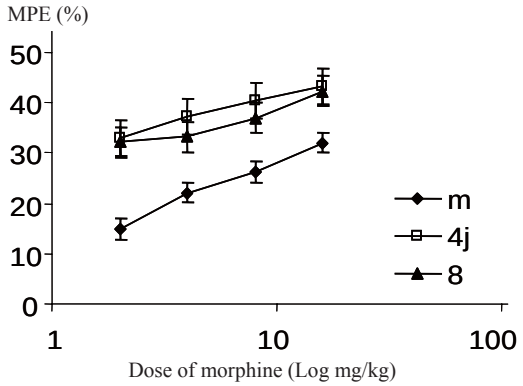

Figure 4. Potentiation effects of **4j** and **8** on morphine-induced analgesia in mice. Mice were injected with 5% DMSO or **4j** or **8** (5 mg/kg BW) (ip) and normal saline (sc) or morphine (sc) (2, 4, 8 or 16 mg/kg BW). There were 8-10 mice in each group and % maximum possible effect (MPE) was expressed as mean ± SD. **P*-value < 0.05 when compared to the control group (Note: **5a** not significantly different from **4j** and **8**). m, morphine; 4j, morphine + 5 mg/kg benzodiazepine **4j**; 8, morphine + 5 mg/kg benzodiazepine **8**.

increased the % MPE in response to morphine, at all doses of morphine tested significantly (Figure 4).

The best enhancement was found at a low dose such as 2 mg/kg of morphine and full investigation of this class of CCK_2 antagonist, further mixed and CCK_1 selective antagonists are in high progress.

As expected no significant difference between the benzodiazepine **5a/4j** and **8** was observed. Overall the dose response curve of morphine was shifted to the left indicating in general a potentiation of the analgesic effects of morphine.

Conclusions

The 3-propylbenzodiazepine **3c** was firstly synthesized by a combinatorial approach, but due to the small scale no further evaluation could be performed. A new chemical approach toward **3c** provided the parent compound in good quantities and new *N*-alkylated analogues were derived thereof. This was completed by a third stereoselective on-step-synthesis of active **8.**

Based on the Oxazepam template an equipotent

N1-alkylated derivative was tested and developed further.

The structurally well known class of non-toxic benzodiazepies displayed as CCK_2 antagonist, antidepressant properties and the dose response curve of morphine was found to be significantly shifted to the left.

Studies are ongoing to evaluate the importance of mixed, CCK_2 or CCK_1 antagonists on the anti-nociceptive effects in conjunction with opiate agonists.

References

1. McDonald IM. CCK_2 receptor antagonists. Expert Opin Ther Pat 2001;11:445-462.
2. Satoh M, Kondoh Y, Okamoto Y, Nishida A, Miyata K, Ohta M, Mase T, Murase K. New 1,4-benzodiazepin-2-one derivatives as gastrin/cholecystokinin-B antagonists. Chem Pharm Bull 1995;43:2159-2176.
3. Bock MG, DiPardo RM, Mellin EC, Newton NC. Second generation benzodiazepine CCK-B antagonists. Development of subnanomolar analogues with selectivity and water solubility. J Med Chem 1994;37:722-724.
4. Lattmann E, Arayarat P. From CNS-drugs to anti-neoplastic agents: Cholecysto-kinin (CCK)-antagonists as modern anti-cancer agents. Science (KKU) 2003;31:178-193.
5. Hughes J, Woodruff GN. Neuropeptides function and clinical applications. Arzneimittelforschung 1992;42:250-255.
6. Rasmussen K, Stockton ME, Czachura JF, Howbert JJ. Cholecystokinin (CCK) and schizophrenia: the selective CCKB antagonist LY262691 decreases midbrain dopamine unit activity. Eur J Pharmacol 1991; 209:135-138.
7. Dourish CT, Rycroft W, Iversen SD. Postponement of satiety by blockade of brain cholecystokinin (CCK-B) receptors. Science 1989;245:1509-1511.
8. Trivedi K, Bharat J. Cholecystokinin receptor antagonists: Current status. Curr Med Chem 1994;1:313-345
9. Bradwejn J, Koszycki D, Meterissian G. Cholecystokinin-tetrapeptide induces panic attacks in patients with panic disorder. Can J Psychiatry 1990;35:83-85.
10. Evans BE, Rittle KE, Bock MG, DiPardo RM, Freidinger RM, Whitter WL, Lundell GF, Veber DF, Anderson PS, Chang RS, Cerino DJ. Methods for drug discovery: development of potent, selective, orally effective cholecystokinin antagonists. J Med Chem 1988;31:2235-2246.
11. Simpson K, Serpell M, McCubbins TD, Padfield NL, Edwards N, Markam K, Eastwood D, Block R, Rowbotham DJ. Management of neuropathic pain in patients using a CCK antagonist Devazepide as an adjunct to strong opioids. 4th International conference on the mechanisms and treatment of neuropathic pain, San Francisco, USA, 2001.
12. Kitchen I, Crowder I. Assessment of the hot-plate antinociceptive test in mice: A new method for the statistical treatment of graded data. J Pharmacol Methods 1985;13:1-7.
13. Lattmann E, Billington DC, Poyner DR, Howitt SB, Offel M. Synthesis and evaluation of Asperlicin analogues as non-peptidal Cholecystokinin-antagonists. Drug Des Discov 2001;17:219-230.
14. Lattmann E, Billington DC, Poyner DR, Arayarat P, Howitt SB, Lawrence S, Offel M. Combinatorial solid phase synthesis of multiply-substituted 1,4-benzodiazepines and affinity studies on the CCK_2 receptor (Part 1). Drug Des Discov 2002;18:9-21.
15. Lattmann E, Sattayasai J, Billington DC, Poyner DR, Puapairoj P, Tiamkao S, Airarat W, Singh H, Offel M. Synthesis and evaluation of N1-substituted-3-propyl-1,4-benzodiazepine-2-ones as cholecystokinin (CCK_2) receptor ligands. J Pharm Pharmacol 2002;54:827-834.
16. Lattmann E, Singh H, Boonprakob Y, Lattmann P, Sattayasai J. Synthesis and evaluation of *N*-(3-oxo-2,3-dihydro-1H-pyrazol-4-yl)-1H-indole-carboxamides as cholecystokinin antagonists. J Pharm Pharmacol 2006;58:393-401.
17. Offel M, Lattmann P, Singh H, Billington DC, Bunprakob Y, Sattayasai J, Lattmann E. Synthesis of substituted 3-anilino-5-phenyl-1,3-dihydro-2H-1,4-benzodiazepine-2-ones and their evaluation as cholecystokinin-ligands. Arch Pharm (Weinheim) 2006;339:163-173.
18. Yu Y, Jawa A, Pan W, Kastin AJ. Effects of peptides, with emphasis on feeding, pain, and behaviour. Peptides 2004;25:2257-2289.
19. Lattmann E, Sattayasai J, Boonprakob J, Lattmann P, Singh H. Synthesis and evaluation of *N*-(5-methyl-3-oxo-1,2- diphenyl-2,3-dihydro-1H-pyrazol-4-yl)-N'-phenylureas as cholecystokinin antagonists. Arzneimittelforschung 2005;55:251-258.
20. Martin IL, Lattmann E. Benzodiazepine recognition site ligands and GABAA receptors. Expert Opin Ther Pat 1999;9:1347-1358.
21. Farghaly AM. Synthesis of some substituted aminophenazones of possible therapeutic interest. Pharmazie 1979;34:70-73.
22. Roth HJ, Kleemann A. Drug synthesis. Pharmaceutical Chemistry (Ellis Horwood). 1999;1:202-205
23. Sternbach LH, Fryer RI, Stempel A. Quinazolines and 1,4-Benzodiazepines. V. o-Aminobenzophenones. J Org Chem 1962;27:3781-3788.
24. Evans BE, Rittle KE, Bock MG, Freidinger RM. Design of nonpeptidal ligands for a peptide receptor: cholecystokin antagonists. J Med Chem 1987;30:1229-1239.
Charpentier B, Pelaprat D, Durieux C, Dor A, Reibaud M, Blanchard JC, Roques BP. Cyclic cholecystokinin analogues with high selectivity for central receptors. Proc Natl Acad Sci U S A 1988;85:1968-1972.
25. Scheibye S, Pederson BS, Lawesson SO. Dithiadiphosphetane and their application for organic syntheses. Bull Soc Chim Belg 1978;87:227-232.
26. Semple G, Ryder H, Kendrick DA, Szelke M, Ohta M, Satoh M, Nisida A, Akuzawa S, Miyata K. Synthesis and biological activity of 1-alkylcarbonyl-methyl analogues of YM022. Bioorg Med Chem Lett 1996;6:51-54.
27. Semple G, Ryder H, Kendrick DA, Szelke M, Ohta M, Satoh M, Nisida A, Akuzawa S, Miyata K, Rooker DP, Batt AR. (3R)-*N*-(tert-Butyl-carbonylmethyl)-2,3-dihydro-2-oxo-5-(2-pyridyl)-1H-1,4-benzodiazepin-3-yl)-*N*'-(3-(methyl-amino)phenyl)urea (YF476): A potent and orally active gastrin/CCK-B antagonist. J Med Chem 1997;40:331-341.
28. O'Neil MF, Dourish CT, Iversen SD. Morphine induced analgesia in the rat paw pressure test is blocked by CCK and enhanced by CCK antagonist MK-329. Neuropharmacology 1989;28:243-247.
29. Vogel HG, Vogel WH. Pharmacological assays. Drug discovery and evaluation (Springer) 1997; pp232-239
30. MattoV, Harro J, Allikmet L. The effects of drugs acting on the CCK receptors and rat exploration in the exploration box. J Physiol Pharmacol 1997;48:239-251.
31. Johnson NJ, Rodgers RJ. Ethological analysis of cholecystokinin (CCK-A and CCK-B) receptor ligands in the elevated plus maze in mice. Psychopharmacology (Berl) 1996;124:355-364.
32. Kilfoil T, Michel A, Montgomery D, Whithing RL. Effects of anxiolytic and anxiogenic drugs on exploratory activity in a simple model of anxiety in mice. Neuropharmacololy 1989;28:901-905.
33. Silverman P. Approach to a conditioned stimulus mazes. Animal behaviour in the laboratory (Chapman and Hall). 1978; pp110-119.
34. Porsolt RD, Le Pichon M, Jalfre M. Depression: a new animal model sensitive to antidepressant treatments. Nature 1977;266:730-732.
35. Walker JM, Dixon WC. A solid state device for the measuring sensitivity to thermal pain. Physiol Behav 1983;30:481-483.
36. Cowan A. Modern methods in pharmacology: Recent approaches in the testing of analgesics in animals. Testing and Evaluation of Drugs of Abuse (Wiley-Liss Inc.) 1990; pp21-33.
37. Speth RC, Wastek GJ, Johnson PC. Benzodiazepine receptors: Temperature dependence of [^{3}H]flunitrazepam binding. Life Sci 1979;24:351-357.

ONIOM DFT/PM3 calculations on the interaction between dapivirine and HIV-1 reverse transcriptase, a theoretical study

Yong-Hong Liang, Fen-Er Chen*

Department of Chemistry, Fudan University, Shanghai, China.

ABSTRACT: Theoretical investigations of the interaction between dapivirine and the HIV-1 RT binding site have been performed by the ONIOM2 (B3LYP/6-31G (d,p): PM3) and B3LYP/6-31G (d,p) methods. The results derived from this study indicate that this inhibitor dapivirine forms two hydrogen bonds with Lys101 and exhibits strong π-π stacking or H…π interaction with Tyr181 and Tyr188. These interactions play a vital role in stabilizing the NNIBP/dapivirine complex. Additionally, the predicted binding energy of the BBF optimized structure for this complex system is -18.20 kcal/mol.

Key Words: Dapivirine, HIV-1 reverse transcriptase, ONIOM, DFT, PM3

Introduction

Human immunodeficiency virus type-1 reverse transcriptase (HIV-1 RT) is an important target for designing RT inhibitors to block the virus's replication and prevent AIDS-related disease (*1*,*2*). Two kinds of RT inhibitors, nucleoside reverse transcriptase inhibitors (NRTIs) and non-nucleoside reverse transcriptase inhibitors (NNRTIs), have been developed over the past twenty years (*3*). Despite NNRTIs such as three FDA-approved drugs, nevirapine (*4*), delavirdine (*5*) and efavirenz (*6*), being highly specific and less toxic than nucleoside inhibitors (*7*), the rapid emergence of resistant HIV viral strains carrying mutation at residues that surround the NNRTI binding pocket limits the usefulness of NNRTI to treat HIV infection (*8*).

Dapivirine (Figure 1), an early compound of NNRTIs diarylpyrimidines (DAPYs) (*9*,*10*), is currently in phase IIB clinical trials in the United States as an RT inhibitor for the treatment of AIDS. Unlike the butterfly-like conformation of nevirapine, delavirdine, and efavirenz in the crystal structures of HIV-1 RT/NNRTI complexes, this inhibitor adopts the horseshoe mode to bind with HIV-1 RT (*12*). Despite intensive experimental research including crystal structure analysis to study the interaction between dapivirine and HIV-1 RT (*11*,*12*), the interaction of dapivirine and amino acid in the non-nucleoside inhibitor binding pocket (NNIBP) and the origin of mutational effects are still not fully understood.

In the present work, the interaction between dapivirine and RT binding sites has been investigated by the ONIOM2 (B3LYP/6-31G (d,p): PM3) and B3LYP/6-31G (d,p) methods. The main aim of this work is to study the following two aspects: 1) the binding mechanism of dapivirine to HIV-1 RT and the nature of drug resistance and 2) the differentia of dapivirine with respect to two other inhibitors studied, nevirapine and efavirenz.

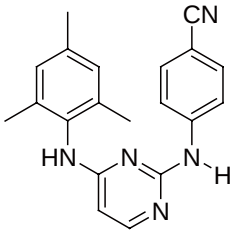

1 dapirivine (TMC 120)

Figure 1. The chemical structure of dapivirine.

Materials and Methods

Construction of the model studied

The model of NNIBP/dapivirine complex has been constructed as in previous reports (*13*,*15*). The binding pocket studied, which contains 19 residues surrounding the NNIBP with at least one atom interacting with any of the atoms of the inhibitor within an interatomic distance of 6 Å (Figure 2), is extracted from the 2.9 Å resolved crystal structure of dapivirine with HIV-1 RT (1S6Q) (*12*). All residues, supposedly in their neutral from, were terminated if not connected to another

**Correspondence to:* Department of Chemistry, Fudan University, Shanghai 200433, China;
e-mail: rfchen@fudan.edu.cn

Received June 9, 2007
Accepted June 20, 2007

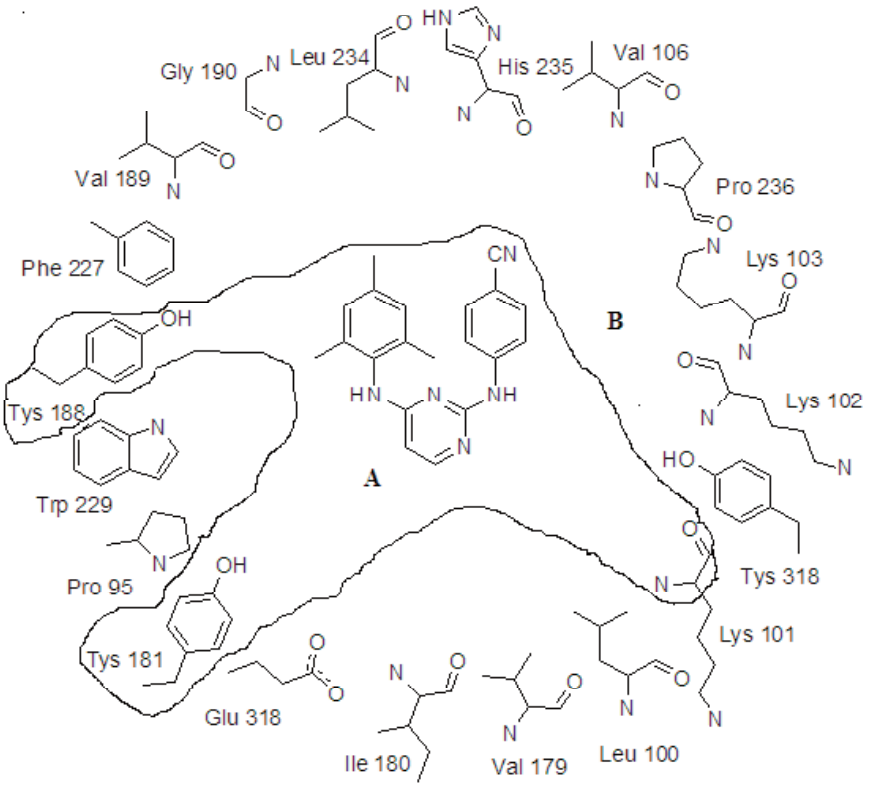

Figure 2. The studied model system of dapivirine bound to the HIV-1 RT binding site. Layer partition is shown for ONIOM2 calculations. (A) is the inner layer and (B) is the outer layer.

residue in the selected model by linking H atoms at the N- and C-terminal with their torsion angles, which are assumed to be the same as in the crystal structure. Hydrogen atoms were added to using the Gauss View program, and their positions were optimized by the semi-empirical PM3 method. This complex was used as the initial structure for this theoretical study.

ONIOM calculations

The ONIOM method was proposed as a reliable tool for studying enzyme-inhibitor interaction (*13-16*). Recently, Morokuma *et al.* (*17*) have systematically investigated all possible three- and two-layer ONIOM combinations of high-level QM (HQ = B3LYP/6-31G (d), low-level QM (LQ = AM1), and MM (Amber) for the deprotonation energy and structure of a zwitterionic peptide molecule, NH_3^+-CH^nBu-CO-NH-CH_2-CO-NH-CH^nBu-COO^-. They found that the errors introduced in the ONIOM approximation, in comparison to the target HQ (or HQ: HQ: HQ) calculation, generally increase in the following order: HQ: HQ: HQ (target) < HQ: HQ: LQ < HQ: LQ: LQ < HQ: HQ: MM < HQ: LQ: MM, HQ: MM: MM, LQ: LQ: LQ < LQ: LQ: MM < LQ: MM: MM. Thus, the two-layer ONIOM (B3LYP/6-31G (d,p): PM3) method is applied to calculate the structure and binding energy of dapivirine at the HIV-RT binding site. Previous reports (*11,12*) indicated that dapivirine has two strong binding sites with HIV-RT--the π-π interaction with aromatic rings of Tyr181 and Tyr188 and the hydrogen bond interaction with Lys101, so dapivirine was selected with two aromatic rings of Tyr181 and Tyr188 and Lys101 as the inner layer (Figure 2).

Optimizations have been performed while considering two approximations, heavy atoms fixing (HAF) and backbone atoms fixing (BBF). The binding energies of dapivirine with individual residues are calculated at the B3LYP/6-31G (d,p) level with correction for the basis set superposition error (BSSE), using the Boys-Bernardi counterpoise technique (*18*). All calculations presented here have been performed with the Gaussian 03 series of programs (*19*).

Results and Discussion

Structure and binding energy of HIV-1 RT binding site/ dapivirine

The main purpose of this work was to study the interaction between dapivirine and the binding sites of HIV-1 RT. Presented first is a discussion of the interaction of dapivirine with individual residues around the NNIBP. As depicted in Figure 3A, Lys101 is found to form two hydrogen bonds with 2-aminopyrimidine in the middle part of dapivirine; one is the nitrogen of the pyrimidine ring with the amino hydrogen of Lys101 and the other H-bond is the amino hydrogen of 2-aminopyrimidine with the backbone carbonyl oxygen of Lys101. Additionally, the distances of two hydrogen bonds in the X-ray structure are 3.51 and 2.75 Å for N…H-N and N-H…

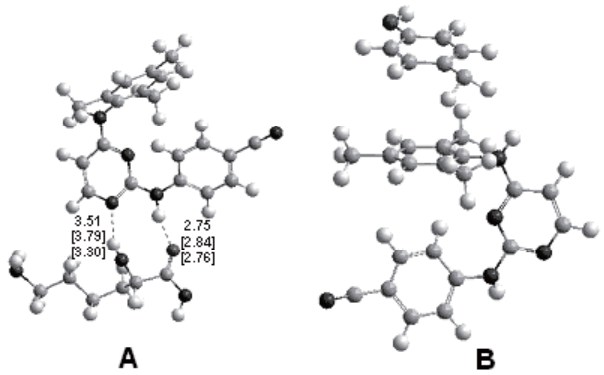

Figure 3. Optimized structure of the dapivirine and Lys101 (A), and Tyr181 (B) complex from ONIOM (B3LYP/6-31G (d,p): PM3).

O, respectively. The predicted H-bond distances of N…H-N and N-H…O in the BBF optimized geometries are consistent with the experimental results (3.38 and 2.76 Å, respectively). However, the H-bond distances in the HAF optimized geometries are predicted to lengthen by 0.28 and 0.09 Å, respectively. Meanwhile, the amino linkages of the two aryl rings provide sufficient flexibility to allow favorable π-π interaction with Tyr181, Tyr188, Trp229 and Tyr318; the aryl ring in the left moiety of dapivirine and the aryl ring of Tyr181 form a strong π-π stacking interaction, and two benzene rings are in parallel as shown in Figure 3B.

Table 1 shows the BSSE-corrected energies of the interaction of dapivirine with individual residues surrounding the NNIBP at the B3LYP/6-31G (d,p) level of theory. The results clearly deny that more attractive interactions are found. The interactions of dapivirine with all residues stabilize the NNIBP/dapivirine complex, and the interaction energies for the X-ray structure range from -0.6 to -4.1 kcal/mol. But the interaction of dapivirine with Leu100, Lys101, Lys103, Tyr181 and Tyr188 are the main contributors to stabilization of the dapivirine/NNIBP complex, and the interaction energies in the X-ray structure are -2.86, -2.06, -4.21, -3.16 and -2.10 kcal/mol, respectively. The calculated interaction energies obtained by the HAF and BBF optimized structures are consistent with those of the X-ray structure. These results are also consistent with the experimental results that the mutations of Leu100Ile, Tyr181Cys, Tyr188Leu and Leu103Asn+Tyr181Cys give rise to drug resistance to dapivirine (*9*). The Leu100Ile and Leu103Asn mutations generally destabilized the complex by diminishing the hydrogen bonds between the inhibitor and Leu101. Additionally, the mutations of Tyr181Cys and Tyr188Leu had resistance to dapivirine by reducing favorable π-π interaction between the tyrosine and aromatic rings of dapivirine.

As the dapivirine/NNIBP complex system is too large for high level calculations, ONIOM2 methods were thus adopted in order to calculate the binding energy of the dapivirine/NNIBP complex. This complex system is divided into two parts: the inner layer,

Table 1. BSSE-corrected interaction energies of dapivirine with individual residues (X_i) (in kcal/mol), calculated at the B3LYP/6-31G (d,p) level

Residue	Crystal	HAF	BBF
Pro95	-0.39	-0.50	-0.54
Leu100	-2.86	-2.64	-2.37
Lys101	-4.21	-4.12	-4.45
Lys102	-0.40	-0.25	-0.24
Lys103	-2.06	-1.94	-1.33
Val106	-0.98	-0.70	-0.73
Val179	-1.65	-1.41	-1.10
Ile180	-0.29	-0.19	-0.28
Tyr181	-3.16	-2.80	-2.37
Tyr188	-2.10	-1.34	-1.08
Val189	-0.31	-0.19	-0.14
Gly190	-0.32	-0.08	-0.09
Phe227	-1.18	-0.36	-0.63
Trp229	-0.83	-0.96	-1.37
Leu234	-1.71	-1.47	-1.37
His235	-1.08	-1.16	-0.84
Pro236	-0.65	-0.93	-0.69
Tyr318	-0.93	-0.66	-0.14
Glu138	-0.62	-0.88	-1.63
Total	-25.76	-22.58	-21.41

Table 2. Binding energies (BE kcal/mol) and their components for the HIV-1 RT/dapivirine complex, calculated by the ONIOM (B3LYP/6-31G (d,p): PM3) method

Method	BE	IE	DE	DE_{TMC120}	DE_{pocket}
HAF	-7.97	-13.95	5.98	3.67	2.31
BBF	-18.20	-23.11	4.91	4.58	0.33

consisting of dapivirine, Lys101, and two aromatic rings of Tyr181 and Tyr188, and the outer layer, consisting of the remaining residues. The B3LYP/6-31G (d,p) method has been proposed as a reliable tool for studying molecular systems containing intermolecular hydrogen bonds (*20*), so this method is applied to the inner layer because the hydrogen bond interaction between dapivirine and Lys101 is the main contributor. The calculated ONIOM2 binding energies (BE), interaction energies (IE), and deformation energies (DE) for the dapivirine/NNIBP complex are shown in Table 2. The binding energy for BBF was found to be -18.20 kcal/mol, while the results obtained by HAF underestimated the binding energy by 10.23 kcal/mol.

Comparison of dapivirine, efavirenz, and nevirapine bound to HIV-1 RT

Upon comparison of two NNRTI drugs studied, efavirenz and nevirapine (*13,14*), dapivirine was found to have the virtues of two inhibitors. Based on previous reports, efavirenz has two strong hydrogen bonds with Lys101 and the aromatic pyridine ring of nevirapine has strong π-π stacking or H…π interaction with two aromatic rings of Tyr181 and Tyr188. In the structure of dapivirine, the 2-aminopyrimidine groups of dapivirine, which are equivalent to the benzoxazin-2-one in efavirenz, form two hydrogen bonds with the carbonyl oxygen and amino hydrogen of Lys101, and the

aromatic ring in the left moiety of dapivirine exhibits strong π-π stacking or H…π interaction with the two aromatic rings of Tyr181 and Tyr188. The calculated interaction energies of dapivirine with all residues stabilize the dapivirine/NNIBP complex; but with some residues the interaction energies of efavirenz and nevirapine destabilize the inhibitor/NNIBP complex.

Conclusions

ONIOM calculations of the NNIBP/dapivirine complexes systems show that dapivirine has strong interaction with NNIBP, and the predicted binding energies of the NNIBP/dapivirine complex are respectively -7.97 and -18.2 kcal/mol for HAF and BBF by the ONIOM2 (B3LYP/6-31G (d,p): PM3) method. The 2-aminopyrimidine groups of dapivirine form two hydrogen bonds with the carbonyl oxygen and amino hydrogen of Lys101, and two aromatic residues, Tyr181 and Tyr188, are found to exhibit strong H… π and π-π interaction with the aromatic ring in the left moiety of dapivirine. These distinctive characteristics of dapivirine binding to NNIBP play a vital role in stabilizing the complex. Therefore, dapivirine is obviously in line to become a new generation of inhibitor to combat AIDS.

Acknowledgements

This work was supported by grants from the National Natural Science Foundation of China (No: 30672536).

References

1. De Clercq E. Strategies in the design of antiviral drugs. Nat Rev Drug Discov 2002;26:13-25.
2. Sarafianos SG, Das K, Lewi PJ, Hughes SH, Arnold E. Taking aim at a moving target: design drugs to inhibit drug-resistant HIV-1 reverse transcriptase. Curr Opin Struct Biol 2004;14:716-730.
3. Jonckheere H, Anné J, De Clercq E. The HIV-1 reverse transcriptase (RT) process as target for RT inhibitors. Med Res Rev 2000;20:129-154.
4. Merluzzi VJ, Hargrave KD, Labadia M, Grozinger K, Skoog M, Wu JC, Shih CK, Eckner K, Hattox S, Adams J. Inhibition of HIV-1 replication by a nonnucleoside HIV-1 reverse transcriptase inhibitor. Science 1990;250:1411-1413.
5. Freimuth WW. Delavirdine mesylate, a potent nonnucleoside HIV-1 reverse transcriptase inhibitor. Adv Exp Med Biol 1996;394:279-289.
6. Young SD, Britcher SF, Tran LO, *et al*. L-743726 (DMP-266): a novel highly potent nonnucleoside inhibitor of the human immunodeficiency virus type 1 reverse transcriptase. Antimicrob Agents Chemother 1995;39:2602-2605.
7. Schinazi RF, Mead JR, Feorino PM. Insights into HIV chemotherapy. AIDS Res Hum Retroviruses 1992;8:963-990.
8. Richman DD, HIV drug resistance. AIDS Res Hum Retroviruses 1992;8:1065-1071.
9. Ludovici DW, De Corte BL, Kukla MJ, *et al*. Evolution of anti-HIV drug candidates. Part 3: diarylpyrimidine (DAPY) analogues. Bioorg Med Chem Lett 2001;11:2235-2239.
10. Guillemont J, Pasquier E, Palandjian P, *et al*. Synthesis of novel diarylpyrimidine analogues and their antiviral activity against human immunodeficiency virus type 1. J Med Chem 2005;48:2072-2072.
11. Das K, Lewi PJ, Hughes SH, Arnold E. Crystallography and the design of anti-AIDS drugs: conformational flexibility and positional adaptability are important in the design of non-nucleoside HIV-1 reverse transcriptase inhibitors. Prog Biophys Mol Biol 2005;8:209-231.
12. Das K, Clark AD, Lewi PJ, *et al*. Roles of conformational and positional adaptability in structure-based design of TMC125-R165335 (etravirine) and related non-nucleoside reverse transcriptase inhibitors that are highly potent and effective against wild-type and drug-resistant HIV-1 variants. J Med Chem 2004;47:2550-2560.
13. Kuno M, Hannongbua S, Morokuma K. Theoretical investigation on nevirapine and HIV-1 reverse transcriptase binding site interaction, based on ONIOM method. Chem Phys Lett 2003;380:456-463.
14. Nunrium P, Kuno M, Saen-oon S, Hannongbua S. Particular interaction between efavirenz and the HIV-1 reverse transcriptase binding site as explained by the ONIOM2 method. Chem Phys Lett 2005;405:198-202.
15. Yao LS, Cukier RI, Yan HG. Catalytic mechanism of guanine deaminase: an ONIOM and molecular dynamics study. J Phys Chem B 2007;111:4200-4210.
16. Majumdar D, Roszak S, Leszczynski J. Probing the acetylcholinesterase inhibition of sarin: A comparative interaction study of the inhibitor and acetylcholine with a model enzyme cavity. J Phys Chem B 2006;110:13597-13607.
17. Morokuma K, Wang Q, Vreven T. Performance evaluation of the three-layer ONIOM method: case study for a zwitterionic peptide. J Chem Theor Comput 2006;2:1317-1324.
18. Boys SF, Bernardi F. The calculation of small molecular interactions by the differences of separate total energies, some procedures with reduced errors. Mol Phys 1970;19:553-566.
19. Frisch MJ, Trucks GW, Schlegel HB, *et al*. Gaussian 03 Revision B.03, Gaussian, Inc., Pittsburgh PA, 2003.
20. Yi PG, Liang YH, Tang ZQ. Theoretical study of intermolecular proton transfer reaction in isolated 5-hydroxyisoxazole--water complexes. Chem Phys 2006;322:387-391.

Studies on the development of rapidly disintegrating hyoscine butylbromide tablets

Ibrahim S Khattab[1,*], Abdel-Azim A Zaghloul[1], Mohsen I Afouna[2]

[1] *Department of Pharmaceutics, Faculty of Pharmacy, Kuwait University, Kuwait;*
[2] *Department of Pharmaceutics, Faculty of Pharmacy, King Abdel-Aziz University, Saudi Arabia.*

ABSTRACT: The objective of this study was to prepare hyoscine butylbromide (a drug with bitter taste) tablets that can rapidly disintegrate in saliva. The granules were prepared by the extrusion method using aminoalkyl methacrylate copolymers (Eudragit E-100). The drugs dissolved rapidly in medium at pH 1.2 in a dissolution test while none of the drugs dissolved from the granules (% of dissolved < 5%) even after 8 h at pH 6.8. Rapidly disintegrating tablets were prepared using prepared taste-masked granules and a mixture of excipients consisting of crystalline cellulose (Avicel PH-102) and low-substituted hydroxypropylcellulose (L-HPC, LH-11). The granules and excipients were mixed well (mixing ratio by weight, crystalline cellulose: L-HPC, was 8:2) with 1% magnesium stearate as a lubricant and subsequently compressed at 500-1,500 kgf in a single-punch tableting machine. The prepared tablets (compressed at 500 kgf) containing the taste-masked granules have significant strength (crushing strength was 3.5 kg), and a rapid disintegration time (within 30 sec) was observed in the saliva of healthy volunteers. None of the volunteers sensed any bitter taste after the disintegration of the tablet that contained the taste-masked granules. The results confirmed that rapidly disintegrating tablets can be prepared using these taste-masked granules and excipients that are commonly used in tablet preparation.

Key Words: Hyuocine butylbromide, fast disintegrant tablets, Eudragit E-100, tast masking

Introduction

Pharmaceutical preparations for the elderly have recently been developed to improve their treatment compliance and quality of life (QOL) (*1*). Fast-disintegrating tablets have been in ever-increasing demand since the last decade, and the field has become a rapidly growing area in the pharmaceutical industry (*2-6*). The preparation of rapidly disintegrating tablets consists of crystalline cellulose (Avicel PH 102) and low-substituted hydroxypropylcellulose (L-HPC), which are commonly used in the manufacture of conventional tablets. The rapidly disintegrating tablet can be prepared by direct compression at a low compression force, 100-300 kgf (*7,8*). The tablets prepared disintegrated rapidly in saliva and a small amount of water, and the disintegration was complete within 30 sec. Other excipients used in the preparation of rapidly disintegrated tablets include amorphous sucrose (*9*), glycine, and carboxymethylcellulose (*10*). High-porosity compressed drug tablets that are soluble in saliva have successfully been prepared using mannitol, a water-soluble excipient (*11*). A tablet prepared by the compression method using only mannitol had a long dissolution time (> 120 sec). However, highly porous tablets could be prepared by subliming camphor after compressing the mixture of the drug and mannitol and camphor particles. High-porosity tablets thus prepared completely dissolved in saliva within 20 sec (*11*). The prepared tablets contained meclizine (HCl salt, powder), an antiemetic and antivertigo agent as the active component, and can be taken for motion sickness even when water is not available (*12*). Thus tablet preparation is highly useful for the treatment of kinetosis. With rapidly disintegrating tablets, there is a problem of the drug' s bitter taste due to the dissolution of the active component in the mouth. Taste masking must be investigated prior to preparing rapidly disintegrating tablets of drugs with a bitter taste. In the present study, hyoscine butylbromide, which is extremely bitter, was chosen as the model drug and prepared as rapidly disintegrating tablets using taste-masked granules such as the aminoalkyl methacrylate copolymers. Hyoscine butylbromide has an antimuscarinic effect and is used as an antispasmodic agent (*13*).

Materials and Methods

**Correspondence to:* Ibrahim S. Khattab, Department of Pharmaceutics, Faculty of Pharmacy, Kuwait University, Kuwait;
e-mail: Khattab@hsc.edu.kw

Received June 16, 2007
Accepted June 21, 2007

Materials

Hyoscine butylbromide, crystalline cellulose (Avicel PH-102), low-substituted hydroxypropylcellulose (L-HPC, LH-110), and magnesium stearate were kindly supplied by the EIPICO Pharmaceutical Company, Egypt. Aminoalkyl methacrylate copolymers (Eudragit E-100) were supplied by Rohm Gmbh (Germany). Ethanol (≥ 99%) and all other reagents used were of analytical grade.

Preparation of granules and rapidly disintegrating tablets

The composition of each tablet tested is listed in Table 1. The drug hyoscine butylbromide (HBB) was mixed with powdered Eudragit E-100 in a drum mixture, and then 10% ethanol was added to the mixture of the drug and Eudragit in a glass beaker. Then, a gel containing the mixture of the drug and Eudragit E-100 was prepared; using this prepared gel, taste-masked granules were prepared by the extrusion method. The prepared gel was manually extended (pressed out) using a syringe. After extrusion of the gel, ethanol was removed by evaporation overnight and subsequently the solidified gel in the shape of a string was crushed into granules using a mortar. An Erweka single-punch tableting machine was used to prepare tablets with an 8-m diameter using a compression force of 500-1500 Kp for a target weight of 180 mg. The taste-masked tablets were prepared using a mixture of the taste-masked granules, excipient mixture, crystalline cellulose and L-HPC at mixing ratios by weight of crystalline cellulose of L-HPC = 8:2, and magnesium stearate (1%). Additionally, tablets were prepared using a powdered mixture of the drug and Eudragit E-100 (without granulation) and magnesium stearate (1%) as a control tablet.

Evaluation of the tablets prepared

The crushing strength of the tablets in response to diametrical compression force was measured with a digital crushing strength measuring machine (Pharma Test hardness tester).

The *in vitro* disintegration time was measured for 6 tablets; one tablet was placed in each tube of the basket, which was then immersed in water (37 ± 2ºC). The time required for complete disintegration of the tablet in each tube of the basket was record in seconds.

The *in vitro* dissolution test was conducted using a USP II dissolution apparatus. The materials (tablet contents and masked granules) were dried overnight in a desiccator to remove excess moisture and subjected to a dissolution test in a machine equipped with an autosampling apparatus (HP, Japan). The USP II dissolution test basket was attached to a spindle and placed in a dissolution bath containing 900 mL of USP II 1st fluid (pH 1.2) and the 2nd fluid (pH 6.8) for the disintegration test or citric acid-NaOH buffer solution (pH 5.0) (*14*) and maintained at 37 ± 0.5ºC. The spindle was rotated at 100 rpm, and the samples were withdrawn and analyzed by UV spectrometry at 211 nm.

Table 1. Composition of the Tablets

Materials	Amount/mg
Hyuocine butylbromide	5
Eudragit E-100	50-75
Crystalline cellulose	78-103
L-HPC	20
Magnesium stearate	2
Total	180

For determination of the *in vivo* disintegration time, ten healthy volunteers, from whom informed consent was first obtained, randomly took one tablet and the time required for complete disintegration of the tablet in the mouth, without biting and without drinking water, was measured (*15*). The sensory test for a bitter taste as described by Kimura *et al*. (*16*) was used with slight modification. Briefly, the same ten volunteers mentioned in the determination of the disintegration time in saliva held the disintegrated materials in their mouths for 30 sec. Immediately after the *in vivo* disintegration test, volunteers rinsed their mouths out without ingesting the disintegrated particles.

Results and Discussion

Dissolution profiles of hyoscine butylbromide from the taste-masked granules prepared from the aminoalkyl methacrylate copolymer

Aminoalkyl Methacrylate Copolymer (Eudragit E-100) dissolved in an acidic pH (low pH region) but not in the neutral pH region. Therefore, Eudragit E-100 was used as an acid-soluble (gastric soluble) coating material for the compound. In the preliminary study, the taste-masked granule using Eudragit E-100 was prepared at various mixing ratios by weight. Although the mixing ratio of the active component and Eudragit E-100 was set arbitrarily, the ratio was ultimately selected to be HBB: Eudragit E-100 = 1:10 (Table 1). Figure 1 shows the dissolution profiles of the drugs from the prepared granules. The prepared granules dissolved slightly in the fluid (pH 6.8) and maintained their granule shape. Consequently, none of the drugs dissolved from the granules (% of dissolved, < 5%) even at 480 min after the beginning of the dissolution test. On the other hand, the dissolution of the drug was rapid at a pH of 1.2. The drug dissolution was complete at 15 min after the beginning of the test. When the pH in the stomach is increased (low gastric acidity) by drug or foods and in patients with greater stomach acidity, dissolution of the

drug from the taste-masked granules should decrease. Therefore, dissolution of HBB from taste-masked granules was tested in a buffer solution at pH 5.0. Consequently, a similar profile of rapid dissolution was obtained at pH 5.0 (Figure 1).

The results of the dissolution test imply that HBB does not dissolve from the prepared granules in saliva with a pH in the neutral region, but they rapidly dissolve in gastric juices where the pH is acidic. As shown in Table 2, the volunteers who took the prepared granules did not sense the bitter taste of the drug. Therefore, taste-masked granules can be prepared using Eudragit E-100.

Evaluation of the rapidly disintegrating tablets prepared using the taste-masked granules and excipients of crystalline cellulose and L-HPC

The HBB content in tablets was chosen to be equal to the dose. Crystalline and L-HPC were used as the excipients for the rapidly disintegrating tablets (*16*).

Figure 2 shows the relationship between the compression force on the mixture of the taste-masked granules and excipients and the crushing strength of the prepared tablet. The crushing strength was about 2 kg for the tablet compressed at 500 kgf while it exceeded 6 kg for tablets compressed at 1,500 kgf. Compressibility decreased when the content of Eudragit E-100 increased in comparison to those of other excipients (crystalline cellulose and L-HPC). Consequently, the crushing strength of the prepared tablets was lower than that of controlled tablets.

Figure 3 illustrates the relationship between the compression force and the *in vitro* disintegration time of the prepared tablet. When the compression force was

Table 2. Disintegration time in mouth and sensory test for the tablets contains taste-masked granules

Volunteer number	Hyuocine butylbromide	
	Masked tablets	Control tablets
1	27 (-)	22 (+)
2	23 (-)	26 (+)
3	25 (-)	23 (+)
4	28 (-)	23 (+)
5	29 (-)	24 (+)
6	26 (-)	22 (+)
7	25 (-)	25 (+)
8	24 (-)	22 (+)
9	27 (-)	20 (+)
10	28 (-)	24 (+)
Mean	26	23.1
+ SD	1.93	1.73

Bitter taste: (-) no, (+) yes

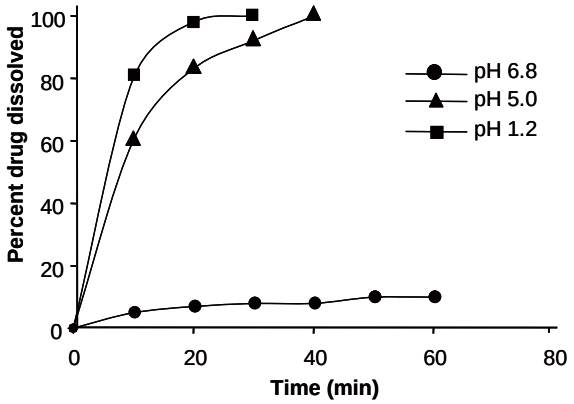

Figure 1. Percent of drug released from the taste-masked granules prepared with Eudragit E-100.

Table 3. Percent of drug released from the granules prepared with Eudragit E-100

Time (sec)	pH		
	1.2	5.0	6.8
10	80	60	5
20	98	83	7
30	100	92	8
40		100	8
50			10
60			10

Table 4. Relationship between crushing strength and *in vivo* disintegration time of the tablets

Compression Force	Crushing Strength	*In vivo* disintegration time
500	2.1	7.5
1000	2.4	12
1500	6.0	26

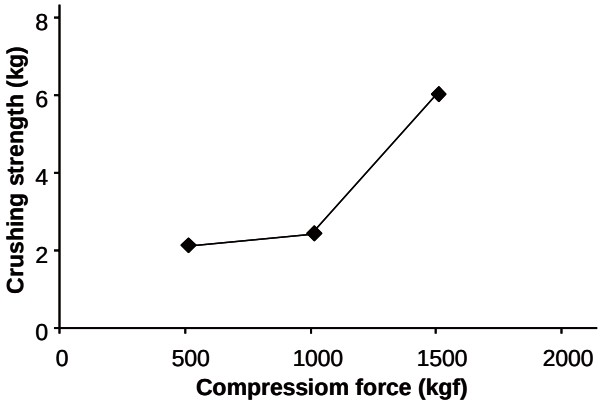

Figure 2. Relationship between compression force and crushing strength of the tablets.

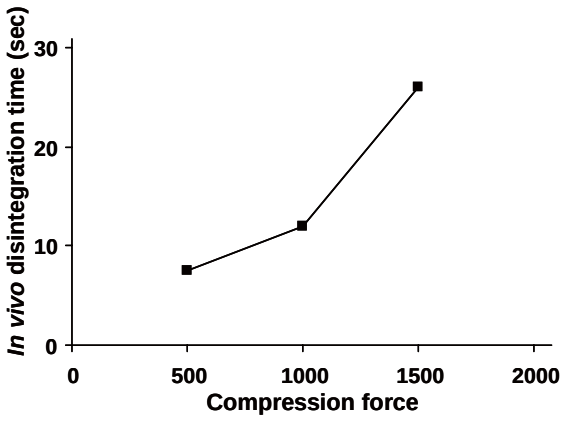

Figure 3. Relationship between compression force and *in vivo* disintegration time of the tablets.

increased, the crushing strength increased markedly and the *in vitro* disintegration time was also prolonged. To date, the best criteria for the disintegration time of rapidly disintegrating tablets have yet to be confirmed. This study sought to achieve a maximum disintegration time of 30 sec. With the tablets in the study, rapid disintegration of the prepared tablets can be achieved by using a mixture of the taste-masked granules and excipients at various compounding ratios when the compression force is adjusted to below 1,000 kgf. The disintegration times of HBB tablets were found to be under 20 sec *in vitro* when the compression force was 500 kgf. To examine the disintegration of the prepared tablet in the mouth, the *in vitro* disintegration time was measured by the method described in Materials and methods. As the same time, a sensory test was performed beforehand to evaluate the degree of taste masking. For the control tablet, the drug, and excipients without granulation, the mixture of the active component, crystalline cellulose, L-HPC and Eudragit E-100 were compressed at the same force as for tablets containing the taste-masked granules. The results are summarized in Table 2. In the mouth, the disintegration time of HBB tablets containing the taste-masked granules prepared using a compression force of 500 kgf was approximately 20 sec. Fortunately, none of the volunteers sensed any bitter taste after disintegration of the tablets containing the taste-masked granules, but they strongly sensed the bitter taste when the control tablet disintegrated in their mouths. The results of the sensory test suggest that formulation of Eudragit E-100 matrices (granules) plays an essential role in the screening of the bitter taste. Although dissolution in the stomach was not examined in the volunteers, rapid dissolution would appear to occur in the gastric juices. Concerning the mechanisms of rapid disintegration by the excipients of crystalline cellulose and L-HPC, a higher level of porosity for compressed tablets using crystalline cellulose and L-HPC would appear to be preferable for disintegration in a small amount of water. Bi *et al*. suggested that the disintegration of crystalline cellulose L-HPC tablet is affected mainly by tablet porosity, hydrophilicity, swelling ability, and interparticle force (*16*).

Conclusion

Rapidly disintegrating tablets were prepared using taste-masking granules and excipients that are commonly used in tablet preparation. The method of preparation is useful for the preparation of rapidly disintegrating tablets containing a bitter-tasting drug like hyoscine butylbromide.

References

1. Watanabe A, Hanawa T, Sugihara M, Yamamoto K. Release profiles of phenytoin from new oral dosage form for the elderly. Chem Pharm Bull (Tokyo) 1994;42:642-645.
2. Fu Y, Yang S, Jeong SH, Kimura S, Park K. Orally fast disintegrating tablets: developments, technologies, taste-masking and clinical studies. Crit Rev Ther Drug Carrier Syst 2004;21:433-476.
3. Fukami J, Yonemochi E, Yoshihashi Y, Terada K. Evaluation of rapidly disintegrating tablets containing glycine and carboxymethylcellulose. Int J Pharm 2006;310:101-109.
4. Sugimoto M, Maejima T, Narisawa S, Matsubara K, Yoshino H. Factors affecting the characteristics of rapidly disintegrating tablets in the mouth prepared by the crystalline transition of amorphous sucrose. Int J Pharm 2005;296:64-72.
5. Abdelbary G, Eouani C, Prinderre P, Joachim J, Reynier J, Piccerelle P.Determination of the *in vitro* disintegration profile of rapidly disintegrating tablets and correlation with oral disintegration. Int J Pharm 2005;292:29-41.
6. Harada T, Narazaki R, Nagira S, Ohwaki T, Aoki S, Iwamoto K. Evaluation of the disintegration properties of commercial famotidine 20 mg orally disintegrating tablets using a simple new test and human sensory test. Chem Pharm Bull (Tokyo) 2006;54:1072-1075.
7. Watanabe Y, Koizumi K, Zama Y, Kiriyama M, Matsumoto Y, Matsumoto M. New compressed tablet rapidly disintegrating in saliva in the mouth using crystalline cellulose and a disintegrant. Biol Pharm Bull 1995;18:1308-1310.
8. Ishikawa T, Mukai B, Shiraishi S, Utoguchi N, Fujii M, Matsumoto M, Watanabe Y. Preparation of rapidly disintegrating tablet using new types of microcrystalline cellulose (PH-M series) and low substituted-hydroxypropylcellulose or spherical sugar granules by direct compression method. Chem Pharm Bull (Tokyo) 2001;49:134-139.
9. Sammour OA, Hammad MA, Megrab NA, Zidan AS. Formulation and optimization of mouth dissolve tablets containing rofecoxib solid dispersion. AAPS PharmSciTech 2006;7:E55.
10. Sugimoto M, Narisawa S, Matsubara K, Yoshino H, Nakano M, Handa T. Development of manufacturing method for rapidly disintegrating oral tablets using the crystalline transition of amorphous sucrose. Int J Pharm 2006;320:71-78.
11. Koizumi K, Watanabe Y, Morita K, Utoguchi M, Matsumoto M. New method of preparing high-porosity rapidly saliva soluble compressed tablets using mannitol with camphor, a subliming material. Int J Pharm 1997;152;127-131.
12. PDR "Physicain Disk Reference", Thomson Corporation, Toronto, 2006.
13. Golding JF, Stott JR. Comparison of the effects of a selective muscarinic receptor antagonist and hyoscine (scopolamine) on motion sickness, skin conductance and heart rate. Br J Clin Pharmacol 1997;43:633-637.
14. Rauniar GP, Gitanjali B, Shashindran C. Comparative effects of hyoscine butylbromide and atropine sulphate on sleep architecture in healthy human volunteers. Indian J Physiol Pharmacol 1998;43:395-400.
15. Kimura S, Imai T, Ueno N, Otagiri M. Pharmaceutical evaluation of ibuprofen fast-absorbed syrup containing low-molecular-weight gelatin. J Pharm Sci 1992;81:141-144.
16. Bi Y, Sunada H, Yonezawa Y, Danjo K, Otsuka A, Iida K. Preparation and evaluation of a compressed tablet rapidly disintegrating in the oral cavity. Chem Pharm Bull 1996;44:2121-2127.

Investigation of the binding behaviors of isonucleoside-incorporated oligonucleotides with complementary sequences

Zhu Guan, Hong-Wei Jin, Zhen-Jun Yang, Liang-Ren Zhang*, Li-He Zhang

State Key Laboratory of Natural and Biomimetic Drugs, School of Pharmaceutical Sciences, Peking University, Beijing, China.

ABSTRACT: Oligonucleotides consisting of isonucleoside 2',5'-anhydro-3'-nucleobase-*D*-mannitol incorporated in 1'→4' linkage mode were synthesized. Their binding behaviors with complementary sequences were investigated via thermal denaturation and CD spectra. 6'-*O*-methyl-2',5'-anhydro-3'-(thymin-1-yl)-*D*-mannitol incorporated oligonucleotide was also synthesized to investigate the effect of hydroxy groups of isonucleosides on duplex formation. The results showed that the 6'-OH free isonucleoside-modified oligonucleotide was able to form a B-like duplex with 3'→5' complementary native oligodeoxynucleotide in the 1'→4' direction. The free hydroxy group in the isonucleoside made a significant contribution to the affinity of the modified oligonucleotide to the complementary sequence, which was confirmed by molecular dynamics simulation.

Key Words: Isonucleoside, nucleoside, oligonucleotide, chemical modification

Introduction

Antisense oligonucleotides manipulate the expression of specific genes by selective hybridization to target mRNA or DNA and can be used as an effective and specific therapeutic agent (*1-5*). They have several disadvantages, though, including instability with respect to cellular nuclease, unsatisfactory binding affinity, insufficient membrane penetration and low bioavailability, and restriction of the application of natural oligonucleotides. Various types of structure-modified oligonucleotides have been developed to overcome these problems (*6*). Modification of the phosphate linkage by phosphorothioate (PS) has been the first successful strategy for antisense drug development, and the first antisense drug (Fomivirsen) was approved by the FDA in 1998 for the treatment of cytomegalovirus-induced retinitis in patients with AIDS. 2'-*O*-substituted oligonucleotide is another type of well investigated modification that has been proven to be stable with respect to DNA or RNA cleaving enzymes (*7*). The mixed backbone containing PS and 2'-*O*-modified oligonucleotide retains RNase H activation properties that are present in PS antisense oligonucleotide and generally absent in 2'-*O*-modified antisense oligonucleotide. Furthermore, this mixed antisense oligonucleotide reduces the side effects caused by PS antisense oligonucleotide and improves the character of pharmacology, pharmacokinetics, and pharmacodynamics (*8*). Locked nucleic acid (LNA), which consists of a conformational restriction with a 2'-*O*-4'-C-methylene bridge, has been reported to exhibit unprecedented affinity to complementary DNA or RNA and shows promise as a therapy (*9-11*).

Isonucleoside is a type of modified nucleoside in which the nucleobase is transferred from C1'- to other positions of ribose, displaying both chemical and enzymatic stabilities (*12,13*). Though the incorporation of isonucleoside in the native structure of oligodeoxynucleotide would slightly decrease the stability of the duplex, the excellent antagonizing ability of the isonucleoside-incorporated oligonucleotide with respect to the hydrolysis of nuclease provides a promising way to design a stable antisense oligonucleotide (*14*). More recent investigation has shown that siRNA with isonucleoside modification on the sense strand still retains the gene silencing effect (*15*). Various types of isonucleoside-modified oligonucleotides (**1**-**5**) are reported to display different hybrid properties than complementary sequences. The homo-oligomer of modified mode **1**, **4**, or **5** was able to bind to the complementary sequence but the modified mode **2** or **3** did not show obvious hybridization ability (*13*). Molecular modeling showed that in the case of modified form **4** or **5** the 6'-OH group of each unit was located in the groove area when hybridized to $d(A)_{14}$, where it was able to form hydrogen bonds with water in

**Correspondence to:* State Key Laboratory of Natural and Biomimetic Drugs, School of Pharmaceutical Sciences, Peking University, Beijing 100083, China; e-mail: liangren@bjmu.edu.cn

Received June 18, 2007
Accepted June 29, 2007

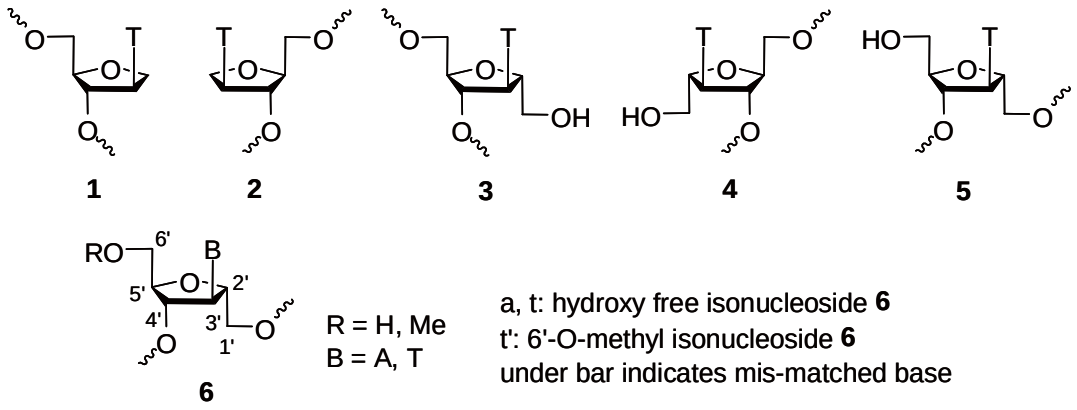

I: 5'-TTT TTT TTT TTTT-3'
II: 1'-ttt ttt ttt ttt-4'-5'-T-3'
III: 1'-t't't' t't't' t't't' t't't' -4'-5'-T-3'
IV: 5'-AAA AAA AAA AAAA-3'
V: 1'-ttt taa att aat aat aa-4'-5'-A-3'
VI: 5'-TTT TAA ATT AAT AAT AAA-3'
VII: 5'-AAA ATT TAA TTA TTA TTT-3'
VIII: 5'-TTT ATT ATT AAT TTA AAA-3'
IX: 5'-TCT AAC CCT AACT-3'
X: 5'-AGT TAG GGT TAGA-3'
XI: 5'-AGT TAG GGT TAG-3'-1'-a-4'
XII: 5'-aGT TAG GGT TAG-3'-1'-a-4'
XIII: 5'-AGT TAG GGT TAGT-3'
XIV: 5'-AGT TAG GGT TAGT-3'

Figure 1. Structures of isonucleosides and the sequences of isonucleoside-incorporated oligonucleotides.

the medium and may have contributed to the stability of duplex formation, while in the case of modified mode **3** most of the 6'-OH groups were directed to the inside of the duplex. These results indicate that the hydoxy group played a crucial role in duplex formation. In this work, an oligonucleotide constructed with isonucleoside **6** was designed and synthesized and the role of 6'-OH was validated by methyl protection. The stability and binding mode of the duplexes (Figure 1) formed by the modified oligonucleotide and its native counterpart were investigated by melting behavior and CD spectra. The results may provide some insight into the design of chemically modified antisense nucleotides.

Materials and Methods

General methods

All solvents were dried and distilled prior to use. Thin layer chromatography (TLC) was performed using silica gel GF-254 (Qing-Dao Chemical Co., China) plates with detection by UV. Column chromatography was performed on silica gel (200-300 mesh or flash, Qing-Dao Chemical Co.). Evaporations were carried out under reduced pressure with a bath temperature below 45°C.

^{1}H-NMR spectra were recorded on Varian VXR-300 or Varian Inova 500 with TMS as an internal standard. ESI-TOF MS were recorded on ABI QSTAR. ^{31}P-NMR spectra were recorded on Bruker AC 2007 or Varian VXR-300. MALDI-TOF MS were recorded on Bruker BIFLEX III or Kratos PC Axima-plus. UV spectra were recorded with Varian Cary 300.

Molecular optimization was performed using the Gaussian 98 program. Unrestrained molecular dynamics simulations were performed for the oligonucleotide duplexes studied by using the Amber 8 suite of programs (*16*). The Amber99 force field was used to describe the DNA. An 8Å truncated octahedron of TIP3P water was added to solvate the structures and counterions of Na^{+} were placed next to each phosphate group. The simulations were conducted for 1.5 ns at a constant pressure (1 atm) and temperature (300K). Stable trajectories of geometry and energy terms were acquired after 500 ps of simulations and the averaged structures during the last 800 ps period of simulations were generated.

Synthesis

1'-O-Benzoyl-3'-deoxy-3'-(adenin-9-yl)-2',5'-anhydro-D-mannitol (10) and 6'-O-benzyol-3'-deoxy-3'-(adenin-9-yl)-2',5'-anhydro-D-mannitol (11)

Saturated ammonia/anhydrous methanol (5 mL) was added to a solution of compound **9** (0.8 g, 1.6 mmol) in anhydrous methanol (10 mL). The reaction mixture was stirred at room temperature for about 1 hour and monitored by TLC. Once the fully deprotected product was detected, the reaction was stopped by removing the solvent under reduced pressure. The mixture was partially separated by silica gel column chromatography (CH_2Cl_2/CH_3OH: 80/1-10/1) to provide the mono-benzoyl protected mixture of products (**10**, **11**) (150 mg, 48.7%) in a ratio of about 1:1, and starting material **9** was collected. Compounds **10** and **11** were separated carefully by silica gel column chromatography for structure characterization.

Compound 10: ^{1}H-NMR (300MHz, DMSO-d_6) δ: 3.65 (m, 2H, 6'-H), 3.91 (dd, 1H, 1'-H), 4.13 (dd, 1H, 6'-H), 4.39 (m, 1H, 5'-H), 4.71 (m, 1H, 4'-H), 4.97 (m, 1H, 2'-H), 5.20 (m, 1H, 3'-H), 7.26 (s, 2H, D_2O exchangeable, 6-NH_2), 7.43 (m, 2H, Ar-H), 7.62 (m, 3H, Ar-H), 8.09 (s, 1H, 2-H), 8.19 (s, 1H, 8-H).

Compound 11: ^{1}H-NMR (300MHz, DMSO-d_6) δ: 3.64 (dd, 2H, 1'-H), 3.90 (m, 1H, 5'-H), 4.37 (m, 2H, 2'-H, 4'-H), 4.73 (m, 2H, 6'-H), 4.93 (m, 1H, 3'-H), 7.30 (s, 2H, D_2O exchangeable, 6-NH_2), 7.48 (m, 2H, Ar-H), 7.65 (m, 1H, Ar-H), 7.79 (d, 2H, Ar-H), 8.11 (s, 1H, 2-H), 8.33 (s, 1H, 8-H).

Mixture of compounds **10** and **11**: ESI-TOF$^+$: 386 $[M + H]^+$.

1'-O-Benzoyl-3'-deoxy-3'-(6-N-benzoyl-adenin-9-yl)-2',5'-anhydro-D-mannitol (12) and 6'-O-benzoyl-3'-deoxy-3'-(6-N-benzoyl-adenin-9-yl)-2',5'-anhydro-D-mannitol (13)

The mixture of compounds **10** and **11** (0.33 g, 0.86 mmol) was dissolved in anhydrous pyridine (10 mL), TMSCl (1.7 mL, 13.4 mmol) was added in an ice bath. The solution was stirred at room temperature for about 1 h till no starting material was detected by TLC, and then benzoyl chloride (0.8 mL, 6.83 mmol) was added. After 2 h of stirring, ammonia was added in drops to adjust the solution to pH 9 and stirred at room temperature for about 3 h. After evaporation, the residue was separated by silica gel chromatography (CH_2Cl_2/CH_3OH: 80/1-30/1) to provide a mixture of compounds **12** and **13** (0.407 g, 96%). Compound **12** was partially obtained as white crystals by recrystallization from ethanol.

Compound **12**: ^{1}H-NMR (300MHz, DMSO-d_6) δ: 3.47 (m, 2H, 6'-H), 4.19 (m, 1H, 5'-H), 4.48 (m, 1H, 4'-H), 4.60 (m, 2H, 1'-H), 5.00 (m, 2H, 2'-H, 3'-H), 7.64 (m, 6H, Ar-H), 8.05 (m, 2H, Ar-H), 8.13 (m, 2H, Ar-H), 8.61 (s, 1H, 2-H), 8.69 (s, 1H, 8-H), 11.19 (s, 1H, D_2O exchangeable, NH).

Mixture of compounds **12** and **13**: ESI-TOF$^+$: 490 $[M]^+$.

6'-O-(4,4-Dimethoxytriphenylmethyl)-1'-O-benzoyl-3'-deoxy-3'-(6-N-benzoyl-adenin-9-yl)-2',5'-anhydro-D-mannitol (14) and 1'-O-(4,4-dimethoxytriphenyl methyl)-6'-O-benzyol-3'-deoxy-3'-(6-N-benzoyl-adenin-9-yl)-2',5'-anhydro-D-mannitol (15)

The mixture of compounds **12** and **13** (0.2 g, 0.41 mmol) was dissolved in anhydrous pyridine (10 mL), and dimethoxytrityl chloride (0.15 g, 0.43 mmol) was added. The solution was stirred at room temperature for 24 h. After evaporation, the residue was purified by silica gel chromatography (CH_2Cl_2/CH_3OH: 100/1-10/1) to provide compound **14** (101 mg, 35%) and compound **15** (111 mg, 34%) as white foam, respectively.

Compound **14**: ^{1}H-NMR (500MHz, DMSO-d_6) δ: 3.24 (m, 2H, 6'-H), 3.73 (2s, 6H, DMT-OCH_3), 4.16 (m, 1H, 5'-H), 4.48 (m, 2H, 1'-H), 4.89 (m, 1H, 4'-H), 4.93 (m, 1H, 2'-H), 5.08 (m, 1H, 3'-H), 5.83 (d, J = 6Hz, 1H, D_2O exchangeable, 4'-OH), 6.86 (m, 4H, Ar-H), 7.23 (m, 1H, Ar-H), 7.30-7.35 (m, 7H, Ar-H), 7.48-7.58 (m, 7H, Ar-H), 7.66 (m, 2H, Ar-H), 7.81 (d, 2H, Ar-H), 8.67 (s, 1H, 2-H), 8.71 (s, 1H, 8-H), 11.20 (s, 1H, D_2O exchangeable, 6-NH). ESI-TOF$^+$: 792 $[M + H]^+$.

Compound **15**: ^{1}H-NMR (500MHz, DMSO-d_6) δ: 3.09 (m, 1H, 1'-H), 3.20 (m, 1H, 1'-H), 4.27 (m, 1H, 5'-H), 4.51 (m, 1H, 6'-H), 4.62 (m, 1H, 6'-H), 4.65 (m, 1H, 2'-H), 4.93 (m, 1H, 4'-H), 5.11 (m, 1H, 3'-H), 5.97 (d, J = 6Hz, 1H, D_2O exchangeable, 4'-OH), 6.77 (m, 4H, Ar-H), 7.08-7.10 (m, 4H, Ar-H), 7.15-7.21 (m, 5H, Ar-H), 7.52-7.72 (m, 6H, Ar-H), 8.06 (d, 2H, Ar-H), 8.11 (m, 2H, Ar-H), 8.65 (s, 1H, 2-H), 8.64 (s, 1H, 8-H), 11.20 (s, 1H, 6-NH, D_2O exchangeable). ESI-TOF$^+$: 792 $[M + H]^+$.

1'-O-(4,4-Dimethoxytriphenylmethyl)-4'-O-(2-cyanoethyl-N,N-diisopropyl) phosphoramidite-1'-O-benzoyl-3'-deoxy-3'-(6-N-benzoyl-adenin-9-yl)-2',5'-anhydro-D-mannitol (16)

Compound **15** (110 mg, 0.14 mmol) was dried in a vacuum and dissolved in anhydrous THF (2 mL) in an argon atmosphere. Diisopropylethylamine (DIPEA, 97 μL, 0.56 mmol) and 2-cyanoethyl-*N,N*-diisopropyl-chlorophosphoramidite (62 mL, 0.28 mmol) were added to the solution. The mixture was stirred at 0°C for 10 min and continued to be stirred at room temperature for 40 min. Then, the reaction mixture was quenched by addition of MeOH (1 mL). After stirring for 10 min, EtOAc (15 mL) was added and the organic layer was washed with 5% aqueous $NaHCO_3$ (2 × 5 mL), followed by H_2O (5 mL) and then drying over anhydrous Na_2SO_4. After evaporation, the oily residue was purified by silica gel column chromatography (petroleum ether/AcOEt/CH_2Cl_2: 10/1/1-4/1/1, 0.3% Et_3N) to provide compound **16** as a white foam (120 mg, 86%). ^{31}P-NMR ($CDCl_3$, ppm) δ: 150.7, 151.6.

6-O-Benzoyl-2,5:3,4-dianhydro-D-talitol (17) and 1-O-benzoyl-2,5:3,4-di-anhydro-D-talitol (18)

Saturated ammonia/anhydrous methanol (20 mL) was added to the solution of compound **7** (7.0 g, 20.0 mmol) in anhydrous methanol (60 mL). The solution was stirred at room temperature till the fully deprotected product was detected by TLC (identified by phosphatomolybdic acid in ethanol). After evaporation, the residue was separated by silica gel column chromatography (petroleum ether/EtOAc: 10/1-2/1) to provide a mixture of compounds **17** and **18** (in total: 1.9 g, 80%), and starting material (3.7 g) was collected.

Compound **17**: ^{1}H-NMR (300MHz, $CDCl_3$) δ: 3.43 (m, 2H, H-1), 3.85 (m, 1H, 2-H), 4.01 (m, 2H, 3-H, 4-H), 4.34 (m, 3H, 5-H, 6-H), 4.88 (m, 1H, 1-OH), 7.55 (m, 2H, Ar-H), 7.67 (m, 1H, Ar-H), 8.01 (m, 2H, Ar-H).

Compound **18**: ^{1}H-NMR (300MHz, $CDCl_3$) δ: 3.43 (m, 2H, 6-H), 4.00 (m, 3H, 3-H, 4-H, 5-H), 4.32 (m, 1H, 2-H), 4.38 (d, 2H, 1-H), 4.90 (m, 1H, 6-OH), 7.56 (m, 2H, Ar-H), 7.68 (m, 1H, Ar-H), 7.97 (m, 2H, Ar-H).

6-O-Benzoyl-1-O-methyl-2,5:3,4-dianhydro-D-talitol (19) and 1-O-benzoyl-6-O-methyl-2,5:3,4-dianhydro-D-talitol (20)

The mixture of compounds **17** and **18** (3.4 g, 13.6 mmol) was dissolved in an ether solution of CH_2N_2 (150 mL), silica gel (5 g, 200-300 mesh) was added, and the solution was stirred at room temperature for 2 h. After evaporation under reduced pressure, the residue was purified on a silica gel column (petroleum ether/EtOAc: 10/1-5/1) to provide a mixture of compounds **19** and **20** (in total: 2.5 g, 70%) as a white syrup. ^{1}H-NMR (300MHz, $CDCl_3$) δ: 3.37 (s, 3H, OCH_3), 3.42 (s, 3H, OCH_3). Anal. Calcd. for $C_{14}H_{16}O_5$: C, 63.63; H, 6.10. Found: C, 63.44; H, 5.98.

6'-O-Benzyl-1'-O-methyl-3'-deoxy-3'-(thymin-l-yl)-2',5'-anhydro-D- mannitol (21) and 1'-O-benzyl-6'-O-methyl-3'-deoxy-3'-(thymin-1-yl)-2',5'-anhydro-D-mannitol (22)

Thymine (2.8 g, 22.6 mmol) in anhydrous DMF, DBU (7 mL, 46 mmol) was added to the solution of compounds **19** and **20** (4 g, 15.1 mmol) in drops at room temperature. The solution was stirred at room temperature for 30 min and then at 90-100°C for 48 h. After evaporation, the residue was applied to a silica gel column (petroleum ether/EtOAc: 5/1-2/1) to provide a mixture of **21** and **22** (in total: 2.0 g, 52%) as a yellow syrup. Unreacted starting materials **19** and **20** were collected. The mixture was characterized by ^{1}H-NMR, and two sets of signals were observed.

1'-O-Methyl-3'-deoxy-3'-(thymin-l-yl)-2',5'-anhydro-D-mannitol (23) and 6'-O-methyl-3'-deoxy-3'-(thymin-l-yl)-2',5'-anhydro-D-mannitol (24)

Saturated ammonia/anhydrous methanol (15 mL) was added to the solution of compounds **21** and **22** (0.29 g, 0.74 mmol) in methanol (15 mL). The solution was stirred at room temperature overnight. After evaporation, the residue was applied to a silica gel column (CH_2Cl_2/CH_3OH: 50/1-10/1) to provide a mixture of **23** and **24** (in total: 0.18 g, 83%) as a yellow syrup. The mixture was characterized by ^{1}H-NMR, and two sets of signals were observed.

Compound **23**: ^{1}H-NMR (500MHz, DMSO-d_6) δ: 1.76 (s, 3H, 5-CH_3), 3.24 (s, 3H, O-CH_3), 3.34 (m, 2H, 1'-H), 3.54 (m, 2H, 6'-H), 3.68 (m, 1H, 5'-H), 4.05 (m, 1H, 2'-H), 4.20 (m, 1H, 4'-H), 4.68 (m, 1H, 3'-H), 7.58 (s, 1H, 6-H).

Compound **24**: ^{1}H-NMR (500MHz, DMSO-d_6) δ: 1.76 (s, 3H, 5-CH_3), 3.24 (s, 3H, O-CH_3), 3.25-3.50 (m, 4H, 1'-H, 6'-H), 3.80 (m, 1H, 5'-H), 3.88 (m, 1H, 2'-H), 4.16 (m, 1H, 4'-H), 4.63 (m, 1H, 3'-H).

6'-O-Dimethoxyltrityl-1'-O-methyl-3'-deoxy-3'-(thymin-l-yl)-2',5'-anhydro-D-mannitol (25) and 1'-O-dimethoxyltrityl-6'-O-methyl-3'-deoxy-3'-(thymin-l-yl)-2',5'-anhydro-D-mannitol (26)

Similar to the preparation of **14** and **15** from **12** and **13**, compounds **25** and **26** were obtained from **23** and **24** as a white foam at a 74% yield.

Compound **25**: ^{1}H-NMR (500MHz, DMSO-d_6) δ: 1.79 (s, 3H, 5-CH_3), 3.09 (m, 2H, 1'-H), 3.32 (s, 3H, 1'-OCH_3), 3.49 (m, 2H, 6'-H), 3.73 (s, 6H, DMT-OCH_3), 3.84 (m, 1H, 5'-H), 4.01 (m, 1H, 2'-H), 4.15 (m, 1H, 4'-H), 4.74 (m, 1H, 3'-H), 5.60 (d, J = 6Hz, 2H, D_2O exchangeable, 4'-OH), 6.84 (m, 4H, Ar-H), 7.20-7.32 (m, 8H, Ar-H), 7.53 (s, 1H, 6-H), 11.28 (s, 1H, D_2O exchangeable, NH). ESI-TOF$^+$ MS: 611 $[M + Na]^+$.

Compound **26**: ^{1}H-NMR (500MHz, DMSO-d_6) δ: 1.79 (s, 3H, 5-CH_3), 3.13 (m, 2H, 6'-H), 3.32 (s, 3H, 6'-OCH_3), 3.45 (m, 2H, 1'-H), 3.73 (s, 6H, DMT-OCH_3), 3.85 (m, 1H, 5'-H), 4.01 (m, 1H, 2'-H), 4.19 (m, 1H, 4'-H), 4.65 (m, 1H, H-3'), 5.61 (d, J = 6Hz, 1H, D_2O exchangeable, 4'-OH), 6.84 (m, 4H, Ar-H), 7.20-7.32 (m, 8H, Ar-H), 7.56 (s, 1H, 6-H), 11.28 (s, 1H, D_2O exchangeable, NH). ESI-TOF$^+$ MS: 611 $[M + Na]^+$.

1'-O-(4,4-Dimethoxytriphenylmethyl)-4'-O-(2-cyanoethyl-N,N-diisopropyl)-phosphoramidite-6'-O-methyl-3'-deoxy-3'-(thymin-l-yl)-2',5'-anhydro-D-mannitol (27)

Similar to the preparation of **16** from **15**, compound **27** was obtained from **26** as a white foam at a 74% yield. ^{31}P-NMR ($CDCl_3$, ppm) δ: 157.2.

Solid-phase synthesis of oligonucleotides

Oligonucleotide synthesis was carried out on a 1-μM scale with a DNA synthesizer (model 392A, Applied Biosystems) applying regular phosphoramidite chemistry. Cleavage and deprotection of the oligonucleotides were performed in a concentrated aqueous ammonia solution at 80°C for 2 h. The oligonucleotides were purified by PAGE (DMT-off) or HPLC (C18, DMT-on) and desalted by OPC (ABI). The pure oligonucleotides were lyophilized and stored at -20°C.

Thermal denaturation and CD spectra

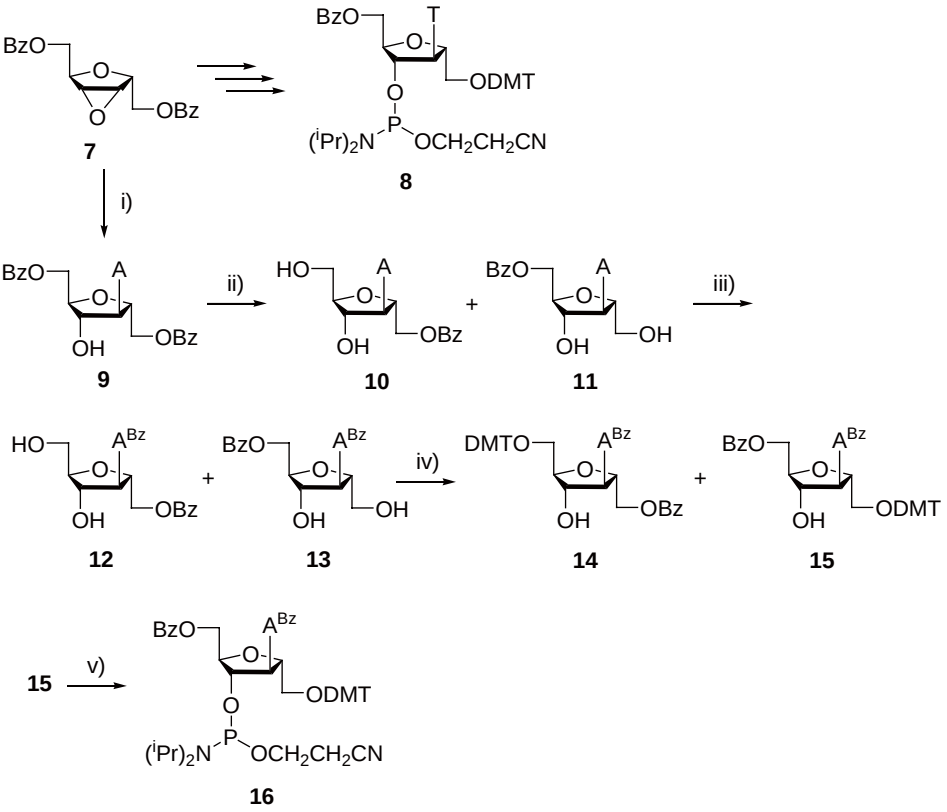

Scheme 1. Reagents and conditions: i) adenine, DBU, DMF, 90-100°C; ii) NH_3/CH_3OH; iii) a. TMSCl, b. BzCl, pyridine, c. NH_3/H_2O; iv) DMTCl, pyridine; v) $ClP(OCH_2CH_2CN)N(^iPr)_2$, $EtN(^iPr)_2$, THF.

The oligomers were dissolved in a buffer containing 0.14 M NaCl, 0.01 M Na_2HPO_4, and 1.0 mM EDTA at pH 7.2. The solution containing oligonucleotide at a concentration of 4 μM was mixed with an equimolar amount of its complementary sequence. Sample were incubated at 80°C for 5 min, then gradually cooled to 4°C, and kept at this temperature for 12 h. Then, the sample was used for the investigation of thermal denaturation and CD spectra. Thermal denaturations were recorded on a Varian Cary 300 spectrophotometer at 260 nm. Sample temperature was increased at 0.5°C/min intervals between 20 and 80°C. CD spectra were measured at 5°C with a J720 polarized spectrophotometer in thermostatically controlled 1 cm cuvettes.

Results and Discussions

Synthesis of oligonucleotides

Isonucleoside phosphoramidite **8**, suitable for solid-phase oligonucleotide synthesis, was obtained by starting with 2',5'-anhydro-1',6'-*O*-dibenzoyl-3'-(thymin-1-yl)-*D*-mannitol, which was prepared from *D*-glucosamine in five steps based on a previous strategy (*13*). The isonucleoside phosphoramidite **16** was also obtained by a similar method (Scheme 1). The amino group of compound **10** or **11** was protected selectively by the "one-pot" method (*17*), in which compound **10** or **11** was first treated with trimethylchlorosilane to protect the hydroxyl groups, and then benzoyl chloride was added to provide *N*-acylation products. Finally, the trimethyl group was hydrolyzed in a basic environment (pH 9) by adding ammonia water (25%) to the reaction solution. Under these pH conditions, the benzoyl group remained. Compounds **10** and **11** or **12** and **13** possessed very similar polarity and were difficult to separate, so the mixture was directly used for the subsequent reaction. The mixture of compounds **12** and **13** reacted with dimethoxytrityl chloride and provided compounds **14** and **15**, which were then separated by silica gel chromatography.

Isonucleoside phosphoramidite **27** was provided by the key intermediate epoxide **7** via six steps (Scheme 2). Compound **7** was debenzoylated with 50% NH_3/CH_3OH at room temperature to provide compounds **17** and **18** in a ratio of about 4:1. Compounds **17** and **18** were difficult to separate, so the mixture was used in the following reaction till the dimethoxytrityl group was used for the protection of the 1'-OH group. Compounds **17** and **18** were methylated in CH_2N_2/ether in which silica gel was used as a catalyst to provide compounds **19** and **20**, which was then reacted with thymine under basic conditions to provide isonucleosides **21** and **22**. After debenzoylation and protection with dimethoxytrityl groups, compounds **25** and **26** were provided, which were then separated

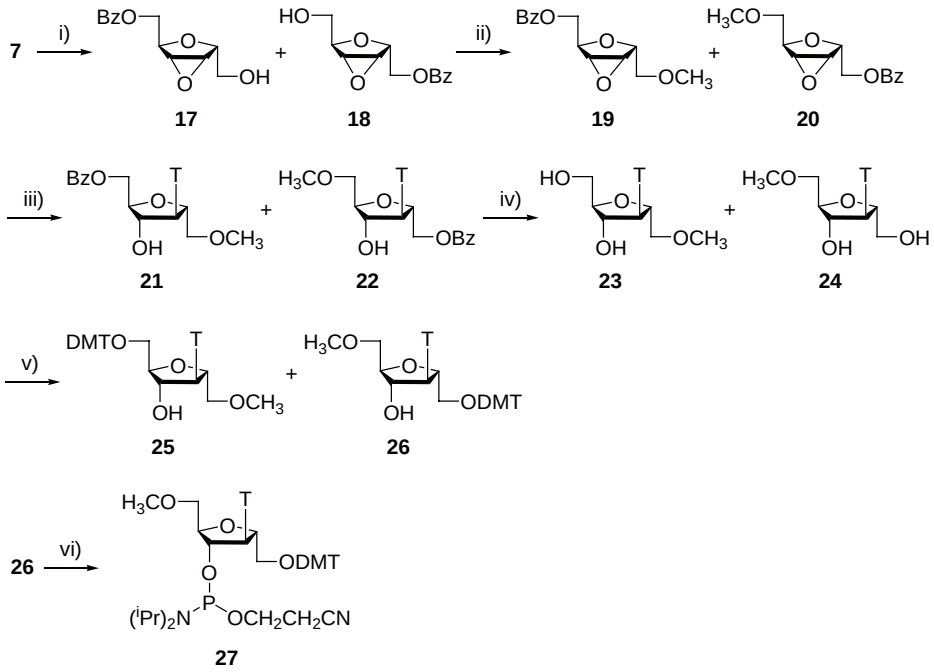

Scheme 2. Reagents and conditions: i) NH_3/CH_3OH; ii) CH_2N_2, ether; iii) Thymine, DBU, DMF, 90-100°C; iv) NH_3/CH_3OH; v) $ClP(OCH_2CH_2CN)N(^iPr)_2$, $EtN(^iPr)_2$, THF.

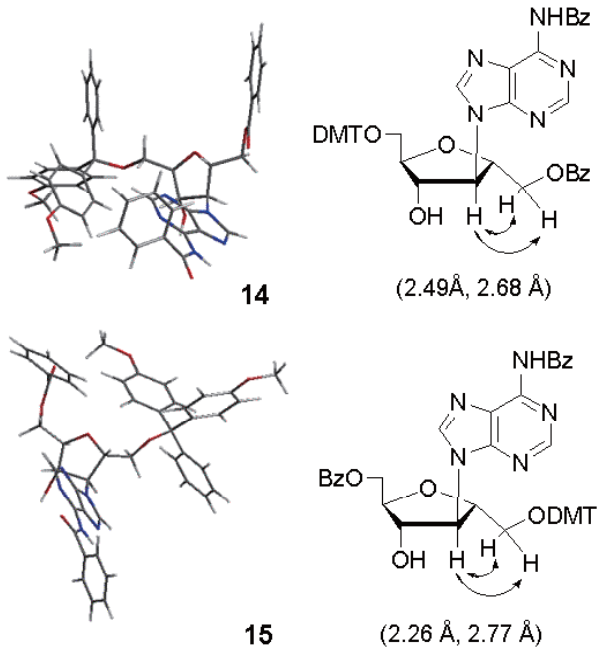

Figure 2. Characterization of compounds **14** and **15** by NOE and molecular modeling.

by silica gel chromatography. The phosphoramidite **27** was obtained by the phosphination of compound **26**. The structures of **14**, **15**, **25** and **26** were identified by ^{1}H-NMR, H-H COSY, and NOESY spectra. The proton signals of the CH_2 connected to OBz appeared to be lower than those of the CH_2 connected to ODMT. Molecular modeling implied that there was a relatively strong NOE between the protons of 1'-H and 3' -H (Figure 2), which was in accordance with NMR characterization.

All isonucleoside-incorporated oligonucleotides were assembled on an automated DNA synthesizer on a 1 μ-mol scale. Synthesis was followed by the standard phosphoramidite protocol except for three injections and a prolonged coupling time of 80 sec every time to ensure adequate coupling yields. For convenience, commercially available nucleotide-attached CPG was used in the synthesis of isonucleoside-incorporated oligonucleotide and one native nucleotide was retained at the 3'-end of the sequence. Universal CPG (Proligo) was used for the synthesis of oligonucleotide with a single isonucleoside modified at the 3'-end. The coupling efficiency was obtained by measuring the release of DMT (95-97%). The crude DMT-protected oligomers were purified by HPLC (C18 column) and then detritylated in 80% acetic acid for 30 min and desalted by OPC (oligonucleotide purification cartridge, ABI) to provide the pure oligomer products. The purities of oligomers were confirmed by capillary electrophoresis or by HPLC analysis. The molecular weights were confirmed by MALDI-TOF mass spectrometry.

The base paring properties of isonucleoside-incorporated oligonucleotides with respect to their complementary sequences were investigated by thermal denaturation and circular dichroism (CD) spectra. Table 1 summarizes the melting temperatures (Tm values) determined by ultra-violet (UV) spectroscopy. The results indicate that oligomer **II** was able to bind with its complementary sequence **IV** though the Tm value was a little lower than that of the native control (**I**/**IV**) (Table 1). When the 6'-OH of isonucleoside was

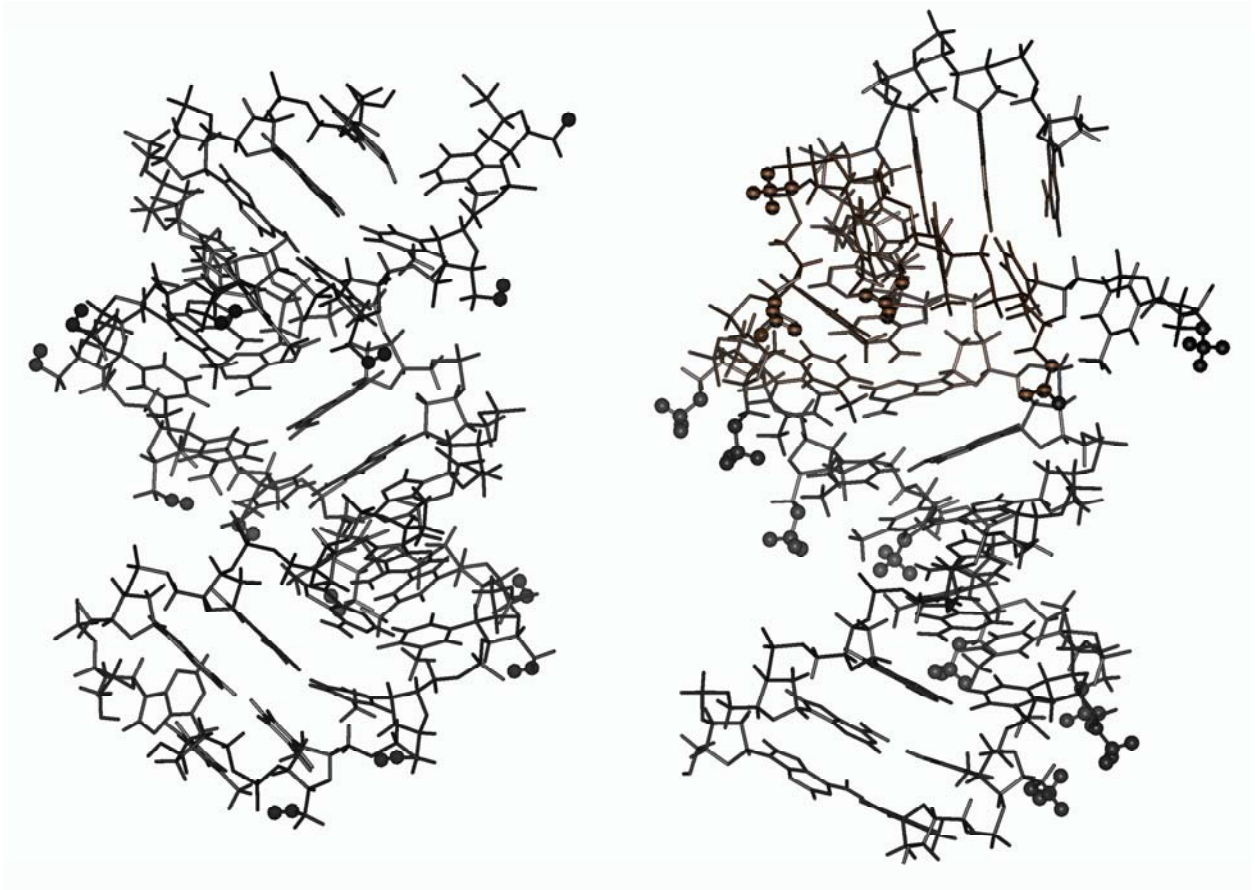

Figure 3. Average structures of duplexes formed by isonucleoside-incorporated oligonucleotides and their native complementary sequences. 6'-OH and 6'-OMe are highlighted with filled-in circles. (Left) duplex **II/IV**; (Right) duplex **III/IV**.

Table 1. Melting temperature of duplexes formed by isonucleoside-incorporated oligonucleotides and their complementary sequences

Duplex	Tm (ΔT) (°C)
I/IV	34.9
II/IV	33.1 (-1.8)
III/IV	-
V/VII	-
V/VIII	29.0 (-8.0)
VI/VII	-
VI/VIII	37.0
X/IX	42.0
XI/IX	40.0 (-2.0)
XII/IX	41.1 (-1.1)
XIII/IX	39.0 (-3.0)
XIV/IX	40.2 (-1.8)

ΔT is the difference in melting temperature between the modified duplex and native oligodeoxynucleotide duplex.

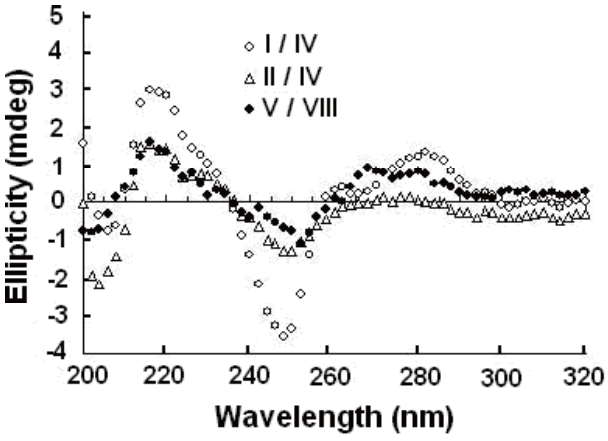

Figure 4. CD spectra of duplexes formed by isonucleoside-incorporated sequences and native complementary sequences.

protected by a methyl group, as shown by oligomer III, no obvious binding to the native complementary sequence was observed. This fact undoubtedly demonstrates that 6'-OH contributed to the stability of the isonucleoside-incorporated duplex. Molecular dynamics simulation also supported this conclusion (Figure 3). Simulation results showed that Watson-Crick base paring and base stacking were retained in the case of free 6'-OH, whereas in the case of 6'-OMe base paring and stacking were disturbed.

Theoretically, isonucleoside-incorporated oligonucleotide has two possible ways to bind with its counterpart, *i.e.*, binding to the 5'→3' native complementary sequence in the 1'→4' or 4'→1' direction. A mixed purine-pyrimidine sequence **V** has been designed to clarify the mode of binding. Thermal denaturation studies showed that a relatively stable duplex was formed between sequences **V** and **VIII**, but no obvious binding was observed between sequence **V** and **VII**. The results indicated that isonucleoside-

incorporated oligonucleotide bound with 5'→3' native complementary oligodeoxynucleotide in the 4' →1' direction. Table 1 also shows that the effect of isonucleoside on the decrease in melting temperature in the mixed purine-pyrimidine sequence (**II/IV**) was much more obvious than in the homo-pyrimidine sequence (**V/VIII**). Single nucleoside modification at one or two ends of the sequence led to the decrease in melting temperature for about 1-2°C, but the effect was a little weaker than the corresponding mis-matched sequence. Considering the increased enzymatic stability of the modified oligonucleotide, the amount of decrease in the binding ability was acceptable. This implied that a stable chemically modified antisense oligonucleotide could be designed by attaching an isonucleoside at the ends of the native sequence.

CD spectra were used to study the conformation of the above duplexes (Figure 4). The spectrum of the duplex dT_{14}/dA_{14} (**I/IV**) showed a positive Cotton peak at 217 nm and a negative Cotton peak at 248 nm, which is the typical character of a B-form DNA conformation. Duplex **II/IV** and **V/VIII** also displayed very similar spectra, which suggested that the modified oligonucleotide duplexes adopted similar B-form conformations. The low intensities of the Cotton peaks of modified duplexes resulted from the poor base stacking of duplexes in which Watson-Crick base paring was disturbed by the torsion of the backbone originating from the introduction of isonucleoside.

In summary, oligonucleotides consisting of isonucleoside 2',5'-anhydro-3'-nucleobase-*D*-mannitol or 6'-*O*-methyl-2',5'-anhydro-3'-(thymin-1-yl)-*D*-mannitol incorporated in 1'→4' linkage mode were synthesized. Their binding behaviors with complementary sequences were investigated via thermal denaturation and CD spectra. A mixed purine-pyrimidine sequence showed that the modified oligonucleotide was able to form a duplex with 3'→5' complementary native oligodeoxynucleotide in the 1'→4' direction. All duplexes were able to adopt B-like DNA conformations. The free hydroxy group in isonucleoside contributed to the modified oligonucleotide's affinity to the complementary sequence, which was in accordance with the results of molecular modeling. The results provided some insight into the design of chemically stable antisense oligonucleotides, *e.g.* by incorporating an isonucleoside at one or two ends of the sequence.

Acknowledgements

This work was supported by the National Natural Science Foundation of China (20132030) and the Ministry of Science and Technology of China (2004CB518904).

References

1. Pirollo KF, Rait A, Sleer LS, Chang EH. Antisense therapeutics: from theory to clinical practice. Pharma Therap 2003;99:55-77.
2. Stahel RA, Zangemeister-Wittke U. Antisense oligonucleotides for cancer therapy-an overview. Lung Cancer 2003;41:581-588.
3. Badros AZ, Goloubeva O, Rapoport AP, Ratterree B, Gahres N, Meisenberg B, Takebe N, Heyman M, Zwiebel J, Streicher H, Gocke CD, Tomic D, Flaws JA, Zhang B, Fenton RG. Phase II study of G3139, a Bcl-2 antisense oligonucleotide, in combination with dexamethasone and thalidomide in relapsed multiple myeloma patients. J Clin Oncol 2005;23:4089-4099.
4. O'Brien SM, Cunningham CC, Golenkov AK, Turkina AG, Novick SC, Rai KR. Phase I to II multicenter study of oblimersen sodium, a Bcl-2 antisense oligonucleotide, in patients with advanced chronic lymphocytic leukemia. J Clin Oncol 2005;23:7697-7702.
5. So A, Rocchi P, Gleave M. Antisense oligonucleotide therapy in the management of bladder cancer. Curr Opin Urol 2005;15:320-327.
6. Urban E, Noe CR. Structural modifications of antisense oligonucleotides. IL Farmaco 2003;58:243-258.
7. Werner D, Brunar H, Noe CR. Investigations on the influence of 2'-*O*-alkyl modifications on the base pairing properties of oligonucleotides. Pharm Acta Helv 1998;73:3-10.
8. Zhou W, Agrawal S. Mixed-backbone oligonucleotides as second- generation antisense agents with reduced phosphorothioate-related side effects. Bioorg Med Chem Lett 1998;8:3269-3274.
9. Wengel J, Koshkin A, Singh SK, Nielsen P, Meldgaard M, Rajwanshi VK, Kumar R, Skouv J, Nielsen CB, Jacobsen JP, Jacobsen N, Olsen CE. LNA (locked nucleic acids). Nucleosides Nucleotides 1999;18:1365-1370.
10. Wahlestedt C, Salmi P, Good L, Kela J, Johnsson T, Hökfelt T, Broberger C, Porreca F, Lai J, Ren K, Ossipov M, Koshkin A, Oerum H, Jacobsen MH, Wengel J. Locked Nucleic Acids (LNA): A novel, efficacious and non-toxic oligonucleotide component for antisense studies. Proc Natl Acad Sci U S A 2000;97:5633-5638.
11. Morita K, Takagi M, Hasegawa C, Kaneko M, Tsutsumi S, Sone J. Synthesis and properties of 2' -O, 4'-C-ethylene-bridged nucleic acids (ENA) as effective antisense oligonucleotides. Bioorg Med Chem 2003;11:2211-2226.
12. Lei Z, Min J, Zhang L. A concise synthesis of 3' -deoxy-3'-nucleobase-2',5'-anhydro-*D*-mannitol: a novel class of hydroxymethyl-branched isonucleosides. Tetrahedron: Asymmetry 2000;11:2899-2906.
13. Lei Z, Zhang L, Zhang L, Chen J, Min J, Zhang L. Hybrid characteristics of oligonucleotides consisting of isonucleoside 2',5'-anhydro-3'-deoxy-3'- (thymin-1-yl)-*D*-mannitol with different linkage modes. Nucleic Acids Res 2001;29:1470-1475.
14. Wang Z, Shi J, Jin H, Zhang L, Lu J, Zhang L. Properties of isonucleotide incorporated oligodeoxynucleotides and inhibition to the expression of spike protein of SARS-CoV. Bioconjugate Chem 2005;16:1081-1087.
15. Li ZS, Qiao RP, Du Q, Yang ZJ, Zhang LR, Zhang PZ, Liang ZC, Zhang LH. Studies on aminoisonucleoside modified siRNAs: stability and silencing activity. Bioconjugate Chem 2007;18 (*in press*).
16. Jin H, Zheng S, Wang Z, Luo C, Shen J, Jiang H, Zhang L, Zhang L. Structural insights into the effect of isonucleosides on B-DNA duplexes using molecular dynamics simulations. J Mol Model 2006;12:781-791.
17. Ti GS, Gaffney BL, Jones RA. Transient protection: efficient one-flask syntheses of protected deoxynucleosides. J Am Chem Soc 1982;104:1316-1319.

Modification of 15-akylidene andrographolide derivatives as alpha-glucosidase inhibitor

Hai-Wei Xu[1, 2], Gai-Zhi Liu[1, 2], Gui-Fu Dai[1], Chun-Li Wu[2], Hong-Min Liu[1, 2, *]

[1] *New Drug Research & Development Center, Zhengzhou University, Zhengzhou, China;*
[2] *School of Pharmaceutical Sciences, Zhengzhou University, Zhengzhou, China.*

ABSTRACT: 15-Alkylidene andrographolide derivatives were specific alpha-glucosidase inhibitors. Semi-synthetic studies of these derivatives led to new alpha-glucosidase inhibitors. Their alpha-glucosidase inhibitory activity was evaluated. Bioactivity results indicated that most of the derivatives were excellent alpha-glucosidase inhibitors. Among them, 6c displayed the best alpha-glucosidase inhibitory bioactivity with an IC_{50} value of 8.3 M.

Key Words: Synthesis, andrographolide derivative, alpha-glucosidase inhibitor

Introduction

Intense interest in glucosidase inhibitors in chemistry, biochemistry, and pharmacology has led to many types of natural and synthetic inhibitors, which aid in both unraveling the mechanism of glucosidase action and development of potential pharmaceuticals such as antitumour agents (*1-3*), antiviral agents (*4,5*), antidiabetics (*6-9*), and immunoregulatory agents (*10*). Various types of inhibitors have also been designed based on structures that resemble the glycosylcations in a transition state of hydrolysis by glucosidase (*11*).

The plant *Andrographis paniculata* (*12,13*) and its constituent andrographolide (**3**) are used extensively in traditional Chinese medicine (*14,15*). Extracts of the plant and the constituents are reported to exhibit a wide spectrum of biological activities including antibacterial (*16,17*), anti-inflammatory (*18,19*), antimalarial (*20,21*), immunological (*22,23*), hepatoprotective (*24*), and antitumor (*25*) properties. In recent years, the antidiabetic activity of the plant has also attracted some researchers' attention (*26-30*).

In the course of the current authors' study of glucosidase inhibitors, some andrographolide derivatives have been proven to be potent and specific α-glucosidase inhibitors (*31*). Previous results indicated that (a) the γ-alkylidene butenolide moiety of andrographolide derivatives and (b) the aromatic group at 3,19-hydroxyls favored α-glucosidase inhibitory activity while (c) the epoxidation of double bonds ($\Delta^{8(17)}$) hampered α-glucosidase inhibitory activity (*31*).

Among the two series of 15-alkylidene derivatives cited in previous work, compounds **1** and **2** were the best α-glucosidase inhibitors with an IC_{50} value of 16 μM and 6 μM, respectively (Figure 1) (*32*).

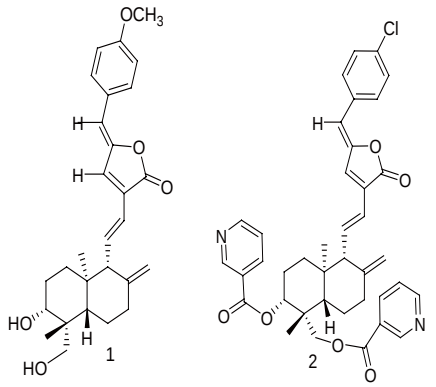

Figure 1. α-glucosidase inhibitors with an IC_{50} value of 16 μM and 6 μM, respectively.

This paper focuses on synthesizing more 15-alkylidene andrographolide analogues and investigating the contribution of ketal to inhibitory activity. Hence, a new series of derivatives were designed and synthesized based on the 15-aklylidene andrographolide derivatives concerned instead of the compound **1,** which displayed excellent bioactivity (IC_{50}, 16 μM).

Materials and Methods

**Correspondence to:* New Drug Research & Development Center, 75 Daxue Road, Zhengzhou City, 450052, Henan Province, China;
e-mail: liuhm@zzu.edu.cn

Received June 20, 2007
Accepted July 6, 2007

General methods

Melting points were determined on a Beijing Keyi XT5 apparatus and are uncorrected. IR spectra were recorded as KBr pellets on a Thermo Nicolet (IR200) Spectrometer. ^{1}H- and ^{13}C-NMR spectra were recorded on a Brüker DPX-400 spectrometer at 400 and 100MHz with TMS as the internal standard. Mass spectra were taken with a Waters Q-Tof micro mass spectrometer. The absorbance at 405 nm was measured with a PowerWaveX Microplate Scanning Spectrophotometer (BIO-TEK INSTRUMENTS, INC).

General procedure for α-glucosidase inhibition assay

The inhibition rate was determined at 37ºC in 0.067 M K_2HPO_4/KH_2PO_4 buffer (pH 6.8).The reaction mixture contained 4 μL of enzyme solution, 40 μL of inhibitor and 20 μL of substrate. *p*-Nitrophenyl-α-*D*-glucopyranoside, the substrate, and α-glucosidase (Baker's yeast) were purchased from Sigma Chemical Co. (St Louis, MO, USA). One mM acarbose (extracted from Glucobay tablets, Bayer Pharmaceuticals Corporation) was tested as a positive control. Both the inhibitor and substrate were first dissolved in dimethyl sulfoxide (DMSO) and then diluted with 0.067 M K_2HPO_4/KH_2PO_4 buffer so that the final concentration of DMSO was 10%. The enzymatic reaction was started after incubation of the enzyme (0.04 units/mL) for 30 min in the presence of the inhibitor (0.1 mM) by the addition of substrate (0.5 mM). The mixture was incubated at 37ºC for 5 min, and the reaction was quenched by the addition of 0.1 M Na_2CO_3 (pH 9.8). The absorption at 405 nm was measured immediately and served as the relative rate for the hydrolysis of the substrate. All experiments were carried out in triplicate.

Synthesis of compound 4 (*33*)

Synthesis of compound 5

Compound **4** (500 mg, 1.4 mmol) and paraform (85 mg, 2.8 mmol) in THF (20 mL) were refluxed for 1 h in the presence of H_2SO_4. The solvent was evaporated under reduced pressure to produce a white powder. The white powder was dissolved in $CHCl_3$. The $CHCl_3$ phase was extracted with brine and water and dried with Na_2SO_4. The solvent was evaporated to produce **5.**

General procedure for the synthesis of compound 6

5 (100 mg, 0.3 mmol) and variant aldehydes (0.45~0.9 mmol) in dry methanol were refluxed in the presence of Na_2CO_3 (10 mg, 0.09 mmol). After completion of the reaction, the mixture was diluted with $CHCl_3$ and washed with water. The organic phase was evaporated in vacuo to produce the corresponding product by flash chromatography or crystallization from methanol.

6a Yield 89%; m.p.: 153.8~156.5ºC; IR 2939, 2847, 1757, 1643, 1449, 1165, 1101, 1029, 941, 900 cm^{-1}; ^{1}H-NMR (400MHz, $CDCl_3$): δ 7.77 (2H, d, *J* = 7.5Hz), 7.38 (1H, t, *J* = 7.3Hz), 7.30 (2H, t, *J* = 7.3Hz), 7.10 (1H, s), 6.97 (1H, dd, *J* = 10.0, 15.6Hz), 6.23 (1H, d, *J* = 15.6Hz), 5.95 (1H, s), 4.93 (1H, d, *J* = 6.5Hz), 4.81 (2H, od), 4.57 (1H, s), 4.06 (1H, d, *J* = 11.2Hz), 3.50 (1H, dd, *J* = 4.6, 13.2Hz), 3.46 (1H, d, *J* = 11.2Hz), 2.50 (1H, dd, *J* = 1.6, 13.7Hz), 2.24 (1H, m), 2.04 (1H, m), 1.76 (1H, m), 1.64 (2H, om), 1.47 (1H, br), 1.42 (3H, s), 1.31 (1H, m), 1.22 (1H, m), 1.14 (1H, m), 0.97 (3H, s); ^{13}C-NMR (100.6MHz, $CDCl_3$): δ 168.8, 147.8, 147.6, 137.5, 135.5, 133.3, 130.4, 128.8, 128.7, 127.7, 127.1, 113.0, 109.6, 87.7, 79.8, 69.1, 61.8, 54.5, 38.7, 37.7, 37.3, 36.3, 25.8, 21.8, 20.9, 16.0. HRMS m/z: $[M+Na]^+$ 455.2189 (calcd.455.2198).

6b Yield 87%; m.p.: 187.0~189.4ºC; IR: 2940, 2847, 1752, 1645, 1596, 1462, 1300, 1245, 1165, 1100, 1029, 939, 752 cm^{-1}; ^{1}H-NMR (400MHz, $CDCl_3$): δ 8.18 (1H, dd, *J* = 1.2, 8.0Hz), 7.28 (1H, m), 7.13 (1H, s), 7.01 (1H, t, *J* = 7.6Hz), 6.92 (1H, dd, *J* = 10.1, 15.8Hz), 6.89 (1H, d, *J* = 8.4Hz), 6.5 (1H, s), 6.29 (1H, d, *J* = 15.6Hz), 4.95 (1H, d, *J* = 6.4Hz), 4.80 (2H, om), 4.57 (1H, s), 4.06 (1H, d, *J* = 11.2Hz), 3.87 (3H, s), 3.50 (1H, dd, *J* = 4.4, 8.8Hz), 3.46 (1H, d, *J* = 11.6Hz), 2.49 (1H, m), 2.46 (1H, d, *J* = 10Hz), 2.26 (1H, m), 2.06 (1H, m). 1.79 (1H, m), 1.64~1.57 (2H, om), 1.41 (3H, s), 1.30 (1H, m), 1.21~1.13 (2H, om), 0.96 (3H, s); ^{13}C-NMR (100.6MHz, $CDCl_3$): δ 168.9, 157.3, 147.9, 147.4, 136.9, 136.1, 131.5, 130.3, 126.4, 122.3, 121.8, 121.1, 110.5, 109.6, 106.9, 87.7, 79.8, 69.1, 61.8, 55.6, 38.7, 37.7, 37.3, 36.3, 25.8, 21.8, 20.9, 16.0.

6c Yield 57%; m.p.: 175.0~176.4ºC; IR 2941, 2849, 1742, 1601, 1565, 1525, 1366, 1165, 1100, 1063, 940, 810 cm^{-1}; ^{1}H-NMR (400MHz, $CDCl_3$): δ 7.70 (2H, d, *J* = 8.8Hz), 7.09 (1H, s), 6.84 (1H, dd, *J* = 10.1, 15.8Hz), 6.70 (2H, d, *J* = 8.8Hz), 6.21 (1H, d, *J* = 15.8Hz), 5.90 (1H, s), 4.94 (1H, d, *J* = 6.4Hz), 4.81 (2H, od), 4.58 (1H, s), 4.06 (1H, d, *J* = 11.2Hz), 3.51 (1H, om), 3.43 (1H, d, *J* = 11.2Hz), 3.0 (6H, od), 2.49 (1H, d, *J* = 13.5Hz), 2.36 (1H, d, *J* = 10Hz), 2.26 (1H, m), 2.10 (1H, m). 1.79 (1H, m), 1.65~1.57 (2H, om), 1.41 (3H, s), 1.28~1.13 (3H, om), 0.96 (3H, s); ^{13}C-NMR (100.6MHz, $CDCl_3$): δ 169.4, 150.5, 148.0, 144.8, 135.7, 135.2, 132.2, 130.4, 124.2, 122.1, 121.4, 114.6, 111.9, 109.6, 87.7, 79.8, 69.1, 61.8, 34.3, 40.1, 38.6, 37.7, 37.2, 36.3, 25.8, 21.8, 20.8, 16.1.

6d Yield 69%; m.p.: 164.8~170.2ºC; IR: 2942, 2847, 1750, 1638, 1599, 1507, 1233, 1161, 1099, 1028, 941, 892 cm^{-1}; ^{1}H-NMR (400MHz, $CDCl_3$): δ 7.83 (2H, om), 7.11 (3H, om), 6.98 (1H, dd, *J* = 10.1, 15.8Hz), 6.23 (1H, d, *J* = 15.8Hz), 5.9 (1H, s), 4.94 (1H, d, *J* = 6.4Hz), 4.82 (2H, od), 4.56 (1H, s), 4.06 (1H, d, *J* = 11.2Hz), 3.51 (1H, om), 3.46 (1H, d, *J* = 11.2Hz), 2.49 (1H, d, *J* = 13.6Hz), 2.46 (1H, d, *J* = 10.0Hz), 2.26 (1H, m), 2.06 (1H, m), 1.78 (1H, br), 1.61 (2H, om), 1.42 (3H, s),

1.31 (1H, m), 1.22 (1H, m), 1.14 (1H, m), 0.97 (3H, s); ^{13}C-NMR (100.6MHz, $CDCl_3$): δ 168.6, 164.0, 161.5, 147.8, 147.1, 137.5, 135.5, 132.3, 129.5, 126.8, 121.6, 116.0, 115.8, 111.8, 109.6, 87.7, 79.7, 69.1, 61.8, 54.3, 38.7, 37.7, 37.3, 36.3, 25.8, 21.8, 20.8, 16.1.

6e Yield 90%; m.p.: 198.2~199.7ºC; IR 2953, 2939, 2849, 1758, 1637, 1488, 1458, 1161, 1097, 1043, 1023, 942, 891, 811 cm^{-1}; H-NMR (400MHz, $CDCl_3$): δ 7.71 (2H, d, *J* = 8.8Hz), 7.36 (2H, d, *J* = 8.8Hz), 7.10 (1H, s), 6.99 (1H, dd, *J* = 10.1, 15.6Hz), 6.23 (1H, d, *J* = 15.8Hz), 5.92 (1H, s), 4.94 (1H, d, *J* = 6.4Hz), 4.81 (2H, od), 4.56 (1H, s), 4.06 (1H, d, *J* = 11.2Hz), 3.51 (1H, dd, *J* = 4.4, 12.8Hz), 3.46 (1H, d, *J* = 11.2Hz), 2.50 (1H, m), 2.46 (1H, d, *J* = 10Hz), 2.29 (1H, m), 2.08 (1H, m). 1.79 (1H, m), 1.63~1.58 (2H, om), 1.42 (3H, s), 1.32 (1H, m), 1.22~1.11 (2H, om), 0.96 (3H, s); ^{13}C-NMR (100.6MHz, $CDCl_3$): δ 168.5, 147.82, 147.86.

6f Yield 77%; m.p.: 168.4~170.2ºC; IR 2970, 2941, 2847, 1761, 1628, 1443, 1261, 1101, 1030, 944, 892 cm^{-1}; ^{1}H-NMR (400MHz, $CDCl_3$): δ 8.25 (1H, d, *J* = 7.7Hz), 7.41 (1H, d, *J* = 7.8Hz), 7.31 (1H, m), 7.24 (1H, m), 7.22 (1H, s), 7.00 (1H, dd, *J* = 10.0, 15.8Hz), 6.45 (1H, s), 6.25 (1H, d, *J* = 15.8Hz), 4.9 (1H, d, *J* = 6.4Hz), 4.8 (2H, od), 4.56 (1H, s), 4.06 (1H, d, *J* = 11.2Hz), 3.51 (1H, dd, *J* = 4.4, 12.8Hz), 3.47 (1H, d, *J* = 11.2Hz), 2.50 (1H, d, *J* = 13.6Hz), 2.38 (1H, d, *J* = 10.1Hz), 2.24 (1H, m), 2.07 (1H, m), 1.78 (1H, m), 1.61 (2H, om), 1.42 (3H, s), 1.31~1.14 (3H, om), 0.97 (3H, s); ^{13}C-NMR (100.6MHz, $CDCl_3$): δ 168.5, 148.5, 147.8, 138.1, 135.8, 134.1, 131.9, 131.0, 129.7, 129.6, 127.5, 127.2, 121.5, 109.7, 105.2, 87.7, 79.7, 69.1, 61.8, 54.2, 38.7, 37.7, 37.2, 36.2, 25.8, 21.8, 20.8, 16.1.

6g Yield 77%; m.p.: 179.3~182.7ºC; IR 2941, 2878, 2847, 1762, 1638, 1582, 1474, 1425, 1163, 1099, 1030, 943, 892 cm^{-1}; ^{1}H-NMR (400MHz, $CDCl_3$): δ 7.73 (1H, s), 7.67 (1H, d, *J* = 7.5Hz), 7.30 (2H, om), 7.11 (1H, s), 7.00 (1H, dd, *J* = 10.0, 15.6Hz), 6.24 (1H, d, *J* = 15.6Hz), 5.89 (1H, s), 4.94 (1H, d, *J* = 6.4Hz), 4.82 (2H, od), 4.56 (1H, s), 4.06 (1H, d, *J* = 11.2Hz), 3.51 (1H, dd, *J* = 4.4, 12.9Hz), 3.47 (1H, d, *J* = 11.2Hz), 2.50 (1H, d, *J* = 12.3Hz), 2.46 (1H, d, *J* = 10.0Hz), 2.24 (1H, m), 2.08 (1H, br), 1.78 (1H, m), 1.63 (2H, om), 1.42 (3H, s), 1.31 (1H, m), 1.22~1.14 (2H, om), 0.97 (3H, s); ^{13}C-NMR (100.6MHz, $CDCl_3$): δ 168.8, 148.7, 148.2, 138.6, 135.8, 135.4, 135.1, 130.43, 130.40, 129.2, 128.8, 128.0, 122.0, 111.8, 110.1, 88.1, 80.1, 69.5, 62.2, 54.7, 39.2, 38.1, 377, 36.7, 26.2, 22.2, 21.3, 16.5.

6h Yield 85%; m.p.: 203.2~203.8ºC; IR 2942, 2851, 1753, 1642, 1495, 1447, 1259, 1038, 940, 891 cm^{-1}; ^{1}H-NMR (400MHz, $CDCl_3$): δ 7.47 (1H, d, *J* = 1.4Hz), 7.15 (1H, dd, *J* = 1.4, 8.1Hz), 7.08 (1H, s), 6.95 (1H, dd, *J* = 10.1, 15.6Hz), 6.83 (1H, d, *J* = 8.1Hz), 6.22 (1H, d, *J* = 15.6Hz), 6.01 (2H, s), 5.89 (1H, s), 4.9 (1H, d, *J* = 6.3Hz), 4.82 (1H, d, *J* = 6.3Hz), 4.80 (1H, s), 4.57 (1H, s), 4.06 (1H, d, *J* = 11.2Hz), 3.51 (1H, m), 3.45 (1H, d, *J* = 11.1Hz), 2.49 (1H, dd, *J* = 1.5, 13.7Hz), 2.38 (1H, d, *J* = 10.0Hz), 2.24 (1H, br), 2.05 (1H, m), 1.76 (1H, m), 1.64~1.57 (2H, om), 1.42 (3H, s), 1.28 (1H, m), 1.22 (1H, m), 1.13 (1H, m), 0.96 (3H, s); ^{13}C-NMR (100.6MHz, $CDCl_3$): δ 169.0, 149.1, 148.9, 148.6, 147.0, 137.6, 136.4, 128.4, 126.6, 122.5, 113.9, 110.6, 110.4, 109.3, 102.2, 88.4, 80.5, 68.0, 62.5, 55.0, 39.4, 38.4, 38.0, 37.0, 26.5, 22.57, 21.6, 16.8.

6i Yield 75%; m.p.: 203.6~205.0ºC; IR 2943, 2851, 1761, 1636, 1573, 1503, 1457, 1422, 1332, 1248, 1156, 1121, 1027, 937, 896 cm^{-1}; ^{1}H-NMR (400MHz, $CDCl_3$): δ 7.09 (1H, s), 7.02 (2H, s), 6.94 (1H, dd, *J* = 10.1, 15.8Hz), 6.23 (1H, d, *J* = 15.8Hz), 5.87 (1H, s), 4.93 (1H, d, *J* = 6Hz), 4.81 (2H, om), 4.5 (1H, s), 4.06 (1H, d, *J* = 11.6Hz), 3.90 (9H, s), 3.50 (1H, m), 3.46 (1H, d, *J* = 11.6Hz), 2.49 (1H, d, *J* = 12.4Hz), 2.4 (1H, d, *J* = 10.0Hz), 2.26 (1H, m), 2.01 (1H, m), 1.79 (1H, m), 1.64~1.57 (2H, o0m), 1.42 (3H, s), 1.31 (1H, m), 1.22~1.14 (2H, om), 0.96 (3H, s); ^{13}C-NMR (100.6MHz, $CDCl_3$): δ 168.7, 153.2, 147.9, 147.0, 139.0, 137.3, 135.5, 128.8, 126.5, 121.6, 113.1, 109.6, 107.6, 87.7, 79.5, 69.1, 61.7, 61.0, 56.2, 54.3, 38.7, 37.7, 37.3, 36.3, 25.8, 21.8, 20.8, 16.0.

6j A mixture of two isomers (1/3); ^{1}H-NMR (400MHz, $CDCl_3$): δ 7.83 (0.3H, s), 7.52 (0.3H, d, *J* = 1.2Hz), 7.50 (0.7H, d, *J* = 1.2Hz), 7.09 (0.7H, s), 7.03 (0.7H, d, *J* = 3.6Hz), 6.99 (03H, dd, *J* = 10.1, 15.6Hz), 6.95 (0.7H, dd, *J* = 10.1, 15.6Hz), 6.55 (0.7H, m), 6.51 (0.3H, d, *J* = 3.2Hz), 6.49 (0.3H, m), 6.35 (0.3H, s), 6.27 (0.3H, d, *J* = 15.6Hz), 6.22 (0.7H, d, *J* = 15.6Hz), 6.01 (0.7H, s), 4.93 (1H, d, *J* = 6.4Hz), 4.81 (2H, om),

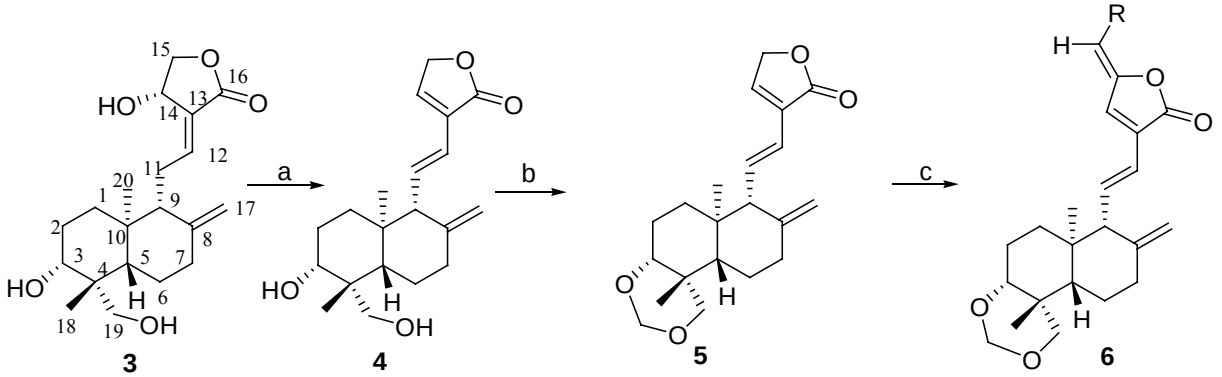

Scheme 1. Synthesis of compound 6. Reagents and conditions: a) xylene, pyridine, Al_2O_3, reflux, 6~10 h. b) THF, H_2SO_4, paraform, reflux, 1 h; c) aldehydes, Na_2CO_3, methanol, reflux, 3~5 h.

Table 1. Structures and α-glucosidase inhibitory activity of compounds **1, 2, 3, 4, 6, and 7**

Comp	R	Bioactivity (IC_{50} μM)	Comp	R	Bioactivity (IC_{50} μM)
1	-	16	**3**	-	Ni [a]
2	-	6	**4**	-	18.5 [b]
6a	C_6H_5	49.1	**7a**	C_6H_5	58
6b	*o*-$OMeC_6H_4$	15.7	**7b**	*o*-$OMeC_6H_4$	Nd [c]
6c	*p*-(*N*,*N*-dimethyl)-C_6H_4	8.3	**7c**	*p*-(*N*,*N*-dimethyl)-C_6H_4	70
6d	*p*-F-C_6H_4	14.1	**7d**	*p*-F-C_6H_4	Ni
6e	*p*-Cl-C_6H_4	> 100	**7e**	*p*-Cl-C_6H_4	Ni
6f	*o*-Cl-C_6H_4	> 100	**7f**	*o*-Cl-C_6H_4	Ni
6g	*m*-Cl-C_6H_4	24.6	**7g**	*m*-Cl-C_6H_4	Nd
6h	benzo[13]dioxole-5-methanyl	> 100	**7h**	benzo[13]dioxole-5-methanyl	82
6i	2,4,5-triMeO-C_6H_4	> 100	**7i**	2,4,5-triMeO-C_6H_4	84
6j	furoyl	Nd	**7j**	furoyl	100

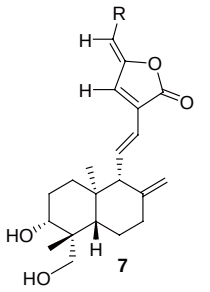

7

Acarbose served as a positive control. The percentage of inhibition of 1 mM acarbose was 56.5%.
[a] No inhibition at100 μM.
[b] % Inhibition determined at 100 μM compound concentration.
[c] No determination.

4.57 (0.3H, s), 4.56 (0.7H, s), 4.06 (1H, d, *J* = 11.2Hz), 3.51 (1H, m), 3.46 (1H, d, *J* = 11.2Hz), 2.49 (1H, m), 2.36 (1H, d, *J* = 10Hz), 2.26 (1H, m), 2.07 (1H, m). 1.76 (1H, m), 1.63~1.58 (2H, om), 1.41 (3H, s), 1.28 (1H, m), 1.22~1.13 (2H, om), 0.96 (3H, s); ^{13}C-NMR (100.6MHz, $CDCl_3$): δ 168.3, 168.0, 149.7, , 87.7, 79.7, 69.1, 61.8, 54.3, 38.7, 37.7, 37.2, 36.3, 25.8, 21.8, 20.149.3, 147.88, 147.84, 147.3, 145.6, 144.3, 143.9, 138.0, 137.3, 134.1, 132.3, 128.9, 127.0, 122.1, 121.8, 114.9, 114.5, 113.1, 112.4, 109.6, 101.8, 101.38, 16.0.

Results and Discussion

Compound **4** was obtained by refluxing andrographolide (**3)** in a mixture of xylene and pyridine in the presence of Al_2O_3. Compound **5** was obtained in an excellent yield by heating **4** and paraform in THF in the presence of H_2SO_4. Compound **6** was synthesized by vinylogous aldol reaction of **4** and varied aldehydes (Scheme 1, Table 1). The structure of **6** was elucidated by NMR and IR spectral analysis. Conjugated olefinic protons in ^{1}H-NMR spectrum of **6** were detected at δ 6.8 (H-11), 6.1 (H-12), 7.2 (H-14) and about δ 5.9~6.5 (H-21). The signal of H-15 (δ 4.8) disappeared in ^{1}H-NMR of **6**. Based on the coupling constant $\boldsymbol{J_{H\text{-}11,H\text{-}12}}$ (15.6Hz), the conformation of double bonds $\Delta^{11(12)}$ was assumed to be **E**. The geometry of double bonds ($\Delta^{15(21)}$) in **6** was confirmed to be a **Z** conformation according to previous research (*32*). Of the **6** compounds, **6j** was a mixture of two isomers (1/3), which differed from the corresponding compound **7j**. The reason for the difference has yet to be indicated.

Bioactivity results showed that compound **6** displayed selective α-glucosidase inhibitory activity. The ketal derivative was able to enhance α-glucosidase inhibitory activity (Table 1). The bioactivities of **6a~g** were better than those of their corresponding compounds **7a~g** (*31*,*32*). **6c** is more effective than other **6** compounds. However, the ketal derivatives **6h** and **6i** of **7h** and **7i** displayed a lower IC_{50} value among the compounds concerned. The above results suggested that the ketal of hydroxyls at C-3 and C-19 favored inhibitory activity.

Comparing the activities of **6** indicated that mono-substitution in the aromatic ring displayed a higher affinity than disubstitution or trisubstitution. On the other hand, substitution of a simple chloro group at the 3-position of the aromatic ring was more effective than at the 2- or 4-position. Introduction of a strong electron-donor displayed the best inhibitory activity.

In α-glucosidase inhibitory activity testing, acarbose served as a positive control. The percentage of inhibition of 1 mM acarbose was 56.5%. Most 15-alkylidene andrographolide derivatives (**6** and **7**) displayed better activity than acarbose, which has proven useful in reducing peak postprandial blood glucose (PPBG) concentrations.

In summary, a new series of 15-alkylidene andrographolide derivatives were designed and synthesized as α-glucosidase inhibitors. Their structures were identified by IR and NMR spectral analysis. Several products exhibited good α-glucosidase inhibition activity. Among the inhibitors, the best was **6c** (8.3 μM), which should prove useful in developing new drugs such as diabetes, anti-tumor, and anti-antiviral medications.

Acknowledgment

We would like to thank the National Natural Science Foundation of China for their support of this work.

References

1. Bernack RJ, Niedbala MJ, Korytnyk W. Glycosidases in cancer and invasion. Cancer Metastasis Rev 1985;4:81-101.
2. Pili R, Chang J, Partis RA, Mueller RA, Chrest FJ, Passaniti A. The α-glucosidase I inhibitor

castanospermine alters endothelial cell glycosylation prevents angiogenesis and inhibits tumor growth. Cancer Res 1995;55:2920-2926.
3. Humphries MJ, Matsumoto K, White SL, Olden K. Inhibition of experimental metastasis by castanospermine in mice: blockage of two distinct stages of tumor colonization by oligosaccharide processing inhibitors. Cancer Res 1986;46:5215-5222.
4. Papandreou MJ, Barbouche R, Guieu R, Kieny MP, Fenouillet E. The alpha-glucosidase inhibitor 1-deoxynojirimycin blocks human immunodeficiency virus envelope glycoprotein-mediated membrane fusion at the CXCR4 binding step. Mol Pharmacol 2002;61:186-193.
5. Ouzounov S, Mehta A, Dwek RA, Block TM, Jordan R. The combination of interferon alpha-2b and *n*-butyl deoxynojirimycin has a greater than additive antiviral effect upon production of infectious bovine viral diarrhea virus (BVDV) *in vitro*: implications for hepatitis C virus (HCV) therapy. Antiviral Res 2002;55:425-435.
6. Schmidt DD, Frommer W, Junge B, Muller L, Wingender W, Truscheit E, Schafer D. alpha-Glucosidase inhibitors. New complex oligosaccharides of microbial origin. Naturwissenschaften 1977;64:535-536.
7. Kameda Y, Asano N, Yoshikawa M, Takeuchi M, Yamaguchi T, Matsui K, Horii S, Fukase H. Valiolamine a new alpha-glucosidase inhibiting aminocyclitol produced by Streptomyces hygroscopicus. J Antibiot 1984;37:1301-1307.
8. Robinson KM, Begovic ME, Rhinehart BL, Heineke EW, Ducep JB, Kastner PR, Marshall FN, Danzin C. New potent alpha-glucohydrolase inhibitor MDL 73945 with long duration of action in rats. Diabetes 1991;40:825-830.
9. Fujisawa T, Ikegami H, Inoue K, Kawabata Y, Ogihara T. Effect of two α-glucosidase inhibitors voglibose and acarbose on postprandial hyperglycemia correlates with subjective abdominal symptoms. Metabolism 2005;54:387-390.
10. Van den Broek LA, Kat-Van Den Nieuwenhof MW, Butters TD, Van Boeckel CA. Synthesis of alpha-glucosidase I inhibitors showing antiviral (HIV-1) and immunosuppressive activity. J Pharm Pharmacol 1996;48:172-178.
11. Look GC, Fotsch CH, Wong CH. Enzyme-catalyzed organic synthesis: practical routes to aza sugars and their analogs for use as glycoprocessing inhibitors. Acc Chem Res 1993;26:182-190.
12. Taki T, Kuroyanagi M, Matsumoto A, Fukushima S, Maeda H, Sato M. Isolation of andrographolide and its deoxy derivative from Andrographis paniculata as antitumor agents and pharmaceutical compositions containing them. JP patent 63088124 A2, 1988.
13. Abeysekera AM, De Silva KTD, Silva WSJ, Ratnayake S, Labadie RP. Proton and carbon-13 NMR spectral analysis of andrographolide. Fitoterapia 1988;59:501-505.
14. Zhang CY, Tan BK. Effects of 14-deoxyandrographolide and 14-deoxy-11,12-didehydroandrographolide on nitric oxide production in cultured human endothelial cells. Phytotherapy Res 1999;13:157-159.
15. Sabu KK, Padmesh P, Seeni S. Intraspecific variation in active principle content and isozymes of Andrographis paniculata (kalmegh): a traditional hepatoprotective medicinal herb of India. J Medicinal and Aromatic Plant Sciences 2001;23:637-647.
16. Zhang WY. Anti-infectious antipyretic and analgesic medicine. Chinese Patent CN 1266699, 2000.
17. Gupata S, Choudhry MA, Yadava JNS, Srivastava V, Tandon JS. Antidiarrheal activity of diterpenes of Andrographis paniculata (Kal-Megh) against Escherichia coli enterotoxin in *in vivo* models. Int J Crude Drug Res 1990;28:273-283.
18. Babish JG, Howell T, Pacioretty L. Combinations of diterpene triepoxide lactones and diterpene lactones or triterpenes for synergistic inhibition of cyclooxygenase-2. U S Patent 20020068098, 2002.
19. Madav S, Tanda SK, Lal J, Tripathi HC. Anti-inflammatory activity of andrographolide. Fitoterapia 1996;67:452-458.
20. Misra P, Pal NL, Guru PY, Katiyar JC, Srivastava V, Tandon JS. Antimalarial activity of traditional plants against erythrocytic stages of Plasmodium berghei. Int J Pharmacog 1992;30:263-274.
21. Najib Nik A Rahman N, Furuta T, Kojima S, Takane K, Ali Mohd M. Antimalarial activity of extracts of Malaysian medicinal plants. J Ethnopharmacology 1999;64:249-254.
22. Puri A, Saxena F, Saxena KC, Srivastava V, Tandon JS. Immunostimulant agents from Andrographis paniculata. J Nat Prod 1993;56:995-999.
23. Chiou WF, Lin JJ, Chen CF. Andrographolide suppresses the expression of inducible nitric oxide synthase in macrophage and restores the vasoconstriction in rat aorta treated with lipopolysaccharide. Br J Pharmacol 1998;125:327-334.
24. Saraswat B, Visen PKS, Patnaik GK, Dhawan BN. Effect of andrographolide against galactosamine-induced hepatotoxicity. Fitoterapia 1995;66:415-420.
25. Nanduri S, Rajagopal S, Akella V. Preparation of andrographolide derivatives for pharmaceutical use in the treatment of a variety of disorders such as cancer and HIV infection. WO 2001085709, 2001.
26. Ahmed M, Talukder SA. Studies on the hypoglycemic activity of Kalmegh (Andrographis paniculata Nees.) on the blood sugar level of rats. Pharm J 1977;6:21-24.
27. Zhang XF, Tan BK. Antihyperglycaemic and anti-oxidant properties of Andrographis paniculata in normal and diabetic rats. Clin Exp Pharmacol Physiol 2000;27:358-363.
28. Zhang XF, Tan BK. Anti-diabetic property of ethanolic extract of Andrographis paniculata in streptozotocin-diabetic rats. Acta Pharmacol Sin 2000;21:1157-1164.
29. Rafidah H, Azimahtol HP, Meenakshii N. Screening for antihyperglycaemic activity in several local herbs of Malaysia. J Ethnopharmacol 2004;95:205-208.
30. Siripong P, Kongkathip B, Preechanukool K, Picha P, Tunsuwan K, Taylor WC. Cytotoxic diterpenoid constituents from Andrographis paniculata Nees leaves. J Sci Soc Thailand 1992;18:187-194.
31. Dai GF, Xu HW, Wang JF, Liu FW, Liu HM. Studies on the novel alpha-glucosidase inhibitory activity and structure-activity relationships for andrographolide analogues. Bioorg Med Chem Lett 2006;16:2710-2713.
32. Xu HW, Dai GF, Liu GZ, Wang JF, Liu HM. Synthesis of andrographolide derivatives: A new family of α-glucosidase inhibitors. Bioorg Med Chem 2007;15:4247-4255.
33. Xu HW, Zhang JY, Liu HM, Wang JF. Synthesis of andrographolide cyclophosphate derivatives and their antitumor activities. Synth Commun 2006;36:407-414.

Evaluation of transdermal permeability of pentoxifylline gel: *in vitro* skin permeation and *in vivo* microdialysis using Wistar rats

Ke-Shu Yan, Ting-Xu Yan, Hong Guo, Ji-Zhong Li, Lan-Lan Wei, Chao Wang, Shu-Fang Nie, Wei-San Pan*

School of Pharmacy, Shenyang Pharmaceutical University, Shenyang, China.

ABSTRACT: The aim of the present work was to evaluate the transdermal permeability of pentoxifylline gel *in vitro* and *in vivo*. Gel was prepared with carbomer 934 as the base, and the Wistar rat was chosen as an animal model. The effects of percutaneous enhancers on the transdermal permeability of pentoxifylline gel were investigated by *in vitro* permeation experiments. Cumulative permeation at different times was determined by HPLC. 3% Azone and 5% propylene glycol were used as collaborative enhancers in an optimal formulation. Topical concentrations at different times were measured by microdialysis *in vivo*. The transdermal process of pentoxifylline fits to a zero-order kinetic equation, and its release profile remains of the zero-order despite the addition of enhancers. In addition, a good *in-vitro-in-vivo* correlation was achieved.

Key Words: Pentoxifylline, gel, transdermal, enhancer, microdialysis, *in vitro*/*in vivo* correlation

1. Introduction

Pentoxifylline (PTX), a derivate of xanthine, is a nonselective phosphodiesterase inhibitor that is commonly used for treatment of symptomatic vascular insufficiency because of its hemorrheological activity (*1*). It can restore erythrocyte deformability, decrease blood viscosity, and prevent thrombocyte adherence and aggregation, which would improve the blood circulation of the brain and the limbs and increase the volume of blood flow in arteries and capillaries. Thus, PTX is used widely in renal transplant recipients (*2*), for the cure of venous leg ulcers (*3*), and for many others diseases related to infection and tumors (*4,5*). However, the manifest first-pass effect results in a low bioavailability of 20% and its half-life is 0.4-0.8 h. Furthermore, oral administration and intravenous injection will cause adverse effects to some extent, including the most common ones of sicchasia, dizziness, headaches, anorexia (*6*). Therefore, PTX is better suited to external use for tropical disease.

The Transdermal Drug Delivery System is a promising method of drug administration that can avoid the variability in rates of absorption and metabolism encountered in oral treatment and that offers several advantages over conventional dosage forms such as tablets and injections, including elimination of first-pass metabolism, minimization of pain and some adverse effects, and possible controlled release of drugs (*7,8*). Additionally, gels are gaining greater popularity with regard to the Transdermal Drug Delivery System due to their bioadhesive properties and biocompatibility (*9*). Based on these considerations, PTX was prepared as a gel for transdermal delivery and the effects of various enhancers, which may increase the diffusion coefficient of the drug into the stratum corneum or improve partitioning between the formulation and the stratum corneum, were studied.

Microdialysis is a semi-invasive, focal sampling method based on the use of probes with a semi-permeable membrane at the probe tip and is a relatively new and effective technology for the assessment of drug distribution and target tissue pharmacokinetics (*10*). Microdialysis has gained more importance due to the fact that tissue concentrations are usually more predictive of clinical outcome than plasma concentrations. In cutaneous microdialysis, a probe is inserted superficially into the dermis, parallel to the skin surface, with or without topical anesthesia at the site of entry. The principle of microdialysis is that a physiological solution pumped through the probe is in equilibrium with the diffusible molecules in the immediate surroundings. This principle can also be used either to remove or to deliver substances to the tissue since the direction of the flux is dependent on the concentration gradient. In this paper, microdialysis was

**Correspondence to:* PO BOX 122#, Department of Pharmaceutics, Shenyang Pharmaceutical University, No. 103 Wen Hua Road, Shenyang 110016, China; e-mail: ppwwss@163.com

Received June 21, 2007
Accepted June 26, 2007

utilized *in vivo* experiment.

2. Materials and Methods

2.1 *Materials*

Materials used were carbopol 934 (BF Goodrich, USA), PTX (Shijiazhuang Pharma Group Pharmaceutical Co., China), acetonitrile (Shandong Yuwang Chemical Co., China), propylene glycol (Guangzhou Jietu Chemical Co., China), oleic acid (Dandong Julong Chemical Co., China), glycerin (Anji Haosen Pharmaceutical Co., China), and azone (Shanxi Ruicheng Fine Chemicals, China).

2.2 *Animals*

Male Wistar rats weighing approximately 170-220 g were provided by the Animal Experimental Center of Shenyang Pharmaceutical University. All studies were conducted in accordance with the Principles of Laboratory Animal Care (NIH publication no. 92-93, revised in 1985) and were approved by the Department of Laboratory Animal Research at Shenyang Pharmaceutical University. Procedures with animals were reviewed and approved by the Animal Ethical Committee at Shenyang Pharmaceutical University.

2.3 *Preparation of PTX gel*

As a base, carbopol 934 was slowly dispersed into distilled water and allowed to swell for 12 h under normal temperature; PTX (200 mg) and enhancer dissolved in 50% glyceryl alcohol solution (8 g) were added to the base while stirring. The carbopol gel was thickened by a few drops of Tris added to adjust the carbopol gel to pH 7. Distilled water was added to the gel for a final weight of 20 g (*11-13*).

2.4 *HPLC determination of PTX*

Drug analysis was performed according to the reverse phase HPLC method previously reported (*14,15*). The optimized mobile phase consisted of a combination of acetonitrile: water (28:72, v/v). The UV detector wavelength was set at 274 nm, the volume of injection was 20 μL, flow rate was 1.0 mL/min, and the temperature of column was 35°C. Under these conditions, the retention time of the PTX peak was found to be 5.1 min.

2.5 *In vitro permeability studies*

2.5.1 *Skin preparation*

Abdominal skin of male Wistar rats, 250 ± 20 g, was used for the permeation studies. The rat was sacrificed with ether and the hair of abdomen was carefully removed using an electric clipper. Full-thickness skin samples were cut, removed, and washed with normal saline. Adhering fat and connective tissues were carefully removed with a blunt-ended forceps. Skin was observed for any damage (*11,16*).

2.5.2 *In vitro skin permeation studies*

Full-thickness skin was mounted on Franz diffusion cells (vertical; available diffusion area, 2.54 cm^2; volume of receiver cell, 13 mL) with a water jacket (32 ± 1°C) to assess skin permeability. The stratum corneum side was facing upward into the donor compartment, and the dermal side was facing downward into the receptor compartment. The receiver cells were filled with distilled water and stirred by a magnetic bar to ensure adequate mixing and maintenance of sink conditions. After the experiment began, all of the solutions were sampled at 1, 2, 4, 6, 8, and 10 h, filtered with micropore film (pore diameter, 0.45 μm), and an equal volume of blank solution was immediately added. Each data point represents the average of five examinations (*17*).

The types of enhancers in gel (1% PTX) were: 1) blank; 2) 1% Azone; 3) 3% Azone; 4) 5% Azone; 5) 5% Oleic acid; 6) 3% Azone + 5% propylene glycol; and 7) 3% Azone + 5% oleic acid.

2.5.3 *Statistical analysis*

The permeation of PTX in gel with different enhancers assayed for 10 h was investigated and plots of the cumulative amount of permeated PTX (μg/cm^2) were plotted versus time. The transdermal flux (J, μg/cm^2/h) was calculated from the steady-state part of the curve and T_{lag} by extrapolation of the linear portion to the x-axis. The effectiveness of penetration enhancers was determined by comparing the flux of PTX in the presence and absence of the enhancer. This was defined as the enhancement factor (EF), which was calculated using the following equation: EF = (drug flux of samples containing an enhancer)/(drug flux of control sample without an enhancer). Data on the cumulative amount of permeation were subjected to a *t*-test at a significance level of $P < 0.01$ (*17,18*).

2.6 *In vivo microdialysis permeability studies*

Microdialysis is based on sampling of analytes from the extracellular space by means of a microdialysis probe that is made of a semipermeable membrane. A microinjection pump is used to deliver normal sodium at a flow rate of 1 μL/min as perfusate to the probe. Once the probe is implanted under the dermis, substances present in the extracellular fluid at concentration (C_{out}) are filtered by diffusion out of

the extracellular fluid into the probe, resulting in a concentration (C_{in}) in the perfusion medium. Samples are collected and determined. For most analytes, equilibrium between extracellular tissue fluid and the perfusion medium is incomplete; therefore: $C_{out} > C_{in}$. The factor by which the concentrations are interrelated is termed recovery (*19*).

2.6.1 *In vivo microdialysis*

2.6.1.1 *Implantation of the probe in vivo*

Male rats were anesthetized with urethane (1.2 g/kg, i.p.). The abdominal fur of rats was shaved. A needle was then inserted into the skin to channel away the probe. After placing the probe under the skin, the needle was withdrawn. The length of the active dialysis window was adjusted to be 1 cm. Environment temperature was kept at 37 ± 1°C using an infrared lamp (*20*).

2.6.1.2 *Permeability of PTX in vivo*

After probe implantation, a hemispherical glass reservoir with the available diffusion area of 2.54 cm^2 was adhered to the abdomen of the rat to be located on the skin above the probe. Two g of gel were added to the reservoir. Primarily, the pump worked for 1 h for washout with normal saline at an optimized flow rate of 1 μL/min. After the gel was added to the reservoir, the dialyzates were collected for 10 h at 1-hour intervals.

2.6.2 *In vitro recovery of PTX*

In order to characterize *in vitro* the influence of drug concentration in the surrounding medium on the transfer rate of the drug across the dialysis membrane, the concentration difference method was used to measure the recovery of the probe (*21*). A custom-made beaker was filled with a 10.0 μg/mL solution of PTX in normal saline, in which a stirrer was rotating. The active dialysis window was immersed in the solution; its length was 1 cm. A series of concentrations (2.0, 5.0, 10.0, 20.0, and 40.0 μg/mL) of PTX in normal saline was used as the perfusate. After each change to a different concentration perfusate, there was a half-hour washout period with the same perfusate, and then the sample was collected for an hour using mini-tubes; accordingly, the volume of the sample was 60 μL.

2.6.3 *In vivo recovery of PTX*

In vivo recovery was assessed according to the retrodialysis method (*22*). The principle of this method relies on the assumption that the diffusion process is quantitatively equal in both directions through the semipermeable membrane, which was verified by the *in vitro* experiment. Therefore, PTX solutions can serve as the perfusate and the elimination coefficient through the probe can serve as the *in vivo* recovery. In the experiment *in vivo*, after the probe was implanted blank normal saline was passed through the probe using an infusion pump as the perfusate to washout the probe for one hour. Afterward, a series of concentrations (2.0, 5.0, 10.0, 20.0, 40.0 μg/mL) of PTX in normal saline was pumped in as the perfusate at a flow rate of 1 μL/min. The dialyzate of each concentration was measured with HPLC. After each change to a different concentration perfusate, there was a half-hour washout period with normal sodium.

3. Results

3.1 *Effect of penetration enhancers*

Data for the *in vitro* permeation of PTX in gel through rat abdominal skin over 10 h are summarized in Figure 1, and J, T_{lag}, and EF are shown in Table 1.

For transdermal delivery, overcoming the barrier of the skin is a crucial step. The use of penetration enhancers offers a simple and convenient method of improving transdermal bioavailability. Several chemical penetration enhancers were examined in order to enhance the permeation of PTX from a carbopol gel base.

The effects of azone and oleic acid were investigated; among the types of enhancers (single enhancers or coalescent enhancers), a coalescent enhancer that consisted of 3% azone and 5% propylene glycol had the most conspicuous effect ($P < 0.01$). Furthermore, it produced a uniform gel.

3.2 *Microdialysis experiments*

Table 1. Effects of penetration enhancers of PTX

	Q (μg/cm^2)	*r*	J (μg/cm^2· h)	T_{lag} (h)	EF
(1)	0.6938t + 0.496	0.9947	0.8010 ± 0.6044	2.143 ± 0.4357	-
(2)	5.682t - 5.236	0.9957	6.755 ± 2.507	2.134 ± 0.5104	8.433
(3)	8.979t - 7.084	0.9995	9.123 ± 3.212	1.852 ± 0.7123	11.39
(4)	6.419t - 2.268	0.9997	6.767 ± 1.514	1.034 ± 0.2586	8.448
(5)	10.64t - 9.377	0.9946	12.79 ± 1.719	2.148 ± 0.3523	15.97
(6)	23.02t - 12.23	0.9995	24.16 ± 11.94	1.409 ± 0.3227	30.16
(7)	11.71t - 7.167	0.9965	15.16 ± 5.228	2.523 ± 0.2867	18.93

Each point and bar represents the mean ± SD of four or five determinations.

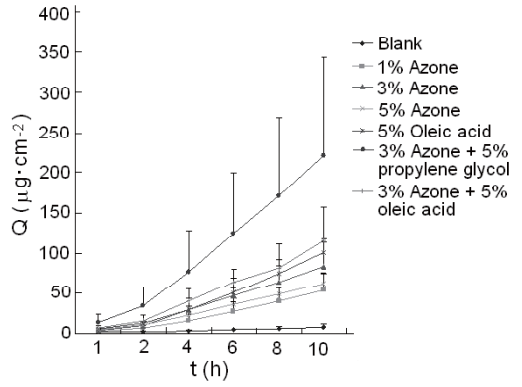

Figure 1. Effects of penetration enhancers of PTX. Each point and bar represents the mean ± SD of four or five.

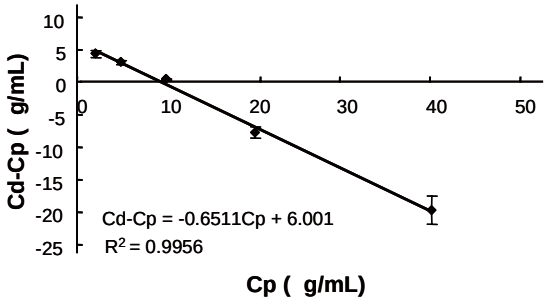

Figure 2. The concentration difference method to estimate *in vitro* recovery of PTX from the microdialysis probe (n = 3).

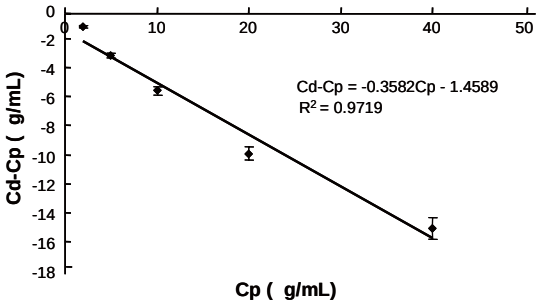

Figure 3. *In vivo* characterization of the probe (n = 3). The slope of the line is the recovery.

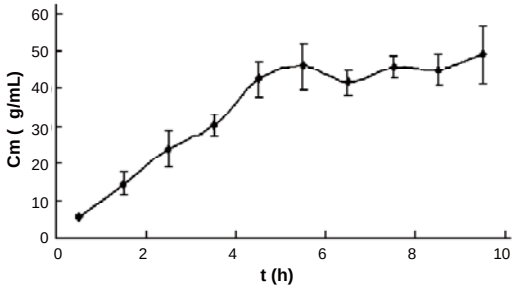

Figure 4. PTX concentration-time profiles under the dermis in rats (n = 3).

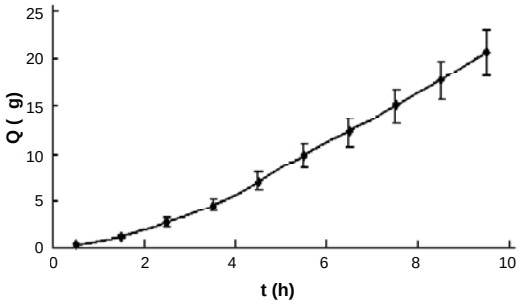

Figure 5. Plots of PTX cumulative amount versus time. The slope of the linear portion is the steady-state flux and the intercept on the time axis is the lag time in rats (n = 3).

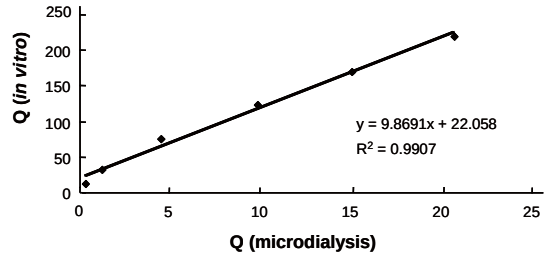

Figure 6. IVIVC model linear regression plots of Q (*in vitro*) *vs.* Q (microdialysis) for PTX.

3.2.1 *In vitro recovery experiments*

Recovery *in vitro* as measured by the concentration difference method is shown in Figure 2. There was a linear correlation for PTX between the difference in concentration in the dialysate and in perfusate (C_d-C_P) and perfusate concentration (C_P) over a wide concentration range *in vitro*. The intersection of the line and horizontal axis showed that the concentration in the surrounding medium was 9.215 μg/mL, which was essentially equal to the assigned concentration (10 μg/mL) (*23*). Accordingly, drug recovery from the tissue to perfusate was verified to be the same as drug loss from perfusate to tissue across the probe membrane in the stated concentration range (*21*). The recovery of PTX from the microdialysis probe was 65.11 ± 0.9%.

3.2.2 *In vivo recovery experiments*

The recovery *in vivo* was measured in rat subcutaneous adipose tissue with the retrodialysis method. Figure 3 shows a linear relationship between (C_d-C_P) and C_P; according to the equation, the recovery *in vivo* was 35.82 ± 1.9% (n = 3). The recovery was used to calculate the dermal PTX concentration in the study (*24*).

3.2.3 *PTX experiments*

Concentration profiles of PTX under the dermis versus time are depicted in Figure 4. The concentration under the dermis reached a plateau at about 6 h, which was in the range of 40-50 μg/mL. The cumulative amount of PTX under the dermis is plotted versus time in Figure 5. The slope of the linear portion of the profile is the transdermal delivery rate (2.724 μg/h) and the intercept on the time axis extrapolated from the linear portion is T_{lag} (1.96 h).

3.2.4 *IVIVC*

The relationship between the cumulative amount *in vitro* and *in vivo* was examined. Linear regression analysis was applied to the IVIVC plots. The values of the correlation coefficient (R^2), slope, and intercept were calculated and are given in Figure 6.

4. Discussion

Because of its hydrophilic characteristics, PTX has difficultly permeating the corneum of the skin. During the *in vitro* experiment, a low permeation of PTX resulted without enhancers. To increase permeation, several kinds of enhancers that would affect the corneum of the skin by changing the construction of the lipidic bilayer or by increasing the rheokinesis of lipoids were added to the gel. Accordingly, the transdermal permeability of PTX increased. The results of the experiment indicated that the transdermal permeability of PTX can be improved by various kinds of penetration enhancers; the mixture of azone (3%) and propylene glycol (5%) had the best improvement ($P < 0.01$) since propylene glycol increased the dissolubility of azone. However, a zero-order kinetic mechanism that was fitted to the transdermal process of PTX was not found to be affected by the addition of penetration enhancers.

In order to investigate the *in vivo* transdermal process of PTX in gel, the sample was microdialyzed. The samples obtained by microdialysis did not contain biomacromolecules, which allowed them to be injected directly into HPLC. The sampling and determination of liber drugs proceeded continuously. Therefore, the variation of the drug concentration was recorded during the whole process in this study.

Results of this study showed that dermal drug concentration can be calculated from the drug concentration in dialysate as a result of recovery, and this is easily assessed by probe characterization *in vitro* and *in vivo*.

Theoretically, the principle of the retrodialysis method is that the probe recovery is equal to the delivery rate for the same drug. However, this must be proven or demonstrated by experiments, for in fact the probe recovery is not always equal to the delivery rate for many drugs (*25*). Thus, use of the retrodialysis method to determine recovery is incorrect. Here, probe recovery was investigated by the *in vitro* experiment. Regarding the linear relationship between (C_d-C_P) and C_P as shown in Figure 2, the portion of the straight line above the horizontal axis is recovery, and the portion of the straight line under the horizontal axis is the delivery rate. The linear relationship indicates that the recovery is equal to the delivery rate for PTX. It also means that there is no interreaction between the drug and the dialyser in normal sodium and that the diffusions from both the obverse and reverse are equal. Furthermore, the concentration of PTX in the surrounding medium has no effect on recovery.

5. Conclusion

PTX gel was prepared by using carbopol 934 as a base and at the same time using 3% azone and 5% propylene glycol as collaborative enhancers. PTX permeates the skin by passive diffusion. Transdermal flux was augmented by the chosen enhancers, but a zero-order kinetic mechanism fitted to the transdermal process of PTX was not affected. Microdialysis was used to investigate the transdermal process of PTX during the *in vivo* experiment. Comparing the evaluations of *in vitro* skin permeation and *in vivo* microdialysis indicates that uniform regularity of the transdermal process was obtained during the evaluation of IVIVC, although the sampling of the two methods differed.

References

1. Ward A, Clissold SP. Pentoxifylline. A review of its pharmacodynamic and pharmacokinetic properties, and its therapeutic efficacy. Drugs 1987;34:50-97.
2. Demir E, Paydas S, Balal M, Kurt C, Sertdemir Y, Erken U. Effects of pentoxifylline on the cytokines that may play a role in rejection and resistive index in renal transplant recipients. Transplant Proc 2006;38:2883-2886.
3. Jull A, Waters J, Arroll B. Pentoxifylline for treatment of venous leg ulcers: a systematic review. Lancet 2002;359:1550-1554.
4. Najdanovic B, Zdravkovic M, Korolija P, Popovic D. Experience with pentoxifylline in the treatment of peripheral arterial desease. Pharmatherapeutica 1978;2:94-99.
5. Yaya R, Aznar J, Vaya A, Villa P, Santos T, Valles J, Martinesz-Sales V. Effect of dipyridamole plus pentoxifylline in patients with diffuse cerebrovascular insufficiency. Thromb Haemost 1985;54:896.
6. Clinical Medication guides. ChP 2005; pp308.
7. Charles SA, Bozena BM. Percutaneous penetration enhancers local versus transdermal activity. Pharm Sci Technolo Today 2000;3:36-41.
8. Hadgraft J, Peck J, Williams DG, Pugh WJ, Allan G. Mechanisms of action of skin penetration enhancers/retarders: Azone and analogues. Int J Pharm 1996;141:17-25.
9. Shin SC, Kim HJ, Oh IJ, Cho CW, Yang KH.

Development of tretinoin gels for enhanced transdermal delivery. Eur J Pharm Biopharm 2005;60:67-71.
10. Brunner M, Derendorf H. Clinical microdialysis: Current applications and potential use in drug development. Trends Analyt Chem 2006;25:674-680.
11. Fang C, Liu Y, Ye X, Rong ZX, Feng XM, Jiang CB, Chen HZ. Synergistically enhanced transdermal permeation and topical analgesia of tetracaine gel containing menthol and ethanol in experimental and clinical studies. Eur J Pharm Biopharm 2007; doi:10.1016/j.ejpb.2007.02.007.
12. Guo H, Liu Z, Li J, Nie S, Pan W. Effects of isopropyl palmitate on the skin permeation of drugs. Biol Pharm Bull 2006;29:2324-2326.
13. Guo H, Nie SF, Yang XG, Pan WS. Study on stability and prescription screening of oxaprozin gel. Chin Pharm J 2006;41:759-762.
14. Best BM, Burns JC, DeVincenzo J, Phelps SJ. Pharmacokinetic and tolerability assessment of a pediatric oral formulation of pentoxifylline in kawasaki disease. Curr Ther Res Clin Exp 2003;64:96-115.
15. Jia Woei Wong, Kah Hay Yuen, Kok Khiang Peh. Simple high-performance liquid chromatographic method for determination of pentoxifylline in human plasma. J Chromatogr B Biomed Sci Appl 1998;716:387-391.
16. Vaddi HK, Wang LZ, Ho PC, Chan SY. Effect of some enhancers on the permeation of haloperidol through rat skin *in vitro*. Int J Pharm 2001;212:247-255.
17. Ammar HO, Ghorab M, El-Nahhas SA, Kamel R. Design of a transdermal delivery system for aspirin as an antithrombotic drug. Int J Pharm 2006;327:81-88.
18. Pillai O, Panchagnula R. Transdermal delivery of insulin from poloxamer gel: *ex vivo* and *in vivo* skin permeation studies in rat using iontophoresis and chemical enhancers. J Control Release 2003;89:127-140.
19. Müller M, Schmid R, Wagner O, Osten Bv, Shayganfar H, Eichler HG. *In vivo* characterization of transdermal drug transport by microdialysis. J Control Release 1995;37:49-57.
20. Fang JY, Hsu LR, Huang YB, Tsai YH. Evaluation of transdermal iontophoresis of enoxacin from polymer formulations: *in vitro* skin permeation and *in vivo* microdialysis using Wistar rat as an animal model. Int J Pharm 1999;180:137-149.
21. Ding P, Xu H, Wei G, Zheng J. Microdialysis sampling coupled to HPLC for transdermal delivery study of ondansetron hydrochloride in rats. Biomed Chromatogr 2000;14:141-143.
22. Sauernheimer C, Williams KM, Brune K, Geisslinger G. Application of microdialysis to the pharmacokinetics of analgesics: problems with reduction of dialysis efficiency *in vivo*. J Pharmacol Toxicol Methods 1994;32:149-154.
23. He HB, Tang X, Cui F. Pharmacokinetic study of ketoprofen in rat by blood microdialysis technique. Yao Xue Xue Bao 2006;41:452-456.
24. Ding PT, Wei G, Li H, Zheng J. Study on the recovery of microdialysis by concentration difference method. Chin Pharm J 2001;36:690-694.
25. Groth L. Cutaneous microdialysis. Methodology and validation. Acta Derm Venereol Suppl (Stockh) 1996;197:1-61.

Drug Discoveries & Therapeutics

Guide for Authors

1. Scope of Articles

Drug Discoveries & Therapeutics mainly publishes articles related to basic and clinical pharmaceutical research such as pharmaceutical and therapeutical chemistry, pharmacology, pharmacy, pharmacokinetics, industrial pharmacy, pharmaceutical manufacturing, pharmaceutical technology, drug delivery, toxicology, and traditional herb medicine. Studies on drug-related fields such as biology, biochemistry, physiology, microbiology, and immunology are also within the scope of this journal.

2. Submission types

Original Articles should be reports new, significant, innovative, and original findings. An Article should contain the following sections: Title page, Abstract, Introduction, Materials and Methods, Results, Discussion, Acknowledgments, References, Figure legends, and Tables. There are no specific length restrictions for the overall manuscript or individual sections. However, we expect authors to present and discuss their findings concisely.

Brief Reports should be short and clear reports on new original findings and not exceed 4000 words with no more than two display items. Drug Discoveries & Therapeutics encourages younger researchers and doctors to report their research findings. Case reports are included in this category. A Brief Report contains the same sections as an Original Article, but Results and Discussion sections must be combined.

Reviews should include educational overviews for general researchers and doctors, and review articles for more specialized readers.

News articles should not exceed 500 words including one display item. These articles should function as an international news source with regard to topics in the life and social sciences and medicine. Submissions are not restricted to journal staff - anyone can submit news articles on subjects that would be of interest to Drug Discoveries & Therapeutics' readers.

Letters discuss material published in Drug Discoveries & Therapeutics in the last 6 months or issues of general interest. Letters should not exceed 800 words and 6 references.

3. Manuscript preparation

Preparation of text. Manuscripts should be written in correct American English and submitted as a Microsoft Word (.doc) file in a single-column format. Manuscripts must be paginated and double-spaced throughout. Use Symbol font for all Greek characters. Do not import the figures into the text file but indicate their approximate locations directly on the manuscript. The manuscript file should be smaller than 5 MB in size.

Title page. The title page must include 1) the title of the paper, 2) name(s) and affiliation(s) of the author(s), 3) a statement indicating to whom correspondence and proofs should be sent along with a complete mailing address, telephone/fax numbers, and e-mail address, and 4) up to five key words or phrases.

Abstract. A one-paragraph abstract consisting of no more than 250 words must be included. It should state the purpose of the study, basic procedures used, main findings, and conclusions.

Abbreviations. All nonstandard abbreviations must be listed in alphabetical order, giving each abbreviation followed by its spelled-out version. Spell out the term upon first mention and follow it with the abbreviated form in parentheses. Thereafter, use the abbreviated form.

Introduction. The introduction should be a concise statement of the basis for the study and its scientific context.

Materials and Methods. Subsections under this heading should include sufficient instruction to replicate experiments, but well-established protocols may be simply referenced. Drug Discoveries & Therapeutics endorses the principles of the Declaration of Helsinki and expects that all research involving humans will have been conducted in accordance with these principles. All laboratory animal studies must be approved by the authors' Institutional Review Board(s).

Results. The results section should provide details of all of the experiments that are required to support the conclusions of the paper. If necessary, subheadings may be used for an orderly presentation. All figures, tables, and photographs must be referred in the text.

Discussion. The discussion should include conclusions derived from the study and supported by the data. Consideration should be given to the impact that these conclusions have on the body of knowledge in which context the experiments were conducted. In Brief Reports, Results and Discussion sections must be combined.

Acknowledgments. All funding sources should be credited in the Acknowledgments section. In addition, people who contributed to the work but who do not fit the criteria for authors should be listed along with their contributions.

References. References should be numbered in the order in which they appear in the text. Cite references in text using a number in parentheses. Citing of unpublished results and personal communications in the reference list is not recommended but these sources may be mentioned in the text. For all references, list all authors, but if there are more than fifteen authors, list the first three authors and add "et al." Abbreviate journal names as they appear in PubMed. Web references can be included in the reference list.

Example 1:
Hamamoto H, Kamura K, Razanajatovo IM, Murakami K, Santa T, Sekimizu K. Effects of molecular mass and hydrophobicity on transport rates through non-specific pathways of the silkworm larva midgut. Int J Antimicrob Agents 2005; 26:38-42.

Example 2:
Mizuochi T. Microscale sequencing

of N-linked oligosacchaides of glycoproteins using hydrazinolysis, Bio-Gel P-4, and sequential exoglycosidase digestion. In: Methods in Molecular Biology: Vol. 14 Glycoprotein analysis in biomedicine (Hounsell T, ed.). Humana Press, Totowa, NJ, USA, 1993; pp. 55-68.

Example 3:
Drug Discoveries & Therapeutics. Hot topics & news: China-Japan Medical Workshop on Drug Discoveries and Therapeutics 2007. http://www.ddtjournal.com/hotnews.php (accessed July 1, 2007).

Figure legends. Include a short title and a short explanation. Methods described in detail in the Materials and methods section should not be repeated in the legend. Symbols used in the figure must be explained. The number of data points represented in a graph must be indicated.

Tables. All tables should have a concise title and be typed double-spaced on pages separate from the text. Do not use vertical rules. Tables should be numbered with Roman numerals consecutively in accordance with their appearance in the text. Place footnotes to tables below the table body and indicate them with lowercase superscript letters.

Language Editing. Manuscripts submitted by authors whose primary language is not English should have their work proofread by a native English speaker before submission. The Editing Support Organization can provide English proofreading, Japanese-English translation, and Chinese-English translation services to authors who want to publish in Drug Discoveries & Therapeutics and need assistance before submitting an article. Authors can contact this organization directly at http://www.iacmhr.com/iac-eso .

IAC-ESO was established in order to facilitate manuscript preparation by researchers whose native language is not English and to help edit work intended for international academic journals. Quality revision, translation, and editing services are offered by our staff, who are native speakers of particular languages and who are familiar with academic writing and journal editing in English.

4. Figure preparation

All figures should be clear and cited in numerical order in the text. Figures must fit a one- or two-column format on the journal page: 8.3 cm (3.3 in.) wide for a single column; 17.3 cm (6.8 in.) wide for a double column; maximum height: 24.0 cm (9.5 in.). Only use the following fonts in the figure: Arial and Helvetica. Provide all figures as separate files. Acceptable file formats are JPEG and TIFF. Please note that files saved in JPEG or TIFF format in PowerPoint lack sufficient resolution for publication. Each Figure file should be smaller than 10 MB in size. Do not compress files. A fee is charged for a color illustration or photograph.

5. Online submission

Manuscripts should be submitted to Drug Discoveries & Therapeutics online at http://www.ddtjournal.com. The manuscript file should be smaller than 10 MB in size. If for any reason you are unable to submit a file online, please contact the Editorial Office by e-mail: office@ddtjournal.com .

Editorial and Head Office
Wei TANG, MD PhD
Secretary-in-General
TSUIN-IKIZAKA 410
2-17-5 Hongo, Bunkyo-ku
Tokyo 113-0033
Japan
Tel: 03-5840-9697
Fax: 03-5840-9698
E-mail: office@ddtjournal.com

Cover letter. A cover letter from the corresponding author including the following information must accompany the submission: name, address, phone and fax numbers, and e-mail address of the corresponding author. This should include a statement affirming that all authors concur with the submission and that the material submitted for publication has not been previously published and is not under consideration for publication elsewhere and a statement regarding conflicting financial interests.

Authors may recommend up to three qualified reviewers other than members of Editorial board. Authors may also request that certain (but not more than three) reviewers not be chosen.

The cover letter should be submitted as a Microsoft Word (.doc) file (smaller than 1 MB) at the same time the work is submitted online.

6. Accepted manuscripts

Proofs. Rough galley proofs in PDF format are supplied to the corresponding author via e-mail. Corrections must be returned within 3 working days of receipt of the proofs. Subsequent corrections will not be possible, so please ensure all desired corrections are indicated. Note that we may proceed with publication of the article if no response is received.

Offprints. Fifty (50) offprints of each article are sent to the corresponding author. Additional offprints can be ordered before the article is published. Offprint requests after publication will be subject to an extra charge.

Page and color charges. A page charge of $140 will be assessed for each printed page of accepted manuscripts and $30 will be charged as a flat fee for each publication. The charge for printing of color figures is $340 for each page.

Transfer of copyrights. Upon acceptance of an article, authors will be asked to agree to a transfer of copyright. This transfer will ensure the widest possible dissemination of information. A letter will be sent to the corresponding author confirming receipt of the manuscript. A form facilitating transfer of copyright will be provided. If excerpts from other copyrighted works are included, the author(s) must obtain written permission from the copyright owners and credit the source(s) in the article.

Cover submissions. Authors whose manuscripts are accepted for publication in Drug Discoveries & Therapeutics may submit cover images. Color submission is welcome. A brief cover legend should be submitted with the image.

Revised July 2007

Drug Discoveries & Therapeutics

Editorial Office
TSUIN-IKIZAKA 410,
2-17-5 Hongo, Bunkyo-ku
Tokyo 113-0033, Japan

Tel: 03-5840-9697
Fax: 03-5840-9698
E-mail: office@ddtjournal.com
URL: http://www.ddtjournal.com

IACMHR CO., LTD.

JOURNAL PUBLISHING AGREEMENT

Ms No:

Article entitled:

Corresponding author:

To be published in Drug Discoveries & Therapeutics

Assignment of publishing rights:

I hereby assign to International Advancement Center for Medicine & Health Research Co., Ltd. (IACMHR Co., Ltd.) publishing Drug Discoveries & Therapeutics the copyright in the manuscript identified above and any supplemental tables and illustrations (the articles) in all forms and media, throughout the world, in all languages, for the full term of copyright, effective when and if the article is accepted for publication. This transfer includes the rights to provide the article in electronic and online forms and systems.

I understand that I retain or am hereby granted (without the need to obtain further permission) rights to use certain versions of the article for certain scholarly purpose and that no rights in patent, trademarks or other intellectual property rights are transferred to the journal. Rights to use the articles for personal use, internal institutional use and scholarly posting are retained.

Author warranties:

I affirm the author warranties noted below.
1) The article I have submitted to the journal is original and has not been published elsewhere.
2) The article is not currently being considered for publication by any other journal. If accepted, it will not be submitted elsewhere.
3) The article contains no libelous or other unlawful statements and does not contain any materials that invade individual privacy or proprietary rights or any statutory copyright.
4) I have obtained written permission from copyright owners for any excerpts from copyrighted works that are included and have credited the sources in my article.
5) I confirm that all commercial affiliations, stock or equity interests, or patent-licensing arrangements that could be considered to pose a financial conflict of interest regarding the article have been disclosed.
6) If the article was prepared jointly with other authors, I have informed the co-authors(s) of the terms of this publishing agreement and that I am signing on their behalf as their agents.

Your Status:

☐ I am the sole author of the manuscript.

☐ I am one author signing on behalf of all co-authors of the manuscript.

Please tick one of the above boxes (as appropriate) and then sign and date the document in black ink.

Signature: **Date:**

Name printed:

Please return the completed and signed original of this form by express mail or fax, or by e-mailing a scanned copy of the signed original to:

Drug Discoveries & Therapeutics office
TSUIN-IKIZAKA 410, 2-17-5 Hongo,
Bunkyo-ku, Tokyo 113-0033, Japan
E-mail: proof-editing@ddtjournal.com
Fax: +81-3-5840-9698